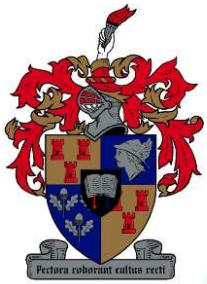

UNIVERSITEIT • STELLENBOSCH • UNIVERSITY

Reliability based codification for the design of overhead travelling crane support structures

by

Juliet Sheryl Dymond

Dissertation presented for the degree of

Doctor of Philosophy in Engineering

at the University of Stellenbosch

Department of Civil Engineering
University of Stellenbosch
Private Bag X1, 7602, Matieland, South Africa

Promoters:

Prof P.E. Dunaiski
Prof J.V. Retief

December 2005

Pectora roborant cultus recti

Declaration

I, the undersigned, hereby declare that the work contained in this dissertation is my own original work and that I have not previously in its entirety or in part submitted it at any university for a degree.

Signature: .....

J.S. Dymond

Date: .....

Pectora roborant cultus recti

Synopsis

Reliability based codification for the design of overhead travelling crane support structures

J.S. Dymond

Department of Civil Engineering
University of Stellenbosch
Private Bag X1, 7602, Matieland, South Africa

Dissertation: PhD (Engineering)

December 2005

Electric overhead travelling bridge cranes are an integral part of many industrial processes, where they are used for moving loads around the industrial area.

Codes of practice on loadings on buildings provide load models for the calculation of the vertical and horizontal loads that cranes impose on their support structures. The crane load models in the South African loading code, SABS 0160:1989 [1], are over-simplistic, therefore it is currently under consideration to adopt the crane load models from the Eurocode crane loading code, prEN 1991-3 [2] into the updated South African loading code, SANS 10160 [3]. There is no reliability basis for the partial load factor applied to crane loads in SABS 0160:1989.

This dissertation presents an investigation into electric overhead travelling crane support structures, focussing on the crane load models from prEN 1991-3. The investigation takes the form of a code calibration in two parts: calibration to current practice and reliability calibration.

The aims of the calibration to current practice were to investigate the load models from prEN 1991-3 to determine their suitability for inclusion into the proposed SANS 10160 and to assess the effect on the cost of the support

structure and the design effort required, of calculating crane loads using the load models from prEN 1991-3 rather than SABS 0160:1989.

The aims of the reliability calibration were to investigate the current level of reliability of crane support structures designed using crane loads calculated from prEN 1991-3 and SABS 0160:1989 and, if necessary, to determine partial load factors required to achieve a consistent, minimum level of reliability.

The calibration process was carried out on three representative cranes and their support structures.

Statistical models for the hoistload lifted by cranes and the modelling uncertainties in the calculation of the wheel loads were developed for use in the reliability calibration.

It was found that the current level of reliability was inadequate and partial load factors were determined, for ultimate limit state, accidental limit state and fatigue, to achieve consistent, selected target levels of reliability.

Samevatting

Reliability based codification for the design of overhead travelling crane support structures

J.S. Dymond

Departement Siviele Ingenieurswese
Universiteit van Stellenbosch
Privaatsak X1, 7602, Matieland, Suid-Afrika

Proefskrif: PhD (Ingenieurswese)

Desember 2005

Elektriese oorhoofse brugkrane vorm 'n ge-integreerde deel van baie nywerheidsprosesse, waar dit gebruik word om swaar laste in die nywerheidsaanleg te verskuif.

Praktykkodes vir belastings op geboue gee lasmodelle vir die berekening van vertikale en horisontale laste wat van die kraan na die ondersteuningsstruktuur oorgedra word. Die kraan-lasmodelle in die huidige Suid-Afrikaanse laskode, SABS 0160:1989 [1], is oorvereenvoudig en daarom word dit oorweeg om die kraan-lasmodelle van die Eurocode, prEN 1991-3 [2], in die nuwe Suid-Afrikaanse laskode, SANS 10160 [3], op te neem. Daar bestaan ook geen betroubaarheidsbasis vir die huidige parsiële lasfaktore vir kraanlaste in SABS 0160:1989 nie.

Hierdie proefskrif bespreek die navorsing oor ondersteuningsstrukture vir elektriese oorhoofse krane, met die klem op die lasmodelle van prEN 1991-3. Die navorsing neem die vorm aan van 'n tweeledige kodekalibrasie : kalibrasie gerig op huidige praktyk en 'n betroubaarheidskalibrasie.

Die doel van die kalibrasie gerig op huidige praktyk is om die lasmodelle van prEN 1991-3 te ondersoek, die geskiktheid daarvan vir die Suid-Afrikaanse kode te bepaal en dit met die huidige lasmodelle in SABS 0160:1989 te vergelyk.

Dit sluit ook die effek daarvan op die koste van ondersteuningsstrukture en die omvang van die ontwerpwerk in.

Die doel van die betroubaarheids gebaseerde kalibrasie is om die huidige vlak van betroubaarheid van ondersteuningsstrukture vir elektriese oorhoofse krane wat volgens die kraanlaste van prEN 1991-3 en SABS 0160:1989 ontwerp is, te bepaal, en indien nodig, parsiële lasfaktore te bepaal wat lei tot 'n volhoubare minimum vlak van betroubaarheid.

Die kalibrasieproses is uitgevoer op drie verteenwoordigende krane en ondersteuningsstrukture.

Statistiese modelle vir die laste wat deur die krane gehys word en die modeleringsonsekerhede vir die bepaling van die kraanwiellaste is ontwikkel vir die gebruik in die betroubaarheidskalibrasie.

Daar is gevind dat die huidige vlak van betroubaarheid ontoereikend is. Parsiële lasfaktore wat 'n gekose vlak van betroubaarheid verseker is bepaal vir die grenstoestand van swigting, die grenstoestand vir ongelukslaste en die grenstoestand van vermoeidheid.

Acknowledgements

I would like to thank the following people for the various ways in which they have assisted me during the course of my PhD:

- My supervisors, Prof PE Dunaiski and Prof JV Retief for their academic guidance during the course of this study
- Prof M Holický from the Klokner institute at the Czech Technical University in Prague for his assistance and guidance with my study during my two month stay in Prague
- The following crane manufacturers and operators for their time and assistance in the collection of data: Coen Lubbe, Coen Jacobs, Trevor Graham, Derek Lidston, Drikus Stander, Mark Walter and the late Tom Reynolds.
- My parents for the support they have given me during the course of all my studies
- My friend Michele van Rooyen, for all her encouragement
- My husband, Jacques, for always believing in me and supporting me and for his assistance in the drawing of Figure 2.1

Contents

Chapter 1

Introduction

Electric overhead travelling cranes are used in industrial applications for moving loads without causing disruption to activities on the ground. Overhead cranes can be described as machines for lifting and moving loads, consisting of a crane bridge which travels on wheels along overhead crane runway beams, a crab which travels across the bridge and a hoist for lifting the loads.

Overhead cranes are often an integral part of the industrial process and any time in which the crane is not able to be used can have severe financial implications for the owner. Cranes can be classified as heavy machinery which lift loads overhead and any mechanical or structural failure which causes the crane or load to fall could become a serious safety hazard.

The overhead travelling crane runway beams and the structural elements which support them are referred to as the crane support structure.

Overhead travelling cranes are supplied by the crane manufacturers whose responsibility it is to ensure the working and safety of the crane itself. The crane support structure is designed by a structural engineer who is responsible for ensuring that the support structure is sufficiently strong and robust to withstand the loads that are imposed by the crane.

Various problems have been encountered with crane support structures in practice, many of these arise from the deflections that result from the crane loads. Cranes, by their nature of moving loads by travelling along the crane runway beams, imposed cyclic loading on the support structure which can lead to fatigue. Fatigue failures are common problems that occur with crane support structures.

These problems which have been observed with crane support structures

prompted this investigation into the design of crane support structures and more specifically crane induced loads on the support structures. Two aspects are considered here, the load models provided in codes of practice for the crane induced loads and the structural reliability of the crane support structures.

1.1 Crane load models

Codes of practice on loadings on buildings give load models for the calculation of vertical and horizontal wheel loads that overhead travelling cranes impose on their support structures.

The crane load models in the South African loading code (SABS 0160:1989 [1]) are over-simplistic as will be shown by a comparison between the crane load models in SABS 0160:1989 and those in the Eurocode 1 Part 3 (prEN 1991-3 [2]), the German code (DIN 15018 Part 1 1984 [4]), the International standard (ISO 8686-1:1989 [5]), the Australian code (AS1418.1-1994 [6]) and the American code (ASCE 7-98 [7]).

Because of the over-simplistic nature of the crane load models in SABS 0160:1989, the crane load models are currently under review by the South African loading code committee, with the intention of adopting more sophisticated crane load models into the updated South African loading code, SANS 10160 [3].

The prEN 1991-3 crane load models have been widely accepted, having been developed from DIN 15018 and ISO 8686-1:1989 and forming the basis of AS1418.1-1994. Because of their wide acceptance, the adoption of the prEN 1991-3 crane load models into proposed SANS 10160 has been proposed and is currently under consideration.

An assessment of the prEN 1991-3 crane load models is required to determine if they are suitable for inclusion into proposed SANS 10160 and to investigate the implications of their adoption into proposed SANS 10160.

1.2 Reliability of crane support structures

There is no reliability basis for the crane partial load factor applied to crane wheel loads in SABS 0160:1989. The imposed load partial factor of 1.6 is used which has been calibrated for floor loads in office buildings. Crane induced loads are caused by the mechanical operations of lifting loads and the crane

movement along the runway beams whereas floor loads in office buildings are due mainly to furniture and the occupants of the building. These loads do not have the same origin, one is mechanical and the other is based on the weight of objects and people, and there is no evidence to suggest that crane loads have the same characteristics as floor loads in office buildings; so it is unclear whether the same partial load factor is suitable for both.

In contrast, prEN 1991-3 prescribes a partial load factor of 1.35 for crane loads which is the same as the permanent load factor in prEN 1991-3.

There is thus a difference in the approach taken to, and the value of, the crane partial load factor between the two codes; SABS 0160:1989 applies a factor equal to the imposed load factor of 1.6 and prEN 1991-3 applies a factor equal to the permanent load factor of 1.35.

The lack of a reliability basis for the crane partial load factors in SABS 0160:1989 indicates a need for a reliability assessment of the crane load models to assess the current level of reliability and if necessary to determine appropriate partial load factors for crane induced loads.

1.3 Code calibration of crane load models

The two aspects of the crane loading code which have been identified as critical and requiring investigation are:

1. Crane load models

   The crane load models in SABS 0160:1989 are over-simplistic, so it is under consideration to adopt the prEN 1991-3 crane load models into proposed SANS 10160.

   An assessment of the prEN 1991-3 crane load models is required to investigate their suitability for inclusion into proposed SANS 10160 and the implications of their inclusion into proposed SANS 10160.

2. Reliability of the crane load models.

   Different partial load factors are applied to crane loads in SABS 0160:1989 and prEN 1991-3 and there is no reliability basis for these crane partial load factors.

A reliability assessment of the crane load models is required to determine the current level of reliability and, if necessary, to determine appropriate partial load factors for the crane loads.

Both of these aspects of crane induced loads that require investigation can be treated as code calibration problems, where the 'code' that is being considered is the code of practice which specifies loads that cranes impose on their support structures.

The code calibration consists of two parts, firstly calibration to current practice and secondly reliability calibration.

1.3.1 Calibration to current practice

The calibration to current practice takes the form of a comparison between the prEN 1991-3 crane load models and the crane load models in SABS 0160:1989. The aims of the calibration to current practice are to assess the manner in which the crane behaviour is modelled and to assess the effect on the cost of the support structure and the difference in design effort, of using the crane load models in prEN 1991-3 rather than those in SABS 0160:1989. The comparison is carried out with respect to these three aspects of the codes which are discussed in more detail below:

1. Load situations

   The crane load situations that are allowed for and the aspects of the crane behaviour that are modelled are assessed. The load cases and load combinations in each code are compared.

2. Cost of support structure

   The effect on the cost of the crane support structure of calculating the crane loads using the prEN 1991-3 crane load models is assessed.

3. Design effort

   The amount of work required to calculate the factored load combinations for each code and the work required for the subsequent design of the support structure is compared.

1.3.2 Reliability calibration

Reliability based code calibration has not previously been applied to crane support structures. In this investigation the methods of reliability code calibration are applied to crane loads to investigate suitable code formats and partial load factors for crane loads as well as combination factors for combinations of crane loads with other time varying loads, i.e. wind and roof imposed loads.

Reliability code calibration has been defined by Faber *&* Sørensen [8] as using reliability analysis methods to choose design equations, characteristic values, combination schemes and partial load and resistance factors to maintain a minimum and consistent target reliability over all choices of material, loading conditions and structural configurations.

As mentioned above, the reliability code calibration is concerned with the crane induced loads on the support structure.

In general code calibration for a body of codes, the calibration of the load factors and resistance factors is carried out separately as described by Kemp *et al.* [9]. This is because of the wide range of load and resistance parameters which need to be taken into account and the need for partial load factors which are independent of the resistance codes. The partial load factors are calibrated first to obtain design loads which have a specified maximum probability of occurrence. The second step is to calibrate the partial resistance factors that result in a consistent probability of failure when combined with the calibrated design loads.

Since a particular structural type, i.e. crane support structures, is considered here, it is practical to include the resistance modelling when calibrating the partial load factors. The code calibration procedure followed here, therefore, will not follow the convention of separating resistances and loads, rather, limit states equations including both loads and resistances are set up for the reliability analysis.

The crane load models are the focus of the code calibration and all the other loads, partial load factors, resistances and partial resistance factors are taken as they are specified in the current South African loading and materials codes (SABS 0160:1989 [1]; SABS 0100-1:1992 [10]; SANS 10162-1:2005 [11]).

The aims of the reliability calibration of the crane load models are given below:

1. A reliability assessment of the two different sets of load models.

   This reliability assessment is carried out to determine the level of reliability of crane support structure for present practice of SABS 0160:1989 as well as for prEN 1991-3.

2. An investigation into different code formats.

   The code format refers to the number and type of partial load factors as well as the load combination schemes [8]. Different code formats are considered here and recommendations for the best alternative are given.

3. Determination of partial load factors and combination factors.

   The final code calibration objective is to find crane partial load factors and combination factors which result in a consistent level of reliability over a range of parameters.

The procedure for the code calibration of the crane load models was based on that given by Faber & Sørensen [8] and is outlined below.

1. Definition of the scope of the code

   The code calibration is focussed on the crane load models and 'the code' therefore refers to the crane loading code. The crane load models which are specifically being considered are those in the Eurocode 1 Part 3, prEN 1991-3 [2] because they are being assessed with a view to being incorporated into proposed SANS 10160.

   The definition of the scope of the proposed new code entails determining the type of cranes whose wheel loads can be calculated by the crane loading code and the range of these cranes in South Africa.

   The code calibration is carried out on specific example structures (cranes and support structures) as recommended by Faber & Sørensen [8] and Hansen & Sørensen [12]. These structures are chosen to be representative of the scope of the code.

2. Definition of the code objective

   The code objective could either be maximisation of the expected utility of the code or to achieve a target reliability [12]. The objective for this calibration is the achievement of a consistent target reliability. An

assessment of recommended target reliabilities is carried out and suitable values are chosen for the calibration of the crane load models for the different limit states considered.

3. Definition of the code format

   As mentioned above, the code format refers to the number and type of partial load factors and load combination schemes.

   Load combinations consist of combinations of crane loads with permanent loads or other time varying loads such as wind or roof imposed loads as well as combinations of actions from more than one crane. Actions from more than one crane are not within the scope of this investigation; so this code calibration focusses on single cranes only in combination with permanent loads, wind loads and roof imposed loads.

   The load combination schemes for crane loads with permanent loads and wind or roof imposed loads are defined by the South African loading code, SABS 0160:1989 [1], so the definition of the code format here will focus on the number and type of crane partial load factors.

   Different code formats are considered for this code calibration, to take into account the different characteristics of various crane induced loads. The different code formats considered are the use of one partial load factor applied to the characteristic wheel loads as is the current practice in both SABS 0160:1989 and prEN 1991-3, and an extension of this format to the use of two partial load factors applied separately to the crane self weight and hoistload before the calculation of the design wheel loads and the option of including an additional partial load factor for the horizontal crane wheel loads.

4. Identification of typical failure modes

   The typical failure modes of the structural elements considered for the code calibration are required to set up the limit states equations.

   Because this code calibration considers the loading and resistance together, not separately as is the convention for the calibration of the Eurocodes, the resistances of the structural elements considered are required for setting up the limit states equations. The elements chosen for the limit states equations are those that are subject to crane loads i.e. the crane girders, crane columns, roof columns, roof trusses and crane

runway bracing. The design of these elements is carried out according to the South African materials codes [10; 11]. The critical failure modes that govern the sizes of the elements are selected for the limit state equations.

Three limit states are considered: ultimate limit state, accidental limit state and fatigue.

5. Development of stochastic models

   The variables in the limit states equations that are considered as random variables for the reliability analysis are identified. Most of the stochastic models are taken from literature.

   Statistical models for crane loads have been presented by Köppe [13] and Pasternak *et al.* [14] but are not suitable for the reliability based code calibration carried out for this investigation. Due to the lack of available suitable models, stochastic models, which are suitable for a range of limit states and load combinations, are developed for this investigation for loads lifted by cranes and the modelling uncertainties in the calculation of the crane wheel loads. The development of these stochastic models is discussed

6. Determination of the optimal partial load factors

   The method of determining the optimal partial load factors is to carry out reliability analyses on the selected structural elements. The reliability analysis is carried out as an iterative process in two steps.

   a) Economic design

      The code calibration exercise is specifically interested in the reliability of the code, therefore the structural element is first designed to exactly satisfy the code requirements. No practical rounding of the element size is carried out. Practical rounding includes conservatism in the resistance of the element so that it no longer represents the code specifications and would have a higher reliability than that implied by the code. Code calibration carried out on conservatively designed elements would underestimate the size of the partial load factor required to achieve a given target reliability.

      The load models used for the crane loads in the economic design are the models in prEN 1991-3, the resistances are calculated using

the South African steel design code SANS 10162-1:2005 [11] and concrete design code SABS 0100-1:1992 [10].

The economic design is carried out using assumed values of the crane partial load factors.

b) Reliability analysis

The size of the element obtained from the economic design is used as the nominal size for the reliability analysis. A time integrated approach using a first order reliability method (FORM) with the Rackwitz-Fiessler procedure as given by Nowak *&* Collins [15] is used for the reliability analysis.

These two steps are repeated, varying the value of the crane partial load factors until the reliability of the element satisfies the code objective.

Finding the optimal partial load factors will entail assessing the different code formats to determine which best meets the code calibration criterion of obtaining a consistent level of reliability over a range of parameters.

7. Verification of partial load factors

The final step in the code calibration procedure is the verification of the partial load factors. All the elements and limit states are assessed to ensure that the code objective is met. The level of conservatism incurred with the chosen partial load factors is evaluated.

The crane partial load factors will also be assessed on the basis of engineering judgement and existing practice.

Pectora roborant cultus recti

Chapter 2

Design of crane support structures

Electric overhead travelling cranes (EOT cranes) are used in industrial applications for mechanically moving loads without interfering with activities on the ground. An EOT crane can be defined as: 'A machine for lifting and moving loads that moves on wheels along overhead crane runway beams. It incorporates one or more hoists mounted on crabs or underslung trolleys' [2]. Cranes are an essential part of the industrial process and any 'down time' can have severe financial consequences for the owner. For this reason it is essential that the running of the crane is kept as problem free as possible, leading to minimum disruption of service.

An overview is given below of electric overhead travelling cranes and their support structures with a discussion of the common problems that are encountered.

2.1 Electric overhead travelling cranes

EOT cranes can either operate within an industrial building or outside a building. Industrial buildings housing EOT cranes generally consist of one or more bays with one or more EOT cranes in each bay.

The magnitude of the loads lifted by EOT cranes varies from 2t up to 630t. The rated weight of the load lifted by an EOT crane is referred to as the 'safe working load' (SWL) and is the way in which EOT cranes are referred to (e.g. a 40t crane).

EOT cranes can have various different configurations depending on the application, the layout of the industrial building housing the crane and the type of loads to be lifted. The three basic types of electric overhead travelling cranes are bridge cranes as shown in Figure 2.1, portal cranes and semi-portal cranes. Portal cranes are a portal frame structure with the bottom of the frame legs running on rails and semi-portal cranes have one end of the crane bridge running on an elevated rail and the other end supported on a column (as with a portal frame) with the bottom of the column running on a lower rail. EOT bridge cranes are the most commonly used cranes in industry and are the type of cranes which fall under the scope of the crane loading codes. These bridge cranes will be the focus of this investigation.

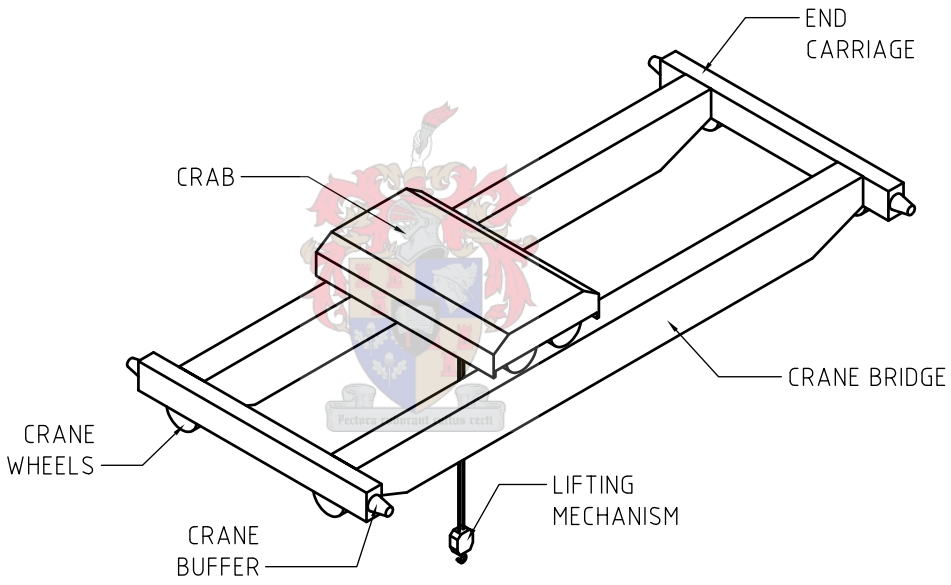

Figure 2.1: Main components of an EOT bridge crane

Within the category of EOT bridge cranes there are various different configurations. The biggest distinction is between underslung overhead travelling cranes and top mounted overhead travelling cranes. Underslung cranes are supported on the bottom flanges of the runway beams and top mounted overhead cranes are supported on rails on the top of the runway beams.

The main components of an EOT crane are the crane bridge which spans the width of the bay between the runway girders and moves longitudinally

down the length of the building, the crane crab which traverses the bridge and houses the hoisting mechanism and the end carriages on either side of the crane bridge which house the wheel blocks. The combined horizontal longitudinal and transverse movements of the crane bridge and crab and the vertical movement of the hoist allow the crane to reach any position in the industrial building for the purpose of lifting or lowering a load. The elements of an EOT crane are shown in Figure 2.1.

Top mounted overhead travelling cranes can have further different configurations. EOT cranes lifting light loads typically have hot rolled I or H sections for the end carriages and a single hot rolled I or H section for the crane bridge with the crab hoist running along the bottom flange of the crane bridge. EOT cranes lifting heavier loads normally have box girders for the end carriages and crane bridge, the crane bridge consists of two parallel box girders with the crab unit mounted on rails on top of the crane bridge girders. In cases of cranes with extremely heavy applications, the crane bridge can consist of four box girders.

There are a wide range of applications for which cranes are used which require different load lifting mechanisms. Hooks are the most common type of load lifting mechanism for general warehouse and industrial use. Ladles are used in metal works for transporting molten metal from the furnace to the casters. Another load lifting mechanism is a grab which is used for applications such as lifting granular material or scrap metal. Cranes equipped with a magnet lifting device are typically used for lifting steel plates. Specialised load lifting mechanisms such as coil lifters are used for specific applications.

The wheels are a very important part of EOT bridge cranes because the smooth running of the crane depends on the quality of the wheels and the wheels transfer the loads from the crane to the support structure. Most cranes have four wheels, two on each end carriage, but larger cranes lifting heavier loads can have eight or sixteen wheels in total. The current practice of wheel configurations is to have independent wheels which are not linked in any way to the wheels on the opposite end carriages [16; 17; 18; 19]. The driven wheels each have their own wheel drive.

Buffers are supplied on the end carriages to reduce the impact forces if the crane runs into the end stops at the end of the runway. The different types of buffers are rubber and cellular plastic which are used mainly for smaller cranes as well as hydraulic buffers which are used mainly for larger cranes.

2.2 EOT Crane support structures

The movement of loads is an integral, essential part of many industrial applications and cranes therefore play a very important role in the smooth running of the industrial process. A crane that is out of commission can have very serious financial implications for the owner. For example, if a crane in a steel works building which carries the molten metal from the furnace to the caster is out of commission, the whole production line comes to a halt with a great loss in production and hence a great financial loss. The problem of the crane being unable to fulfil its intended purpose is considered a serviceability problem because the implications are financial and not safety related.

The crane is also an important aspect when considering the safety of the industrial area. Cranes are a type of heavy machinery which lift large loads and if something should cause the load or the crane to fall it would endanger the lives of the people working in the industrial area.

Problems which could cause cranes to be out of commission or cause a safety hazard could be related to either the crane itself or the support structure. Ensuring the functioning and safety of the crane itself when it is manufactured is the responsibility of the crane manufacturer and ensuring the continued functioning and safety of the crane by means of regular inspection and maintenance is the responsibility of the owner. The functioning and safety of the support structure initially is the responsibility of the structural engineer and the responsibility for the ongoing functioning and safety of the support structure lies partly with the structural engineer in designing a durable structure and partly with the owner in regular inspection and maintenance. The aspects of the functioning and safety of the EOT crane in the industrial area that will be focussed on here are those which are the responsibility of the structural engineer, viz. to design a support structure which is sufficiently reliable over the lifetime of the crane.

Ensuring sufficient reliability of the support structure is a twofold process. The first aspect is the accurate structural modelling of the support structure in the design process, this includes both load modelling and structure response modelling. The second aspect is ensuring sufficient statistical reliability of the support structure by means of suitable partial safety factors.

2.3 Design process for EOT crane support structures

The crane support structure consists of the rails, rail fastening system, crane runway girders, crane columns, crane column bracing, crane column foundations, crane stops and conductor rail supports (Ricker [20]). The crane induced loads are applied by the wheels to the rails which transmit the loads into the girders which in turn transmit the loads to the columns and bracing and down to the foundations. Figure 2.2 shows the main components of the crane support structure.

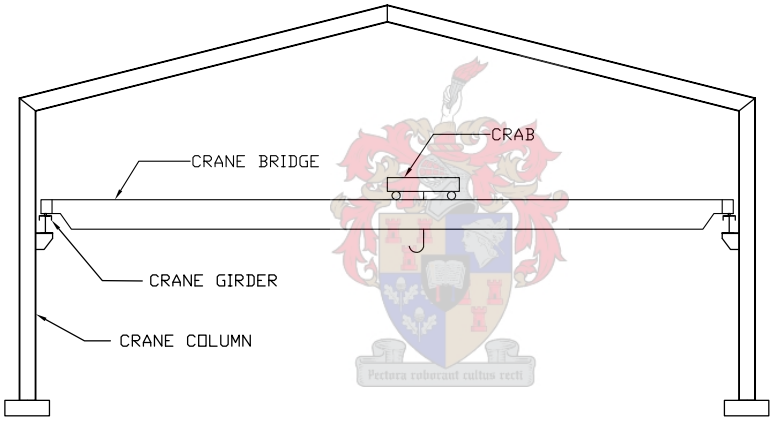

(a) Crane bay

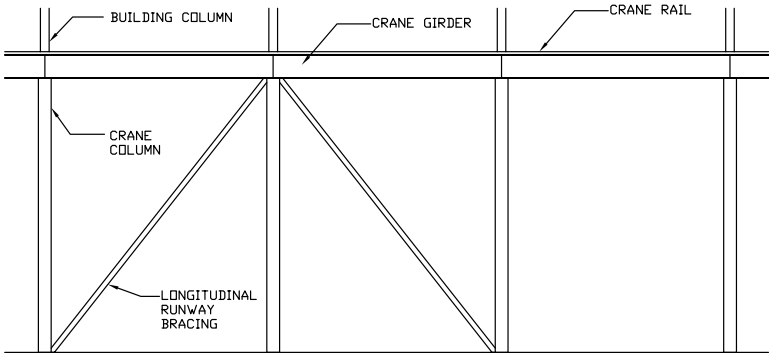

(b) Crane runway

Figure 2.2: Crane support structure

EOT cranes can either operate within an industrial building or outside a building. In the case where EOT cranes operate inside a building, the building withstands the environmental actions of wind or temperature and the crane girders are subject to crane loads only. The crane support structure can be integrated with the building structure (e.g. the crane girders are supported on corbels connected to the building column) and in this case the roof members are affected by the crane loads. Heavier cranes are typically supported on columns that are separate from the building columns and in this case the roof members are not subject to crane loads. In the case where EOT cranes operate outside a building, the crane support structure carries the crane loads as well as the environmental loads.

Ensuring an EOT crane support structure which does not cause down time for the crane or cause a safety hazard is the responsibility of the structural engineer. In order to properly design an EOT crane support structure the designer must have a good understanding of all the steps in the design process:

1. Identifying the loads that the crane imposes on the support structure
2. Modelling the response of the structure
3. Choosing the correct structural system and details to ensure a durable structure

2.3.1 Loads imposed by cranes on the support structure

In order to be able to design the EOT crane support structure, the designer must understand and take into account the various loads that the support structure will be subject to during its lifetime.

There is very little literature available on loads that EOT cranes impose on their support structures. A series of articles has been published by Lobov [21; 22; 23; 24] and Spitsyna *&* Anoskin [25] which investigate the dynamic forces on the crane caused by acceleration of the crane bridge, skewing of the crane bridge and contact of the wheel flange with the rail. The effects on the crane have been investigated considering the equations of motion of the crane. The results of these investigations are not in a form where they are applicable for the calculation of loads that cranes impose on their support structures.

In the absence of literature on crane loads, recourse must be made to design codes of practice which specify crane loads to be considered in the design of support structures.

An important point is raised by Lobov [21], and that is that crane loads are primarily dynamic loads. These dynamic loads are caused by the hoisting of loads and movement of the crane and crab in order to transport the loads around the industrial area. In the design codes these dynamic loads are treated as static loads with amplification factors, usually represented by ϕ, to allow for dynamic effects.

The crane loads are transferred to the support structure by the wheels. For this reason the loads that cranes impose on their support structures are often referred to as crane 'wheel loads'.

Crane loads can be divided into three basic categories.

1. Loads arising from normal operation of the crane
2. Loads arising from accidental situations
3. Loads arising from improper construction, lack of maintenance or misuse of the crane

Dunaiski *et al.* [26] give a review of crane load provisions from various codes, considering only vertical and horizontal crane loads due to normal operation of the crane. A more extensive discussion is presented here of the crane provisions, with respect to the three types of loads listed above, in the following design codes.

1. South African loading code SABS 0160:1989 [1]
2. Eurocode on crane loading prEN 1991-3 [2]
3. German standard on cranes DIN 15018 Part 1 1984 [4]
4. International standard on crane loading ISO 8686-1:1989 [5]
5. Australian code on crane loading AS1418.1-1994 [6]
6. American standard for loading on buildings ASCE 7-98 [7]

SABS 0160:1989, prEN 1991-3, DIN 15018, AS1418.1-1994 and ASCE 7-98 specify loads that cranes impose on the support structure. ISO 8686-1:1989 specifies the wheel loads that cranes is subject to, the support structure would be subject to equal and opposite reaction forces from the crane wheels.

2.3.1.1 Classification of cranes

In many of the design codes on crane loading, the crane wheel loads depend on the crane classification. The various classification systems in the codes are discussed below.

SABS 0160:1989 classifies cranes into four classes based on a description of the usage of the crane as given in Table 2.1.

Table 2.1: Classification of cranes in SABS 0160:1989

Class of crane	Description of crane
Class 1 Light duty	Hand cranes
Class 2 Medium duty	Cranes for general use in factories and workshops Warehouse cranes - intermittent operation Power station cranes Machine shop cranes Foundry cranes
Class 3 Heavy duty	Warehouse cranes - continuous operation Scrapyard cranes Rolling mill cranes Grab and magnet cranes - intermittent operation Ladle cranes in steelworks
Class 4 Extra Heavy duty	Grab and magnet cranes - continuous operation Soaking pit cranes Ingot stripping cranes Furnace charging cranes Forging cranes Claw cranes

The classification of the crane influences the magnitude of the vertical and horizontal forces as will be discussed in the sections below.

ASCE 7-98 does not have a classification system for cranes beyond distinguishing between hand operated cranes, powered cab or remotely operated cranes and powered pendant operated cranes. This nominal classification affects only the vertical impact forces.

prEN 1991-3, ISO 8686-1:1989, AS1418.1-1994 and DIN 15018 all classify cranes into 'Hoist Classes'. The hoist class of the crane affects only the dynamic factor applied to the hoistload to model the dynamic effects of lifting the hoistload off the ground.

The rationale behind the classification of the cranes into different hoist classes is given by DIN 15018 as: 'The softer the springing of the hoisting gear, the larger the elasticity of the supporting structure, the smaller the actual hoisting speed at the commencement of the hoisting of the useful load, the smaller and steadier the acceleration and deceleration during changes in the hoisting motion, the smaller the factor ϕ. Accordingly, the cranes are classified into lifting classes ... with different factors ϕ' [4]. Where ϕ is the dynamic factor applied to the hoistload to allow for the dynamic effects of lifting a load off the ground.

prEN 1991-3 and DIN 15018 provide a table giving the hoist class of cranes depending on a description of their usage, some types of cranes fall into more than one class. The crane descriptions and classes are given in Table 2.2.

Table 2.2: Classification of cranes in DIN 15018 and prEN 1991-3

Hoist class of crane	Description of crane
HC1	Hand cranes Powerhouse cranes
HC1, HC2	Assembly cranes
HC2	Storage cranes - intermittent usage
HC2, HC3	Workshop cranes Casting cranes
HC3, HC4	Storage cranes - continuous operation Scrapyard cranes - continuous operation Soaking pit cranes
HC4	Stripper cranes Charging cranes Forging cranes

ISO 8686-1:1989 recommends that the designer select the hoist class of the crane on the basis of experience.

AS1418.1-1994 provides a table for the selection of the hoist class of the crane which is related to the rationale behind the hoist classes as given by DIN 15018. The table relates the natural frequency of the crane structure in the vertical plane to the hoisting acceleration and is shown in Table 2.3.

Whereas the classification method given in AS1418.1-1994 reflects more the rationale behind the classification it would be more difficult to obtain the information required for the classification.

Table 2.3: Classification of cranes into hoist classes in AS1418.1-1994

Fundamental natural frequency of structure (vertical plane) Hz	Hoisting application group			
	Hoisting acceleration m/s^2			
	≤ 0.2	0.2 - 0.4	0.4 - 0.6	>0.6
$\leq$3.2	H1	H1	H2	H3
3.2 - 5.0	H1	H2	H2	H3 to H4
>5.0	H2	H2	H3	H4

2.3.1.2 Loads arising from normal operation of the crane

The loads that arise from normal operation of the crane can be divided into vertical loads and horizontal loads. The vertical loads can be divided into two parts, firstly the static part arising from gravitational effects on the crane and hoistload and secondly the dynamic part which is caused by inertial effects acting on the mass of the crane and hoistload. Horizontal transverse and longitudinal loads arise due to the movement of the crane.

2.3.1.2.1 Vertical crane loads due to gravitational effects

All the codes agree that the nominal weights of the crane bridge, crab and pay load as given by the crane manufacturer are to be used for the calculation of characteristic vertical gravitational loads.

ISO 8686-1:1989, DIN 15018 and AS1418.1-1994 give no guidance on the method of the calculation of the vertical gravitational loads. The calculation of the vertical gravitational loads is generally carried out by considering equilibrium of the crane bridge supported by the wheels and as such does not require specification.

SABS 0160:1989 recommends using the wheel loads supplied by the crane manufacturer.

ASCE 7-98 states simply that the gravitational vertical wheel loads should be calculated considering the hoistload and crab placed at the position where the wheel load is a maximum.

prEN 1991-3 specifies the crab position and whether the crane is to be loaded or unloaded for the calculation of the wheel loads. This results in four values of wheel load:

- maximum - crab closest to wheel being considered, loaded crane

- accompanying maximum - crab furthest from wheel being considered, loaded crane
- minimum - crab furthest from wheel being considered, unloaded crane
- accompanying minimum - crab closest to wheel being considered, unloaded crane

2.3.1.2.2 Vertical crane loads due to inertial effects

The codes differ more on the inertial effects to be considered for the vertical crane loads. Four basic situations have been identified for which inertial effects are taken into account.

(a) Generic dynamic effects

Both SABS 0160:1989 and ASCE 7-98 specify a dynamic factor to be applied to the static vertical wheel loads to account for general dynamic and impact effects. The value of the dynamic factor in SABS 0160:1989 depends on the class of crane and in ASCE 7-98 on the type of crane. Tables 2.4 & 2.5 give the dynamic factors for the vertical loads from SABS 0160:1989 and ASCE 7-98.

Table 2.4: Dynamic factors for vertical loads from SABS 0160:1989

Class of crane	Dynamic factor ϕ
Class 1	1.10
Class 2	1.20
Class 3	1.25
Class 4	1.30

Table 2.5: Dynamic factors for vertical loads from ASCE 7-98

Powered monorail cranes	1.25
Powered cab-operated or remotely operated bridge cranes	1.25
Powered pendant-operated bridge cranes	1.10
Hand-operated bridge and monorail cranes	1.00

(b) Dynamic effects caused by lifting a hoistload off the ground

prEN 1991-3 and ISO 8686-1:1989 take into account the dynamic effects on the crane self weight and hoistload caused by lifting a load off the ground. ISO 8686-1:1989 states that these dynamic effects are due to the drive coming up to speed before the lifting attachment engages the loads and are the result of a build up of kinetic energy and drive torque.

AS1418.1-1994 and DIN 15018 take into account the dynamic effect on the hoistload only, caused by lifting a load off the ground.

prEN 1991-3 and ISO 8686-1:1989 specify a dynamic factor, ϕ_1, to be applied to the crane self weight to account for dynamic effects of lifting a hoistload off the ground.

prEN 1991-3 specifies the value of ϕ_1 as:

$$0.9 \leq \phi_1 \leq 1.1 \tag{2.3.1}$$

In a similar way, ISO 8686-1:1989 specifies the value of ϕ_1 as:

$$\phi_1 = 1 \pm a \quad 0 \leq a \leq 0.1 \tag{2.3.2}$$

The two values that are given represent the upper and lower values of the vibrational pulse. For overhead travelling bridge cranes, typically only the upper value is of interest. The lower value is relevant for tower or jib type cranes which could have instability problems with lower hoistloads.

prEN 1991-3, ISO 8686-1:1989, AS1418.1-1994 and DIN 15018 specify a dynamic factor, ϕ_2, to be applied to the hoistload to account for the dynamic effects of lifting a load off the ground. The value of ϕ_2 in all cases depends on the Hoist Class of the crane and on the steady hoisting speed v_h. The equations are given below, in all cases the lifting speed is in m/s:

prEN 1991-3:

$$\phi_2 = \phi_{2,min} + \beta_2 \times v_h \tag{2.3.3}$$

ISO 8686-1:1989:

$$\begin{aligned} &\phi_2 = \phi_{2,min} \quad \text{for } v_h \leq 0.2\,\text{m/s} \\ &\phi_2 = \phi_{2,min} + \beta_2\,(v_h - 0.2) \quad \text{for } v_h > 0.2\,\text{m/s} \end{aligned} \tag{2.3.4}$$

AS1418.1-1994:

$$\begin{aligned} \phi_2 &= \phi_{2,min} \quad \text{for } v_h \leq 0.2\,\text{m/s} \\ \phi_2 &= \phi_{2,min} + \beta_2\,(v_h - 0.2) \quad \text{for } 0.2 < v_h \leq 1.52\,\text{m/s} \\ \phi_2 &= \phi_{2,max} \quad \text{for } v_h > 1.52\,\text{m/s} \end{aligned} \tag{2.3.5}$$

DIN 15018:

$$\begin{aligned} \phi_2 &= \phi_{2,min} + \beta_2\,(v_h - 0.2) \quad \text{for } v_h \leq 1.5\,\text{m/s} \\ \phi_2 &= \phi_{2,max} \quad \text{for } v_h > 1.5\,\text{m/s} \end{aligned} \tag{2.3.6}$$

Table 2.6: Factors for the calculation of ϕ_2

	prEN 1991-3		ISO 8686 & AS1418			DIN 15018		
Hoist class	β_2	$\phi_{2,min}$	β_2	$\phi_{2,min}$	$\phi_{2,max}$	β_2	$\phi_{2,min}$	$\phi_{2,max}$
HC1	0.17	1.05	0.2	1.00	1.3	0.132	1.1	1.3
HC2	0.34	1.10	0.4	1.05	1.6	0.264	1.2	1.6
HC3	0.51	1.15	0.6	1.10	1.9	0.396	1.3	1.9
HC4	0.68	1.20	0.8	1.15	2.2	0.528	1.4	2.2

The equations for the dynamic factor ϕ_2 as well as the values of $\phi_{2,min}$ and β_2 are similar for all the codes. The effect of the differences is shown in Figure 2.3 which shows the values of the dynamic factor ϕ_2 for the different codes over a range of lifting speeds ranging from 1 m/min to 120 m/min. The largest difference in values between the codes is in the region of 1 - 20 m/min which is the most common range of hoisting speeds. Enlarged graphs showing the dynamic factors ϕ_2 for a range of hoisting speeds from 0 - 30 m/min are shown in Figure 2.4. DIN 15018 gives the largest values, AS1418.1-1994 and ISO 8686-1:1989 have the lowest values and prEN 1991-3 gives intermediate values.

This spread in the values of the dynamic factors indicate the uncertainty about the true values of these dynamic factors.

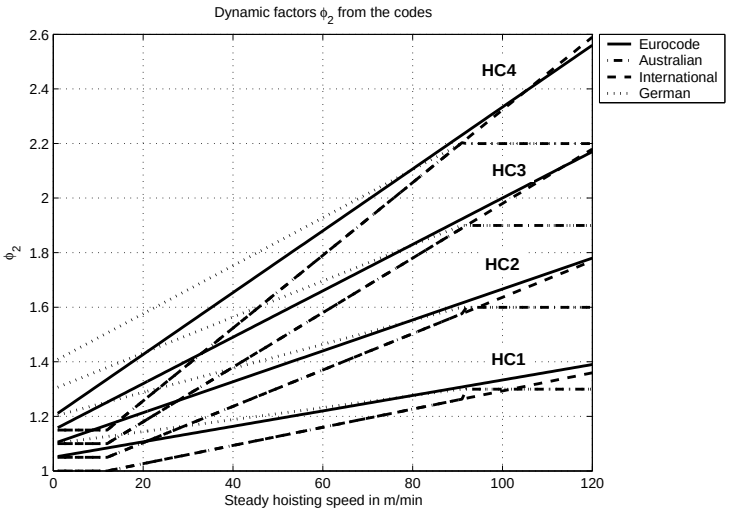

Figure 2.3: Dynamic factor ϕ_2 values for four design codes

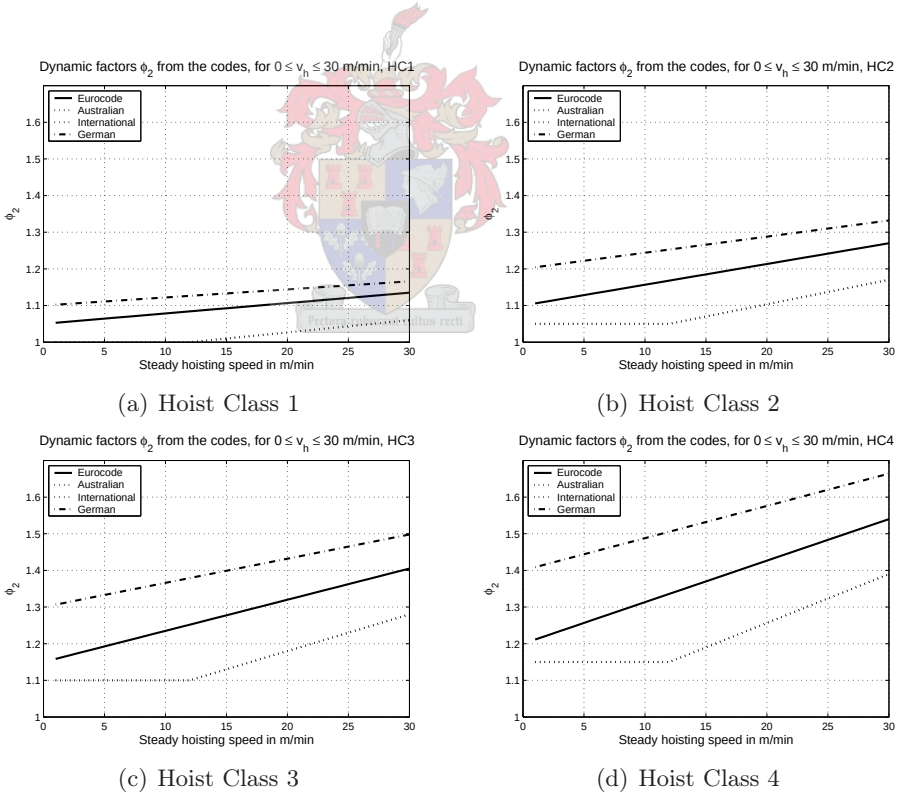

(a) Hoist Class 1

(b) Hoist Class 2

(c) Hoist Class 3

(d) Hoist Class 4

Figure 2.4: Dynamic factor ϕ_2 values for four design codes for $0 \le v_h \le 30\,\mathrm{m/min}$

(c) Dynamic effects caused by sudden release of part of the hoist-load

prEN 1991-3, ISO 8686-1:1989, AS1418.1-1994 and DIN 15018 consider the dynamic effects of the situation when a crane suddenly releases part of, or the whole of, the hoistload. This occurs in cranes which use grabs or magnets to lift loads and often release them suddenly as part of the normal operation of the crane.

prEN 1991-3, ISO 8686-1:1989 and AS1418.1-1994 specify a dynamic factor ϕ_3 to be applied to the hoistload to allow for the dynamic effects of suddenly releasing a load. The equation given in these three codes is:

$$\phi_3 = 1 - \frac{\Delta m}{m}(1 + \beta_3) \tag{2.3.7}$$

Where:

Δm – released part of the load

m – total hoisted load

β_3 = 0.5 for cranes with slow release devices like grabs

β_3 = 1.0 for cranes with rapid release devices like magnets

The dynamic factor ϕ_3 will always be less than one and, like the lower values of ϕ_1, is not generally a critical consideration for EOT bridge cranes but more for tower or jib cranes for instability considerations.

DIN 15018 specifically states that this load situation is only for jib cranes and recommends a value of:

$$\phi_3 = -0.25\phi_2 \tag{2.3.8}$$

(d) Dynamic effects caused by the crane travelling on the rails

prEN 1991-3 and ISO 8686-1:1989 adopt the same approach with regards to the dynamic effects caused by the crane travelling at a constant speed along the rails. Both codes recommend applying a dynamic factor ϕ_4 to the crane self weight and hoistload to allow for the dynamic effects of travelling along uneven rails. The value of ϕ_4 depends on the unevenness of the rails and both codes state that if the tolerances of the rails meet specifications the value of ϕ_4 may be taken as 1.0.

Rails which have a vertical or horizontal step or gap at the rail splices can induce large dynamic forces as the crane travels over the joint. These forces may lead to a fatigue failure in the web of the crane girder at the weld to the flange or stiffener, even at a relatively low number of cycles. A step or gap in the rail may also lead to increased wear of the crane rails or wheels

In the event that the rail tolerances do not meet given standards prEN 1991-3 refers to an alternative model in EN 13001-2 [27], the standard for the design of cranes. ISO 8686-1:1989 contains a model for the calculation of ϕ_4 for the crane travelling over either a gap or a step in the rail. The model is based on elasto-kinetic principles.

AS1418.1-1994 and DIN 15018 apply a dynamic factor ϕ_1 to the crane self weight to allow for the inertial forces caused by movement of the crane or crane components. The value of ϕ_1 depends on the type of wheel, type of wheel suspension, type of runway, condition of runway and travel speed of the crane. Tables 2.7 & 2.8 are given in the codes for the determination of ϕ_1. DIN 15018 states that in the case of spring suspended wheels running on rails ϕ_1 may be taken as 1.1 regardless of the travelling speed or type of runway.

Table 2.7: Determination of ϕ_1 in AS1418.1-1994

Type of runway	Condition of runway	Wheel type	Suspension type	Dynamic multiplier ϕ_1 Travel velocity, m/s				
				0	≤1.0	>1.0 ≤1.5	>1.5 ≤3.5	>3.5
Steel rails or beams	Smooth welded continuous	Steel	Unsprung	1.0	1.1	1.1	1.2	1.2
			Sprung	1.0	1.1	1.1	1.1	1.1
	Joints ≤ 4 mm wide	Steel	Unsprung	1.0	1.1	1.2	1.2	1.2
			Sprung	1.0	1.1	1.1	1.1	1.1
Concrete	No joints	Rubber	Sprung	1.0	1.1	1.1	1.1	1.1
	Jointed	Rubber	Sprung	1.0	1.2	1.2	1.25	1.25
Roadway or flexible pavement	—	Rubber	Sprung	1.0	1.1	1.1	1.15	1.15
		Crawler tracks	Sprung	1.0	1.1	1.2	1.25	1.25

The value of ϕ_1 that would most commonly be used is $\phi_1 = 1.1$. This is the same value given in prEN 1991-3 and ISO 8686-1:1989 for the factor applied to the crane self weight to allow for the dynamic effects on the crane self weight

of lifting a load off the ground, although the rationale behind the factors is different.

Table 2.8: Determination of ϕ_1 in DIN 15018

Travelling speed in m/min		Self weight factor ϕ_1
Runways		
with rail joints or irregularities (road)	without rail joints or with welded and machined rail joints	
Up to 60	Up to 90	1.1
Over 60 up to 200	Over 90 up to 300	1.2
Over 200	—	≥ 1.2

2.3.1.2.3 Horizontal crane loads due to inertial effects

As cranes accelerate or travel along the runway, horizontal transverse and longitudinal wheel loads are developed due to eccentric masses or the direction of long travel motion of the crane not coinciding with the longitudinal axis of the rails. The different horizontal load situations which are taken into account in the codes are discussed below.

(a) Generic horizontal loads

ASCE 7-98 specifies only general horizontal transverse and longitudinal loads without giving any indication of the crane load situation which is being modelled.

The transverse forces are taken to be 20% of the sum of the weights of the hoistload and the crab. The forces act in either direction perpendicular to the runway beam and are to be distributed taking into account the stiffness of the runway beams and supporting structure.

The longitudinal forces are taken to be 10% of the maximum wheel loads of the crane and act in either direction parallel to the beam.

Because of these specifications being all that is given in ASCE 7-98 with regards to horizontal loads, this code will not be considered in the further discussions.

(b) Acceleration and braking of the crane bridge

SABS 0160:1989 specifies horizontal longitudinal forces only for the case of acceleration or braking of the crane bridge. The longitudinal force on each rail is specified to be 10% of the sum of the maximum static wheel loads on that rail.

ISO 8686-1:1989 recommends, in the main body of the code, the use of a rigid body kinetic model to calculate the loads due to the acceleration and braking of the crane bridge, taking into account the geometry and mass distribution of the drives and the crane. A dynamic factor ϕ_5 is applied to allow for the elastic effects of the drives. The values of ϕ_5 range from 1.0 to 2.0 depending on the smoothness of change of the drive forces. A detailed model for the calculation of these loads is given in an Appendix of ISO 8686-1:1989. The model assumes wheel pairs that are fixed on one side and movable on the other. However, this wheel combination is not common practice amongst crane manufacturers today, the current practice is crane wheels that are fixed laterally on both end carriages [16; 17; 18; 19]. The model is a complex fully kinetic model of the drives and crane structure.

prEN 1991-3, AS1418.1-1994 and DIN 15018 specify transverse and longitudinal loads caused by acceleration and braking of the crane. The longitudinal loads are caused by the drive forces and the transverse loads are the result of the crab being positioned eccentric to the centre of mass of the crane.

For independent wheels which are laterally fixed on both sides, the drive force is calculated, assuming no slip, as the minimum possible wheel loads multiplied by the friction coefficient between the wheel and rail:

$$K = \mu \left(n \times V_{min} \right) \tag{2.3.9}$$

Where:

K – total drive force

μ – friction coefficient

n – number of driven wheels

V_{min} – minimum possible wheel load (crab furthest from wheel being considered, unloaded crane)

The drive force acts at the geometric centre of the crane. The configuration which results in the maximum transverse loads is the crab at the extreme of its

travel causing the maximum offset between the geometric centre of the crane and the centre of mass. The drive force then causes a moment about the centre of mass of the crane which is resisted by couples acting on the wheels of each end carriage. Figure 2.5 shows the configuration of the crane and the resulting forces.

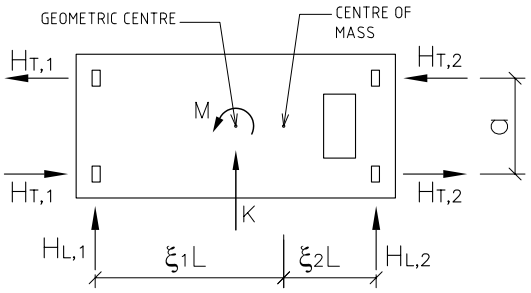

Figure 2.5: Wheel loads due to acceleration of crane bridge

The values of the horizontal transverse loads are calculated using the equation below:

$$H_{T,1} = \phi_5 \xi_2 \frac{K l_s}{a}$$
$$H_{T,2} = \phi_5 \xi_1 \frac{K l_s}{a} \tag{2.3.10}$$

Where:

$H_{T,i}$ – horizontal transverse force on wheels on rail i

ϕ_5 – dynamic factor to take into account the dynamic effects of the change of drive forces

ξ_i – distance from rail i to centre of mass of the crane

l_s – distance between geometric centre and centre of mass of the crane

a – distance between the guide rollers or flanged wheels

The value of the dynamic factor ϕ_5 in DIN 15018 and AS1418.1-1994 is given as 1.5 on condition that the drives are free from backlash.

Different values of the dynamic factor ϕ_5 are given in prEN 1991-3 depending on the type of drive and the behaviour of the drive. The values are shown in Table 2.9.

Table 2.9: Values of the dynamic factor ϕ_5 in prEN 1991-3

$\phi_5 = 1.0$	centrifugal forces
$1.0 \leq \phi_5 \leq 1.5$	systems in which drive forces change smoothly
$1.5 \leq \phi_5 \leq 2.0$	systems in which drive forces change suddenly
$\phi_5 = 3.0$	for drives with considerable backlash

(c) Acceleration and braking of the crab

SABS 0160:1989 specifies the total force due to the acceleration and braking of the crab as equal to the weight of the hoistload and crab multiplied by a factor depending on the class of the crane. The factors are given in Table 2.10. It is recommended in the code that the load be divided among all the wheels of the crane taking into account the transverse stiffness of the crane rail supports.

Table 2.10: Factors from SABS 0160:1989 for the loads due to acceleration and braking of the crab

Class of crane	Factor
Class 1	0.05
Class 2	0.10
Class 3	0.15
Class 4	0.20

prEN 1991-3 states that the transverse forces due to the acceleration or braking of the crab are taken into account by the buffer forces resulting from the accidental situation where the crab runs into the end stops on the end of the crane bridge. This approach is problematic in that it is a conservative estimate of the forces that would be caused due to the acceleration or braking of the crab and its use in fatigue calculations, for example, could lead to over conservative designs.

ISO 8686-1:1989 recommends the same method for calculating the forces due to the acceleration and braking of the crab as those due to the accelera-

tion and braking of the crane, i.e. the rigid body kinetic model given in the appendix of the code.

AS1418.1-1994 and DIN 15018 also take the same approach to the calculation of the loads due to acceleration or braking of the crab as to those due to the acceleration or braking of the crane. The drive forces are calculated, assuming no slip at the wheel-rail interface, by multiplying the friction factor by the minimum possible crab wheel loads. The resulting transverse force is distributed between the crane wheels taking into account whether they are fixed/fixed wheel pairs (divide the total drive force by the number of wheels) or fixed/movable wheel pairs (divide the total drive force by the number of fixed wheels).

(d) Misalignment of crane wheels or gantry rails

SABS 0160:1989 takes into account the situation where there is misalignment of either the crane wheels, in a 'toe-in' or 'toe out' manner, or gantry rails which causes horizontal transverse forces on each side of the crane tending to either pull the rails together or push them apart. These forces are due to horizontal friction forces induced by the crane wheels rolling at an angle to the longitudinal axis of the rail. Wheels or rails which are aligned according to specified tolerances may still be at an angle sufficient to cause these misalignment loads so this load case does fall under the 'loads arising from normal operation of the crane'. The value of the misalignment load for each wheel is calculated according to the equation given below.

$$H_{T,m} = \frac{XM}{N} \tag{2.3.11}$$

Where:

$H_{T,m}$ – horizontal transverse load on each wheel caused by misalignment of wheels or rails

X – factor depending on the class of the crane, given in Table 2.11.

M – combined weight of the crane bridge, crab and hoistload

N – total number of crane wheels

prEN 1991-3, ISO 8686-1:1989, AS1418.1-1994 and DIN 15018 do not give a load model for the calculation of loads due to misalignment of crane wheels or gantry rails.

Table 2.11: Factors from SABS 0160:1989 for the loads due to misalignment of crane wheels or gantry rails

Class of crane	Factor
Class 1	0.05
Class 2	0.12
Class 3	0.15
Class 4	0.20

(e) Skewing of the crane in plan

Skewing of the crane in plan can be caused by a number of factors such as the drive force on one side being larger than on the other side, one motor failing, applying brakes too suddenly so one side takes before the other or different diameters of wheels on either side of the crane. In short, any difference between the long travel speed on one side of the crane from the other can cause the crane to skew in plan thereby causing transverse forces to be applied to the runway.

SABS 0160:1989 specifies loads caused by skewing of the crane in plan. Different methods are given for cranes guided by guide rollers and those guided by wheel flanges.

In the case of a crane guided by wheel flanges, the load applied to each wheel is taken as 1.5 times the load due to misalignment of the wheels or rails. The loads are applied as couples on the wheels of each end carriage.

In the case of a crane guided by guide rollers, the loads applied as a couple to the guide rollers should result in a couple 1.3 times the couple that would have been produced by the skewing forces on one end carriage if the crane did not have guide rollers. The note in the code states that it is not known precisely what the forces imposed on guide rollers are and the recommendation given is empirically based and conservative.

prEN 1991-3, ISO 8686-1:1989, AS1418.1-1994 and DIN 15018 all have the same basic load model for skewing. The model assumes a crane travelling at a constant speed and rotating about an 'instantaneous centre of rotation' to an angle to the runway. A guide force develops on the front guidance means which comes into contact with the rail and tries to straighten the crane. This guide force is then resisted by horizontal transverse forces on the wheels which are due to the transverse component of friction as the wheels slide horizontally. The model takes into account the angle of skew and the configuration of the

wheels.

The guide force and transverse forces due to skewing are calculated as given below:

$$\begin{aligned} S &= f\lambda_{s,j}\Sigma Q_r \\ H_{S,i,j,k} &= f\lambda_{s,i,j,k}\Sigma Q_r \end{aligned} \tag{2.3.12}$$

Where:

S – guide force on the front guidance means

$H_{S,i,j,k}$ – transverse skewing forces on the wheels

f – friction coefficient in the transverse direction

$\lambda_{s,i,j,k}$ – skewing force factors

ΣQ_r – total weight of the crane and hoistload

i – rail i

j – wheel pair j

k – direction of the force, T = transverse, L = longitudinal

Figure 2.6 shows the configuration of the skewing loads.

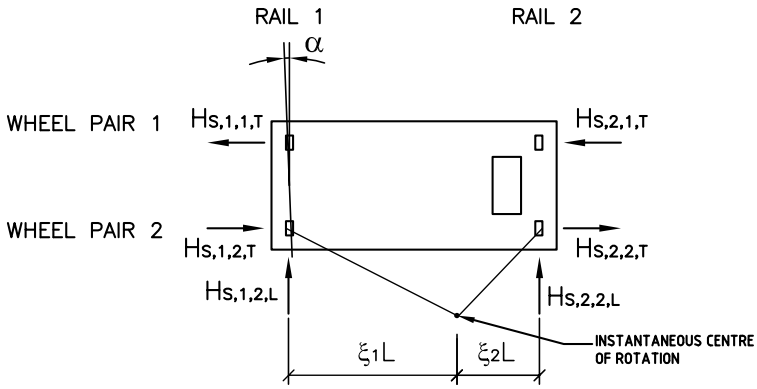

Figure 2.6: Configuration of skewing loads

prEN 1991-3 gives the most guidance on the skewing angle α, recommending that three aspects of skewing be taken into account: initial skewness from slight rail and wheel misalignment, clearance between rail and guidance means and wear of rail and guidance means.

The component of the friction coefficient in the transverse direction is stated by ISO 8686-1:1989 to be empirically based and is given by all four codes as:

$$f = 0.3\,(1 - exp\,(-250\alpha)) \leq 0.3 \tag{2.3.13}$$

The possible configurations of wheel pairs for EOT cranes are either coupled or independent with either movable or fixed wheels. A wheel pair is considered to be a pair of wheels, opposite each other, one on each end carriage, refer to Figure 2.6. Coupled wheel pairs are wheel pairs whose rotation is either electrically or mechanically synchronised, as in the case of central wheel drives. Independent wheel pairs are not linked together in any way and are free to rotate independently of each other. Movable wheels have a lateral degree of freedom, i.e. they are able to move horizontally transverse to the rail direction and are thus unable to transfer any lateral forces to the rails. Fixed wheels do not have this lateral degree of freedom but are horizontally fixed on their axes.

The combinations of coupled or independent and movable or fixed wheels which are considered in prEN 1991-3 for the skewing load model are:

- CFF: Coupled, fixed - fixed: the wheels pairs are coupled and none of the wheels can translate horizontally on their axes.

- CFM: Couple, fixed - movable: the wheel pairs are coupled and the wheels on one end carriage are fixed on their axes while the wheels on the other end carriage have a horizontal transverse degree of freedom.

- IFF: Independent, fixed - fixed: the wheel pairs are independent, the wheels on both end carriages are fixed on their axes.

- IFM: Independent, fixed - movable: the wheel pairs are independent and the wheels on one end carriage are fixed on their axes while the wheels on the other end carriage have a horizontal transverse degree of freedom.

Current common practice is to have independent, fixed - fixed wheels [16; 17; 18; 19], however, the load models for the other configurations of wheels will be presented here as well. Tables 2.12 & 2.13 give the equations for the distance from the front guidance means to the instantaneous centre of rotation and the factors for the determination of the guide force and transverse skewing forces. Figure 2.7 shows the configuration of the skewing loads for a four wheeled crane guided by wheel flanges for the four different wheel combinations identified in Table 2.12.

Table 2.12: Distance to instantaneous centre of rotation for skewing

Combination of wheel pairs	h
Continuous or independent, fixed/fixed (CFF, IFF)	$\frac{m\xi_1\xi_2 l^2+\Sigma e_j^2}{\Sigma e_j}$
Continuous or independent, fixed/movable (CFM, IFM)	$\frac{m\xi_1 l^2+\Sigma e_j^2}{\Sigma e_j}$

Table 2.13: Force factors for skewing forces

Wheels	$\lambda_{s,j}$	$\lambda_{S,1,j,L}$	$\lambda_{S,1,j,T}$	$\lambda_{S,2,j,L}$	$\lambda_{S,2,j,T}$
CFF	$1-\frac{\Sigma e_j}{nh}$	$\frac{\xi_1\xi_2 l}{nh}$	$\frac{\xi_2}{n}\left(1-\frac{e_j}{h}\right)$	$\frac{\xi_1\xi_2 l}{nh}$	$\frac{\xi_1}{n}\left(1-\frac{e_j}{h}\right)$
IFF	$1-\frac{\Sigma e_j}{nh}$	0	$\frac{\xi_2}{n}\left(1-\frac{e_j}{h}\right)$	0	$\frac{\xi_1}{n}\left(1-\frac{e_j}{h}\right)$
CFM	$\xi_2\left(1-\frac{\Sigma e_j}{nh}\right)$	$\frac{\xi_1\xi_2 l}{nh}$	$\frac{\xi_2}{n}\left(1-\frac{e_j}{h}\right)$	$\frac{\xi_1\xi_2 l}{nh}$	0
IFM	$\xi_2\left(1-\frac{\Sigma e_j}{nh}\right)$	0	$\frac{\xi_2}{n}\left(1-\frac{e_j}{h}\right)$	0	0

Where:

h – distance from the front guidance means to the instantaneous centre of rotation

e_j – distance of wheel pair j from the front guidance means

l – span of the crane

m – number of coupled wheel pairs

n – number of wheel pairs

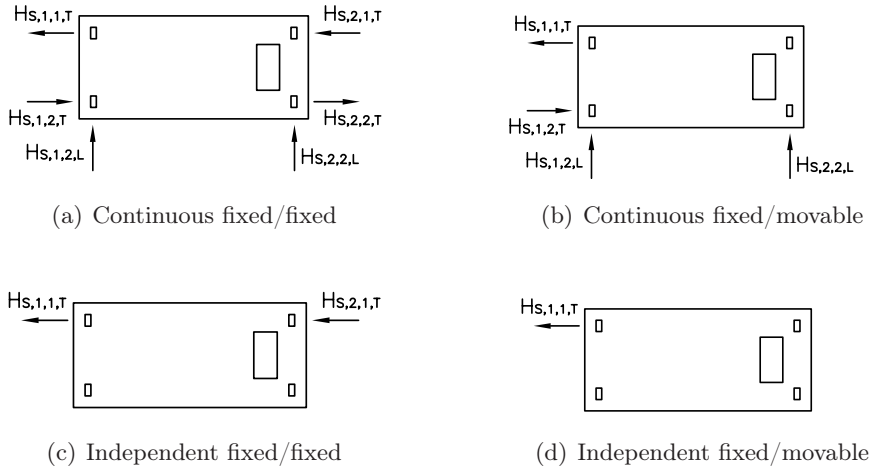

(a) Continuous fixed/fixed

(b) Continuous fixed/movable

(c) Independent fixed/fixed

(d) Independent fixed/movable

Figure 2.7: Configuration of skewing forces for different wheel combinations

2.3.1.2.4 In-service wind

Cranes on outside gantries will be subject to wind forces during crane service. prEN 1991-3, ISO 8686-1:1989, DIN 15018 and AS1418.1-1994 all make provision for these loads when considering load combinations and refer to the relevant parts of their set of standards for the calculation of the in-service wind loads.

2.3.1.2.5 Test Loads

Cranes are required to undergo testing by the lifting of a test load. There are two types of load tests [16]:

- Tests carried out on cranes after initial installation, refurbishment, upgrading or modification. The test consists of loading the crane to 125% safe working load, lifting the load and lowering it with the crane stationary.
- Tests carried out on all cranes each year. The test consists of loading the crane to 110% safe working load and moving the load in the manner of normal operation of the crane, i.e. all motions: long travel, cross travel and hoisting.

SABS 0160:1989 and ASCE 7-98 do not mention the test loads.

prEN 1991-3 specifies a dynamic test load of 110% safe working load and a static test load of 125% safe working load. For design, the dynamic test load is assumed to be moved by the drives in the way in which the crane will be used and is multiplied by a dynamic factor ϕ_6 to allow for vertical inertial effects of lifting the load. The same dynamic factor for the test loads is also used in ISO 8686-1:1989, AS1418.1-1994 and DIN 15018 and is calculated by:

$$\phi_6 = \frac{1 + \phi_2}{2} \tag{2.3.14}$$

ISO 8686-1:1989 specifies that the values of the test loads should be taken from ISO 4310 and that in the case of dynamic test loads the load should be multiplied by the dynamic factor ϕ_6.

AS1418.1-1994 does not state the value of the test load or a reference but merely states that the value of the load should be appropriate for the crane and that the dynamic load should be multiplied by the dynamic factor ϕ_6.

DIN 15018 specifies a small test load of 125% safe working load as a dynamic test load to be multiplied by the dynamic factor ϕ_6 and a large test load of either 133% safe working load for hoist class one or two cranes or 150% safe working load for hoist class three and four cranes as a static test load.

2.3.1.3 Loads arising from accidental situations

Accidental crane load situations can arise from the movement of the crane or the hoistload. The various types of accidental loads are discussed below.

2.3.1.3.1 Crane running into the end stops

This situation occurs when the crane is allowed to run into the end stops on the end of the runway. This is classified as an accidental situation because most cranes are provided with limit switches on the runway which are designed to stop the crane before it collides with the end stops. Buffers are provided on the crane to lessen the impact force. This accidental situation is provided for in the codes.

SABS 0160:1989 recommends taking for the force on each end stop, assuming that the hoistload is free to swing, the lower value of:

(a) A force equal to the self weight of the crane, i.e. crane bridge and crab.

(b) A force calculated assuming the crane to be travelling at full rated speed, taking into account the resilience of the end stops and buffers.

prEN 1991-3 and ISO 8686-1:1989 take the same basic approach in the determination of the buffer forces due to crane movement. They state that the buffer forces are to be calculated considering the kinetic energy from all parts of the crane moving at 70% - 100% of the long travel speed, taking into account the distribution of mass and the buffer characteristics. prEN 1991-3 gives the following equation for the calculation of the buffer forces on each end stop:

$$H_{B,1} = \phi_7 v_1 \sqrt{m_c S_B} \tag{2.3.15}$$

Where:

$H_{B,1}$ – force on each end stop

ϕ_7 – dynamic factor taking into account non-linearity of buffer

v_1 – 70% of the full long travel speed in m/s

m_c – mass of the crane and hoistload in kg

S_B – spring constant of the buffer in N/m

ISO 8686-1:1989 differs from prEN 1991-3 in that it states that the effects of hoistloads which are free to swing need not be included.

The value of the dynamic factor ϕ_7 depends on the non-linearity of the buffer which is represented by the buffer characteristic ξ. ISO 8686-1:1989 refers to the buffer characteristic as the relative buffer energy and defines it as:

$$\xi = \frac{1}{F_{max} u_{max}} \int_0^{u_{max}} F_x \mathrm{d}u \tag{2.3.16}$$

Where:

F_{max} – buffer maximum force

u_{max} – buffer maximum deflection

$\int_0^{u_{max}} F_x \mathrm{d}u$ – area under buffer force displacement curve, shown in Figure 2.8

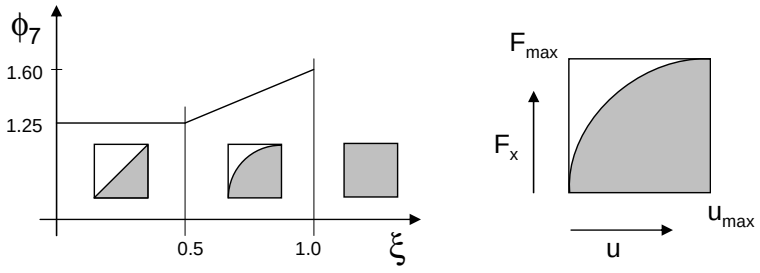

Figure 2.8: Buffer force-displacement characteristic curve

prEN 1991-3 recommends values of the dynamic factor ϕ_7 as depicted in Figure 2.8 and given by the following equations:

$$\begin{aligned} \phi_7 &= 1.25 && \text{if } 0 \leq \xi \leq 0.5 \\ \phi_7 &= 1.25 + 0.7\,(\xi - 0.5) && \text{if } 0.5 \leq \xi \leq 1.0 \end{aligned}$$

Where:

ξ – degree of non-linearity of buffer, ratio of the area under the force displacement curve to the product of the maximum force and maximum displacement. Refer to Figure 2.8 for a graphical representation of the buffer characteristic ξ.

AS1418.1-1994 and DIN 15018 give the same recommendations for the calculation of buffer forces due to crane movement. The buffer forces are calculated assuming the crane to be moving at 85% to 100% of its full long travel speed except in the case where a reliable system is provided to slow the crane down, such as limit switches, in which case a speed of 70% of the full long travel speed may be used. It is stated that hoistloads that are free to swing need not be taken into consideration.

The buffer forces are calculated on the basis of the kinetic energy of the crane before collision with the buffer. The same recommendations as in prEN 1991-3 and ISO 8686-1:1989 are given regarding the dynamic factor ϕ_7.

2.3.1.3.2 Crab running into the end stops

This load situation occurs when the crab runs into the end stops on the end of the crane bridge in a similar way to the crane running into the ends stops on the end of the runway.

SABS 0160:1989 does not make provision for this load situation.

prEN 1991-3 specifies that the total buffer force relating to crab movement, in the case when the hoistload is free to swing, shall be taken as 10% of the weight of the crab and hoistload.

ISO 8686-1:1989, AS1418.1-1994 and DIN 15018 do not make specific provision for this load situation but include it under the buffer forces due to crane movement and recommend that the same procedure be used for both the crane and crab.

2.3.1.3.3 Crane tilting

The crane can tilt if the hoistload is rigidly fixed, for example on a mast, and collides with an obstacle.

SABS 0160:1989 and AS1418.1-1994 do not consider this load situation.

prEN 1991-3 and ISO 8686-1:1989 merely state that in the case when tilting of the crane can occur, the resulting static forces should be considered and the dynamic effects of the crane falling back onto the rails should be taken into account.

DIN 15018 gives more guidance on this load situation by stating that a horizontal load shall be applied at the obstacle level with the crab in the most unfavourable position.

2.3.1.3.4 Wind blowing crane onto end stops

Cranes on outside gantries or in buildings which are not fully clad are subject to wind forces. There have been several cases of cranes without an appropriate anchorage system or without storm brakes activated, where the wind forces have exceeded either the braking force or the friction force between the rails and the wheels and the crane has travelled along the runway, through the end stops and fallen to the ground [18; 20].

Out-of-service wind is mentioned in ISO 8686-1:1989, AS1418.1-1994 and DIN 15018 but no mention is made of this specific consequence of the wind loads which could possibly be the reason why many cases of this type of failure have been observed.

A crane running off the end of the runway has financial and safety implications and is therefore a highly undesirable occurrence.

Two approaches are possible to prevent this behaviour of the crane. The first is to anchor the crane so that it is unable to move due to the wind forces.

This anchorage system should be easy to apply to ensure that it is actually used when the crane is out of service. The second approach is to ensure that the structural elements which could prevent this crane behaviour have sufficient resistance to withstand the loads. The structural elements which resist these loads are the end stops on the ends of the runway and longitudinal runway bracing. The cost of these elements in comparison to the cost of the entire gantry is relatively small so a small increase in cost of the crane support structure would result in a significantly lower risk of financial losses and safety hazards.

2.3.1.3.5 Hoistload colliding with column

In the case when the hoistload is free to swing and the crab suddenly stops as it is traversing, due to inertia effects, the hoistload could swing and collide with a crane column or other structural member. This accidental situation is not considered in any of the codes.

This type of accidental situation is discussed by Lynch [28] who addresses it from a crane operator training point of view. This raises the issue of whether the responsibility for the functioning and safety of the crane support structure under these loads lies with the crane operator preventing these situations or with the structural engineer designing a structure strong enough to withstand loads from these situations. The answer lies in the distinction between accidental loads and loads due to abuse of the structure. Accidental loads are loads which should not occur but occasionally due to unforseen circumstances do occur. Loads due to abuse of the structure occur through the fault of the occupant of the structure who deliberately uses the structure for a purpose for which it was not originally intended. It is prudent for structural engineers to design buildings against accidental loads but the design of a structure for abuse would in many cases be uneconomical. Loads due to abuse of the structure are discussed further in the next section.

2.3.1.3.6 Failure of mechanisms or emergency cut-out

In the case where cranes are supplied with emergency brakes as well as service brakes, failure of a component or an emergency cut-out causes the application of the emergency brakes. ISO 8686-1:1989 and AS1418.1-1994 recommend that the provisions for acceleration or braking of the crane or crab be used to determine these forces.

2.3.1.4 Loads arising from improper construction, lack of maintenance or misuse of the crane

There are many loads which can be imposed by the crane on its support structure resulting from improper construction, lack of maintenance of the support structure or misuse of the crane.

The main issue in the proper construction and maintenance of a EOT crane support structures is the alignment of the rails, this consists of two parts: alignment of the rails with respect to the rest of the support structure and alignment of the rails with respect to each other and the intended rail position. In the construction phase the correct alignment starts at floor level and works upwards with the correct alignment of the column, girders on the columns and rails on the girders. If the alignment is correctly carried out during construction then the maintenance of the rail alignment consists of realigning the rails on the girders with respect to one another and the intended rail position.

Tolerances on rail alignment in South Africa are given by SAISC [29]. Experience shows that correct rail alignment is difficult to achieve and many crane support structures have rails which are not aligned to these tolerances. Misaligned rails cause wear on the tracks and wheel flanges and place stress on the rail connections.

Misaligned rails may cause an increase in the frequency of skewing of the crane and misalignment type of crane loads where the crane bridge is either trying to pull the rails together or force them apart as provided for in SABS 0160:1989.

Rails that are misaligned on the girders cause torsion in the girder and in severe cases of rails being misaligned with respect to the centre of the web, rotation of the top flange and bending of the top of the web can result. These are load effects that are not generally taken into account during the design of the girders and could therefore cause an ultimate limit state type of failure or increase the fatigue damage considerably.

Girders which are not properly aligned on the columns or corbels could cause larger bending moments in the columns than those taken into account during the design.

There are many ways in which the crane itself could be misused thereby leading to loads not considered in the design. Examples of such misuse are

oblique hoisting of a load, dragging a load along the ground, routinely running the crane into the end stops to straighten it, allowing a hoistload to swing into a column or turning off the overload limit switch to pick up loads larger than the safe working load [20]. All of these misuses subject the crane support structure to much larger loads that it was originally designed for and could cause failures or shorten the fatigue life of the structure.

The question raised is: how much should a structural engineer design an EOT crane support structure for loads resulting from these types of improper construction, maintenance and misuse of the crane? This question can be taken further to ask: how far should design codes go to make provision for this sort of load?

The initial response to questions like this is that structures are generally not designed for abuse and the construction of a structure to withstand any possible abuse that may occur would be prohibitively expensive. The owner or occupant of a structure should take the responsibility to ensure that the structure is not subject to these types of abuses. In the case of crane structures this would entail strict control and monitoring of the construction phase to ensure that alignment tolerances were met and a routine maintenance plan to ensure that rails remained aligned within the tolerances. The second aspect of responsible use of crane support structures is the correct training, and/or supervision, of crane operators to ensure that the crane is not misused.

Experience shows, however, that correct rail alignment is often *not* achieved and that misuse of cranes *does* occur. In the light of this a structural engineer may choose to include additional load cases for these situations to be on the conservative side, however, what should be the response of the code writing committee? Three options are available:

1. State that the load models presented in the code are based on the assumption that the alignment tolerances are met and that the crane is used in the manner for which it was intended.

2. Suggest regular inspection and maintenance to ensure rail alignment and crane operator training to ensure that the crane is not misused.

3. Recommend load models for rails misaligned outside the tolerances or the load situations occurring from crane misuse.

Of the codes that were considered here, the only code which makes reference to the correct alignment of the rails to specified construction tolerances is DIN 15018 which states that unless otherwise specified, the loads shall be calculated on the assumption that the runway has been properly horizontally and vertically aligned thereby following option 1.

The question of whether design codes should make provision for lack of maintenance or misuse of the structure, even in the event that it is common knowledge that these occur, is a contentious issue and no firm answer has been reached.

2.3.1.5 Additional loads

Some additional loads can act on crane support structures and are taken into account by the various codes as shown in Table 2.14.

Table 2.14: Additional loads on crane support structures

Additional load	prEN 1991-3	ISO 8686	DIN 15018	AS 1418
Loads due to displacements		X		X
Temperature variation	X	X	X	X
Snow and ice		X	X	X
Off-vertical hoisting				X
Seismic loads		X		X
Construction loads		X		X
Loads on walkways	X	X	X	X

2.3.1.6 Summary of crane loads considered by the codes

Table 2.15 below gives a summary of the basic crane loads that are taken into account by the six codes that were considered.

Table 2.15: Summary of crane loads considered by the codes

Crane load	SABS 0160	ASCE 7-98	prEN 1991-3	ISO 8686-1	DIN 15018	AS 1418
Vertical						
Generic impact	X	X				
Hoisting:						
effect on self weight			X	X		
effect on hoistload			X	X	X	X
Running on rails			X	X	X	X
Release of payload			X	X	X	X
Test loads			X	X	X	X
Horiz transverse						
Generic transverse		X				
Acceleration of crane			X	X	X	X
Acceleration of crab	X			X	X	X
Skewing	X		X	X	X	X
Misalignment	X					
Crab buffer forces			X	X	X	X
Horiz longitudinal						
Generic longitudinal		X				
Acceleration of crane	X		X	X	X	X
Crane buffer forces	X		X	X	X	X

2.3.1.7 Combinations of vertical and horizontal crane loads

Crane load combinations consist of vertical crane loads combined with horizontal crane loads to be considered as one characteristic crane action for combination with other actions such as wind.

SABS 0160:1989 gives little guidance on the combinations of crane actions to be considered, merely stating that the horizontal transverse forces need not be considered to act together. This results in three ultimate limit state combinations and one accidental combination:

Ultimate limit state:

1. Vertical with impact + Acceleration or braking of crab + Acceleration or braking of crane
2. Vertical with impact + Misalignment of wheels or rails + Acceleration or braking of crane
3. Vertical with impact + Skewing + Acceleration or braking of crane

Accidental limit state:

1. Vertical without impact + End stop forces

ASCE 7-98 does not mention combinations of crane actions but as there is only one horizontal transverse force and one horizontal longitudinal force it is assumed that these will be combined resulting in only one load combination:

Ultimate limit state:

1. Vertical with impact + horizontal transverse + horizontal longitudinal

prEN 1991-3 provides a table specifying load combinations resulting in seven ultimate limit state combinations, two accidental combinations and one combination for test loads. The load combination table from prEN 1991-3 is given in Table 2.16. The various individual crane loads are given in the first column and the load combinations are specified in the succeeding columns. The ϕ symbols represent the dynamic factors applicable for each load combination.

Table 2.16: Crane load combinations

		Groups of loads								
		ULS							Test load	Accidental
		1	2	3	4	5	6	7	8	9
1	Self weight of crane	ϕ_1	ϕ_1	1	ϕ_4	ϕ_4	ϕ_4	1	ϕ_1	1
2	Hoist load	ϕ_2	ϕ_3	-	ϕ_4	ϕ_4	ϕ_4	η[1]	-	1
3	Acceleration of crane bridge	ϕ_5	ϕ_5	ϕ_5	ϕ_5	-	-	-	ϕ_5	-
4	Skewing of crane bridge	-	-	-	-	1	-	-	-	-
5	Acceleration or braking of crab or hoist block	-	-	-	-	-	1	-	-	-
6	Test load	-	-	-	-	-	-	-	1	-
7	Buffer force	-	-	-	-	-	-	-	-	ϕ_7

[1] η is the part of the hoist load that remains when the payload is removed, but is not included in the self weight of the crane

From an inspection of the load combinations recommended by prEN 1991-3, it was observed that of the combinations given as ultimate limit state combinations, for overhead travelling bridge cranes, only load combinations 1, 5 and

6 are likely to be critical. Load combination 2 considers the case when the crane releases part of the load where the hoistload value is multiplied by the dynamic factor ϕ_3 which was shown earlier to be always less than one. Load combination 3 is the same as load combination 1 except that an unloaded crane is considered. Load combination 4 considers the case when the crane is accelerating on the runway with a load, and as ϕ_4 is usually equal to one and is therefore less than both ϕ_1 and ϕ_2, this load combination would have smaller vertical loads than load combination 1. Load combination 7 considers a stationary unloaded crane with no horizontal forces and would therefore have smaller loads than the other load combinations.

The conclusion drawn from this observation is that the load combinations which are not critical for the ultimate limit state, are given for the purposes of fatigue calculations.

ISO 8686-1:1989 classifies crane loads as regular, occasional or exceptional. Three types of load combinations are considered: combinations of regular loads, combinations of regular and occasional loads and combinations of regular, occasional and exceptional loads. DIN 15018 classifies crane loads into main loads, additional loads and special loads and load combinations as normal or special. AS1418.1-1994 takes a similar approach to ISO 8686-1:1989 and DIN 15018 by classifying the crane loads as principal loads, additional loads and special loads and the load combinations as frequently, infrequently and rarely occurring combinations.

For ISO 8686-1:1989 and AS1418.1-1994 the regular or frequent load combinations consist of combinations of crane loads which result from normal operation of the crane such as acceleration of the crane and hoist drives, corresponding to prEN 1991-3 load combinations 1 - 4, 6 and 7. The occasional and infrequent combinations include skewing, corresponding to prEN 1991-3 load combination 5. DIN 15018 considers the regular and occasional or frequent and infrequent combinations together as the normal combinations. The exceptional, special or rare load combinations include test loading, tilting, end stop forces etc. corresponding to prEN 1991-3 load combinations 8 and 9.

ISO 8686-1:1989, AS1418.1-1994 and DIN 15018 also recommend load combinations including the additional loads such as deformations, snow and ice, temperature etc.

2.3.2 Fatigue

Crane support structures are subject to fatigue due to the cyclic nature of crane loading as the crane lifts and lowers loads and moves around the building. Many problems that are encountered with crane support structures in practice are fatigue problems, indicating that correct fatigue design is an important consideration.

Fatigue damage is unlike the ultimate limit states where the loading and resistance of the structure can be treated separately. In the assessment of fatigue damage a knowledge of both the fatigue loads and the fatigue resistance, normally in the form of S-N curves, is required.

The question raised then is should crane loading design codes give guidance on loads to be considered for fatigue or should the onus be on the designer to ensure that fatigue has been adequately taken into account.

Varying degrees of guidance on fatigue loads for crane support structures are given in the design codes which have been considered. SABS 0160:1989 and ASCE 7-98 do not give any guidance on the loads to be considered for fatigue. DIN 15018 discusses fatigue but from the point of view of allowable stress rather than crane loading. The guidance given in ISO 8686-1:1989 is that generally the only load combinations taken into account for fatigue verification are the regular load combinations, which model the hoisting of a load or sudden release of a load with acceleration of the drives and that, in some cases, in-service wind, skewing or test loads should be taken into account. AS1418.1-1994 also states that the fatigue assessment should be carried out considering only the frequently applied load combinations, which involve hoisting a load, sudden release of a load and acceleration of drives.

prEN 1991-3 gives a detailed method of fatigue analysis which was derived from the design code for the design of the crane. This method will be outlined below.

The basis for the determination of the fatigue loads is the normalisation of the maximum nominal wheel load resulting in an equivalent constant amplitude load for two million cycles. This normalised load is called the 'fatigue damage equivalent load'. The normalisation is carried out by multiplying the maximum nominal wheel load by a factor (λ), as shown below.

$$Q_e = \phi_{fat} \times \lambda \times Q_{max} \tag{2.3.17}$$

Where:

Q_e – fatigue damage equivalent load

ϕ_{fat} – damage equivalent dynamic impact factor, the factor applied to the crane self weight $\phi_{fat,1} = \frac{1}{2}(1+\phi_1)$ and the factor applied to the hoistload $\phi_{fat,2} = \frac{1}{2}(1+\phi_2)$

Q_{max} – maximum nominal wheel load

The λ factor is determined from the fatigue class of the crane. Cranes are classified into fatigue classes depending on the total number of cycles (N) performed over the lifetime of 25 years and the load spectrum (kQ). One λ factor is given for each fatigue class for the calculation of normal stresses and another for the calculation of shear stresses. Table 2.17 shows the λ factors and Table 2.18 shows the classification table from prEN 1991-3.

Table 2.17: λ factors according to the classification of cranes

Class	S_0	S_1	S_2	S_3	S_4	S_5	S_6	S_7	S_8	S_9
normal stresses	0.198	0.250	0.315	0.397	0.500	0.630	0.794	1.00	1.260	1.587
shear stresses	0.379	0.436	0.500	0.575	0.660	0.758	0.871	1.00	1.149	1.320

The load spectrum definition in prEN 1991-3 is:

$$kQ = \sum_j \left(\left(\frac{\Delta Q_{i,j}}{\max \Delta Q_i} \right)^m \frac{n_{i,j}}{\sum n_{i,j}} \right) \tag{2.3.18}$$

Where:

$\Delta Q_{i,j}$ – load amplitude of range j for wheel i: $\Delta Q_{i,j} = Q_{i,j} - Q_{min,i}$

$\max \Delta Q_i$ – maximum load amplitude for wheel i: $\max \Delta Q_i = Q_{\max,i} - Q_{\min,i}$

$n_{i,j}$ – number of applications of range j for wheel i

$\sum n_{i,j}$ – total number of load applications

m – slope of the S-N curve

This is the definition of the load spectrum when fatigue of the crane itself is being considered. For the fatigue of a simply supported crane girder it was considered more reasonable to use the values of the wheel loads rather than the wheel load amplitudes to define the load spectrum. This is because the load amplitude that is felt by the girder ranges from a load of zero when the crane is not yet on the girder to a load equal to the wheel load for that given crane cycle. This will result in a larger load spectrum than that calculated using the wheel load amplitudes. The suggested load spectrum to take into account that it is the effect on the girder that is being considered is:

$$kQ = \sum_j \left(\left(\frac{Q_{i,j}}{\max Q_i} \right)^m \frac{n_{i,j}}{\sum n_{i,j}} \right) \tag{2.3.19}$$

Where:

$Q_{i,j}$ – wheel load of value j for wheel i

maxQ_i – maximum wheel load for wheel i

The effects of a crane moving along a continuous beam would not be accurately modelled using this definition of the load spectrum. The load effect in a continuous beam could vary from negative when the crane is on the adjacent span to positive when the crane is on the span being considered. This highlights the fact that a generic definition of a load spectrum for the fatigue of a crane support structure element is not as simple as for the crane itself, due to the variety of possible support structure configurations.

The manner in which the fatigue damage equivalent load is used to assess the fatigue of an element of the support structure is outlined below.

The fatigue stresses in the support structure element being considered are calculated by considering one movement of the crane along the girder with the wheel loads equal to the fatigue damage equivalent load and the stress cycles causing fatigue are calculated. If the structural element is subject to only one stress cycle from one pass of the crane, the fatigue resistance is taken as the stress level at two million cycles on the relevant S-N curve. If more than one stress cycle is obtained, the parameters of the relevant S-N curve are used to calculate the accumulative fatigue damage according to Miner's rule and the resistance is taken as the fatigue damage at failure equal to one.

Table 2.18: Classification of the fatigue actions from cranes

Class of load spectrum		Q_0	Q_1	Q_2	Q_3	Q_4	Q_5
		$kQ \leq 0.0313$	$0.0313 < kQ \leq 0.0625$	$0.0625 < kQ \leq 0.125$	$0.125 < kQ \leq 0.25$	$0.25 < kQ \leq 0.5$	$0.5 < kQ \leq 1.0$
Class of total number of cycles							
U_0	$N \leq 1.6 \times 10^4$	S_0	S_0	S_0	S_0	S_0	S_0
U_1	$1.60 \times 10^4 < N \leq 3.15 \times 10^4$	S_0	S_0	S_0	S_0	S_0	S_1
U_2	$3.15 \times 10^4 < N \leq 6.30 \times 10^4$	S_0	S_0	S_0	S_0	S_1	S_2
U_3	$6.30 \times 10^4 < N \leq 1.25 \times 10^5$	S_0	S_0	S_0	S_1	S_2	S_3
U_4	$1.25 \times 10^5 < N \leq 2.50 \times 10^5$	S_0	S_0	S_1	S_2	S_3	S_4
U_5	$2.50 \times 10^5 < N \leq 5.00 \times 10^5$	S_0	S_1	S_2	S_3	S_4	S_5
U_6	$5.00 \times 10^5 < N \leq 1.00 \times 10^6$	S_1	S_2	S_3	S_4	S_5	S_6
U_7	$1.00 \times 10^6 < N \leq 2.00 \times 10^6$	S_2	S_3	S_4	S_5	S_6	S_7
U_8	$2.00 \times 10^6 < N \leq 4.00 \times 10^6$	S_3	S_4	S_5	S_6	S_7	S_8
U_9	$4.00 \times 10^6 < N \leq 8.00 \times 10^6$	S_4	S_5	S_6	S_7	S_8	S_9

The advantage of the fatigue assessment approach given by prEN 1991-3 is that it is a quick method of carrying out fatigue assessment requiring the calculation of only one set of stresses and the designer is not required to consider the various different loads that the crane will lift as well as the various different crab positions. Being a simplified method though, it should be conservative.

There are many disadvantages to this approach to fatigue assessment. The first is the uncertainty in the derivation of the method. As has already been pointed out in the discussion on the load spectrum, the method still appears to be based on the fatigue of the crane itself rather than the support structure.

The method is specified to be used with vertical wheel loads and no guidance is given on the method to be used with horizontal wheel loads. No guidance is given either on the load combinations to be considered for fatigue.

Using this method restricts the freedom of the designer to tailor the fatigue assessment to a specific crane installation. For example, consider a ladle crane in a steelworks building moving in a very set pattern, it always lifts a full ladle at one end of the gantry with the crab at one end of the crane bridge and travels the full length of the gantry where it brakes and unloads the ladle, it then moves back the whole length of the gantry and stops in position to refill the ladle. This crane is always accelerating and braking over the same girders with the crab at the extreme of its travel and thus a worst-case fatigue situation is realised for those girders which should be taken into account. In comparison if a workshop crane is considered, where the movement of the crane is more random, the girders need not be considered to be subject to the horizontal loads caused by acceleration of the crane for every crane cycle.

Another disadvantage of this method is that it is less transparent for the designer and it is difficult to see the relative importance of each different load case.

2.3.3 Crane - support structure interaction

Most of the load models given in the crane loading codes assume the crane and the support structure to be rigid. This is not the case in reality and the issue of crane - support structure interaction could cause additional loads or different distributions of the wheel loads that are not taken into account by the codes. It is therefore important that the designer takes possible crane - support structure interaction into account when carrying out the design, either

in the calculation of the loads or in selecting the structural configuration of the building.

The structural configuration that would cause the wheel loads to deviate the most from those given in the codes is one where the runway is not symmetrical. If the asymmetry is in the columns, e.g. the columns on one side of the runway are stiffer than the columns on the other side, the side with the stiffer columns would be subject to higher lateral loads than the other side. If the asymmetry is in the girders, e.g. the girder on one side of the runway has a larger span than the girder on the other side, the difference in vertical deflections could cause the vertical wheel loads to be distributed unequally. In the worst case of the girders having unequal deflections, one wheel could lift off the rails causing an increase in vertical loads on the remaining wheels and placing large torsion forces on the crane itself.

Crane - support structure interaction causing additional loads on the runway can also be caused by the configuration of the crane. In the case where the crane bridge consists of an I beam supported on top of the end carriage beams, where the neutral axis of the crane bridge is above the level of the wheels, when the crane lifts a load, the crane wheels will tend to move outwards placing lateral forces on the crane runway.

Most of the codes do not mention the possibility of crane - support structure interaction, with the exception of SABS 0160:1989 and ASCE 7-98 which recommend distributing the lateral forces to the crane wheels with regard to the relative lateral stiffness of the support structure. The onus is therefore on the support structure designer to make adequate provision for the possible effects of the crane support structure interaction when distributing the loads or calculating load effects.

2.3.4 Support structure configurations and details

Buildings housing cranes differ from those without cranes in that they are subject to dynamic loads and this needs to be taken into account for the design of the crane girders, columns and connections. Ricker [20] has considered many aspects of crane support structures, pointing out the crane specific issues involved in their design and recommending structural configurations to withstand these crane specific forces and movements. These issues will be briefly discussed here.

The correct vertical and horizontal alignment of the girders is an important aspect of crane support structures, therefore provision must be made in the support structure components for the adjustment of vertical and horizontal alignment. Fabrication and construction tolerances need to be taken into account in allowing for alignment, including inaccuracies in foundations, skewness of columns, rolling or fabrication tolerances of steel members, sweep in crane beams and fabrication tolerances of the crane itself. The construction tolerances for South Africa are given by SAISC [29] and adherence to these tolerances for all structural members would be critical for the correct alignment of the crane runway.

The crane girders are the most important part of the crane support structure and are the members that are most directly loaded by crane loads. The different types of crane girders are [30]:

1. Wide flange shape, rolled I section
2. Wide flange shape with channel cap
3. Welded wide flange shape with channel as top flange
4. Welded wide flange shape with unequal flanges
5. Welded wide flange shape for narrow clearances
6. Welded wide flange shape with surge plate
7. Welded wide flange shape with surge plate and backup truss

In general simply supported girders are preferable over continuous girders. Midspan points of continuous girders are subject to stress reversals as the crane moves over the girder and combinations of maximum bending moments and shear forces at internal supports which could cause fatigue problems.

In order to select the structural configurations that are appropriate for crane support structures, an understanding is required of the manner in which the various crane actions are resisted. The vertical crane loads are resisted by the vertical crane girder, the transverse crane loads are resisted by the top flange of the crane girder and the longitudinal loads are resisted by the columns and the longitudinal runway bracing.

Considering the transverse wheel loads which are resisted by the top flange of the crane girder. Wide flange shapes with channel caps or unequal flanges

will generally have sufficient resistance for small to medium cranes. Large cranes will generally require surge plates to resist the transverse crane forces. The ends of the girders will typically have some type of lateral restraint consisting of a tie-back connection to the column.

The horizontal longitudinal crane loads are applied to the support structure at the level of the wheel-rail contact. These loads are resisted by the columns and primarily by the longitudinal runway bracing. The connection of the crane girder to the column should ensure that the longitudinal forces can be carried to the bracing system by means of continuity plates on the column cap linking the bottom flanges of the girders.

The vertical crane wheel loads, which are resisted by the main vertical crane girder, cause bending of the girder and accompanying rotation of the girder ends. According to Ricker [20] it is this end rotation which is the major cause of problems in crane runways because structural configurations which can accommodate these end rotations are not employed. In order to overcome these problems, the deflections of the girders should be kept as small as possible (i.e. short spans and deep beams) and the correct details should be chosen to handle these deflections.

Tie-back connections from the top flange to the column which have holes slotted in the longitudinal direction can accommodate the longitudinal movement of the top flange of the girder which results from the vertical deflection. Details that should be avoided are connections between the ends of adjacent girders on webs or top flanges and tie-back type of connections from the web of the girder to the column, both of which will place severe stresses on the girder due to the end rotations.

Off-centre rails should also be taken into account in the design of the girder. An off-centre rail causes torsion in the girder and possible top flange rotation and web bending. The tolerance given by SAISC [29] is that the offset of the centre of the rail from the centre of the web may not be more than half the thickness of the web.

The crane columns are also an important part of the crane support structure in that they provide the support for the crane girders. The different column configurations are:

1. Bracketed column (with corbel)

2. Step column, solid web

3. Step column, laced web

4. Step column, vierendeel

5. Step column, battened

6. Separate building and crane column

An important point which could easily be overlooked is that in cases where the crane girders are eccentric to the centre of the columns, the longitudinal crane loads cause torsion of the columns and column bases.

This is by no means an exhaustive discussion on crane support structure details and design but highlights a few important issues for the purpose of demonstrating that special considerations are required for the design of buildings containing EOT cranes.

2.3.5 Correct construction

The issue which is the most important when considering construction of crane support structures is the issue of rail alignment. Misaligned rails could cause the crane to skew more often and cause more wear on the rails and wheel flanges. Rails which are badly out of alignment may place additional torsion on the crane girders and may even cause the crane to get wedged between the rails thereby placing very large lateral forces on the girders. Misaligned rails also cause larger lateral forces to be placed on the rail clips. These type of forces, which are larger than those allowed for in the design codes, could significantly shorten the fatigue life of the structure.

The correct alignment of the rails starts with the correct alignment of the column bases and foundations and continues up to the columns and girders and finally the rails. Allowance should be made in the details of the connections of the girders to the columns and the rails to the girders for vertical and horizontal alignment. Correct alignment of the rails during the construction phase and continual maintenance to ensure that the rails stay in alignment could significantly prolong the lifetime of the structure. Rail alignment tolerances in the vertical and horizontal directions are given by the SAISC [29].

2.4 Reliability of EOT crane support structures

Ensuring sufficient statistical reliability of the EOT crane support structures is achieved by the application of appropriate partial load factors which are provided by codes of practice.

The appropriate partial load factors are determined by means of reliability based code calibration which takes into account the statistical variability in the loads and resistances, i.e. inherent variability as well as statistical uncertainty of the calculations.

The calibration of the partial load factors is undertaken by assessing the experience and judgement based code specifications and carrying out reliability modelling of the loads and load models.

The objectives of reliability code calibration encompass both concerns of structural engineering, viz. the safety and economics of a structure. The selection of appropriate partial safety factors addresses these two concerns by:

- ensuring sufficiently reliable performance of the structure for the ultimate limit state as well as the serviceability limit state
- obtaining more consistent reliability levels over a range of load situations, material choices and structural configurations. Unnecessary conservatism can be avoided thereby resulting in more economic designs.

The reliability assessment is carried out assuming that all load situations have been accounted for, the correct structural details have been chosen and the design has been carried out correctly. These matters are the responsibility of the designer and a neglect of these issues cannot be compensated for by the partial safety factors.

As mentioned in Chapter 1, there is no reliability basis for the crane partial load factor applied to crane wheel loads in the South African loading code, SABS 0160:1989 [1] and the crane partial load factor applied in SABS 0160:1989 differs from that applied in prEN 1991-3.

The difference in crane partial load factor between SABS 0160:1989 and prEN 1991-3 and the lack of a reliability basis for the crane partial load factor, indicates that an investigation into the reliability of structures subject to crane loads is required.

This investigation will comprise an assessment of the crane load models in prEN 1991-3, an assessment of the level of reliability of structures designed

according to SABS 0160:1989 and prEN 1991-3 and a code calibration exercise to determine appropriate partial load factors for crane loads.

Chapter 3

Scope of the code

The scope of the new South African crane loading code (SANS 10160 [3]) was defined as the same as the scope of the current South African crane loading code, SABS 0160:1989 [1], i.e. electric overhead travelling bridge cranes with wheels at the same level, therefore excluding portal or semi-portal cranes.

The specific example cranes and support structures chosen for the code calibration process should be representative of the scope of the updated South African crane loading code. Due to the fact that the scope of the updated crane loading code is the same as the current code, the requirement that the example cranes should cover the scope of the updated crane loading code will be met by ensuring that they cover the range of cranes currently found in practice. This would be ensured if the range of the parameters of the example cranes cover the range of parameters of cranes found in practice.

The crane parameters that affect the loads imposed by cranes were identified and their ranges and distributions were investigated. Example cranes were selected to cover the range of parameters. These example cranes will from now on be referred to as the representative cranes.

3.1 Crane parameters

The crane parameters that affect the loads imposed by cranes were identified as those that affect the crane wheel loads calculated from the load models in prEN 1991-3, as discussed in Chapter 2. The ranges and distributions of the parameters were determined by consultation with a leading crane manufacturer and an assessment of their database of 563 cranes manufactured since 1956 [18].

The parameters and their ranges and distributions are given below.

3.1.1 Configuration of crane

- Top mounted or underslung

  The crane load models that are used to calculate the crane loads are different for top mounted and underslung cranes. Top mounted cranes are the focus of this investigation and it can be seen below that this is reasonable because 95% of the cranes in South Africa are top mounted cranes.

  - Distribution: Overhead - 95% of cranes
    Underslung - 5% of cranes

3.1.2 Nominal weights of crane and hoistload

The weights of the crane, self weight of the crane bridge and crab, and the weight of the hoistload lifted affect all the crane induced loads - vertical, horizontal longitudinal and horizontal transverse loads due to acceleration of the crane bridge, acceleration of the crab, skewing of the crane bridge in plan and the buffer forces due to crane movement.

- Weight of crane bridge
  - Range: 0.5t - 211t
- Weight of crab
  - Range: 0.08t - 112t
- Nominal weight of the hoistload (crane capacity or safe working load (SWL) of the crane)
  - Range: 2t - 630t
  - Distribution: 63% of cranes 20t - 130t
    42% of cranes 30t - 60t

3.1.3 Crane geometry

- Span of the crane bridge

  The span of the crane bridge has an effect on the vertical loads and horizontal transverse loads due to acceleration of the crane bridge and skewing of the crane in plan.

  - Range: 4 m - 54 m

- Wheel spacing - distance between the wheels on one end carriage

  The wheel spacing affects the horizontal transverse wheel loads due to acceleration of the crane bridge and skewing of the crane in plan. The wheel spacing is also required for the calculation of the load effects in the girder and crane loads to be applied to the column, in that it is needed for the positioning of the crane wheel loads on the support structure.

  - Dependent on bridge span:
    span $<$ 15 m: wheelbase = 1.75 m
    span $>$ 15 m (4 wheels): wheelbase = span/7
    span $>$ 15 m (8 or 16 wheels): wheelbase = span/5

- Minimum distance between hoist and rail

  The minimum distance between the hoist and the rail defines the closest position that the crab, and hence the hoistload, can come to the rail. This influences the magnitude of the vertical loads and the horizontal transverse loads due to acceleration of the crane bridge and skewing of the crane in plan.

  - Range: 0.4 m - 5 m
  - Distribution: most common 1.5 m - 2.5 m (dependent on span)

- Rail head width

  The rail head width is required for the calculation of the skewing angle for the horizontal loads due to skewing of the crane in plan. The rail head width is also needed for the calculation of the load effects in the girder. The vertical wheel load is assumed to act at an eccentricity of a quarter of the rail head width for the calculation of the torsion in the girder.

  - Range: rails range from 40×40 square bar - DIN A120 rail (dependent on size of crane), rail head width ranges from 40 mm - 120 mm

3.1.4 Travel and hoist speeds

- Long travel speed

  The long travel speed is the speed that the crane bridge travels down the length of the runway. This has an effect on the loads arising from the accidental load situation of the crane running into the end stops on the end of the runway.

  - Range: 25 m/min - 100 m/min
  - Distribution (dependent on length of gantry):
    standard cranes: most common 40 m/min
    process cranes: most common 60 m/min

- Steady hoisting speed

  The hoisting speed of the crane has an effect on the dynamic factor ϕ_2 which takes into account the dynamic effects of lifting a hoist load off the ground. The larger the hoisting speed, the greater the dynamic effects will be.

  - Range: 2 m/min - 20 m/min

3.1.5 Hoist type and characteristics

- Hoist class

  Cranes are classified into four 'hoist classes' to allow for the dynamic effects of hoisting a load from the ground. The hoist class represents the springing of the hoisting gear which affects the dynamic effects of lifting a load. The classification is dependent on the use of the crane. The hoist class has an effect on the dynamic factor ϕ_2 which takes into account the dynamic effects of lifting a load off the ground.

  - Distribution: standard cranes: HC1
    process cranes: HC2 - HC4

- Type of load lifting mechanism

  The type of load lifting mechanism refers to whether the crane lifts loads with a hook, grab or magnet or whether it is a ladle crane or coil lifter etc. This has an effect on the crane loads only in the event of the crane being equipped with a grab or magnet in the case when the normal operating behaviour of the crane involves the crane suddenly releasing a part of the hoistload. In this case, the type of load lifting mechanism has an effect on the dynamic factor ϕ_3 which takes into account the dynamic effects of a sudden release of part of the hoistload.

  – Distribution: hook - 89% of cranes
  ladle - 2% of cranes
  grab or magnet - 8% of cranes
  other (e.g. coil lifter) - 1% of cranes

- Hoistload free to swing

  Whether the hoistload is free to swing or not, determines whether the crane is prone to tilting due to the hoistload colliding with an obstacle.

  – Distribution:

  hoistload is free to swing - 97% of cranes
  hoistload suspended by mast and not free to swing - 1% of cranes
  cables have anti-sway reaving - 2% of cranes

3.1.6 Wheels and wheel drives

- Number of wheels

  The number of wheels that a crane has determines the size of the loads on each wheel as the total load is divided among the individual wheels. This has an effect on the magnitude of all the vertical and horizontal transverse loads.

  – Distribution: (dependent on size of crane)

  4 wheels - 75% of cranes
  8 wheels - 20% of cranes
  16 wheels - 5% of cranes

- Combination of wheel pairs

  prEN 1991-3 allows for four configurations of wheel pairs which are combinations of either independent or continuous wheels, and fixed or movable wheels.

  Continuous wheel pairs are wheels which are joined together between the end carriages by mechanical or electrical means, e.g. in the case of central wheel drives. Independent wheels are not linked in any way to the wheels on the opposite end carriage. The current practice of all the crane manufacturers in South Africa is to use independent wheels, continuous wheel pairs were common in the past but are not in use anymore.

  Movable wheels are wheels which have a lateral degree of freedom, i.e. are able to move horizontally along their axis, and fixed wheels are wheels which do not have this lateral degree of freedom. Cranes with movable wheels would have fixed wheels on one end carriage and movable wheels on the other end carriage. Movable wheels affect the distribution of horizontal transverse forces on the crane as only the fixed wheels can transmit horizontal transverse forces to the rail. It is the current practice of all the crane manufacturers in South Africa to use fixed wheels on both end carriages.

  – always independent, fixed wheels

- Type of wheel drive

  The type of wheel drive refers to whether the crane is driven by means of a central wheel drive on continuous wheels or single wheel drives on independent wheels. This affects the horizontal forces due to the acceleration of the crane and skewing of the crane in plan. As mentioned above, the current practice of crane manufacturers is to use independent wheels and hence single wheel drives.

  – always single wheel drives, no central wheel drives

- Number of wheel drives

  The number of wheel drives refers to the number of single wheel drives on a crane. This affects the horizontal forces due to acceleration of the crane bridge.

  - Distribution:
    all standard cranes: 2 out of 4 (2/4) wheels driven
    30% of process cranes: 50% driven (i.e. 2/4, 4/8, 8/16)
    70% of process cranes: 25% driven (i.e. 2/8, 4/16)

- Smoothness of change of drive forces

  The smoothness of change of the longitudinal drive forces affects the dynamic factor ϕ_5 which takes into account the dynamic effects due to the acceleration of the crane bridge. Values of ϕ_5 are given in prEN 1991-3 for drives which have smooth changes, e.g. drives with frequency inverters rather than gears, drives which have sudden changes, i.e. drives with gears, and drives which have considerable backlash.

  - Distribution:
    sudden changes - 70% of cranes (mostly standard cranes)
    smooth changes - 30% of cranes (mostly process cranes)

3.1.7 Guide means

- Type of guide means

  The guide means refers to the way in which the crane is guided horizontally on the rails. The crane is guided by either the flanges of the crane wheels or by guide rollers. Flanged wheels are the most common guide means. Guide rollers are typically used in buildings that have furnaces where one rail is close to the furnace, this rail could deform due to the heat of the furnace thereby making it unsuitable for flanged wheels.

  The type of guide means influences the horizontal transverse forces caused by skewing.

  - Distribution:
    guided by wheel flanges - 99% of cranes
    guided by guide rollers - 1% of cranes

- Clearance between rail and guide means

  The clearance between the rail and guide means refers to the clear space between the guide means (typically the wheel flange) and the side of the rail. This distance influences the skewing angle of the crane for the calculation of the horizontal forces caused by skewing.

– short span cranes - 15 mm
long span cranes - 25 mm

3.1.8 Buffers

- Buffer type

  The buffer type has an effect on the accidental load case of the buffer forces due to the crane running into the end stops. The type of buffer will define the spring constant and buffer characteristic which are needed for the calculation of these loads.

  – Distribution light cranes - rubber or cellular rubber
  heavy cranes - hydraulic

3.1.9 Governing parameters

The two governing parameters were the span of the crane bridge and the capacity of the crane (SWL); most of the other parameters are dependent on these two. The spans and capacities of the cranes in the database were investigated further to determine more information on their distributions.

It was found that the crane bridge spans were Normally distributed with a mean of 24.5 m. The capacities displayed a Lognormal type distribution. The mean of the capacities was 70t and the mode was 35t. Figures 3.1 and 3.2 show histograms of the crane bridge spans and crane capacities for the 563 cranes in the database. The capacities along the x-axis in Figure 3.2 are shown in a $\log_{10}$ scale.

Three representative cranes were selected from actual crane installations in South Africa. A summary of the main parameters of the representative cranes is given in Table 3.1. A scatter plot of all the cranes in the crane manufacturer's database as well as the representative cranes is shown in Figure 3.3 where the spans are plotted against the capacities of the cranes, the capacities on the x-axis are again shown in a $\log_{10}$ scale. The small squares represent all the cranes in the database and the circles show the representative cranes. The mean of the spans and the mode of the capacities are indicated on the plot.

The representative cranes, having capacities of 5t, 40t and 260t, cover the full range of capacities, with only 5% of the cranes in the manufacturer's database falling outside the 5t - 260t range. The crane bridge spans of the representative cranes of 19.2 m, 23.8 m and 28.5 m, cover the most likely range

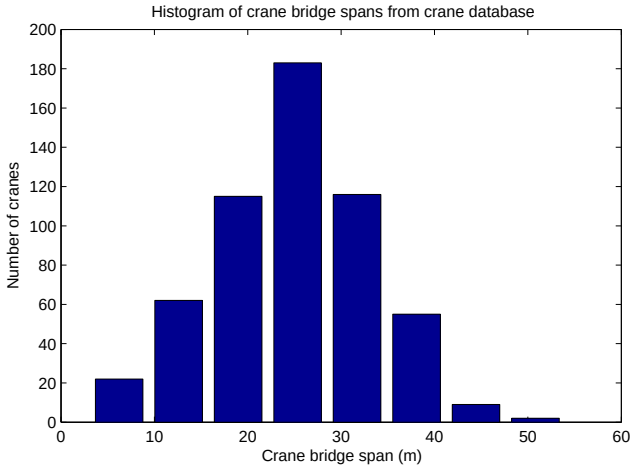

Figure 3.1: Histogram of crane bridge spans

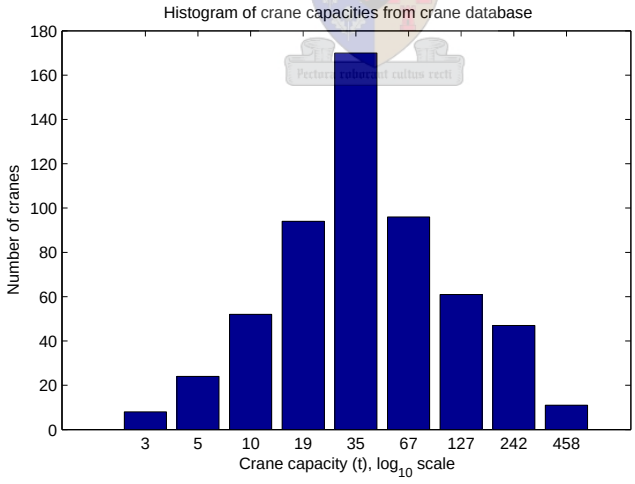

Figure 3.2: Histogram of crane capacities

of spans (refer to Figure 3.1) with 44% of cranes having spans in the range of 19.2 m - 28.5 m, and 57% of cranes having spans in the slightly larger range of 19 m - 30 m. This is shown graphically on the scatter plot in Figure 3.3 which shows that the representative cranes cover the full range of capacities but not the full range of spans. The implications for the results for cranes with longer or shorter spans will be investigated by means of parametric studies.

The 40t crane can be considered to be the 'most representative' crane for South Africa because its capacity and span are close to the mode of the capacities and mean of the spans of the cranes considered, which were produced by one of the leading South African crane manufacturers [18].

A more detailed description of the representative cranes and their support structures is given in section 3.3.

Table 3.1: Parameters of representative cranes

Crane capacity (SWL)	Crane bridge span	Weight of bridge	Weight of crab	Number of wheels	Outer wheel spacing	Hoist type
t	m	kN	kN		m	
5	19.2	55	6.4	4	3	hook
40	23.8	298	98	4	4.4	hook
260	28.5	1970	1298	16	12	ladle

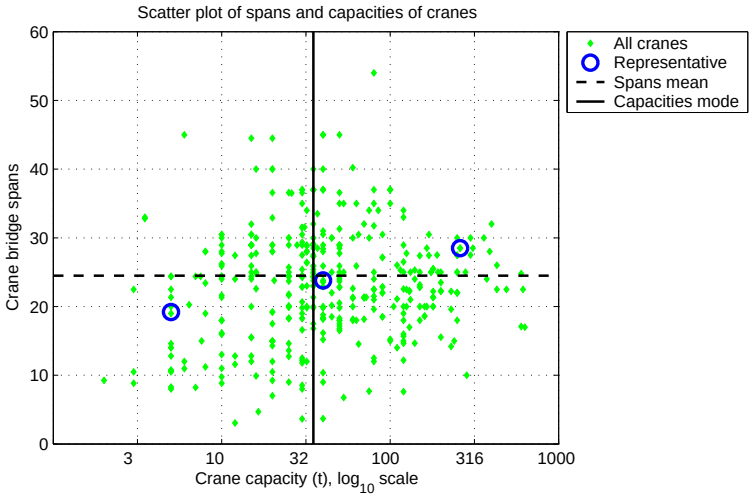

Figure 3.3: Scatter plot of cranes from database

3.2 Range of support structure configurations

For the example structures to be truly representative, both the crane and the support structures should be representative of those found in practice. The crane girders and columns are the elements of the support structure that are most directly loaded by the crane loads so these elements will be discussed. The different types of crane girders and columns described by Rowswell [30] and Ricker [20] that were mentioned in Chapter 2 are outlined below.

3.2.1 Crane Girders

1. Wide flange shape, rolled I section
2. Wide flange shape with channel cap
3. Welded wide flange shape with channel as top flange
4. Welded wide flange shape with unequal flanges
5. Welded wide flange shape for narrow clearances
6. Welded wide flange shape with surge plate
7. Welded wide flange shape with surge plate and backup truss

The different crane girder configurations are suitable for different types of cranes. Rolled I sections or I sections with channel caps are typically used for light cranes where the channel cap would be sufficient for resisting the horizontal loads, this is the crane girder configuration for the 5t crane. Welded wide flange girders with unequal flanges are generally used for medium cranes, this is the girder configuration of the 40t crane. Large cranes which impose large horizontal forces on the crane girders typically have a surge plate with or without a backup truss. This configuration is the most economical way of resisting the large horizontal forces. The 260t crane girder is a welded wide flange shape with a surge plate and backup truss.

The 40t crane girder and the 260t crane girder are simply supported girders and the 5t crane girder is a two span continuous girder. Simply supported girders are preferable to continuous girders due to the fatigue problems encountered with continuous girders, however, continuous girders are still used for crane girders.

3.2.2 Crane columns

1. Separate building and crane column
2. Bracketed column
3. Step column, solid web
4. Step column, laced web
5. Step column, vierendeel
6. Step column, battened

Light cranes typically have bracketed columns where the crane girder is supported by a bracket (corbel) connected to the building column, this is the configuration of the 5t crane column. Heavier cranes are supported on step columns. Step columns can have either solid webs, laced webs, vierendeel truss types webs or battened webs. Heavy cranes in low buildings are typically supported on crane columns which are separate from the building columns. The 40t crane column is a step column with a concrete column supporting the crane girders and a steel roof column extending from the concrete column. The 260t crane column is also a step column consisting of steel crane columns and building columns with a laced web. The 260t crane is in a tall building with the crane girders 24 m from floor level which would make it uneconomical to use separate building and crane columns.

The support structures for the three representative cranes fall into the recognised support structure configurations and cover a range of different configurations. The support structures can therefore also be considered to be representative of those found in practice.

3.3 Representative cranes and their support structures

Detailed descriptions of the representative cranes and their support structures are given below. The representative cranes will be referred to by their capacities.

The crane support structure consists of the crane girders and the building structure which houses the crane. The girders are an important part of the

support structure as they are the members which are most directly loaded by crane loads being subject to only their own weight and the crane wheel loads.

3.3.1 5t crane

The 5t crane is one of five cranes in a container making factory. The building consists of four bays, bays 1, 2 and 4 have one crane each and bay 2 has two cranes (see Figure 3.4). The 5t crane considered here is in bay 1 on one end of the building. The container assembly process starts in bay 4 on the far side of the building and each bay handles a stage of the assembly process which is completed in bay 1. The 5t crane lifts the almost completed containers for the final stages of the assembly process.

3.3.1.1 Description of crane

The 5t crane is an overhead, double box girder crane with four wheels and two wheel drives. The parameters of the crane are given in Table 3.2.

3.3.1.2 Description of support structure

The crane girders for the 5t crane are two span continuous girders, each span of 6.5 m. The girder section is a compound section consisting of a hot rolled I section with a channel on the top flange (305×165×41 UB + PFC 220×80). The channel is welded to the I section with a longitudinal continuous fillet weld along the edges of the top flange of the I girder. A cross section of the girder is shown in Figure 3.5.

The four bay building housing the 5t crane is shown in Figure 3.4. For the purposes of this investigation bay 1 was considered in isolation and the building was modelled as shown in Figure 3.6. The frame consists of steel columns (305×165×54 UB) with corbels to support the crane girders and a truss for the roof member. The corbels are 178×102×19 UB sections.

Table 3.2: Parameters of the 5t crane

Nominal weights of crane and hoistload	
Weight of crane bridge	55 kN
Weight of crab	6.5 kN
Hoistload	50 kN
Crane geometry	
Span of crane bridge	19200 mm
Minimum distance between hoist and rail	570 mm
Rail type	22 kg/m
Width of top of rail	50 mm
Height of rail	95.3 mm
Travel and hoist speeds	
Steady hoisting speed	10 m/min
Long travel speed	20 m/min
Cross travel speed	20 m/min
Hoist type and characteristics	
Hoist class	HC2
Type of load lifting mechanism	hook
Hoistload free to swing	Yes
Wheels and wheel drives	
Number of wheels	4
Wheel spacing	3000 mm
Type of wheel drive	Single
Number of single wheel drives	2
Behaviour of drives	Smooth changes
Combination of wheel pairs	Independent
	Fixed/Fixed
Guide means	
Guide rollers present	No
Clearance between rail and wheel flange	15 mm
Buffers	
Buffer type	rubber DPG 80
Buffer characteristic (degree of plasticity)	0.7
Spring constant	750×10^3 N/m

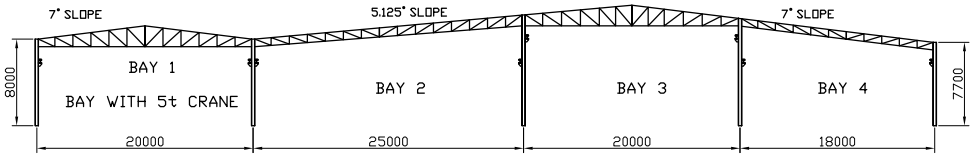

Figure 3.4: Building housing the 5t crane

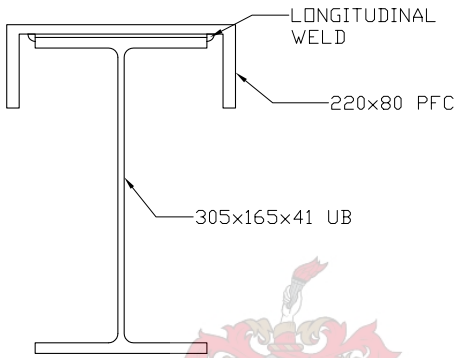

Figure 3.5: Cross section of 5t crane girder

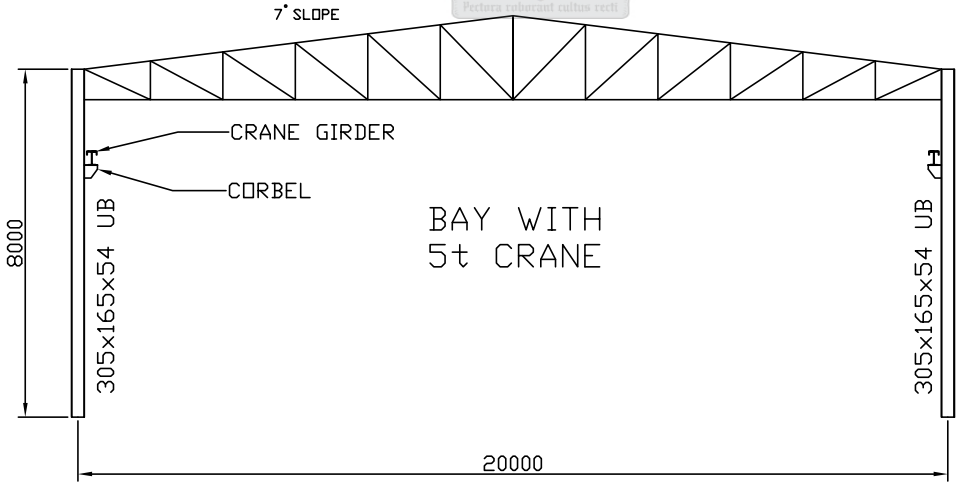

Figure 3.6: Bay considered for 5t crane

3.3.2 40t crane

The 40t crane is one of two cranes in a two bay mono-pitch portal frame building which houses a car manufacturing stamping plant. Figure 3.7 shows a diagram of the structure. The 40t crane is in bay 1 which is the press line, bay 2 is a maintenance area. The primary purpose of the 40t crane is to move the stamping press dies for the tool changes. This entails fetching the new tools from the storage area and lining them up ready for the stamping press as well as removing the old tools and taking them back to the storage area. The tool changes happen approximately every hour.

3.3.2.1 Description of crane

The 40t crane is an overhead, double box girder crane with four wheels and two wheel drives. The span of the crane is 23.8 m. The parameters of the crane are given in Table 3.3.

3.3.2.2 Description of support structure

The 40t crane girders are simply supported, 8 m span, mono-symmetric, welded plate girders. The girders have bearing stiffeners at the supports and intermediate stiffeners at a spacing of 2 m. The intermediate stiffeners are welded to the top flange and web but have a cope around the top flange to web weld of the girder. There is a clearance of four times the thickness of the web between the bottom of the stiffener and the bottom flange of the girder. Figure 3.8 shows the cross section of the girder and the intermediate stiffeners. The ends of the girders are supported laterally by means of tie back connections to the columns.

The crane runways are braced in the longitudinal direction by means of a pair of circular hollow sections per runway as shown in Figure 3.9.

The building consists of reinforced concrete crane columns (1500×450) with steel building columns (356×171×51 UB) and roof members (406×140×39 UB) with knee braces. Step type columns have been utilised with the crane girders resting on steel girder 'chairs' on top of the concrete columns, see Figure 3.7.

Table 3.3: Parameters of the 40t crane

Nominal weights of crane and hoistload	
Weight of crane bridge	298 kN
Weight of crab	98 kN
Hoistload	400 kN
Crane geometry	
Span of crane bridge	23800 mm
Minimum distance between hoist and rail	1650 mm
Rail type	DIN A100
Width of top of rail	100 mm
Height of rail	95 mm
Travel and hoist speeds	
Steady hoisting speed	10 m/min
Long travel speed	50 m/min
Cross travel speed	40 m/min
Hoist type and characteristics	
Hoist class	HC3
Type of load lifting mechanism	hook
Hoistload free to swing	Yes
Wheels and wheel drives	
Number of wheels	4
Wheel spacing	4400 mm
Type of wheel drive	Single
Number of single wheel drives	2
Behaviour of drives	Smooth changes
Combination of wheel pairs	Independent
	Fixed/Fixed
Guide means	
Guide rollers present	No
Clearance between rail and wheel flange	25 mm
Buffers	
Buffer type	hydraulic
	PUDZ II ϕ 63
Buffer characteristic (degree of plasticity)	0.9
Spring constant	2×10^6 N/m

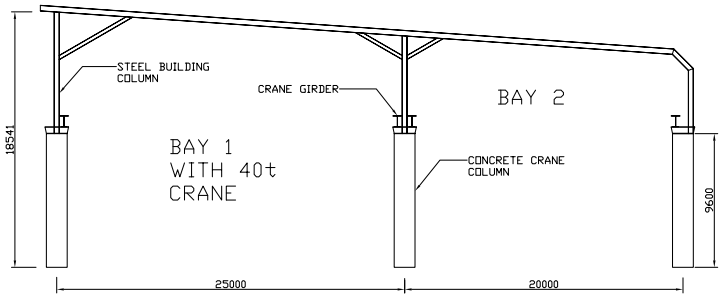

Figure 3.7: Building housing the 40t crane

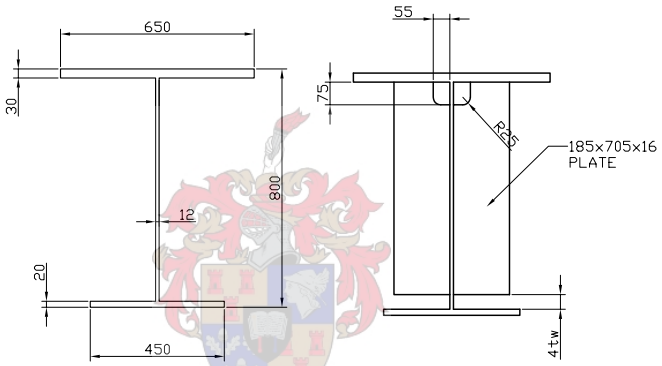

(a) Cross section of girder (b) Stiffener dimensions

Figure 3.8: 40t crane girder

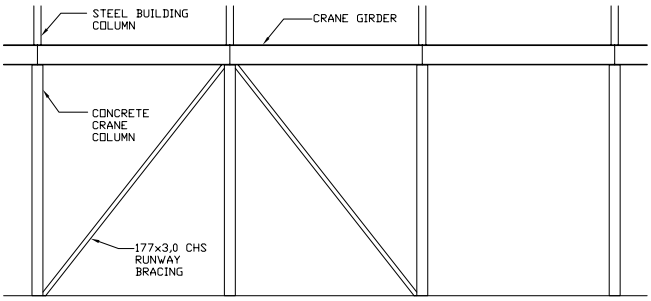

Figure 3.9: Crane runway longitudinal bracing for the 40t crane

3.3.3 260t crane

The 260t crane is a ladle crane for a steel making and rolling mill. The building housing the 260t crane consists of five bays where all except bay 2 contain cranes, the 260t crane is in bay 3 (see Figure 3.10). The primary purpose of the 260t crane is to carry molten steel from the furnace to the caster.

3.3.3.1 Description of crane

The 260t crane is an overhead, double box girder crane with sixteen wheels and four wheel drives. The span of the crane bridge is 28.5 m. The parameters of the crane are given in Table 3.4.

3.3.3.2 Description of support structure

The crane girder for the 260t crane is a 42 m span doubly symmetric plate girder with a 2940×10 mm surge plate and lattice auxiliary girder. A cross section of the crane girder is given in Figure 3.11 and a diagram of the lattice auxiliary girder is shown in Figure 3.12.

The building consists of step crane columns and building columns with a lattice girder roof truss. The step columns are steel laced columns with a cross girder supporting the building column, see Figure 3.10. The entire building was modelled for this investigation.

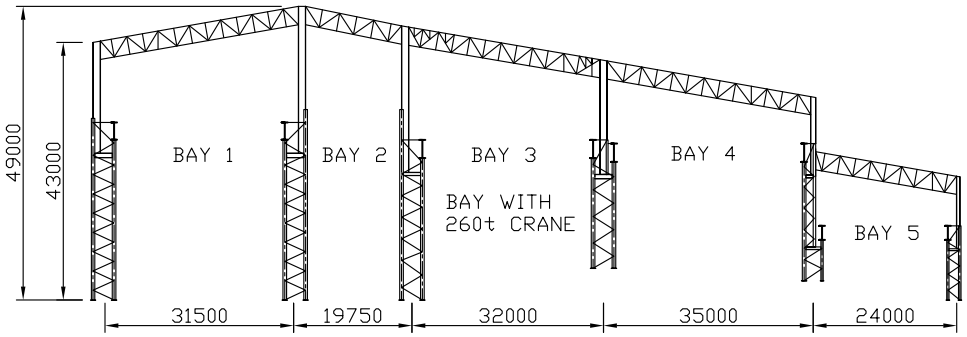

Figure 3.10: Building housing the 260t crane

Table 3.4: Parameters of the 260t crane

Nominal weights of crane and hoistload	
Weight of crane bridge	1970 kN
Weight of crab	1298 kN
Hoistload	2600 kN
Crane geometry	
Span of crane bridge	28500 mm
Minimum distance between hoist and rail	3500 mm
Rail type	DIN A120
Width of top of rail	120 mm
Height of rail	105 mm
Travel and hoist speeds	
Steady hoisting speed	6 m/min
Long travel speed	81.1 m/min
Cross travel speed	27.6 m/min
Hoist type and characteristics	
Hoist class	HC4
Type of load lifting mechanism	ladle
Hoistload free to swing	Yes
Wheels and wheel drives	
Number of wheels	16
Wheel spacing	
Outside wheel span:	12000 mm
Individual wheel spacing: 1000/1800/1000/4400/1000/1800/1000	mm
Type of wheel drive	Single
Number of single wheel drives	4
Behaviour of drives	Smooth changes
Combination of wheel pairs	Independent
	Fixed/Fixed
Guide means	
Guide rollers present	No
Clearance between rail and wheel flange	25 mm
Buffers	
Buffer type	hydraulic
	OLEO 54 MFZ 140 412
Buffer characteristic (degree of plasticity)	0.9
Spring constant	1.25×10^6 N/m

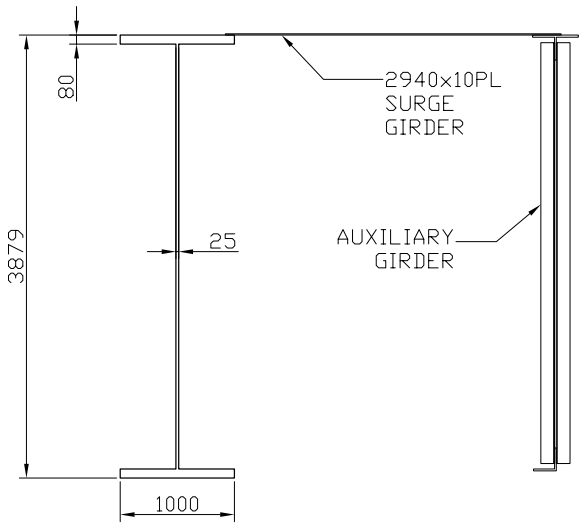

Figure 3.11: Cross section of the 260t crane girder

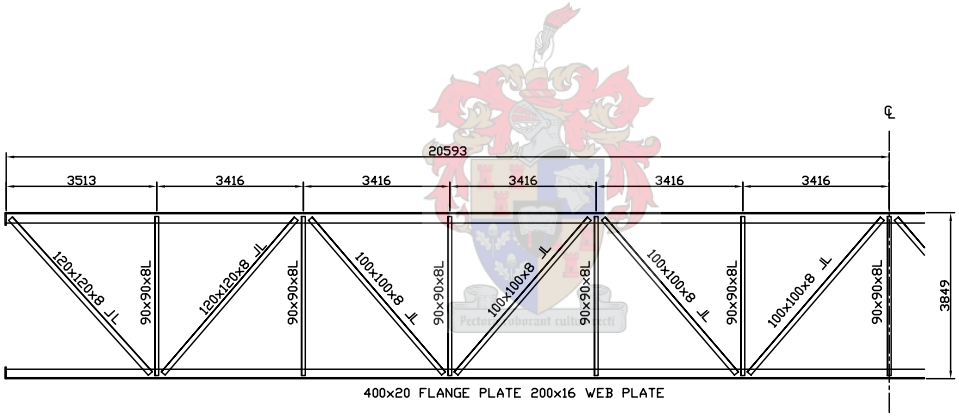

Figure 3.12: 260t crane auxiliary girder

3.4 Summary

The scope of the new South African crane loading code (SANS 10160 [3]) was defined as the same as the scope of the current code, SABS 0160:1989 [1], i.e overhead travelling bridge cranes with wheels elevated at the same level. As mentioned before, the code calibration procedure is carried out on specific example cranes which should be representative of the cranes found in practice i.e. their parameters should cover the range of parameters found in practice.

The ranges and distributions of the crane parameters affecting the crane wheel loads were investigated. It was found that the two governing parameters were the crane bridge span and the capacity of the crane.

Three actual crane installations in South Africa were chosen as the representative cranes and support structures to be used as example structures for the code calibration. The representative cranes were shown to cover the full range of capacities found in practice and the most likely range of spans. Descriptions of the cranes and their support structures were given. It was shown that the support structures are also representative of the range of configurations found in practice.

Chapter 4

Calibration to current practice

The calibration to current practice involves the comparison between the code provisions in SABS 0160:1989 and prEN 1991-3. The comparison was carried out with respect to the load situations modelled, the cost of the support structure and the design effort required. The comparison was carried out on the girders, columns and longitudinal bracing members of the three representative cranes discussed in Chapter 3.

4.1 Crane code provisions

The behaviour of cranes and therefore the loads imposed on the support structure is modelled differently in SABS 0160:1989 and prEN 1991-3. There are differences in the classification of cranes and the influence it has on the loads, the load situations modelled and the recommended crane load combinations.

4.1.1 Crane classification

In both SABS 0160:1989 and prEN 1991-3, cranes are classified into four classes. The methods of classification are similar in that they are both based on descriptions of the cranes. The influence of the crane classification on the wheel loads differs vastly between the two codes.

4.1.1.1 Definition of crane classes

In SABS 0160:1989, cranes are classified into four classes according to a description of the crane usage. prEN 1991-3 divides cranes into four hoist classes

also according to the crane use. Table 4.1 gives descriptions of crane usage as given in the two codes along with the classification of each crane.

Table 4.1: Crane classification

Description of crane usage	Class in SABS 0160:1989	Hoist class in prEN 1991-3
Hand cranes	C1	HC1
Assembly cranes		HC1, HC2
Warehouse cranes - intermittent operation	C2	HC2
Power station cranes	C2	HC2
Foundry cranes	C2	HC2
Casting cranes		HC2
General factory and workshop cranes	C2	HC2, HC3
Machine shop cranes	C2	HC2, HC3
Warehouse cranes - continuous operation	C3	HC3
Rolling mill cranes	C3	
Ladle cranes in steelworks	C3	HC3
Scrapyard cranes	C3	HC3, HC4
Grab and magnet cranes - intermittent operation	C3	HC3, HC4
Grab and magnet cranes - continuous operation	C4	HC3, HC4
Soaking pit cranes	C4	HC4
Ingot stripping cranes	C4	HC4
Furnace charging cranes	C4	HC4
Forging cranes	C4	HC4
Claw cranes	C4	HC4

There is no explanation given in SABS 0160:1989 as to the reasoning behind the crane classification. The rationale behind the division of cranes into hoist classes is given in the German code DIN 15018 Part 1 1984 [4] and was given in Chapter 2 as representing the springing of the hoisting gear and thus the dynamic effects of lifting a load.

With reference to Table 4.1, the same type of cranes tend to fall in the same class for both codes, even though the basis for crane classification in the two codes cannot be shown to be the same and the influence of the crane classification on the crane loads is vastly different.

4.1.1.2 Influence of crane classification in SABS 0160:1989

The class of crane influences the impact factor for the vertical loads and also the magnitude of the horizontal loads. For example, the vertical wheel loads including dynamic effects are calculated by multiplying the nominal static wheel loads by an impact factor which is dependent on the class of the crane. The horizontal wheel loads caused by misalignment of the crane wheels or rails are calculated by multiplying the total crane weight by a factor dependent on the class of the crane. These factors are given in Table 4.2.

Table 4.2: Class dependent factors in SABS 0160:1989

Class of crane	Vertical dynamic factor	Horizontal factor
Class 1	1.10	0.05
Class 2	1.20	0.12
Class 3	1.25	0.15
Class 4	1.30	0.20

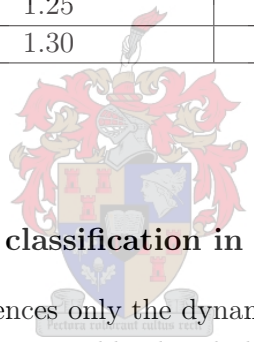

4.1.1.3 Influence of crane classification in prEN 1991-3

The hoist class of the crane influences only the dynamic factor applied to the hoistload for the calculation of the vertical load with dynamic effects caused by the hoisting of a load off the ground. The horizontal forces are not influenced by the hoist class of the crane. The equation for the calculation of the dynamic factor is given below.

$$\phi_2 = \phi_{2,min} + \beta_2 \times v_h \tag{4.1.1}$$

Where:

ϕ_2 – the dynamic factor applied to the hoistload to model the dynamic effects of lifting a load off the ground.

v_h – the steady hoisting speed of the crane

$\phi_{2,min}$ & β_2 – class dependent factors given in Table 4.3.

Table 4.3: Hoist class dependent dynamic factors in prEN 1991-3

Hoist class of crane	$\phi_{2,min}$	β_2
HC1	1.05	0.17
HC2	1.10	0.34
HC3	1.15	0.51
HC4	1.20	0.68

4.1.2 Load cases

The modelling of the crane behaviour as the crane travels on the runways, picks up and sets down loads, results in different load cases for the crane wheel loads. The loading situations considered by the two codes differ and are discussed below.

4.1.2.1 SABS 0160:1989

The following load situations are provided for in SABS 0160:1989:

- Vertical wheel loads
  - Static wheel loads
  - Dynamic wheel loads, impact and other dynamic effects are provided for by multiplying the static wheel load by a factor depending on the crane class as given above.
- Horizontal transverse loads due to
  - Acceleration and braking of the crab
  - Misalignment of rails or wheels
  - Skewing of the crane in plan
- Horizontal longitudinal force due to acceleration or braking of the crane.
- End stop forces due to collision of the crane bridge with the end stops at the end of the runway.

4.1.2.2 prEN 1991-3

prEN 1991-3 makes provision for the following load situations:

- Vertical wheel loads due to
  - Lifting a hoistload off the ground
  - Part of the hoistload suddenly being released
  - The crane travelling along the runway at a constant speed
  - Test loads
- Horizontal longitudinal and transverse forces due to
  - Acceleration or braking of the crane
  - Skewing of the crane in plan
- Horizontal transverse forces due to
  - Acceleration or braking of the crab
  - Buffer forces due to the crab running into the end stops at the end of the crane bridge
- Horizontal longitudinal forces due to buffer forces from the crane running into the end stops at the end of the runway

4.1.2.3 Comparison of load cases

prEN 1991-3 considers in more detail the actual crane behaviour especially with regards to the vertical loads.

One horizontal load situation which is provided for by SABS 0160:1989 but not by prEN 1991-3 is misalignment of the crane wheels or gantry rails. The misalignment load case in SABS 0160:1989 takes into account the wheels of the crane being misaligned in a 'toe-in' or 'toe-out' manner or a similar misalignment of the rails. The horizontal loads are due to the horizontal transverse friction force that is developed due to the rolling direction of the wheel not coinciding with the longitudinal axis of the rail.

The amount of misalignment which causes these horizontal loads still falls within the construction tolerances as specified by SAISC [29] and the misalignment loads can thus be classified as 'load occurring during normal operation of the crane'. This load case does not take into account the situation where the rails or wheels are out of misalignment to such an extent that the flanges of the wheels on each end carriage come into contact with the rails and tend

to either pull the rails together or push them apart. Such a misalignment does not fall within the construction tolerances and would thus not be classed as 'normal operation of the crane'.

Perfect alignment of the rails is impossible to achieve so some allowance in the crane loads for misalignment of the rails within construction tolerances should be made.

4.1.3 Load combinations

The guidelines for load combinations for each of the codes are discussed. For comparison purposes, the design wheel loads resulting from each code are presented here for the 40t representative crane described in Chapter 3 which is classified as a class 3 crane in SABS 0160:1989 and a hoist class 3 crane in prEN 1991-3.

4.1.3.1 SABS 0160:1989

The only guidance given on load combinations is that the three horizontal transverse loads need not be considered to act simultaneously. The resulting load combinations and forces for the 40t crane are given in Figures 4.1 - 4.5. The full load calculations are given in Appendix A.

The loads given in Figures 4.1 - 4.5 are design loads that have been factored using SABS 0160:1989 load factors i.e. 1.6 for ultimate limit state and 1.0 for accidental loads (end stop forces).

All loads shown are in kN. The horizontal transverse loads may act either in the directions shown or in the opposite direction.

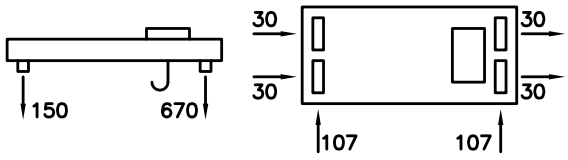

Figure 4.1: SABS 0160:1989 load combination 1: Vertical + Acceleration of crab + Acceleration of crane

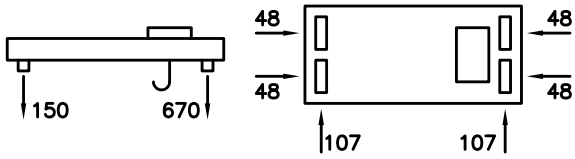

Figure 4.2: SABS 0160:1989 load combination 2: Vertical + Misalignment + Acceleration of crane

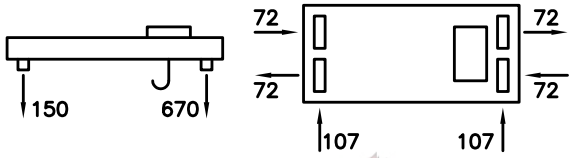

Figure 4.3: SABS 0160:1989 load combination 3: Vertical + Skewing + Acceleration of crane

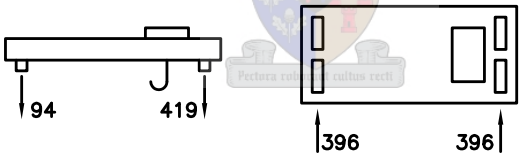

Figure 4.4: SABS 0160:1989 load combination 4a: Vertical + End stop force

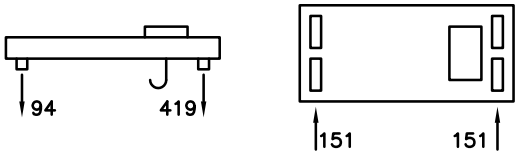

Figure 4.5: SABS 0160:1989 load combination 4b: Vertical + End stop force

4.1.3.2 prEN 1991-3

prEN 1991-3 gives a table which describes the combinations of crane loads which are to be considered as one crane action for combination with other loads. The table was given in Chapter 2, Table 2.16 on page 46.

The load combinations resulting from prEN 1991-3 for the 40t crane are given below. The ultimate limit state load combinations are shown in Figures 4.6 - 4.11, the serviceability limit state combination is shown in Figure 4.12 and the accidental limit state load combination is shown in Figure 4.13. The full load calculations are given in Appendix A.

Load combination 2 is not relevant for the 40t crane because its normal working does not entail sudden release of the hoistload.

The loads shown in Figures 4.6 - 4.13 are design loads which have been factored using the SABS 0160:1989 load factors i.e. 1.6 for ultimate limit state, 1.0 for serviceability limit state and 1.0 for accidental loads.

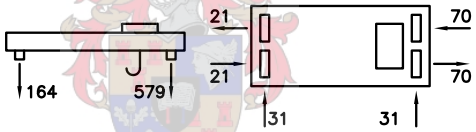

Figure 4.6: prEN 1991-3 load combination 1: ϕ_1(Self weight) + ϕ_2(Hoistload) + ϕ_5(Acceleration of crane)

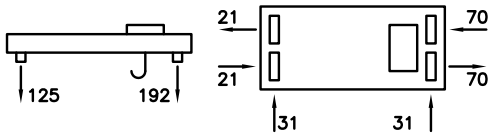

Figure 4.7: prEN 1991-3 load combination 3: Self weight + ϕ_5(Acceleration of crane)

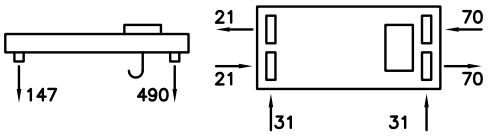

Figure 4.8: prEN 1991-3 load combination 4: ϕ_4(Self weight) + ϕ_4(Hoistload) + ϕ_5(Acceleration of crane)

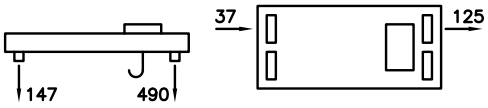

Figure 4.9: prEN 1991-3 load combination 5: ϕ_4(Self weight) + ϕ_4(Hoistload) + Skewing)

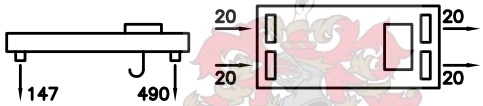

Figure 4.10: prEN 1991-3 load combination 6: ϕ_4(Self weight) + ϕ_4(Hoistload) + Acceleration of crab

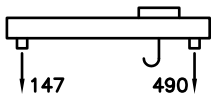

Figure 4.11: prEN 1991-3 load combination 7: Self weight + η(Hoistload)

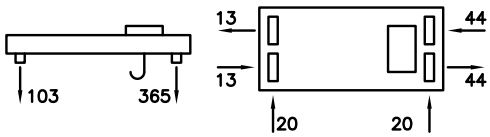

Figure 4.12: prEN 1991-3 load combination 8: ϕ_1(Self weight) + ϕ_6(Test load) + ϕ_5(Acceleration of crane)

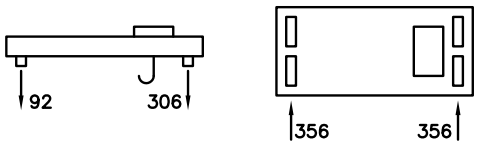

Figure 4.13: prEN 1991-3 load combination 9: Self weight + Hoistload + ϕ_7(Crane buffer forces)

4.1.4 Fatigue loading

4.1.4.1 SABS 0160:1989

The South African loading code, SABS 0160:1989, does not specify the crane loads which are to be used for fatigue verification of the crane support structure, nor how the crane loads are to be applied to the structure for the fatigue assessment. The South African steel design code, SANS 10162-1:2005 [11], recommends the use of Miner's rule of accumulative damage for the assessment of fatigue for loads not applied at a constant amplitude.

4.1.4.2 prEN 1991-3

prEN 1991-3 gives simplified rules for the assessment of the fatigue of crane support structures. Cranes are divided into fatigue classes depending on the range of loads lifted and the total number of cycles performed during the lifetime. Depending on the fatigue class of the crane, the 'fatigue damage equivalent load' is calculated which is the equivalent constant amplitude load for two million cycles and is used for the calculation of the fatigue stresses. The fatigue provisions were discussed in more detail in Chapter 2.

4.1.4.3 Comparison of fatigue loading

Fatigue is an issue where the loads and resistance are traditionally not separated. The fatigue damage, which is used as a measure of the fatigue life of a structure, is a function of both the loads and the resistance of the member in the form of S-N curves.

SABS 0160:1989 follows the traditional method of not specifying fatigue loads in the loading code whereas prEN 1991-3 separates the fatigue loads from the resistances by providing a method of calculating the 'fatigue damage

equivalent load'.

Another approach which could be adopted by a crane loading code is that taken by the International code ISO 8686-1:1989 [5] where recommendations are made on the crane load combinations that are to be considered for fatigue. It is then up to the support structure designer to model the crane behaviour to determine at what level the loads are applied. The modelling of the crane behaviour would entail considering the frequency at which each value of hoist-load is lifted as well as the position of the crab on the crane and the crane on the runway.

Both the method given by prEN 1991-3 and the alternative method of modelling the crane behaviour will be considered for the further investigations of fatigue.

The modelling of the crane behaviour entails a full analysis of the crane movements and loading to determine the range of stress amplitudes and the number of times they will be applied over the crane lifetime.

4.2 Cost of support structure

The critical load combinations for the ultimate limit state resulting from each code were identified as load combinations 2 and 3 from SABS 0160:1989 and load combinations 1 and 5 from prEN 1991-3. The design (factored) loads for the 40t crane for these load combinations are shown in Figures 4.14 - 4.17. The wheel loads have been factored using the South African load factors of 1.6 for ultimate limit state.

The critical load combinations for the accidental limit state of the crane running into the end stop were load combination 4a and 4b from SABS 0160:1989 and load combination 9 from prEN 1991-3. These load combinations are shown in Figures 4.18 - 4.20. For the purpose of comparison between the different methods of calculating the end stop forces in SABS 0160:1989, the forces resulting from both the simplified method and the more detailed method, taking into account the resilience of the buffer, are shown.

The comparison between the loads from SABS 0160:1989 and prEN 1991-3 could not be carried out directly by considering the crane load combinations because the configurations of the loads from the two codes are different. The comparison was therefore carried out on the load effects in the support structures.

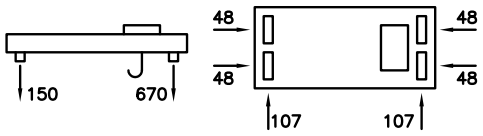

Figure 4.14: SABS 0160:1989 critical load combination 2: Vertical + Misalignment + Acceleration of crane

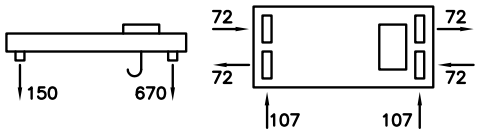

Figure 4.15: SABS 0160:1989 critical load combination 3: Vertical + Skewing + Acceleration of crane

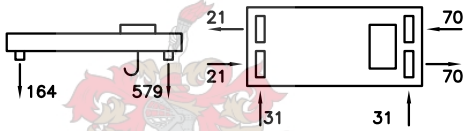

Figure 4.16: prEN 1991-3 critical load combination 1: ϕ_1(Self weight) + ϕ_2(Hoistload) + ϕ_5(Acceleration of crane)

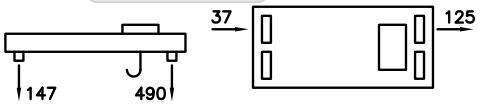

Figure 4.17: prEN 1991-3 critical load combination 5: ϕ_4(Self weight) + ϕ_4(Hoistload) + Skewing)

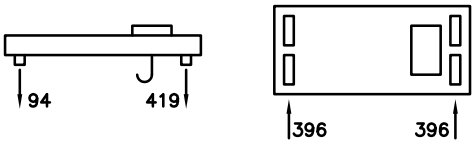

Figure 4.18: SABS 0160:1989 critical load combination 4a: Vertical + End stop force

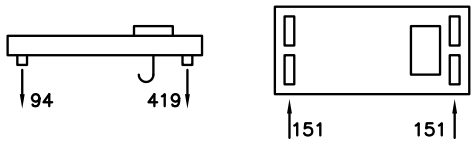

Figure 4.19: SABS 0160:1989 critical load combination 4b: Vertical + End stop force

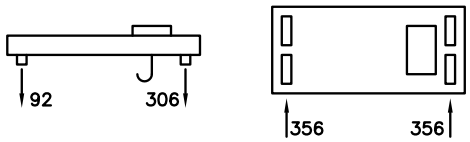

Figure 4.20: prEN 1991-3 critical load combination 9: Self weight + Hoistload + ϕ_7(Crane buffer forces)

4.2.1 Structural elements

The elements of the support structures that were considered for the comparison were the elements most directly loaded by crane loads i.e. crane girders, crane columns and longitudinal runway bracing.

The load effects considered for the crane girder were moments about the z and y axes, shear in the y and z directions, torsion about the x axis and axial force in the x direction. The axes of the girder are defined in Figure 4.21.

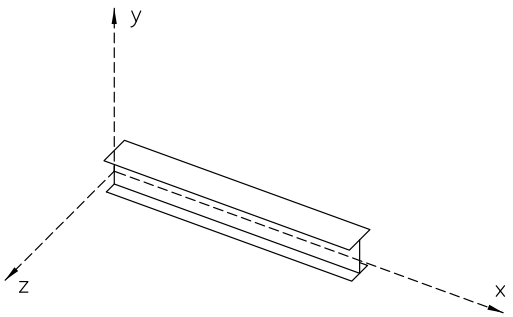

Figure 4.21: Crane girder axes

The load effects considered for the crane columns were axial force and

bending moment. The load effect considered for the longitudinal bracing was axial force.

4.2.2 Crane class

The class of the crane in SABS 0160:1989 affects the magnitude of the vertical impact forces as well as the horizontal forces due to acceleration of the crab, misalignment of the rails or wheels and skewing of the crane in plan. The hoist class of the crane in prEN 1991-3 affects only the dynamic factor ϕ_2 modelling the dynamic effects caused by hoisting a load off the ground, which is part of load combination 1.

A parametric study was carried out for the class or hoist class of the crane in order to assess the sensitivity of the load effects to the class of crane in SABS 0160:1989 or hoist class in prEN 1991-3.

The loads and load effects were calculated for each crane assuming the crane to be, in turn, a class 2, 3 or 4 crane for SABS 0160:1989 and a hoist class 2, 3 or 4 crane for prEN 1991-3. Class 1 and hoist class 1 crane were omitted because these classes consist mostly of hand operated cranes which are not of interest for this study.

The load effects from the SABS 0160:1989 class 2 cranes were compared with prEN 1991-3 hoist class 2 cranes etc. This is reasonable because it was shown earlier, with reference to Table 4.1 that the same type of cranes tend to fall into the same class for each code, e.g. a warehouse crane with intermittent operation will be classified as class 2 in SABS 0160:1989 and hoist class 2 in prEN 1991-3.

The 5t crane is classified as a class or hoist class 2 crane, the 40t crane is a class or hoist class 3 crane and the 260t crane is a class or hoist class 4 crane.

4.2.3 Comparison of load effects

The load effects in the crane girders and columns were calculated for the critical load combinations. The maximum load effects were identified and the ratio of load effect from SABS 0160:1989 to the load effect from prEN 1991-3 were calculated. The load effect ratios for the three representative cranes for class or hoist class 2 - 4 are given in Table 4.4. The columns containing the ratios for the actual class of each crane are shown in bold.

Table 4.4: Load effect ratios: SABS 0160:1989/prEN 1991-3

Load effect	5t crane			40t crane			260t crane		
	Crane class or hoist class								
	2	3	4	2	**3**	4	2	3	**4**
Crane girder									
Moment about z axis	**1.06**	1.06	1.06	1.16	**1.16**	1.16	1.11	1.12	**1.13**
Shear in y direction	**1.06**	1.06	1.06	1.16	**1.16**	1.16	1.11	1.12	**1.13**
Moment about y axis	**0.51**	0.64	0.85	0.46	**0.58**	0.77	1.04	1.30	**1.73**
Shear in z direction	**0.64**	0.80	1.07	0.46	**0.58**	0.77	1.03	1.29	**1.72**
Torsion	**0.81**	0.91	1.07	0.76	**0.85**	0.99	1.16	1.40	**1.80**
Axial force	**2.38**	2.38	2.38	3.43	**3.43**	3.43	6.37	6.37	**6.37**
Crane column									
Moment	**0.46**	0.55	0.70	0.64	**0.73**	0.87	1.15	1.39	**1.79**
Axial force	**1.06**	1.06	1.06	1.16	**1.16**	1.16	1.22	1.34	**1.53**
Bracing									
Axial force SABS (a)	**2.08**	2.08	2.08	1.11	**1.11**	1.11	2.68	2.68	**2.68**
Axial force SABS (b)	**0.74**	0.74	0.74	0.42	**0.42**	0.42	0.65	0.65	**0.65**

The load effects that are due solely to vertical loads are for all the girders - the moment about the z axis and shear in the y direction and for the columns of the 5t and 40t cranes - the axial force. These load effects are all greater than one with the largest being 1.16. This shows that the vertical loads due to SABS 0160:1989 can be up to 16% larger than those due to prEN 1991-3.

The load effects due to the vertical loads only remain the same, or within a very small range, over the three classes being considered. The maximum vertical wheel loads from both SABS 0160:1989 and prEN 1991-3 are dependent on the class of the crane, and for both codes, the vertical wheel loads increase by the same amount as the class of the crane increases.

The load effect ratios influenced by only the horizontal transverse loads are for all the girders - the moment about the y axis and shear in the z direction. The load effect ratios which are due to a combination of vertical and horizontal wheel loads are for all the girders - the torsion, the column for the 260t crane - the axial force and moment and the columns for the 5t and 40t cranes - the moment.

The load effect ratios due to horizontal loads only and a combination of horizontal and vertical loads vary across the different crane classes. The horizontal transverse loads in prEN 1991-3 are not affected by the hoist class of

the crane so this range in load ratios is due to the change in magnitude of the loads in SABS 0160:1989.

The load effects resulting from both horizontal load only and a combination of horizontal and vertical loads have ratios that range from 0.46 for the 40t crane, class 2, moment in the girder about the y axis to 1.80 for the 260t crane, class 4, torsion in the girder. This means that for a crane configuration like the 40t crane, considering a class 2 crane, the horizontal load effects due to prEN 1991-3 are 2.17 times those due to SABS 0160:1989. For a crane configuration like the 260t crane, the horizontal load effects from prEN 1991-3 are only 56% of those given by SABS 0160:1989.

The ratios of the load effects influenced by the horizontal transverse loads for the 5t crane and the 40t crane are similar but the 260t crane has much higher ratios indicating that for this crane SABS 0160:1989 gives much larger horizontal transverse loads than prEN 1991-3. The difference in the ratios between the 5t crane, 40t crane and the 260t crane can be explained by examining the load models for the horizontal loads.

The two critical load cases for horizontal loads from SABS 0160:1989 are misalignment of the rails or wheels and skewing of the crane in plan. The magnitude of the loads is dependent only on the crane self weight and hoistload, the number of wheels and the class of the crane.

The two critical load cases for horizontal loads from prEN 1991-3 are acceleration of the crane bridge with the crab eccentric to the centre of mass and skewing of the crane in plan. Both of these load models are dependent on the parameters mentioned above as well as the geometry of the crane, i.e. the span of the crane bridge, the wheel spacing, the minimum distance between hoist and rail and the clearance between the wheel flange and rail. Both load cases are most sensitive to the crane bridge span and wheel spacing.

The 5t crane and the 40t crane have similar span to wheel spacing ratios of 6.4 and 5.4 respectively, whereas the 260t crane has a span to wheel spacing ratio of 2.4. This could account for the large difference between the load effect ratios between the 5t and 40t cranes and the 260t crane.

Theoretically, it seems reasonable that the horizontal loads due to acceleration of the crane and skewing are dependent on the span and wheel spacing because the horizontal loads are caused by moments acting on the crane which are resolved into horizontal couples. SABS 0160:1989, however, does not take this into account. The crane load models in prEN 1991-3 are therefore more

sophisticated than the crane load models in SABS 0160:1989 in that they consider the effect of the different crane parameters in more detail and are more likely to be a true representation of the behaviour of the crane.

Such large differences in the horizontal wheel loads between the two codes, as is demonstrated by the ratios of load effects influenced by horizontal loads, highlights the need for experimental data to verify the load models.

The load effect ratio for axial force in the girders is large compared to the other load effect ratios. This is because SABS 0160:1989 includes the weight of the hoistload when determining longitudinal forces caused by acceleration of the crane and prEN 1991-3 does not. In the design of the girder, the effect of the axial force is very small compared to the moments and torsion so the large ratio is not of great significance.

The axial force that is carried by the bracing is due to the horizontal longitudinal forces caused by collision of the crane with the end stops. SABS 0160:1989 does not include the hoistload in the calculation of these forces whereas prEN 1991-3 does include the hoistload. These ratios remain constant across the classes of crane because in neither SABS 0160:1989 nor prEN 1991-3 are the end stop forces dependent on the crane class.

The ratios of the axial forces in the bracing calculated using the SABS 0160:1989 method (a) of assuming a maximum deceleration of g, are all greater than one, and in the cases of the 5t crane and the 260t crane are greater than two. As expected, this shows that the simplified method in SABS 0160:1989 gives much larger values than a method which takes the buffer characteristics into account.

The ratios of axial forces in the bracing calculated using the SABS 0160:1989 method (b) where the resilience of the buffers is taken into account are all less than one. The methods used for the calculation of the end stop forces according to SABS 0160:1989 method (b) and the prEN 1991-3 method differ in that the prEN 1991-3 method specifies a force based on the spring constant of the buffer, whereas SABS 0160:1989 does not give a specific calculation method but merely states that the resilience of the buffers should be taken into account. The method used to calculate the end stop forces for SABS 0160:1989 method (b) was the method used by the crane manufacturers for the selection of the buffers by considering the absorption of the crane's kinetic energy.

For the SABS 0160:1989 method (b), the ratios of axial force in the bracing being less than one can be partially explained by the fact that prEN 1991-3

specifies that the mass of the crane and the hoistload should be considered whereas SABS 0160:1989 considers only the mass of the crane and not the hoistload.

The ratios of end stop forces are small for the 40t crane compared to the other two cranes. The 40t crane has a relatively stiff buffer ($S_B = 2 \times 10^6$) compared to the 5t crane ($S_B = 0.75 \times 10^6$) and 260t crane ($S_B = 1.25 \times 10^6$) causing the prEN 1991-3 calculation method to give larger forces.

End stop forces calculated according to prEN 1991-3 lie between the forces from the two methods recommended by SABS 0160:1989. Therefore, depending on which method was selected by the designer previously, using the prEN 1991-3 load model would sometimes result in heavier end stops and bracing and something in lighter end stops and bracing.

4.2.4 Design effects

As an example, to assess the effect of the combination of the various load effects, the design of the 40t crane girder was carried out using the loads from each code. The size of the girder was determined by keeping the proportions of the cross sectional dimensions the same (as given in Chapter 3) and scaling the cross section until the design resistance was equal to the design loading. The cross sectional area of the girder was calculated, Table 4.5 gives the ratios of the cross sectional areas calculated using loads from SABS 0160:1989 to those calculated using loads from prEN 1991-3.

Table 4.5: Ratio of areas: SABS 0160:1989/prEN 1991-3

Class or hoist class	ratio
2	1.19
3	1.20
4	1.22

The loads calculated from SABS 0160:1989 result in girders approximately 20% larger than those designed using the loads from prEN 1991-3.

The load effect ratios, given in Table 4.4, for the three representative cranes, indicate that crane girders designed using prEN 1991-3 crane loads would differ in shape to the those designed using the SABS 0160:1989 crane loads. The vertical forces from prEN 1991-3 are slightly smaller than those from SABS

0160:1989 and this would result in girders which are slightly shallower. For cranes with a large span to wheel spacing ratio, the horizontal forces from prEN 1991-3 are mostly larger than those in SABS 0160:1989. Using the prEN 1991-3 crane load models for the design of the girder for these cranes would result in the girders with larger top flanges. In contrast, for cranes with a small span to wheel spacing ratio, the horizontal forces from prEN 1991-3 are smaller than those in SABS 0160:1989. Using the prEN 1991-3 crane load models would therefore result in smaller top flanges and surge plates for these cranes.

4.3 Design effort

The design effort required for the design of the support structure using the crane load models in SABS 0160:1989 and prEN 1991-3 was assessed with respect to the amount of crane information it is necessary to obtain, the work required to determine the loads and the amount of work required for the subsequent design of the support structure.

4.3.1 Information required for design

The information required for the support structure design can be divided into two parts, the information required to calculate the loads and the information required to carry out the design of the crane support structure. All the crane information listed in Table 4.6 is required by prEN 1991-3 for the calculation of the crane wheel loads. The crane information that is required by SABS 0160:1989 is shown in Table 4.6, classifying the information into that required for the load calculations and that required for the support structure design.

Slightly more information is required by prEN 1991-3 for the calculation of the crane loads and design of the support structure than SABS 0160:1989. The extra information relates mostly to the travel and hoisting speeds, wheel drives and wheel characteristics and buffers.

Based on Table 4.6, there is slightly more effort involved in obtaining the crane information required for prEN 1991-3 than for SABS 0160:1989. The amount of extra effort depends on the availability of the required information at the stage of the support structure design.

It is often difficult to obtain detailed crane information at the stage of support structure design. This is because the crane is only installed near the end of the construction phase of the building and the crane manufacture is

Table 4.6: Crane information required for design of support structure

	SABS 0160:1989
Nominal weights of crane and hoistload	
Weight of crane bridge	Loads
Weight of crab	Loads
Hoistload	Loads
Crane geometry	
Span of crane bridge	Support structure
Minimum distance between hoist and rail	Support structure
Rail type	Support structure
Width of top of rail	Support structure
Height of rail	Support structure
Travel and hoist speeds	
Steady hoisting speed	
Long travel speed	
Cross travel speed	
Hoist type and characteristics	
Hoist class	Loads
Type of load lifting mechanism	
Hoistload free to swing	Loads
Wheels and wheel drives	
Number of wheels	Loads
Wheel spacing	Support structure
Type of wheel drive	
Number of single wheel drives	
Behaviour of drives	
Combination of wheel pairs	
Guide means	
Guide rollers present	Loads
Clearance between rail and wheel flange	
Buffers	
Buffer type	
Buffer characteristic (degree of plasticity)	

scheduled so as to be completed just before installation. This means that the support structure design is carried out before the crane has been manufactured, or in some cases even designed, and thus before the details of the crane are known.

This difficulty in obtaining crane information is more relevant for process cranes than standard cranes. Process cranes are custom made for a particular process and are typically the larger cranes, whereas standard cranes are manufactured by the crane company and bought in an 'off the shelf' manner. The crane parameters of the standard cranes would therefore be available in advance. The breakdown of cranes sold by a leading crane manufacturer is 30% process cranes and 70% standard cranes. Therefore for 70% of cranes, the crane information would be readily available in advance.

4.3.2 Work required for load calculations

A rough indication of the amount of work that is required for the calculation of the loads is the number of pages of hand calculations to obtain the design crane actions, i.e. factored crane load combinations. Using the SABS 0160:1989 load models, four pages of calculations were required to arrive at factored load combinations compared to ten pages for the load models in prEN 1991-3.

4.3.3 Work required for support structure design

By inspection of all the ultimate limit state load combinations from SABS 0160:1989 and prEN 1991-3, two critical crane load combinations were identified for each code.

The initial calculation of the crane loads is only a small part of the total design effort for the building housing the crane. Because there are the same number of critical load combinations for each code, the resulting effort for the subsequent design of the support structure would not be increased by using prEN 1991-3.

It can be concluded that using prEN 1991-3 for the calculation of the crane loads would not significantly increase the total work required for the design of a structure housing an overhead travelling crane.

4.4 Summary

The crane provisions in SABS 0160:1989 were compared to those in prEN 1991-3. The comparison was carried out with respect to the load situations modelled, the cost of the support structure and the design effort required.

prEN 1991-3 considers in more detail the actual behaviour and geometry of the crane in the crane load modelling. More guidance is given by prEN 1991-3 on the crane load combinations. prEN 1991-3, however, lacks a load model for the misalignment of the wheels or rails. There is no guidance given in SABS 0160:1989 on loading to be considered for the fatigue of the support structure whereas prEN 1991-3 provides a method for the calculation of fatigue loads.

The cost of the support structure was assessed on the basis of the ratios of load effects obtained from SABS 0160:1989 to those obtained from prEN 1991-3. The load effects were calculated for the crane girders, crane columns and longitudinal bracing for the support structures of the three representative cranes.

It was found that the prEN 1991-3 crane load models resulted in smaller vertical loads than the crane load models from SABS 0160:1989. For cranes that have a large span to wheel spacing ratio, the prEN 1991-3 load models result in horizontal load effects that are 217% of the load effects from SABS 0160:1989. In contrast, for cranes with small span to wheel spacing ratios, the prEN 1991-3 load models result in horizontal loads 56% of the SABS 0160:1989 load models. The resulting girder size was about 20% larger for SABS 0160:1989 than for prEN 1991-3. The load effects in the bracing calculated using the load model in prEN 1991-3 were smaller than the SABS 0160:1989 simplified method and larger than the SABS 0160:1989 more detailed method.

The design effort required was assessed on the basis of information required for the design, work required for the calculation of the crane loads and work required for the design of the support structure. prEN 1991-3 requires more crane information than SABS 0160:1989 and also more work for the calculation of the crane loads. The same number of critical crane load combinations result from each code so the subsequent design of the support structure would entail the same amount of work.

Chapter 5

Development of limit states equations

The development of the limit states equations entailed selecting which limit states to consider, selecting the elements to assess for each limit state, determining the loading on the element and determining the failure mode to be considered for the resistance of the element. The identification of the basic variables for use in the reliability analysis is also part of setting up the limit states equations.

The limit states that were considered for this investigation were ultimate limit state, accidental limit state and fatigue. The elements that were chosen for the assessment of each limit state were individual structural elements from the three representative structures. The loading scenarios considered were the various load combinations that include crane loads. For the ultimate limit state this included combinations with permanent loads, wind and roof imposed loads. The failure modes that were considered for the resistance of the elements were the critical failure modes which, in the design, governed the element size. Each limit state will be discussed below, along with the elements chosen for assessment, the loading and the resistance.

The two step reliability assessment process consisting of the economic design of the member and then the reliability analysis, as described in Chapter 1, results in two equations for each member. Firstly the design equation (including all the partial factors) and secondly the limit state equation used as the performance function for the reliability assessment. Both of these equations will be outlined in this chapter.

5.1 Ultimate limit state

The structural elements considered for the assessment of the ultimate limit state were the crane girders and those elements in the building frame that were subject to crane loads. These elements were the crane column, the building column and in some cases the roof members. The elements that were chosen from each representative structure are discussed in detail in section 5.1.2.

5.1.1 Loading

The load combinations considered for the ultimate limit state were taken from SABS 0160:1989 [1] with the addition of the crane load only case. The loading is discussed separately for the two steps of the code calibration process: firstly the loads imposed for the design of the elements and secondly setting up the limit states equations for the reliability analysis.

5.1.1.1 Design

The load combinations considered for the design of the elements are outlined below, along with the design equations including the partial load factors and combination factors.

1. Crane load only
   a) γ_C(Crane)
2. Permanent + Crane
   a) $\gamma_{P'}$(Permanent)
   b) γ_{P_u}(Permanent) + γ_C(Crane)
3. Permanent + Crane + Wind
   a) γ_{P_f}(Permanent) + γ_C(Crane) + $\psi_{WC}\gamma_W$(Wind)
   b) γ_{P_f}(Permanent) + $\psi_{CW}\gamma_C$(Crane) + γ_W(Wind)
4. Permanent + Crane + Roof Imposed
   a) γ_{P_u}(Permanent) + γ_C(Crane) + $\psi_{RC}\gamma_R$(Roof Imposed)
   b) γ_{P_u}(Permanent) + $\psi_{CR}\gamma_C$(Crane) + γ_R(Roof Imposed)

The crane related partial load factors and combination factors are the focus of this investigation and are to be determined in the code calibration exercise. The values of the remaining partial load factors and combination factors were taken as given in SABS 0160:1989. The definitions of the partial factors and combination factors are given in Table 5.1. The values of the partial load factors from SABS 0160:1989 are given in Table & 5.2.

Table 5.1: Definitions of crane related partial load factors and combination factors

Symbol	Definition
γ_C	represents the factoring of the crane load by whichever code format is being considered
ψ_{WC}	combination factor for wind load as the accompanying load with crane load as the leading load
ψ_{CW}	combination factor for crane load as the accompanying load with wind load as the leading load
ψ_{RC}	combination factor for roof imposed load as the accompanying load with crane load as the leading load
ψ_{CR}	combination factor for crane load as the accompanying load with roof imposed load as the leading load

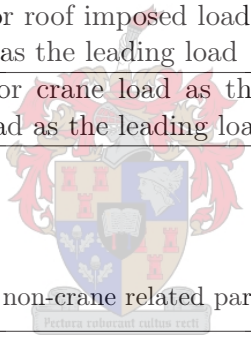

Table 5.2: Definitions of non-crane related partial load factors

Symbol	Definition	Value
$\gamma_{P'}$	partial load factor for permanent load only	1.5
γ_{P_u}	partial load factor for permanent load in unfavourable combination with another load	1.2
γ_{P_f}	partial load factor for permanent load in favourable combination with another load	0.9
γ_W	partial load factor for wind load	1.3
γ_R	partial load factor for roof imposed loads	1.6

Example calculations of all the loads for the 40t crane are given in Appendix A.

The crane loads consist of both vertical and horizontal wheel loads. prEN 1991-3 specifies six ultimate limit state crane loading scenarios consisting of combinations of vertical and horizontal crane wheel loads. The two combinations that were found by inspection to be critical were load combinations

one and five which are described below. From all the ultimate limit state load combinations shown in Chapter 4, the two critical combinations are shown in Figures 5.1 & 5.2. The loads shown are characteristic, unfactored wheel loads.

Load Combination 1 : Represents the crane lifting a load off the ground and accelerating with the crab eccentric to the centre of mass of the crane.

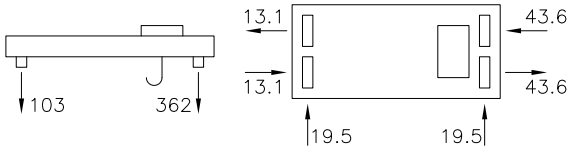

Figure 5.1: Load Combination 1: ϕ_1(Self weight) + ϕ_2(Hoistload) + ϕ_5(Acceleration of crane bridge)

Load Combination 5 : Represents the crane travelling along the runway at constant speed and skewing of the crane bridge occurring.

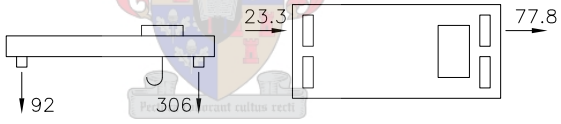

Figure 5.2: Load Combination 5: ϕ_4(Self weight) + ϕ_4(Hoistload) + (Skewing)

Where:

ϕ_1 – dynamic factor applied to the self weight of the crane to take into account the dynamic effects of lifting a load

ϕ_2 – dynamic factor applied to the hoistload to take into account the dynamic effects of lifting a load

ϕ_4 – dynamic factor to take into account the dynamic effects induced when the crane travels along the rails

ϕ_5 – dynamic factor to take into account the dynamic effects of the drive forces

The crane loading for the building frames was calculated by considering the different possible positions of the crane which gave different loading cases. The resulting loading cases were either the vertical loads or the horizontal loads at a maximum with the maximum loads either on the left or right hand side, for each crane load combination.

The load effects in the crane girders were calculated by simple structural analysis methods. A structural analysis computer program [31] was used for the determination of the load effects in the building frames. Linear, two dimensional analyses of the frames were carried out.

5.1.1.2 Reliability analysis

The actual loads that the elements were subject to were considered for the reliability analysis. The methods of calculating these actual loads were assumed to be the same methods that are given in the codes i.e. those used for the economic design of the element. Modelling factors were included to take into account the uncertainties in the calculation of the loads and load effects. The modelling factors will be discussed in more detail below.

The load effects in the girders were still determined by simple structural analysis methods, however, it was not practical to use the structural analysis program directly for the determination of the load effects in the frame, due to the iterative nature of the reliability analysis procedure. In order to be able to determine the load effect in a member, given the load applied to the frame, influence coefficients were calculated. The basis for the calculation of the influence coefficients was that a load effect in a linear analysis can be modelled by the following equation as given by Ellingwood *et al.* [32]:

$$Q_i = c_i \theta_i A_i \tag{5.1.1}$$

Where:

Q_i – load effect

c_i – influence coefficient for calculation of load effects

θ_i – modelling uncertainty in the calculation of the load effect

A_i – applied load

Each load was applied separately to the frame in the structural analysis program and the influence coefficients were found by:

$$c_i = \frac{Q_i}{A_i} \tag{5.1.2}$$

Modelling uncertainties for the loading arose from two sources: the uncertainty in the calculation of the loads and the uncertainty in the calculation of the load effects. The modelling uncertainties involved in the load calculations affected only the crane loads and were included as:

$$\begin{aligned} A_{\text{vertical wheel load}} &= \theta_v \times \text{Calculated vertical crane wheel load} \\ A_{\text{horizontal wheel load}} &= \theta_h \times \text{Calculated horizontal crane wheel load} \end{aligned} \tag{5.1.3}$$

The load effect calculations that included modelling uncertainties were the additional moment due to slenderness effects in the concrete column for the 40t crane, the stress in the girders for the 40t crane and the axial forces and bending moments in the frame elements from the structural analysis program. These modelling uncertainties were included in the limit states equations in the manner shown above.

5.1.2 Resistances

The method of calculating the resistances of the elements for both the economic design and the reliability analysis were taken from the South African materials design codes (SANS 10162-1:2005 [11]; SABS 0100-1:1992 [10]). Modelling factors were included in the reliability analysis to account for the uncertainties involved in the resistance calculations. The modelling uncertainties were included in the limit states equations in a similar manner to the modelling uncertainties for the loads and load effects.

The structural elements that were considered for each representative structure are discussed below, along with the failure modes that were considered for the economic design and reliability analysis.

5.1.2.1 5t crane

5.1.2.1.1 Crane girder

The two span continuous crane girder for the 5t crane was subject to combined vertical and horizontal bending due to the vertical and horizontal crane wheel loads. The design equation and the limit state equation were interaction equations for the combination of vertical and horizontal bending. The different load cases for the assessment of the 5t crane girder and the specific failure modes for each load case are given below.

Bending moment diagrams for each load case are given in Appendix B.

1. Maximum positive vertical moment

   Three resistance checks for the crane girder were carried out when the maximum positive vertical moment was considered.

   a) Combined vertical and horizontal bending for the top flange in compression in the first span of the girder, i.e. the span subject to the maximum positive vertical moment. The failure mode considered for vertical bending was lateral torsional buckling and the failure mode for horizontal bending was elastic bending.

   b) Tension in the bottom flange of the first span of the girder. The failure mode considered was elastic bending.

   c) Accompanying negative vertical moment in the second span of the girder. The failure mode considered was lateral torsional buckling.

2. Maximum negative vertical moment over the internal support. The failure mode considered was lateral torsional buckling.

3. Maximum horizontal moment. Combined vertical and horizontal bending was considered for the top flange in compression. The failure mode considered for vertical bending was lateral torsional buckling and the failure mode for horizontal bending was elastic bending.

5.1.2.1.2 Building frame

The structural elements that were considered for the building frame of the 5t crane were the column, the corbel connection to the column and a roof truss element. These three elements are discussed separately below:

1. Column

   The failure mode considered for the column was a combination of axial compression and bending about the major axis. Three failure modes were considered: cross sectional resistance, buckling about the major axis and lateral torsional buckling.

2. Corbel connection to the column

   Two separate connection details were considered for the corbel to column connection: a bolted connection and a welded connection. The connection was subject to both a bending moment and a shear force from the vertical crane wheel loads. The failure mode for the bolts and the weld was combined shear and tension.

3. Truss element

   The truss element selected for analysis was the one subject to the largest stress. Different load cases and combinations resulted in the truss element being subject in some cases to axial compression and in other cases to axial tension. Both of these failure modes were considered.

5.1.2.2 40t crane

5.1.2.2.1 Crane girder

The crane girder was subject to vertical and horizontal crane wheel loads. Eccentricity of the vertical load combined with the horizontal load caused torsion in the girder. An analysis method given by Rowswell [30] was used where axial stresses in the top and bottom flanges, due to the vertical and horizontal bending and torsion, were considered as the load effects for the crane girder. The resistance of the flanges was taken as the yield stress.

5.1.2.2.2 Building frame

The structural elements of the building frame that were considered were the concrete crane column and the steel building column. The effect of the crane loads on the roof members was very small and they were thus not considered for analysis.

1. Concrete crane column.

   The concrete crane column was subject to combined axial compression and bending about its major axis. According to the South African concrete design code, SABS 0100-1:1992 [10], the column was classified as slender and an additional moment about the minor axis due to slenderness effects was induced. An approximate method of analysis for columns subject to both axial force and bending moment is given by SABS 0100-1:1992 [10] in the absence of a more accurate analysis method. It was decided to use a more accurate analysis method for this investigation. A method of analysis designed for use with a computer has been given by Kwan & Liauw [33]. This method combined with general concrete design principles given by Nawy [34] and the specifications given by SABS 0100-1:1992 was implemented as the more accurate analysis method.

   The analysis was an iterative process first using elastic methods to determine an initial position of the neutral axis following the method given by Kwan & Liauw [33] and then using the compressive stress block method prescribed by SABS 0100-1:1992 to find the final position of the neutral axis and the resistance of the section. The output from the analysis was the ratio of the resistance of the column to the applied loads.

2. Steel building column

   The steel building column was subject to a combination of axial compression and bending about the major axis. As for the column of the 5t crane, three failure modes were considered: cross sectional resistance, buckling about the major axis and lateral torsional buckling.

5.1.2.3 260t crane

5.1.2.3.1 Crane girder

The crane girder for the 260t crane consisted of a main girder with a surge plate and an auxiliary lattice girder. The main girder supported the vertical crane loads. A combined girder consisting of the top flange of the main girder, the surge plate and the top chord of the auxiliary girder carried the horizontal crane wheel loads. Elastic bending was considered for the resistance of the girders.

5.1.2.3.2 Building frame

The structural elements that were considered in the building frame were the steel crane column, the steel building column and two roof truss members.

1. Steel crane column

   The crane column was subject to combined axial compression and bending about the minor axis. The failure modes that were considered were cross sectional resistance and buckling about the minor axis.

2. Steel building column

   The building column was subject to combined compression and bending about the major axis. As for the column of the 5t crane, three failure modes were considered: cross sectional resistance, buckling about the major axis and lateral torsional buckling.

3. Roof truss elements

   As with the 5t crane, some load combinations caused tension in the roof truss member and some caused compression. Both of these failure modes were considered.

5.1.3 Limit states equations

The general performance function for the ultimate limit states was:

$$g(\mathbf{X}) = R\theta_R - \sum c_i A_i \theta_L \tag{5.1.4}$$

Where:

R – resistance of the member

θ_R – modelling uncertainty in the calculation of the resistance

c_i – influence coefficient for calculation of load effects

A_i – applied load

θ_L – modelling uncertainty in the calculation of the load effects

In cases when the failure mode considered was a combination of axial compression and bending, the limit state equation took the form:

$$g(\mathbf{X}) = \theta_R - \left(\frac{(\sum c_i A_i \theta_L)_{\text{axial}}}{R_{\text{axial}}} + \frac{(\sum c_i A_i \theta_L)_{\text{bending}}}{R_{\text{bending}}} \right) \tag{5.1.5}$$

5.2 Accidental limit state

The possible accidental load situations for cranes are outlined below:

1. The crane bridge running into the end stops.

   This is considered as an accidental load because there are generally limit switches on the runways close to the ends which cause the crane to stop when it passes over them. In the event of the limit switches failing, the crane will fail to stop and the crane will run at full travel speed into the end stops. The buffers on the crane are used to lessen this impact force.

2. The crab running into the end stops.

   This is a similar situation to the crane bridge running into the end stops. There are generally limit switches to stop the crab before it reaches the end stops. This load case is considered for the ultimate limit state in that prEN 1991-3 considers this case to allow for the effects of acceleration or deceleration of the crab. In the ultimate limit state this load case is not critical and it will thus not be considered for the investigation of the accidental limit state.

3. The hoistload colliding with a column.

   This could occur if the crane bridge was between a pair of columns with the crab travelling such that the line of travel of the crab was directly towards a column, and the crab suddenly stopped. In this situation the hoistload could swing and collide with a column.

The case that was chosen for the assessment of the accidental limit state was the crane bridge running into the end stops because this is the accidental load that is provided for in prEN 1991-3.

For all the cranes, the longitudinal buffer forces are resisted by the longitudinal runway bracing and all have the same failure mode so the 40t crane was selected to be representative of all the cranes for the accidental limit state and the accidental load case has been considered for the 40t crane only.

5.2.1 Loading

The loads caused by the crane bridge running into the end stops are longitudinal loads along the runway. The loads are calculated assuming that the crane is travelling at 70% of the full rated long travel speed, taking into account the mass of the crane and hoistload. The load combination is shown in Chapter 4, the load calculations are given in Appendix A.

This method was used for the calculation of the load for the economic design and the reliability assessment. A modelling factor to take into account the uncertainty of the load calculation was included in the limit state equation.

5.2.2 Resistance

The longitudinal loads from the crane bridge colliding with the end stops are resisted by the longitudinal runway bracing. A diagram of the bracing for the 40t crane is given in Figure 3.9 on page 76. The behaviour of the bracing was modelled as the compressive leg buckling and the tensile leg carrying the load. The resistance was thus considered as the resistance of one bracing leg in tension.

5.2.3 Design equation

The design equation for the accidental case is given by:

$$\phi_R A f_y = \gamma_A H_B \tag{5.2.1}$$

Where:

ϕ_R – partial resistance factor

A – cross sectional area of one bracing leg

f_y – yield strength of steel

γ_A – partial load factor for accidental crane actions

H_B – longitudinal load from the crane bridge colliding with the end stops

5.2.4 Limit state equation

The limit state equation for the accidental limit state is given by:

$$g(\mathbf{X}) = Af_y - H_B\theta_{H_B} \tag{5.2.2}$$

Where:

θ_{H_B} – modelling factor to allow for uncertainty in the load calculation

5.3 Fatigue

The procedure for the calculation of fatigue reliability is the same two step procedure carried out for the other limit states. The first step is the economic design of the element considered according to the code provisions to ensure that the resulting element exactly meets the code requirements. The second step is to carry out the reliability analysis where the loading and the resistance in the limit state equation represent the actual loads imposed on, and the resistance behaviour of the element.

The elements that are most susceptible to crane induced fatigue are those most directly loaded by crane loads i.e. the crane girder, columns and related connections. The elements chosen for the assessment of fatigue reliability in this study were taken from two of the three representative cranes and are:

1. 40t crane girder, fatigue at the bottom of the intermediate stiffeners

2. 40t crane girder, fatigue of the top flange to web weld caused by rotation of the top flange

3. 5t crane, corbel to column welded connection

The 260t crane girder is similar to the 40t crane girder in that they are both welded plate girders and would therefore display the same behaviour. The surge plate for the 260t crane girder would to some extent reduce the top flange rotation, therefore the 40t crane girder represents the worst case. The 5t crane girder is a two span continuous hot rolled I section with a channel on the top flange. The only weld in a tension region is the weld connecting the channel to the top flange over the support. This is a longitudinal weld in the same direction as the stresses and is thus not critical for fatigue.

5.3.1 Economic design method

The two fatigue design methods that were discussed in section 4.1.4 on page 90 were considered for the economic design. The first method is that given in prEN 1991-3 where the fatigue loads and resistance are separated and prEN 1991-3 specifies the crane fatigue loading. The second method is that assumed by SABS 0160:1989 where the crane fatigue loading is not specified and it is the responsibility of the support structure designer to model the behaviour of the crane. In both cases, the fatigue resistance, in the form of S-N curves, was taken from the South African steel design code SANS 10162-1:2005 [11].

5.3.1.1 prEN 1991-3 fatigue loads

The method given in prEN 1991-3 of determining the crane loads to be considered for fatigue is described in detail in Chapter 2 but will be briefly outlined below.

The basis for the determination of the fatigue loads in prEN 1991-3 is the normalisation of the maximum nominal wheel load, resulting in the equivalent constant amplitude load for two million cycles. This normalised load is called the 'fatigue damage equivalent load'. The rationale behind the calculation of this load is that two million crane cycles with the crane wheel loads equal to the fatigue damage equivalent load, will result in the same amount of fatigue damage as the normal operating conditions of the crane with the number of cycles it is likely to perform over its lifetime. The normalisation is carried out by multiplying the maximum nominal wheel load by a factor (λ):

$$Q_e = \phi_{fat} \times \lambda \times Q_{max} \tag{5.3.1}$$

Where:

Q_e – fatigue damage equivalent load

ϕ_{fat} – damage equivalent dynamic impact factor, the factor applied to the crane self weight $\phi_{fat,1} = \frac{1}{2}(1+\phi_1)$ and the factor applied to the hoistload $\phi_{fat,2} = \frac{1}{2}(1+\phi_2)$

Q_{max} – maximum nominal wheel load

The λ factor is determined from the fatigue class of the crane. Cranes are classified into fatigue classes depending on the total number of cycles (N)

performed over the lifetime of 25 years and the load spectrum (kQ). One λ factor is given for each fatigue class for the calculation of normal stresses and another for the calculation of shear stresses.

As discussed in Chapter 2, the load spectrum definition in prEN 1991-3 is based on the fatigue of the crane itself and not the support structure. The load spectrum used for this investigation has been modified to more accurately represent the stress cycles caused by the crane wheel loads on the girder and is given by:

$$kQ = \sum_j \left(\left(\frac{Q_{i,j}}{\max Q_i} \right)^m \frac{n_{i,j}}{\sum n_{i,j}} \right) \tag{5.3.2}$$

Where:

$Q_{i,j}$ – wheel load of value j for wheel i

$\max Q_i$ – maximum wheel load for wheel i

$n_{i,j}$ – number of applications of range j for wheel i

$\sum n_{i,j}$ – total number of load applications

m – slope of the S-N curve

The fatigue stresses in the element were calculated by considering one movement of the crane along the girder with the wheel loads equal to the fatigue damage equivalent load. The stress cycles causing fatigue were calculated and in the event of there being more than one stress cycle for one pass of the crane over the girder, Miner's rule of accumulative damage was used. A description of the design procedure for each element is given in section 5.3.2.

5.3.1.2 Resistance

The resistances of the elements were determined using the S-N curves in SANS 10162-1:2005 [11]. The S-N curves in SANS 10162-1:2005 [11] consist of two slopes, the first in the region of higher stress with a slope of $m_1 = 3$ and the second in the region of lower stress with a slope of $m_2 = 5$. The equation for the S-N curves is given by:

$$(S)^m = \frac{A}{N} \tag{5.3.3}$$

Where:

S – stress amplitude

m – slope of the S-N curve

A – material parameter

N – number of cycles to failure for a given stress amplitude, S

If only one stress cycle resulted from the stress calculations, the fatigue resistance was taken as the stress level at two million cycles on the relevant S-N curve. If more than one stress cycle was obtained, the parameters of the relevant S-N curve were used to calculate the accumulative fatigue damage according to Miner's rule and the resistance was taken as the fatigue damage at failure equal to one.

5.3.2 Economic design

The economic design was carried out by determining the size of the member for which the fatigue load effect calculated with the fatigue damage equivalent load was exactly equal to the resistance.

In order to carry out the economic design, the stress histories for the relevant fatigue stresses in the three elements were required.

The stress history was produced by calculating the stresses at the point where fatigue was considered as the crane moved incrementally along the girder. The stress histories for one crane cycle (loaded and unloaded) for the 40t crane girder intermediate stiffener and the 5t corbel to column connection are shown in Figures 5.3 and 5.5. The stress history for the 40t crane girder top flange to web weld is shown in Figure 5.4 where only the loaded part of the cycle is shown. In Figures 5.3 and 5.5 the movement of the crane along the girder is expressed in terms of time, this was assuming an arbitrary velocity of the crane of 30 m/min.

A brief description of the specific design procedure for each element is given below.

1. 40t crane girder, fatigue at the bottom of the intermediate stiffeners

   The stress causing fatigue at the bottom of the intermediate stiffener was the longitudinal tension due to global bending of the beam. It was

assumed that there was a stiffener at the point of maximum bending in the beam i.e. at 5.1m from the support. Figure 5.3 shows the stress history at this point for the crane travelling over the girder twice, the first time the crane is travelling from left to right along the girder and the second time the crane is returning in the other direction. The first peak in the first pass of the crane is when the leading wheel is at 5.1 m and the following wheel is at 0.7 m, the second peak is when the following wheel is at 5.1 m and the leading wheel is off the girder.

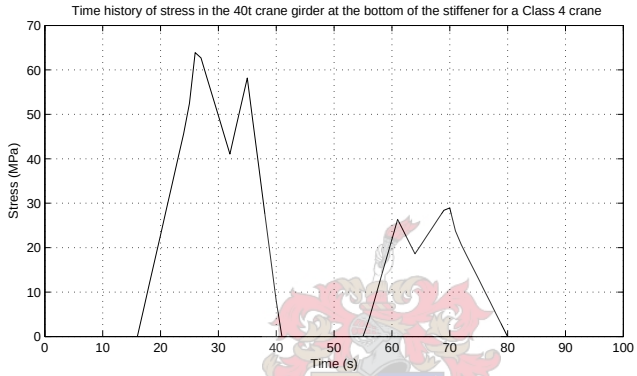

Figure 5.3: Stress history for 40t crane girder at bottom of stiffener

In this case two stress cycles resulted from one pass of the crane over the girder. A rainflow counting method was used to identify the stress cycles and their amplitudes. The first cycle was identified as ranging from zero to 64 MPa (the top of the first peak). The second cycle was identified as ranging from 40 MPa (the lowest point between the peaks) to 58 MPa (the top of the second peak) resulting in a stress amplitude of 18 MPa.

The bottom of the stiffener was classified as detail category C1 which is described as 'Base metal at the toe of transverse stiffener-to-flange and transverse stiffener-to-web welds' according to SANS 10162-1:2005 [11].

Miner's rule for accumulative damage was used to determine the damage caused by the two stress cycles. The stresses were calculated using the fatigue damage equivalent load which is normalised to two million crane cycles, therefore the damage caused by two stress cycles was multiplied by two million to give the total damage over the girder lifetime.

The fatigue resistance was taken as the fatigue damage at failure equal to one.

The method of carrying out the economic design was to scale the dimensions of the crane girder, keeping the original proportions, until the total damage resulting from two million cycles of the fatigue damage equivalent load was exactly equal to the fatigue damage at failure.

2. 40t crane girder, fatigue of the top flange to web weld caused by rotation of the top flange

   The wheel loads that were considered for this fatigue case were the vertical load and the horizontal transverse load due to the acceleration of the crane bridge with the crab eccentric to the centre of mass. Considering the horizontal load as a fatigue load is a conservative but not unrealistic assumption. In the case where a crane has very fixed movements around a building it is possible that it will always accelerate over the same girder. For example a ladle crane in a steelworks building always collects the molten steel at one end of the building and runs the full length of the runway and back again with an empty ladle. In this case the crane bridge always accelerates in the same place. The configuration of the horizontal transverse loads caused by acceleration of the crane bridge are shown in Figure 5.1.

   The stresses that caused fatigue in the top flange to web weld were global and local bending stresses and global and local shear stresses. These stresses were calculated using the method given in the steel design part of the Eurocode (ENV 1993-6 [35]) because no guidance is given on the calculation of these type of stresses in the South African design codes. The individual stresses are outlined below.

   - Compressive longitudinal stress due to global bending
   - Global shear due to vertical loads
   - Local shear due to vertical loads
   - Local vertical compressive stresses due to concentrated wheel loads
   - Vertical bending stresses due to the rotation of the top flange caused by the horizontal wheel load and the eccentricity of the vertical wheel load. When considering one side of the web, the bending

stress for the first wheel was tensile due to the horizontal and vertical loads causing rotation of the top flange away from the side of the web being considered. The bending stresses for the second wheel were compressive because the horizontal wheel loads act in opposite directions (see Figure 5.1) and the vertical and horizontal forces from the second wheel tend to rotate the flange towards the side of the web being considered.

The stress that was considered for the fatigue analysis was the maximum resulting principal stress. The stress history in terms of the resultant principal stress from the stresses given above for one pass of the crane over the girder is shown in Figure 5.4. The stress cycles were broad banded so a rainflow counting method was used to identify the cycles and find their amplitudes. Three stress cycles were identified:

- the first cycle ranges from zero to 80 MPa and back to zero.
- the second cycle ranges from zero, up to 20 MPa, down to -50 MPa and back up to zero resulting in an amplitude of 70 MPa.
- the third cycle ranges from zero up to 8 MPa and back to zero.

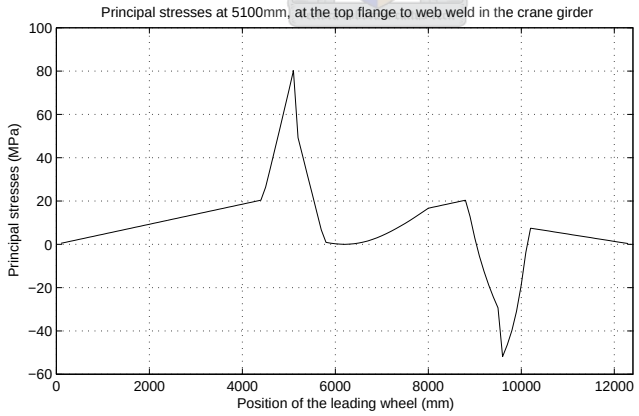

Figure 5.4: Stress history for 40t crane girder at top flange to web weld

The top flange to web weld was classified as fatigue detail B which is described as 'Built up members - Base metal and weld metal in components,

without attachments, connected by continuous full penetration groove welds with backing bars removed' according to SANS 10162-1:2005 [11].

Miner's rule for accumulative damage was used to determine the damage caused by the three stress cycles and the damage was multiplied by two million to get the total damage over the lifetime of the girder. The resistance of the girder was taken as the fatigue damage at failure equal to one.

The method of carrying out the economic design was the same as that for the fatigue at the bottom of the intermediate stiffener, viz. to scale the dimensions of the crane girder, keeping the original proportions, until the total damage resulting from two million cycles of the fatigue damage equivalent load was exactly equal to the fatigue damage at failure.

3. 5t crane, corbel to column welded connection

   The weld that was considered for the corbel to column welded connection was the horizontal weld along the top flange of the corbel. The stress causing fatigue was the tension stress from the moment resulting from the eccentricity of the crane vertical load. It was assumed that the vertical welds carried the shear and the horizontal welds carried the moment. Figure 5.5 shows the stress history for two passes of the crane along the girder. In this case there is only one stress cycle for each pass of the crane. The fatigue loading was taken as the amplitude of the stress cycle.

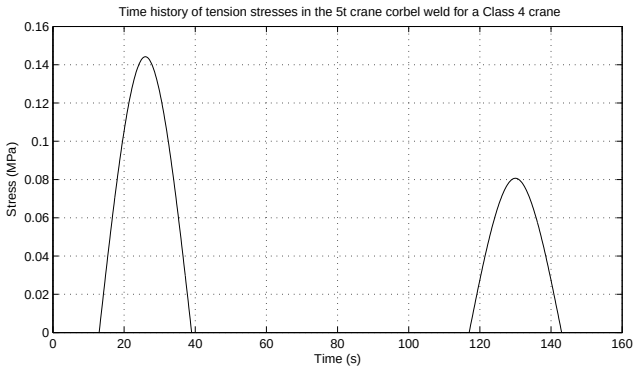

Figure 5.5: Stress history for 5t crane at corbel to column welded connection

The corbel to column welded connection was classified as detail category C with an additional reduction factor to allow for the fact that it is a transversely loaded fillet weld, according to SANS 10162-1:2005 [11]. The resistance of the weld was taken as the stress in the S-N curve for detail category C at two million cycles, multiplied by the reduction factor.

The economic design was carried out by keeping the size of the column and the corbel constant and determining the weld thickness required for the fatigue resistance to be exactly equal to the fatigue loading.

The difference between the fatigue loading calculated according to the method given in prEN 1991-3 and that calculated by considering the crane behaviour was assessed by calculating the damage in the element which had been economically designed using prEN 1991-3, resulting from simulating the crane behaviour. The assessment was carried out by simulating the crane behaviour to obtain a stress history for the element being considered and determining the resulting fatigue damage using Miner's rule of accumulative damage.

Two aspects of the crane behaviour were simulated in order to produce a stress history:

1. Crane movement along the gantry

   One crane cycle was defined as the crane lifting a load at one end of the gantry, travelling along the gantry, setting down the load and travelling back, unloaded, to the starting point. It was assumed that the crane travels over the girder being considered, twice for each crane cycle; the first time carrying a load and the second time with no load.

2. Crane wheel loads

   To simulate the crane loading a set of hoistload values and crab positions were generated. In order to assess the fatigue reliability of the code provisions, hoistload values were generated to give a specified load spectrum value kQ. These load spectrum values were generated considering the crab always at the extreme of its travel, closest to the wheel being considered. The generated hoistload values were used to calculate the crane wheel loads.

5.3.3 Reliability analysis

In the reliability analysis the actual loads applied to the element were modelled along with the actual resistance of the element.

The actual loading for the reliability analysis was determined by simulating the crane behaviour to produce a stress history for the member and using Miner's rule to determine the accumulative damage. The actual resistance of the element was taken as the fatigue damage at failure with a mean of one.

5.3.3.1 Loading

The simulation of the crane behaviour was carried out as described in the previous section. The stress histories for the three elements are shown in Figures 5.3 - 5.5. In the cases where the stress histories were broad-banded, a rainflow counting method was used to identify the stress cycles [36] as described in Section 5.3.2. Miner's rule for accumulative damage was used to determine the fatigue damage caused by the crane loads.

The properties of the S-N curves for the reliability analysis were derived from those in SANS 10162-1:2005 [11]. The statistical models used for the fatigue analysis are discussed in Chapter 6. The S-N curves have two slopes, the first in the region of higher stresses with a gradient of $m_1 = 3$, the second in the region of lower stresses with a gradient of $m_2 = 5$. In order to simplify the reliability analysis procedure, investigations were also carried out considering the S-N curve having a single slope of $m = 3$. The single slope S-N curve was taken as an extension of the first slope in the double slope curve i.e. instead of a change of slope the curve continues into the region of lower stresses with a slope of $m = 3$.

5.3.3.2 Resistance

The resistance of each element was taken as the fatigue damage at failure with a mean of one.

5.3.3.3 Limit state equations

For the case when a double slope S-N curve was considered, the limit state equation is given by:

$$g(\mathbf{X}) = D - \left(\sum_i \frac{(S_i)^{m_1}}{A_1} \frac{n_i}{N} + \sum_j \frac{(S_j)^{m_2}}{A_2} \frac{n_j}{N} \right) \tag{5.3.4}$$

Where:

D – fatigue resistance

S_i – amplitude of stress cycle i which falls into the higher stress region

S_j – amplitude of stress cycle j which falls into the lower stress region

A_1 – fatigue material property from the S-N curve for slope 1

A_2 – fatigue material property from the S-N curve for slope 2

m_1 – slope of S-N curve in region of higher stresses

m_2 – slope of S-N curve in region of lower stresses

n_i – number of stress cycles with amplitude S_i

n_j – number of stress cycles with amplitude S_j

N – total number of stress cycles

In the case where a single slope S-N curve was considered, the limit state equation is given by:

$$g(\mathbf{X}) = D - \sum_i \frac{(S_i)^{m_1}}{A_1} \frac{n_i}{N} \tag{5.3.5}$$

Where:

S_i – in this case is the amplitude of stress cycle i for stresses in the higher and lower regions.

5.4 Summary

The limit states equations that will be used for the reliability assessment and code calibration of the crane load models were developed. The three representative cranes discussed in Chapter 3 are used as example structures for the code calibration. Limit states equations were developed considering specific elements of the support structures for the three representative cranes. Because

specific examples structures are considered for the reliability analysis, the limit states equations include both the loading on the element and the resistance of the structural element.

The three limit states that were considered critical for crane support structures and were considered for the code calibration were ultimate limit state, accidental limit state and fatigue.

A methodology was demonstrated on how to obtain a design that just satisfies the code requirements, the so called 'economic design'. The element so designed is then used in the reliability analysis. This ensures that the reliability of the code requirements are assessed without any conservatism included due to practical rounding of elements sizes.

The crane loads that were considered for the ultimate limit state were the loads due to normal operation of the crane. The structural elements from the three representative structures that were considered for the ultimate limit state were those that were subject to crane loads, i.e. crane girders, crane columns, building columns and the roof trusses from the 5t and 260t cranes.

The load combinations that were considered for the ultimate limit state were crane load only, crane with permanent load, crane with permanent and wind loads and crane with permanent and roof imposed loads. The critical failure mode, i.e. the failure mode that governed the element size, was considered for the resistance of the element.

The economic design of the elements was carried out considering the crane loads from prEN 1991-3, the permanent, wind and roof imposed loads from the South African loading code SABS 0160:1989 [1] and the resistances from the South African materials codes.

For the reliability analysis, the actual loads that the element were subject to and the actual resistance behaviour was considered. The true behaviour of both the loads and resistances was assumed to be represented by the models given the loading and materials codes, with the inclusion of modelling uncertainties. The modelling uncertainties were included in the limit states equations by multiplying the load or resistance, calculated from the code models, by the relevant modelling factor.

The limit states equations for the ultimate limit state were defined for the general case when only one load effect was considered, e.g. tension in a roof truss member, and for the interaction case, e.g. combination of axial load and bending moment for the columns.

The situation considered for the accidental limit state was the case that is provided for in the crane load models in prEN 1991-3, viz. the crane running into the end stops on the end of the runway. The structural element that was considered for the accidental limit state was the structural element that resists the resulting longitudinal force, i.e. the longitudinal runway bracing.

Three fatigue situations were considered as critical for the three crane configurations investigated and were considered as representative of fatigue design of crane support structures. The three fatigue situations were: 5t crane - corbel to column welded connection, 40t crane girder - bottom of the intermediate stiffener, 40t crane girder - top flange to web weld.

The loading considered for the economic design was calculated using the method given in prEN 1991-3 of calculating a fatigue damage equivalent load which is the constant amplitude crane wheel load normalised to two million cycles which will result in the same fatigue damage as the normal crane operation. The fatigue resistance for the economic design was determined from the S-N curves in the South African steel design code [11].

The loading considered for the fatigue reliability analysis was determined by simulating the crane behaviour to obtain stress histories for the fatigue detail being considered. Two aspects of the crane behaviour were simulated: the loads lifted by the crane and the movement of the crane around the building. The resulting stress cycles were counted using a rainflow counting method and the fatigue damage due to the crane loads was calculated using Miner's rule for accumulative damage.

The variables that have been selected from the limit states equations to be considered as random variables for the reliability analysis are identified and discussed in Chapter 6.

Pectora roborant cultus recti

Chapter 6

Stochastic models

The stochastic models for the material properties, geometric properties, loads and modelling uncertainties that have been taken from literature are discussed here. The new stochastic models that were developed for this code calibration (viz. the stochastic models for the crane hoistload) are discussed in Chapter 7.

6.1 Basis for statistical modelling

There are two types of statistical uncertainties: aleatory uncertainties and epistemic uncertainties. Aleatory uncertainties are due to the inherent variability and randomness of basic variables and epistemic uncertainties are due to lack of knowledge, imperfect representations of the real world or imperfect predictions.

The two types of uncertainties may be combined in the following manner [32]:

If X represents a basic variable then estimates of the mean and coefficient of variation of X, $\hat{\bar{X}}$ and $\hat{\delta}_x$, can be obtained from an idealised model. Then $\hat{\delta}_x$ represents the aleatory uncertainty, resulting from the inherent variability of X and does not include all sources of uncertainty which contribute to the total uncertainty in X. The mean and coefficient of variation attributed to the additional (epistemic) uncertainty can be treated as a bias factor B with mean and coefficient of variation $\bar{B}$ and δ_B. Then the true mean and coefficient of variation of the basic variable are given by:

$$\bar{X} = \bar{B}\hat{\bar{X}} \tag{6.1.1}$$

$$\delta_X = \sqrt{\hat{\delta}_X{}^2 + \delta_B{}^2} \tag{6.1.2}$$

6.2 Sources of information

Two fundamental sources of information have been consulted on the statistical modelling of the basic variables:

1. The work that was carried out for the development of the American National Standard A58, Ellingwood *et al.* [32] circa 1980. Extensive investigations were carried out on loads and resistances, both material properties and resistance models. Due to the importance of the development of the code, the work has been subject to extensive peer review. The references which form part of this study are: [32; 37; 38; 39; 40; 41; 42; 43; 44; 45; 46; 47; 48]

2. The probabilistic model code developed by the Joint Committee on Structural Safety, JCSS [36], in 2001. This model code was developed with the intention of compiling the information required to design new structures or assess existing structures probabilistically. This code has also undergone extensive peer review.

The remaining references in this chapter do not form a part of either of the two projects mentioned above.

6.3 Material properties

6.3.1 Structural steel

The steel was assumed to have been drawn from different mills due to the fact that this investigation deals with a code calibration and the code considers general structures.

6.3.1.1 Yield strength of structural steel, (f_y)

$f_{y,nom} = 300\,\text{MPa}$ $\mu_{f_y} = 315\,\text{MPa}$ $\delta_{f_y} = 10\%$ Distribution = LN

A summary of the statistical properties given in the literature is shown in Table 6.1. The nominal value of the yield strength has been taken as 300 MPa.

Table 6.1: Statistical parameters of the yield strength of structural steel

Item	Mean MPa	c.o.v. %	Distr.	Reference
Steel members	316.5	7	LN	JCSS [36]
Flanges	315	10	N	Galambos & Ravindra [37] Ellingwood *et al.* [32] Bjorhovde *et al.* [38]
Webs and plates	330	11	N	Galambos & Ravindra [37] Ellingwood *et al.* [32] Bjorhovde *et al.* [38]
Steel members	321	12	N	Ellingwood & Reinhold [39]
Steel members	315	10	N	Cooper *et al.* [40] Ravindra & Galambos [41]

The distribution that was used was based on that recommended by JCSS [36]. The main reasons for this are that it is a more recent publication and that it is accepted as the standard for statistical models. The parameters of the distribution given by JCSS [36] are similar to those given in the other references and a Lognormal distribution is thought to be more suitable to resistance parameters as it cannot go below zero. The coefficient of variation was increased from 7% to 10% to reflect the additional uncertainty due to the spread in mean values from the various sources.

6.3.1.2 Moduli of elasticity (E, G)

$$\mu_E = E_{\text{nom}} \qquad \delta_E = 3\% \qquad \text{Distribution} = \text{N}$$

$$\mu_G = G_{\text{nom}} \qquad \delta_G = 3\% \qquad \text{Distribution} = \text{N}$$

The statistical properties given above are recommended by JCSS [36]. The statistical properties recommended by Galambos & Ravindra [37] are the same

except that the coefficient of variation is given as 6%. The models given by JCSS [36] were used for the same reasons as for the yield strength of structural steel.

6.3.2 Bolts

The stochastic models for the properties of bolts were taken from Fisher *et al.* [48].

6.3.2.1 Ultimate tensile strength (f_u)

$$\mu_{f_u} = 1.2 f_{u,nom} \qquad \delta_{f_u} = 7\% \qquad \text{Distribution} = \text{N}$$

The statistical parameters of the ultimate tensile strength of bolts were obtained by Fisher *et al.* [48] from a number of sets of published experimental data obtained from tests on high strength bolts. The statistical model for A325 bolts was used. The A325 bolts have a minimum tensile strength of 845 MPa which corresponds to the Grade 8.8 bolts, considered for the code calibration, which have a minimum tensile strength of 800 MPa.

6.3.2.2 Ratio of shear strength to tensile strength ($\frac{\tau}{\sigma}$)

$$\left(\frac{\tau}{\sigma}\right)_{nom} = 0.60 \qquad \mu_{\frac{\tau}{\sigma}} = 0.625 \qquad \delta_{\frac{\tau}{\sigma}} = 5.3\% \qquad \text{Distribution} = \text{N}$$

Design codes specify a ratio of shear strength to tensile strength for the calculation of the resistance of bolts subject to shear. The statistical parameters obtained by Fisher *et al.* [48] for the ratio of shear to tensile strength were based on experimental data and are valid for both the A325 bolts and the higher strength A490 bolts.

6.3.3 Welds

The stochastic models for the strength of the welds were taken from Fisher *et al.* [48]. The models were based on experimental data obtained from strength tests of welds from various electrode types. Longitudinal fillet welds were considered as they result in the lower bound of strength.

6.3.3.1 Ultimate tensile strength (f_{uw})

$$\mu_{f_{uw}} = 1.05 f_{uw,nom} \qquad \delta_{f_{uw}} = 4\% \qquad \text{Distribution} = \text{N}$$

6.3.3.2 Ratio of shear strength to tensile strength ($\frac{\tau}{\sigma}$)

$$\left(\frac{\tau}{\sigma}\right)_{nom} = 0.67 \qquad \mu_{\frac{\tau}{\sigma}} = 0.84 \qquad \delta_{\frac{\tau}{\sigma}} = 10\% \qquad \text{Distribution} = \text{N}$$

Design codes specify a ratio of weld shear strength to tensile strength for the assessment of welds subject to tension and shear. Experimental data was assessed by Fisher *et al.* [48] to determine the statistical parameters of the ratio of shear to tensile strength.

6.3.4 Concrete

6.3.4.1 Compressive strength of concrete (f_c)

$$f_{c,nom} = 30\,\text{MPa} \qquad \mu_{f_c} = 32\,\text{MPa} \qquad \delta_{f_c} = 15\% \qquad \text{Distribution} = \text{N}$$

The assumptions made in the statistical modelling of the compressive strength of concrete were [32]:

1. The quality of construction is average. Because this is a code calibration exercise, the models should be representative of the overall variability in construction.

2. The 'static' strengths are considered, i.e. assuming slow loading rates. For concrete compressive strength this relates to testing at a rate of one hour to failure. The slower the rate of loading, the lower the strength of the concrete. Considering the static strength is thus a conservative assumption.

3. Long term changes in the concrete and reinforcing strengths are ignored. This has been shown to be conservative as the strength of reinforced concrete increases over time [32; 42].

The statistical model for concrete compressive strength presented by JCSS [36] is comprehensive but complicated and not suitable or practical for this application which is concerned primarily with crane loads.

The model that was used was that proposed by Mirza *et al.* [43]. This model was also used in reliability analyses carried out by Ellingwood *et al.* [32], Grant *et al.* [44] and MacGregor *et al.* [42]. Ruiz & Aguilar [49] use a simpler model suggested by Ellingwood [45]. The model given by Mirza *et al.* [43] was preferred because it resulted from a more in-depth study and it was developed more recently than the model given by Ellingwood [45].

The model for the mean value of the concrete compressive strength is based on three correction factors and is given by:

$$\mu_{f_c} = f_{c,nom}\, r_{creal}\, r_{in-situ}\, r_R \tag{6.3.1}$$

Where:

$f_{c,nom}$ – specified characteristic concrete strength = 30 MPa.

r_{creal} – corrects the characteristic value to the mean cube strength

$r_{in-situ}$ – corrects the cube strength to the in-situ concrete strength

r_R – converts the strength to a 'static' concrete strength considering failure in one hour

The South African concrete materials code SABS 0100-2:1992 [50] specifies that the characteristic strength of concrete is the 0.05 fractile, i.e. only 5% of the cube tests should fall below the characteristic strength. For a normal distribution, the value of r_{creal} is given by:

$$r_{creal} = \frac{1}{1 - 1.645\delta} \tag{6.3.2}$$

Where:

δ – the coefficient of variation of the concrete strength, given as 15% below.

Mirza *et al.* [43] recommend values of the in-situ and rate of loading correction factors as:

$$r_{in-situ} = 0.9 \tag{6.3.3}$$

$$r_R = 0.89\,(1.173 + 0.08 \log R) \tag{6.3.4}$$

Where:

R – is the rate of loading in MPa/s

For failure in one hour ('static' concrete strength):

$$R = \frac{f_{c,nom}}{3600} = \frac{30}{3600}\frac{\text{MPa}}{\text{s}} = \frac{1}{120}\,\text{MPa/s} \tag{6.3.5}$$

This gives:

$$\mu_{f_c} = 32.1\,\text{MPa}$$

The coefficient of variation of the concrete compressive strength is given as [43]:

$$\delta_{f_c} = \sqrt{\left(\delta_{ccyl}{}^2 + 0.0084\right)} \tag{6.3.6}$$

Where:

δ_{ccyl} – coefficient of variation of the test cylinders

Ellingwood *et al.* [32] give the coefficient of variation for average quality control 5000 psi (≈ 35 MPa) concrete to be 12% which results in:

$$\delta_{f_c} = 15\%$$

Mirza *et al.* [43] state that a Normal distribution describes the compressive strength of concrete where there is good to average quality control whereas a Lognormal distribution is better for poor quality control. Average quality control was considered for this investigation, therefore a Normal distribution was used.

6.3.4.2 Yield strength of reinforcing (f_{yr})

$f_{yr,nom} = 450\,\text{MPa}$ $\mu_{f_{yr}} = 510\,\text{MPa}$ $\delta_{f_{yr}} = 6\%$ Distribution = N

The reinforcement was assumed to be drawn from many locations due to the same reasons that the concrete was assumed to have average quality control, i.e. this is a code calibration exercise and therefore describes the variability expected for any project.

The 'static' yield strength was considered here so as to be consistent with the concrete rate of loading. The yield strength is based on the nominal cross

sectional area thus the variation in bar diameter is taken into account in the variation of yield strength.

A summary of the parameters found in the literature for the yield strength of reinforcing is given in Table 6.2.

Table 6.2: Statistical parameters of the yield strength of reinforcing steel

Mean (MPa)	c.o.v. %	Distribution	Reference
500	8.6	Beta	Mirza & MacGregor [46] cited by: Grant *et al.* [44] MacGregor *et al.* [42] Lu *et al.* [51] Ellingwood *et al.* [32]
510 (nom + 2σ)	5.8 (σ = 30 MPa)	N	JCSS [36]

The model used was that given by JCSS [36] for the same reasons as those given before.

6.4 Geometric properties

The variation in a dimension x, is often best described by considering the variation of the error y, where:

$$x_{actual} = x_{spec} + y \tag{6.4.1}$$

6.4.1 Steel members

The statistical properties of cross sectional dimensions and section properties of steel members were modelled by Bjorhovde *et al.* [38] as Normal distributions with mean values equal to the nominal values and coefficients of variation of 5%. This distribution was used in reliability work carried out by Ellingwood *et al.* [32], Ellingwood & Reinhold [39] and Ravindra & Galambos [41].

JCSS [36] base their suggested statistical models on preliminary results from a study in the Czech Republic on I profiles ranging in size from IPE 80-200. A Normal distribution is recommended for all section properties. Cross

sectional dimensions have the Normal parameters given below:
Mean:

$$-1.0\,\text{mm} \leq \mu_y \leq +1.0\,\text{mm}$$

Standard deviation:

$$\sigma_y \leq 1.0\,\text{mm}$$

The mean values of the section properties such as area and section modulus are given as equal to the nominal values and the recommended coefficients of variation are given below:
Coefficient of variation for cross sectional area:

$$\delta_A = 3.2\%$$

Coefficient of variation for section modulus:

$$\delta_Z = 4\%$$

The statistical model that was chosen for the cross sectional dimensions was a Normal distribution with the mean value equal to the nominal value. Based on both suggested models; the coefficient of variation was taken to be 5% with an upper limit of the standard deviation of 1.0 mm.

The statistical model that was chosen for the section properties was also a Normal distribution with the mean value equal to the nominal value. The coefficients of variation for the area and section modulus were those given by JCSS [36] and for all other properties the coefficient of variation was taken as 5%.

6.4.2 Welds

6.4.2.1 Weld throat thickness (a)

$$\mu_a = a_{nom} \qquad \delta_a = 15\% \qquad \text{Distribution} = \text{N}$$

The statistical properties of the thickness of the weld were taken from Fisher *et al.* [48]. The parameters recommended were not based on quantitative studies due to a lack of data. With the parameters given, there is a 50% chance that the shear area of the weld will be within 10% of the specified area, which

was considered to be a conservative assumption [48].

6.4.3 Concrete column

6.4.3.1 Column dimensions

$$\mu_y = +1.59\,\text{mm} \qquad \sigma_y = 6.35\,\text{mm} \qquad \text{Distribution} = \text{N}$$

A study on the statistical parameters of rectangular columns with nominal dimensions from 280 - 760 mm was carried out by Mirza *&* MacGregor [47]. A Normal distribution for the error on column cross sectional dimensions was recommended, with the parameters given above.

Ellingwood *et al.* [32], MacGregor *et al.* [42] and Grant *et al.* [44] use the statistical model given by Mirza *&* MacGregor [47] for the cross sectional dimensions. Ellingwood *et al.* [32] further state that the standard deviations are independent of the size of the member, therefore the models based on columns with dimensions 280 - 760 mm can be applied to the concrete column under consideration here with cross sectional dimensions 450 × 1500 mm.

JCSS [36] suggests a Normal distribution with the range of parameters given below.
Mean:

$$0 \leq \mu_y \leq 0.003 x_{\text{nom}} \leq 3\,\text{mm}$$

$$\therefore \mu_{y,(h\,=\,1500)} = +3\,\text{mm} \qquad \mu_{y,(b\,=\,450)} = +1.35\,\text{mm}$$

Standard deviation:

$$\sigma_y = 4 + 0.006 x_{\text{nom}} \leq 10\,\text{mm}$$

$$\therefore \sigma_{y,(h\,=\,1500)} = 10\,\text{mm} \qquad \sigma_{y,(b\,=\,450)} = 6.7\,\text{mm}$$

This model does not reflect what is stated by Ellingwood *et al.* [32], i.e. that the standard deviation is independent of the size of the member and will thus not be used for this investigation.

The statistical model that was chosen for the cross sectional dimensions of the concrete column was that given by Mirza *&* MacGregor [47].

6.5 Loads

6.5.1 Permanent loads

The self weight of a structure is modelled by JCSS [36] as a function of the density and the volume of an element:

$$D = \gamma V$$

The variability of the permanent load is assumed to be due to the inherent variability of the density and volume of a given element. Very small coefficients of variation and bias factors close to one are obtained for this model ($\lambda_D = 1.005, \delta_D = 4\%$). The shortcoming in this model is that it considers aleatory uncertainty only and does not make any allowance for imperfect modelling or prediction. Ellingwood *et al.* [32] state that most designers tend to underestimate the permanent load of a structure and therefore recommend a Normal distribution with the bias factor and coefficient of variation given below. These values allow for both aleatory and epistemic uncertainties.

$$\lambda_D = 1.05 \qquad \delta_D = 10\%$$

A set of Normal distributions was used for the various different permanent loads with the statistical parameters given in Table 6.3. The values of the bias and coefficient of variation reflect the perceived degree of uncertainty in, and difficulty of estimation of, the various permanent loads. Values of the coefficients of variation are taken as less than 10% because the structures dealt with in this investigation are steel structures where the permanent load is easier to estimate than for concrete structures.

Table 6.3: Statistical parameters of the permanent loads

Permanent Load	Bias	c.o.v. %
Sheeting, purlins and utilities, D_s, D_p, D_u	1.02	5
Own weight of the structure, D_o	1.05	8
Crane bridge weight, Q_{br} and crab weight, Q_{cr}	1.02	3

6.5.2 Roof imposed loads

6.5.2.1 Lifetime maximum roof imposed load

$$\mu_R = \frac{R_{nom}}{3.75} \qquad \delta_R = 12.5\% \qquad \text{Distribution} = \text{EV I (Gumbel)}$$

The statistical model for roof imposed loads was taken from de Villiers [52]. Roof imposed loads can be classified into those due to maintenance and those due to construction. The roof imposed load under consideration was that due to maintenance as it was used in combination with the crane running under normal operating conditions. The roof loads were further classified as those imposed on large areas (for frame analysis) and those imposed on small areas (for purlin analysis). As it was the frame that was under consideration here, the statistical model used for the roof imposed load was that derived for maintenance roof imposed loads on large areas.

6.5.2.2 Point-in-time roof imposed load

The point-in-time roof load is assumed to be equal to zero for the combination with other time varying loads. Maintenance roof loading is not a common occurrence and the chance of roof loading being present when another time varying load is at its maximum is negligible.

6.5.3 Wind loads

6.5.3.1 Lifetime maximum wind load

$$\mu_{v^2} = 0.41 v_{nom}^2 \qquad \delta_{v^2} = 52\% \qquad \text{Distribution} = \text{EV I (Gumbel)}$$

The statistical parameters of the wind loads were taken from Ter Haar & Retief [53]. The statistical model for the wind load was based on the square of the wind speed because the load effects are linear with respect to this value.

6.5.3.2 Point-in-time wind load

$$\mu_{v^2} = 0.05 v_{nom}^2 \qquad \delta_{v^2} = 108\% \qquad \text{Distribution} = \text{EV III (Weibull)}$$

As for the lifetime maximum wind load, the parameters for the point-in-time wind load were taken from Ter Haar & Retief [53].

6.6 Modelling uncertainties

6.6.1 Basis for modelling uncertainties

The response of a structure can be expressed as [36]:

$$Y = f\left(X_1,\ X_2,\ \ldots\ X_n\right) \tag{6.6.1}$$

Where:

Y – structural response

X_i – basic variables

f – model function

Generally the model function does not completely and exactly describe the physical process thus some errors are induced in the structural response Y. The real outcome of an experiment can be expressed as:

$$Y' = \theta f\left(X_1,\ X_2,\ \ldots\ X_n\right) \tag{6.6.2}$$

Where:

θ – modelling uncertainty

Modelling uncertainties arise because of:

- random effects neglected in the models
- simplification in mathematical relations
- neglecting 3D effects
- inhomogeneities in the material
- simplifications of connection behaviour

Ideally modelling factors should be obtained from many laboratory tests or measurements on actual structures where the random variables are measured, then the only uncertainties are the uncertainties inherent in the model. If the number of measurements is small then there will be some statistical uncertainty as well. Additional uncertainty could arise due to measurement errors in Y and X. Ellingwood *et al.* [32] combine the uncertainties due to measurements with the modelling uncertainty in the following way:

$$\delta_{T/C} = \sqrt{{\delta_m}^2 + {\delta_{test}}^2 + {\delta_{spec}}^2} \tag{6.6.3}$$

Where:

$\delta_{T/C}$ – variability in the ratios of test values to calculated values.

δ_m – variability of the model.

δ_{test} – variability in the measurements during the test, i.e. measurement errors in Y.

δ_{spec} – variability in the measurements of the test specimens, i.e. measurement errors in X.

This gives the modelling uncertainty as:

$$\delta_m = \sqrt{\delta_{T/C}^2 - {\delta_{test}}^2 - {\delta_{spec}}^2} \tag{6.6.4}$$

6.6.2 Distributions for modelling uncertainties

6.6.2.1 Introduction

The different modelling processes that are involved in calculating the loadings and resistances have been identified and treated separately. This allows the contribution of each individual modelling process to the overall reliability to be investigated. The modelling processes were identified as the calculation of the loads, the calculation of the load effects and the calculation of the resistances.

The methods followed for determining parameters for the modelling uncertainties can be summarised as follows:

1. In the case when information is available, the parameters are based on an assessment of the information.

2. In the case when no information is available two levels of parameter selection can be considered:

   a) Engineering reasoning and judgement can be employed for the selection of parameters. This could include consultations with experts.

   b) Nominal provision can be made for modelling uncertainties by applying a modelling factor with no bias and an upper bound of the coefficient of variation.

The modelling uncertainties that are critical for the reliability should be identified and more emphasis placed on determining accurate parameters of these uncertainties.

The three modelling processes are discussed below with their specific applications. The statistical parameters of the modelling uncertainties are given for each application.

Lognormal distributions were used for the modelling uncertainties as recommended by JCSS [36] for modelling uncertainties which are applied by multiplication, as shown in the equation below from Chapter 5, rather than by addition.

$$Q_i = c_i \theta_i A_i \tag{6.6.5}$$

Where:

Q_i – load effect

c_i – influence coefficient for calculation of load effects

θ_i – modelling uncertainty in the calculation of the load effect

A_i – applied load

The mean value of the modelling uncertainty will be referred to as the bias, λ, because it indicates the bias with respect to the expected value of the calculation model.

6.6.2.2 Crane loads

There was no information available on the model accuracy of the calculation models for the crane wheel loads so the parameters of the modelling factors were selected on the basis of reasoning.

6.6.2.2.1 Vertical wheel load

$$\lambda = 0.95 \qquad \delta = 5\%$$

The bias factor for the vertical wheel load was taken as less than one because the dynamic factors model the maximum vertical force that will occur, which will be greater than the mean values.

The vertical crane loads are calculated using simple vertical equilibrium and as such the uncertainty in the calculation procedure is small. The assumption is made, that all the crane wheels are in contact with the rails and each wheel is treated as a simple support. It is possible for one wheel to lift from the rail in the case where the girders are misaligned vertically or the girders on each side of the runway are of different lengths causing unequal deflections. In the case where one wheel lifts off the rail, the remaining wheels will carry a greater load. This phenomenon was thought to be most critical for cranes with four wheels because cranes with eight or sixteen wheels have spreader mechanisms between the wheels to distribute the load more evenly.

An assessment was carried out of four crane configurations (outlined below) to determine the percentage increase of the maximum wheel load from removing the support at one wheel or lowering the wheel by a given amount.

1. Single I girder crane, 8 m span
2. Single box girder crane, 8 m span
3. Double box girder crane, 8 m span
4. Double box girder crane, 24 m span

The cranes were modelled in a finite element analysis with the crab at the extreme of its travel carrying the hoistload. One of the wheels on the far side of the crane, furthest away from the hoistload, was either removed or lowered by 5 or 10 mm. A displacement of 10 mm was considered to be a reasonable maximum because the tolerances of vertical girder alignment given by SAISC [29] state that the maximum relative vertical misalignment of crane girders is 10 mm. The percentage increase of the maximum wheel load and, where applicable, the displacement of the wheel, were noted. The results are given in Table 6.4 below.

Table 6.4: Investigation into vertical wheel load modelling uncertainty

Crane configuration	Wheel support removed		Wheel lowered by	
			5 mm	10 mm
	% increase	displacement	% increase	% increase
1	N/A crane too flexible		0.02	0.03
2	25	41.28 mm	3	6
3	33	27.5 mm	6	12
4	20	47.0 mm		4.4

As can be seen from Table 6.4, the stiffer the crane, the greater the increase of the maximum wheel load. The maximum percentage increase of 33% was for the stiffest crane (double box girder, 8 m span). This was accompanied by a 27.5 mm displacement of the wheel which was considered unreasonably large.

If the worst case is considered to be a displacement of 10 mm and the crane configuration taken as a double box girder short span crane, then the percentage increase of 12% can be considered the upper limit. A coefficient of variation of 5% for the vertical load would mean that the worst case would lie 2.4σ away from the mean and would have a 1.09% chance of occurring which was judged to be reasonable.

6.6.2.2.2 Horizontal wheel loads

$$\lambda = 1.0 \qquad \delta = 15\%$$

The load models for the horizontal loads are much more complex and less transparent than the simple equilibrium used for the calculation of the vertical loads. Therefore it was felt that there was greater uncertainty in the calculation models for the horizontal loads than the vertical loads and this was reflected in the larger coefficient of variation.

6.6.2.2.3 Horizontal longitudinal loads due to buffer forces

$$\lambda = 0.75 \qquad \delta = 10\%$$

A series of tests on end buffer loads was carried out by Kohlhaas [54]. The tests were carried out on a crane with cellular rubber buffers.

Although the buffers considered for the end stop forces for the code calibra-

tion are hydraulic buffers and the tests were carried out with cellular rubber buffers, this test data is the best available data and so will be used for the development of the modelling uncertainty parameters.

Two end stop situations were considered, firstly the end stops being in alignment so the buffers strike the end stops at approximately the same time and secondly, the end stops 20 mm out of alignment in the longitudinal direction so the buffer on one end carriage will strike the end stop before the other side.

Three hoistload positions were considered, firstly the crab in the centre with the hoistload 150 mm from the ground, secondly the crab in the centre with the hoistload 800 mm from the ground and thirdly the crab at one end of the crane bridge with the hoistload 890 mm from the ground.

The force on both end stops, one on each line of rails, were measured. It was found that the end stop forces increased with the height of the hoistload. With the crab on one side of the crane bridge, as expected, the end stop forces on one side of the runway were greater than those on the other side. The same trend was observed when the end stops were offset in the longitudinal direction.

The maximum end stop force, from the forces on each buffer, for each crane run, were analysed to obtain the modelling factor.

The bias values obtained considering the various different hoistload positions are given in table 6.5.

Table 6.5: Bias values for end stop forces

Hoistload position	bias value
crab in centre, hoistload height = 150 mm	0.59
crab in centre, hoistload height = 800 mm	0.61
crab off centre, hoistload height = 890 mm	0.70

As was mentioned before and as can be seen from Table 6.5, as the height of the hoistload increases, the bias increases. The crab positioned on one side of the crane bridge results in a larger bias than the crab positioned at the centre of the crane bridge.

Because of the configuration of the experimental setup, the hoistload could not be lifted to very close under the crane bridge. For this reason, the bias values in the table were considered to be less than the maximum possible bias

values and a bias value of 0.75 was selected for the modelling uncertainty in the calculation of the end stop forces.

The coefficient of variation considering all the end stop forces was 8.77%. The coefficient of variation has been increased to 10% for this analysis, to take into account additional uncertainty included for the fact that the buffers considered for the code calibration are hydraulic buffers and the test data was gathered for cellular rubber buffers.

6.6.2.3 Load effects

6.6.2.3.1 Additional moment due to slenderness in concrete column

$$\lambda = 1.0 \qquad \delta = 5\%$$

The method of calculating the additional moment in the concrete column due to second order effects is given in the South African concrete design code SABS 0100-1:1992 [10]. There was no data available on the accuracy of the method so the parameters of the distribution were estimated.

6.6.2.3.2 Axial stress in flanges of crane girder

$$\lambda = 1.0 \qquad \delta = 5\%$$

For the 40t crane the normal stresses in the girder flanges due to vertical and horizontal crane loads were calculated. The uncertainty in the stresses is mostly due to the uncertainty in the section properties of the girder combined with the elastomeric pad and the rail. The distribution parameters were estimated because no information was available.

6.6.2.3.3 Axial forces from an analysis model

$$\lambda = 1.0 \qquad \delta = 5\%$$

These parameters were taken from JCSS [36].

6.6.2.3.4 Bending moments from an analysis model

$$\lambda = 1.0 \qquad \delta = 10\%$$

These parameters were taken from JCSS [36].

6.6.2.4 Resistances

6.6.2.4.1 Concrete column - biaxial bending and axial force

$$\lambda = 1.10 \qquad \delta = 15\%$$

A bias of 1.20 is suggested by Holický [55] for the resistance of concrete columns. This value was reduced to 1.10 because a more accurate calculation method than the code method was used. The coefficient of variation given by Holický [55] was adopted.

6.6.2.4.2 Steel column - bending and axial force

$$\lambda = 1.10 \qquad \delta = 15\%$$

Table 6.6 gives a summary of the modelling uncertainty parameters in the literature.

Table 6.6: Modelling uncertainty of resistance of steel columns

Failure mode	Bias	c.o.v. %	Reference
In plane strength	1.107	16.4	Kotoguchi *et al.* [56]
Out of plane strength	1.18	14	Kotoguchi *et al.* [56]
In plane strength	0.98	8	Rojiani *&* Woeste [57]
Out of plane strength	0.88	4	Rojiani *&* Woeste [57]
In plane strength	1.07	10	Bjorhovde *et al.* [38]
Bending and compression	1.02	10	Bjorhovde *et al.* [38]
Bending and compression	1.20	10	Holický [55]

The bias ranges from 0.88 to 1.20 and the coefficient of variation from 4% to 16.4%. The parameters given by Rojiani *&* Woeste [57] were neglected because of their vast difference from the rest of the parameters. The value

of the mean selected as 1.10 was considered to be representative of the range given. The value of 15% selected for the coefficient of variation is on the upper side of the values given, in order to reflect the additional uncertainty due to the wide range in the mean values.

6.6.2.4.3 Crane girder - elastic bending

$$\lambda = 1.0 \qquad \delta = 5\%$$

The parameters were taken from JCSS [36] for bending moment capacity of steel members.

6.6.2.4.4 Truss members - axial tension

There is no modelling uncertainty in the resistance of a member to axial tension because the tension model is the same as the tension test coupon so all the variability is assumed to be in the material and the dimensions (Ellingwood *et al.* [32]).

6.6.2.4.5 Truss members - axial compression

$$\lambda = 1.10 \qquad \delta = 10\%$$

The parameters of the modelling uncertainty for the truss members in axial compression was based on the modelling uncertainty for steel columns. The coefficient of variation was reduced from 15% to 10% because of the simpler load case of only axial load, no bending moment.

6.6.2.4.6 Resistance of bolts

$$\lambda = 1.25 \qquad \delta = 15\%$$

These parameters were taken from JCSS [36].

6.6.2.4.7 Resistance of welds

$$\lambda = 1.15 \qquad \delta = 15\%$$

These parameters were taken from JCSS [36].

6.7 Fatigue

The method used for the fatigue analysis was the S-N curve approach. This is one of the methods recommended by JCSS [36] for the consideration of fatigue. Unless otherwise stated, the statistical models for fatigue are those recommended by JCSS [36].

6.7.1 Fatigue resistance

6.7.1.1 Fatigue damage at failure (D)

$$D_{nom} = 1 \qquad \mu_D = 1 \qquad \delta_D = 30\% \qquad \text{Distribution} = \text{LN}$$

6.7.1.2 S-N curve material property (A)

$$\mu_A = \frac{A_{nom}}{\Delta^2} \qquad \delta_A = 58\% \qquad \text{Distribution} = \text{LN}$$

The S-N curves that are given in SANS 10162-1:2005 [11] are given in terms of mean minus two standard deviations on the fatigue life [58]. The method for determining the mean value of the material parameter from a mean minus two standard deviations S-N curve was given by Maddox [59] as:

$$a = \frac{A}{\Delta^d} \tag{6.7.1}$$

Where:

A – the mean minus two standard deviations material factor

Δ – is related to the standard deviation on the fatigue life by: $\sigma = log\left(\frac{1}{\Delta}\right)$

d – number of standard deviations of $log(N)$ away from the mean, in this case $d = 2$.

Values of Δ have been given by Maddox [59] for various fatigue details corresponding to different welded joint configurations. The fatigue detail categories given by Maddox [59] were compared to the fatigue detail categories

for each crane girder fatigue situation as classified by the South African steel design code and the relevant values of Δ were selected as described below.

1. 40t crane girder, fatigue at the bottom of the intermediate stiffeners

   The bottom of the stiffener was classified as detail category C1 which is described as 'Base metal at the toe of transverse stiffener-to-flange and transverse stiffener-to-web welds' according to SANS 10162-1:2005 [11]. This corresponds to detail category E according to Maddox [59], described as: 'Welded attachments on the surface or edge of a stressed member - attachment to girder webs in regions of combined bending and shear'. The value of Δ for this detail category is:

   $$\Delta_E = 0.561$$

2. 40t crane girder, fatigue of the top flange to web weld caused by rotation of the top flange

   The top flange to web weld was classified as fatigue detail B which is described as 'Built up members - Base metal and weld metal in components, without attachments, connected by continuous full penetration groove welds with backing bars removed' according to SANS 10162-1:2005 [11]. This corresponds to detail category F_2 according to Maddox [59], which is described as 'web-to-flange fillet weld in crane girder'. The value of Δ for this detail category is:

   $$\Delta_{F_2} = 0.592$$

3. 5t crane, corbel to column welded connection

   The corbel to column welded connection was classified as detail category C with an additional reduction factor to allow for the fact that it is a transversely loaded fillet weld according to SANS 10162-1:2005 [11]. This detail is also classified as detail category F_2 according to Maddox [59], described as 'fillet welded T joint between plates or built up members, transverse to direction of stress'. The value of Δ for this detail category is given above.

6.7.1.3 Stress level for slope change in S-N curve (S_o)

$$\mu_{S_o} = S_{o,nom} \qquad \delta_{S_o} = 30\% \qquad \text{Distribution} = \text{N}$$

The slopes of the S-N curve were taken as deterministic, the slope of the first part of the curve $m_1 = 3$, and the slope of the second part of the curve $m_2 = 5$. The nominal values of the material properties for both parts of the curve are given in SANS 10162-1:2005 [11] and the nominal value of the slope change in the S-N curve was calculated in the following manner:

$$S_{o,nom} = \left(\frac{A_2}{A_1}\right)^{\frac{1}{m_2 - m_1}} \tag{6.7.2}$$

During the reliability analysis, the material property for the second part of the S-N curve was calculated in the following manner:

$$A_2 = A_1 S_o^{(m_2 - m_1)} \tag{6.7.3}$$

6.7.2 Fatigue loading

6.7.2.1 Modelling factors for stress calculations (B_{glob} and B_{loc})

$$\mu_{B_{glob}} = 1 \qquad \delta_{B_{glob}} = 10\% \qquad \text{Distribution} = \text{LN}$$

$$\mu_{B_{loc}} = 1 \qquad \delta_{B_{loc}} = 25\% \qquad \text{Distribution} = \text{LN}$$

B_{glob} and B_{loc} are the modelling factors for the uncertainties associated with the global and local stress calculations respectively.

6.7.2.2 Fatigue stresses (S)

$$\mu_S = S_{nom} \qquad \delta_S = 25\% \qquad \text{Distribution} = \text{LN}$$

The nominal values of the fatigue stresses in the girder were calculated by simulating the crane running over the gantry and obtaining a stress history for the girder. The stress process obtained was broad-banded therefore a rainflow counting method was used to determine the stress cycles as recommended by JCSS [36]. There was no statistical data given for the stresses obtained by a

rainflow counting method but it was judged that there was some uncertainty in the stresses, therefore a coefficient of variation of 25% was assigned to the stress values. A Lognormal distribution was used in order to prevent the stresses becoming negative.

Sensitivity studies on the effect of the statistical parameters of the fatigue stresses on the fatigue reliability showed that they have a limited effect. Therefore the parameters were not investigated further and were taken as those given above.

6.7.2.3 Number of stress cycles (N)

$$\mu_N = N_{nom} \qquad \delta_N = 20\% \qquad \text{Distribution} = \text{N}$$

There was no statistical model given by JCSS [36] for the number of stress cycles but it was judged that this was an uncertain parameter so a coefficient of variation of 20% and a Normal distribution were assumed.

As with the fatigue stresses, sensitivity studies showed that the statistical parameters of the number of stress cycles have a limited effect on the fatigue reliability therefore the parameters were taken as those given above.

The fact that the sensitivity studies on the fatigue stresses and number of cycles showed that these variables have a limited effect on the fatigue reliability could explain why no statistical models are provided in JCSS [36] for these variables.

6.8 Summary

A summary of all the statistical models is given in Tables 6.7 - 6.11.

Table 6.7: Statistical models for material properties

Material property	Nominal	Mean	c.o.v. %	Distr.
Yield strength of structural steel	300 MPa	315 MPa	10	LN
Modulus of elasticity of steel	200 GPa	Nom	3	N
Shear modulus of elasticity of steel	70 GPa	Nom	3	N
Bolt ultimate tensile strength	800 MPa	1.2 Nom	7	N
Bolt shear/normal strength	0.60	0.625	5.3	N
Weld ultimate tensile strength	480 MPa	1.05 Nom	4	N
Weld shear/normal strength	0.67	0.84	10	N
Compressive strength of concrete	30 MPa	32 MPa	15	N
Yield strength of reinforcement	450 MPa	510 MPa	6	N

Table 6.8: Statistical models for geometric properties

Geometric property	Mean	c.o.v. %	Distr.
Dimensions of steel members	Nominal	5, $\sigma < 1$ mm	N
Cross sectional area of steel members	Nominal	3.2	N
Section moduli of steel members	Nominal	4	N
Section properties of steel members	Nominal	5	N
Weld throat thickness	Nominal	15	N
Error in concrete column dimension	+1.59 mm	$\sigma = 6.35$ mm	N

Table 6.9: Statistical models for loads

Load	Bias	c.o.v. %	Distr.
Permanent load (sheeting, purlins, utilities)	1.02	5	N
Permanent load from structure self weight	1.05	8	N
Crane self weight (bridge and crab)	1.02	3	N
Lifetime maximum roof imposed load	1/3.75	12.5	EV I
Point-in-time roof imposed load	0		
Lifetime maximum wind load	0.41	52	EV I
Point-in-time wind load	0.05	108	EV III

Table 6.10: Statistical models for modelling uncertainties

Model	Bias	c.o.v. %	Distr.
Vertical crane wheel loads	0.95	5	LN
Horizontal crane wheel loads	1.00	15	LN
Longitudinal crane buffer forces	0.75	10	LN
Second order moment in concrete column	1.00	5	LN
Axial stress in crane girder flanges	1.00	5	LN
Axial forces from an analysis model	1.00	5	LN
Bending moments from an analysis model	1.00	10	LN
Concrete column resistance	1.10	15	LN
Steel column resistance	1.10	15	LN
Crane girder resistance to bending	1.00	5	LN
Roof truss member resistance to tension	1.00	0	
Roof truss member resistance to compression	1.10	10	LN
Bolt resistance	1.25	15	LN
Weld resistance	1.15	15	LN

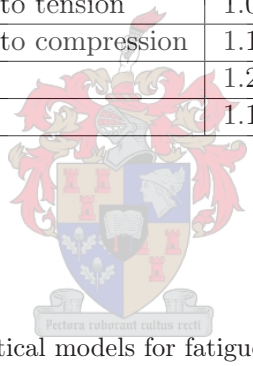

Table 6.11: Statistical models for fatigue analysis

Property	Mean	c.o.v. %	Distr.
Miner's sum at failure	1	30	LN
S-N curve material property	A_{nom}/Δ^2	58	LN
40t crane intermediate stiffener	$\Delta = 0.561$		
40t crane top flange to web weld	$\Delta = 0.592$		
5t crane corbel to column weld	$\Delta = 0.592$		
Slope change in S-N curve	Nominal	30	N
Global stress calculation uncertainty	1	10	LN
Local stress calculation uncertainty	1	25	LN
Fatigue stresses in the girder	Nominal	25	LN
Number of stress cycles	Nominal	20	N

Pectora roborant cultus recti

Chapter 7

Stochastic modelling of crane hoistload

The new stochastic models that were developed for the code calibration were the models that describe the hoistload lifted by the crane. The stochastic models that are required for the hoistload are those that represent 'arbitrary point-in-time' models as well as extreme value type models.

7.1 'One cycle' distribution

A crane cycle is defined as the crane lifting a load, moving to the position where it puts down the load, unloading and moving to the position where it will lift the next load. The 'one cycle' distribution models the probability distribution of the size of the hoistload for one lift of a load, i.e. one crane cycle. The 'one cycle' distribution can be considered as the frequency distribution of all the loads lifted during the crane lifetime.

Hoistload distributions for grab cranes lifting granular material have been presented by Köppe [13] as a combination of Normal distributions with an upper limit of 1.2 times the safe working load (SWL). Cranes were divided into four classes depending on their intensity of work from light to very heavy and a hoistload distribution was provided for each class of crane. The philosophy in the development of the upper region of the distributions presented by Köppe [13] was that if too large a load was lifted, some of the granular material could be released until the load was just of a size where it could be lifted without triggering the overload limit switch. This caused a concentration of loads in

the region of the overload limit.

Most of the overhead travelling cranes in South Africa have hooks as their load lifting mechanism (see Chapter 3) and the characteristics of loads lifted by a hook differ from loads in the form of granular material lifted by a grab in that they are of a set size and cannot be adjusted, as with a granular material, to be just within the overload limit. Distributions of loads lifted by hook cranes would therefore not have such a concentration of loads around the overload limit. It was also unclear whether the value of 1.2 SWL for the upper limit was reasonable for hook cranes in South Africa.

For these reasons, the hoistload distributions presented by Köppe [13] were not considered to be suitable for the purposes of the calibration process and new models were developed.

In the development of the new hoistload distributions, information was obtained from crane manufacturers and operators about the upper limit and the distribution of loads lifted. Cranes were again divided into four classes, as given by Dunaiski *et al.* [26], described as:

1. Light – rarely lifts the SWL and normally only small proportions of the SWL
2. Medium – fairly frequently lifts the SWL and normally moderate proportions of the SWL
3. Heavy – frequently lifts the SWL and normally high proportions of the SWL
4. Very heavy – regularly lifts the SWL

The class one and two cranes are generally workshop and maintenance type cranes where the level of control over the usage of the crane is relatively low. Class three cranes are generally process cranes and class four cranes are typically ladle cranes in metal works where the level of control over the usage of the crane is higher.

7.1.1 Type of distribution

In the modelling of the loads lifted by cranes, it was judged to be reasonable to use a distribution with upper and lower limits. The hoistload lifted cannot be lower than zero and as loads lifted by cranes have a mechanical origin the

upper tail of the distribution cannot tend to infinity as with loads of natural origin.

One hoistload distribution was required to model the distribution of hoistloads lifted by each of the four classes of crane. There were therefore four different shaped distributions to be developed and the distribution type selected for the hoistload distribution was required to be able to easily deal with the different shapes.

The statistical distribution that best fulfilled these requirements was the beta distribution because of the ease of generating the required shape and because the beta distribution has lower and upper bounds.

7.1.2 Upper limit of distribution

All the crane manufacturers and operators stated that the overload limit switches on cranes are set to 10% overload. Overloading of cranes does, however, occur and it is possible to turn off the overload limit switch and to pick up a load greater than 1.1 SWL. This is more likely to occur with the class one and two cranes than the class three and four cranes.

The load that is used as the test load for the commissioning of the crane after installation is 1.25 SWL. The crane operators therefore know that the crane is capable of lifting this load and would be confident to overload the crane to this level but would probably be unwilling to lift loads larger than 1.25 SWL. For this reason, the upper limit of the distribution was chosen as 1.25 SWL.

7.1.3 Shape of distribution

Information was gathered from crane manufacturers and operators in the form of expert opinion giving descriptions of the usage of the crane and histograms of loads lifted. These were used, together with the descriptions of the classes of the cranes, to develop the shapes of the 'one cycle' distributions. Appendix C contains all the information gathered from the manufacturers and operators, i.e. the histograms of loads lifted and descriptions of usage of the cranes.

7.1.3.1 Information gathered from crane operators

The histogram data obtained from the crane operators was based on production records and in one case on measurements of loads lifted. All the histograms

are given in Appendix C. The histograms have been normalised with respect to the SWL.

A class one crane was investigated at a boiler making factory as part of a study carried out by Van der Walt [60]. Instrumentation was fitted to the crane and the loads that were lifted over a four week period were recorded. Four weeks has been determined by Pasternak *et al.* [14] to be the period over which the lifting history of a crane is representative. The histogram for this boiler making crane is shown in Figure C.3.

Three cranes were investigated at a car manufacturing plant, two class two cranes on press lines and a class one maintenance crane. The main duty of the press line cranes is to carry the press tools from the storage area to the press and back again for the tool changes. The maintenance crane is used for moving the tools around the maintenance area.

The histograms were developed by assessing the production information combined with the weights of the tools. For one crane there were 38 different car parts that were manufactured in the press line and for the other crane there were 28. The production data was assessed to determine how many times each car part was manufactured in a given year. It was assumed that the crane lifted the tools required for the manufacture of each part twice for each time the part was manufactured, once to take the tool to the press, and once to take it back to storage. The weights of the tools for each part were known therefore it was possible to determine how often the cranes lifted a particular weight. The histograms for the two press line cranes are given in Figures C.4 & C.5.

The histogram for the maintenance crane was developed based on the assumption that each tool requires an equal amount of maintenance. Each tool consists of two parts, an upper part and a lower part. It was assumed that the maintenance crane lifted the entire tool and each part of the tool, an equal number of times. The weights of all the tools were known and these were used to develop the histogram. The histogram for the maintenance crane is given in Figure C.1.

Production data was obtained on a class three slab handling crane in a steel works. The data was in the form of delivery records of slabs that had been transferred. The histogram for this crane is shown in Figure C.11.

The other histograms given in Appendix C were generated based on descriptions of the loads that the various cranes lift, obtained from the crane

operators. This is the type of information that would be given to the structural engineer for the design of the support structure. For process cranes with a fixed operating routine, this type of information is more accurate than for maintenance and general workshop cranes.

7.1.3.2 Distribution parameters

Histogram data was available for the class one to three cranes but not for the class four, ladle cranes. The hoistload distributions for classes one to three were therefore based on both histogram data and descriptions given by the crane operators of the loads lifted, whereas the distribution for the class four cranes was based on the range of ladle weights given by the operators.

The parameters of the beta distributions for the class one to three cranes were determined by fitting the shape of the beta distribution to the shape of the histograms of loads lifted and the description of the crane classes. The parameters of the beta distributions for the class four crane were determined by fitting a beta distribution to the information given by the crane operators on the ladle weights for the class four cranes, combined with the description of the crane class. Each class will be discussed in turn below.

Figures 7.1 - 7.3 show histograms of loads lifted and the beta distributions for crane classes one to three. The distributions and histograms have been normalised with respect to the SWL.

Class 1: The definition of class one cranes is that they rarely lift the SWL and normally only small proportions of the SWL. The peak of the class one distribution was therefore chosen as a small proportion of the SWL, taken as 16% SWL, which corresponded well to the peak of the histogram. The upper tail of the distribution was modelled so as to reflect the fact that class one cranes will rarely lift the SWL. The probability given by the chosen beta distribution of the class one crane lifting a load equal to or greater than the SWL is 1.25%, which was judged to represent rarely lifting such large loads.

An example of an histogram of loads lifted for a class one crane is shown in Figure 7.1. Most loads that were lifted were in the region of 0.1 to 0.6 SWL which corresponds well with the beta distribution for this class.

Class 2: The definition of the class two cranes is that they fairly frequently

lift the SWL and normally moderate proportions of the SWL. The peak of the class two distribution was taken as 56% SWL. The probability of the class two cranes lifting the SWL is higher than the class one cranes and this is modelled in the upper tail of the beta distribution.

An histogram of loads lifted by a class two crane is shown in Figure 7.2 along with the beta distribution for the class two cranes. The histogram is symmetrical with the peak at 0.6 SWL which corresponds well to the beta distribution.

Class 3: The definition of the class three cranes is that they frequently lift the SWL and normally high proportions of the SWL. The peak of the class three distribution, representing 'high proportions of the SWL' was taken as 80% SWL.

An histogram of loads lifted by a class three crane is shown in Figure 7.3 together with the beta distribution. Most of the loads lifted are in the region of 80% to 100% SWL which corresponds well with the beta distribution.

Class 4: The definition of the class four cranes is that they regularly lift the SWL. The information given by two crane operators about the loads lifted by the class four, ladle cranes was that the ladle weights range from 98% SWL to 110% SWL with most ladle weights being equal to the safe working load. The beta distribution was fitted to the descriptions by the peak being at the SWL and setting the lower limit at 90% SWL. From the beta distribution, the probability that a class four crane would lift loads equal to or greater than the SWL is 58%.

The parameters of the beta distributions, for the 'one cycle' distributions, are summarised in Table 7.1.

The 'one cycle' distributions for classes one to three are shown in Figure 7.4(a). The 'one cycle' distribution for class four cranes is given in Figure 7.4(b). The distributions have been normalized with respect to the SWL.

Figure 7.5 shows an enlargement of the upper tails of the 'one cycle' distributions for all four classes of crane. The class one and two cranes are typically more general use cranes, such as maintenance or workshop cranes, rather than fixed process cranes as for the class three and four cranes. The class one and two cranes therefore have less control over their usage and it is more likely

than for the class three or four crane for the overload limit switch to be turned off and to lift loads higher than SWL. The upper tails model the greater level of control over the usage of the class three and four cranes than the class one and two cranes.

Table 7.1: Parameters of 'one cycle' beta distributions

			Shape factors	
	lower bound	upper bound	q	r
Class 1	0	1.25	1.3	3
Class 2	0	1.25	3.2	3.7
Class 3	0	1.25	8	4.9
Class 4	0.9	1.25	3.5	7

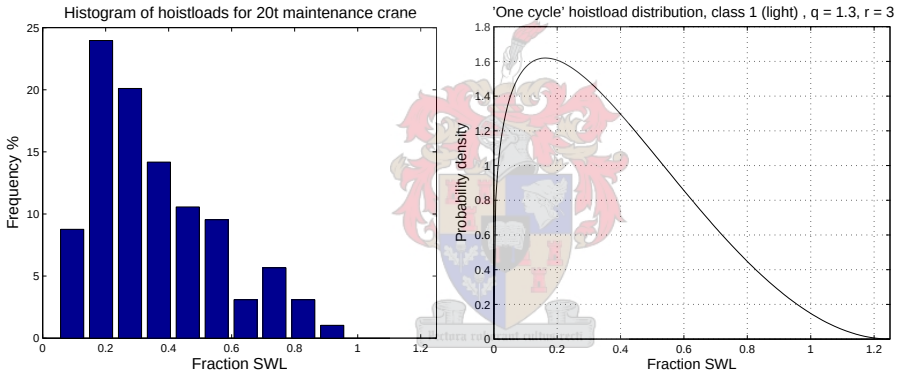

(a) Histogram of hoistloads (b) Beta distribution

Figure 7.1: Class 1 crane 'one cycle' distribution

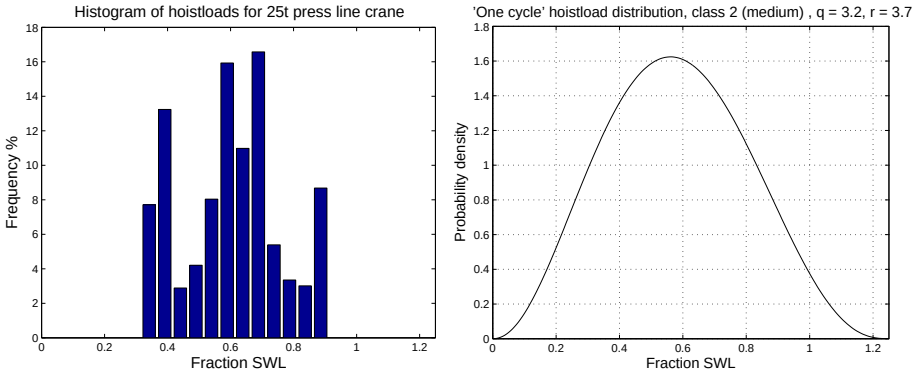

(a) Histogram of hoistloads (b) Beta distribution

Figure 7.2: Class 2 crane 'one cycle' distribution

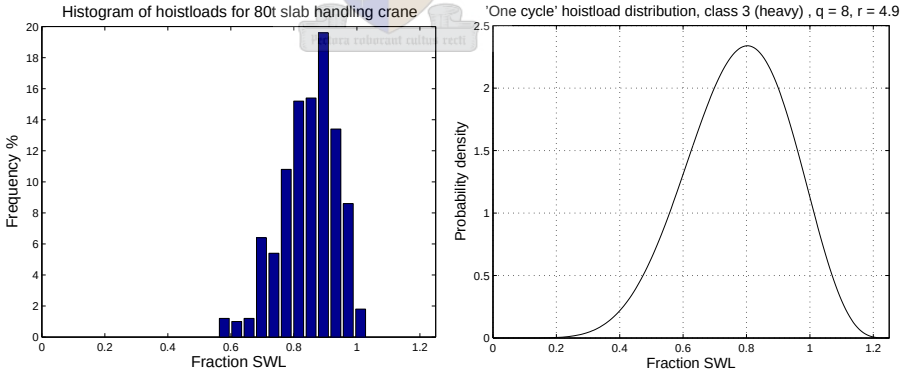

(a) Histogram of hoistloads (b) Beta distribution

Figure 7.3: Class 3 crane 'one cycle' distribution

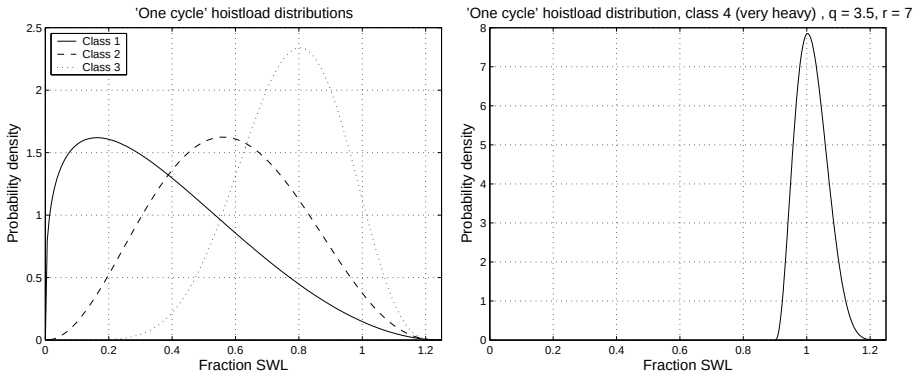

(a) Classes 1 to 3 (b) Class 4

Figure 7.4: 'One cycle' distributions for all crane classes

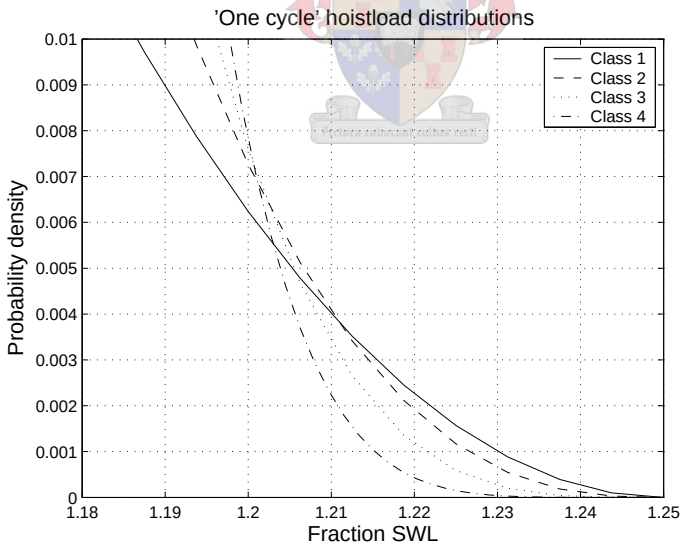

Figure 7.5: Upper tails of 'one cycle' hoistload distributions

7.2 Extreme hoistload distributions

Two possible types of extreme value distributions were identified: either an extreme value distribution for the wheel load or an extreme value distribution for the hoistload.

The method of calculating the vertical wheel load for a four wheel crane is given in Equation 7.2.1

$$Q_{max} = \frac{1}{2}\left[\frac{Q_{br}}{2} + \frac{L-y}{L}\left(Q_{cr} + Q_h\right)\right] \tag{7.2.1}$$

Where:

Q_{max} – maximum vertical wheel load

Q_{br} – weight of the crane bridge

Q_{cr} – weight of the crab

Q_h – weight of the hoistload being lifted

y – distance of the crab from the wheel being considered

L – span of the crane bridge

The four parameters that can be considered as basic variables are the weights of the crane bridge, crab and hoistload and the position of the crab on the bridge. The same four parameters were identified in the calculation of the horizontal wheel loads. The methods of developing the two possible types of extreme value distributions are discussed below.

1. Extreme value distribution for the wheel load. This extreme distribution could be developed by simulating 'one cycle' hoistloads, self weight values and crab positions to generate histories of crane wheel loads. A distribution could be fitted to the extreme 'observed' wheel loads and the wheel loads would be considered as random variables for the reliability analysis.

2. Extreme value distribution for the hoistload. The reliability analysis would be carried out considering the crane self weight and hoistload as basic variables. The position of the crab would be considered deterministic at some point along its travel. The wheel loads would be calculated during the reliability analysis process.

The second approach was adopted for this code calibration procedure. The motivation for using this approach is outlined below.

1. The second approach enables the sensitivity of the reliability analysis to the individual variables to be assessed. The first approach of extreme value distributions for the wheel loads loses the information about the relative importance of the separate variables.

2. Developing extreme value distributions for the wheel loads combines the crane parameters into one basic variable. This would require new models to be developed for each crane considered. Developing an extreme value distribution for the hoistload only, results in more generic models which can be used for any crane. The extreme value hoistload distributions could be used for future code calibration or reliability assessment work on crane loading.

The position of the crab was treated as a deterministic variable and was taken conservatively as at the extreme of its travel closest to the wheel being considered.

7.2.1 Basis for development

The basis for the development of the extreme hoistload distributions was that structural reliability is always considered with reference to a given time period. The extreme distributions model the probability distribution of the largest load that will occur in the time period considered and are therefore dependent on the given time period. When considering crane loads, the extreme hoistload distributions are dependent on the number of crane cycles carried out during the given time period.

The extreme hoistload distributions are referred to by the number of cycles considered (N_{extr}), e.g. a '100 cycle' hoistload distribution is the probability model for the size of the largest load that will be lifted in 100 crane cycles, i.e. $N_{extr} = 100$.

The value of N_{extr} depends on the limit state and load combination being considered. For the ultimate limit state when crane loads are the leading load, N_{extr} would be the total number of cycles a crane would perform during its lifetime. When the crane load is the accompanying load for combination with wind, N_{extr} would be the number of cycles that the crane would perform

during the extreme wind event. In the case of the accidental load situation of the crane running into the end stops, the number of times during the crane lifetime that this will occur is estimated and that number of cycles is used as N_{extr} for determining the hoistload distribution for the accidental limit state. In this way it is relatively simple to obtain appropriate hoistload distributions for any limit state and for the combination of crane loads with other loads or combinations of more than one crane.

7.2.2 Method of development

A simulation technique was used for the development of the extreme hoistload distributions. A set of hoistload values was generated from the 'one cycle' distribution for a given number of cycles, N_{extr}, and the largest value from that set was selected as the extreme value, H_{extr}. This process was repeated E_n times to obtain a set of E_n number of extreme values.

For N_{extr} less than 1000, there was a greater spread in the extreme values and a greater E_n was required to determine the extreme hoistload distribution parameters than for N_{extr} greater than 1000. For N_{extr} less than 1000, the number of extreme values generated was $E_n = 3000$ and for N_{extr} greater than 1000, the number of extreme values were generated was $E_n = 200$.

Histograms of extreme values generated for a class one crane for N_{extr} = 100, 1000 and 3000 are shown in Figures 7.6 - 7.8 where it was observed that as N_{extr} increases, the mean value of the extreme hoistload increases and the standard deviation decreases.

A linear relationship between the log of the cycles and the log of the standard deviations was obtained. Polynomials were fitted to the curves for the trend of the mean values. The trend lines allow interpolation and extrapolation of the mean values and standard deviations for a given value of N_{extr}. Extrapolation is valid up to two million cycles.

The trends of the mean values and standard deviations are shown for the four crane classes in Figures 7.9 & 7.10. The trend lines were plotted from extreme values generated for N_{extr} ranging from 30 to 300 000 and extrapolation was carried out to two million cycles. Equations for the trends of the mean values and standard deviations are given in Appendix C.

The extreme hoistloads generated were plotted on probability paper so as to investigate the best distribution type to use for the extreme hoistloads. The coefficients of skewness of the sets of extreme hoistloads were all very close to

zero indicating that a Normal distribution could be considered. Figure 7.11 shows extreme hoistload values for $N_{extr} = 3000$ for a class one crane plotted on Normal probability paper and it was observed that there is a good fit to a Normal distribution.

The 'one cycle' distributions have an upper bound at 1.25 SWL which means that the extreme hoistloads have the same upper bound. The final distribution type that was chosen for the extreme hoistload distributions was a truncated Normal distribution with an upper limit of 1.25 SWL.

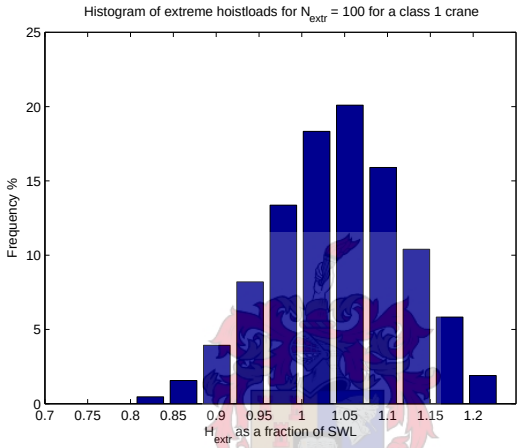

Figure 7.6: Histogram of extreme hoistloads for $N_{extr} = 100$

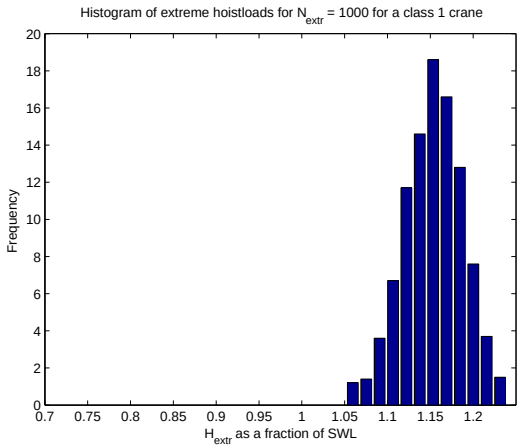

Figure 7.7: Histogram of extreme hoistloads for $N_{extr} = 1000$

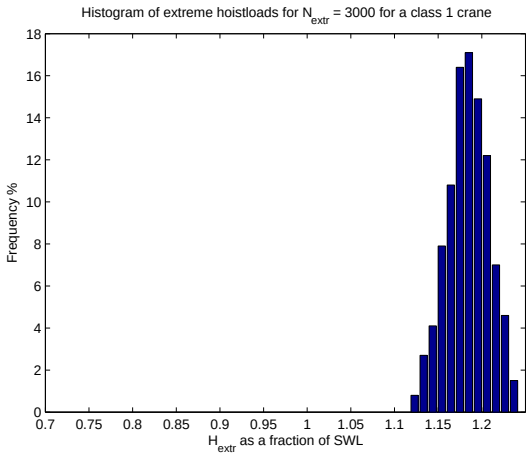

Figure 7.8: Histogram of extreme hoistloads for $N_{extr} = 3000$

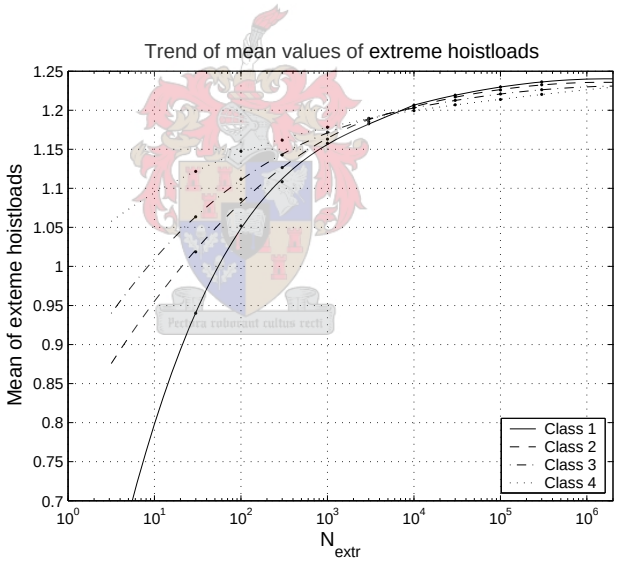

Figure 7.9: Trend of the mean values of the extreme hoistload distributions

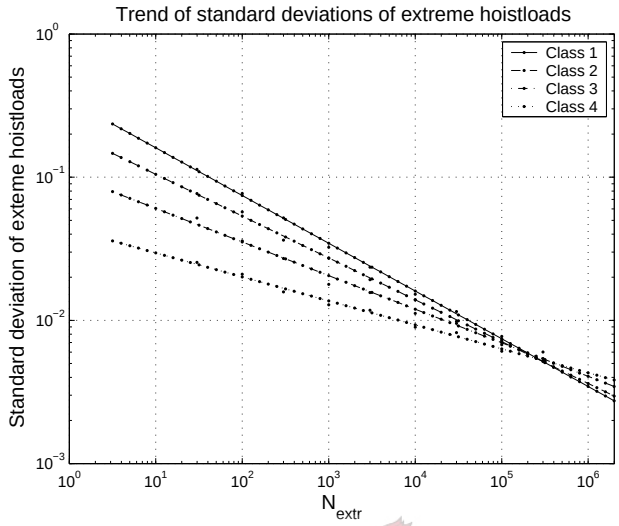

Figure 7.10: Trend of the standard deviations of the extreme hoistload distributions

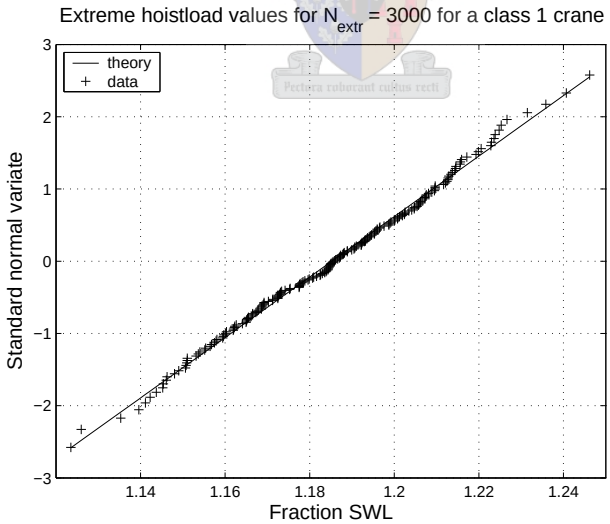

Figure 7.11: Normal probability plot of extreme hoistload values

The cumulative distribution functions of the extreme hoistload distributions are shown in Figure 7.12 for all the crane classes for various values of N_{extr}.

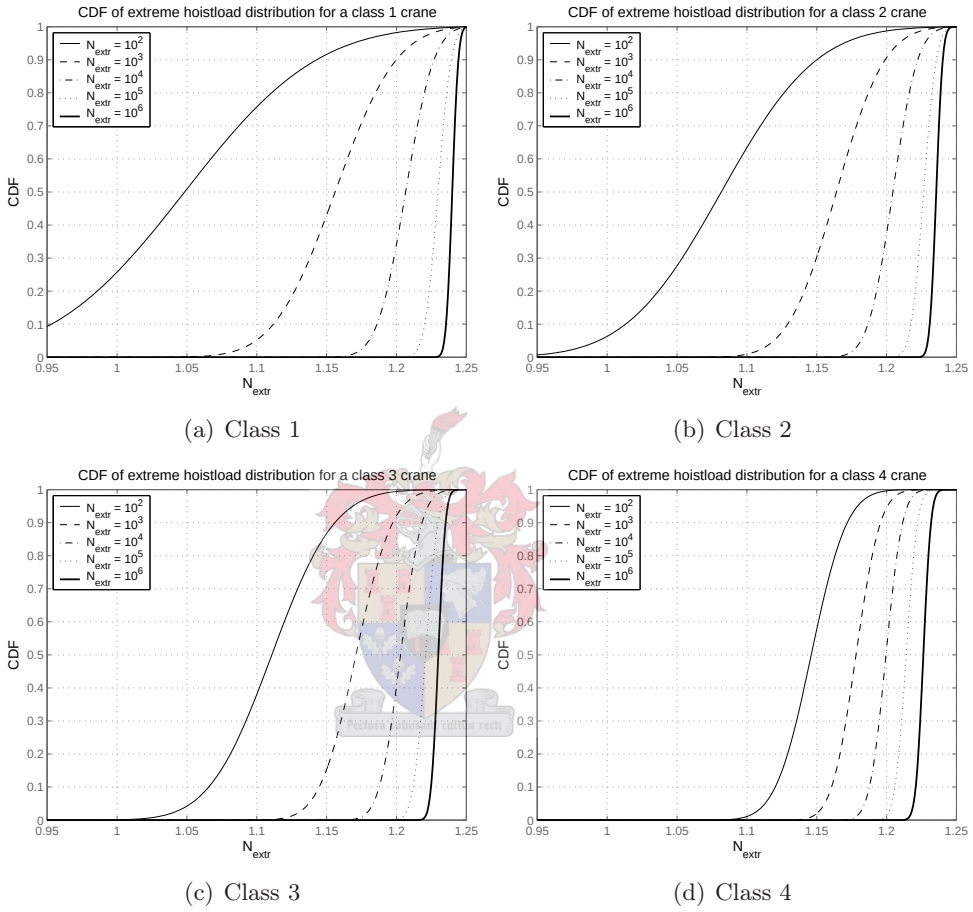

(a) Class 1 (b) Class 2

(c) Class 3 (d) Class 4

Figure 7.12: Cumulative distributions functions for extreme hoistload distributions

7.3 Summary

The stochastic models of the loads lifted by a crane were discussed. Both arbitrary point-in-time models as well as extreme value type models were developed.

Cranes were divided into four classes defined as light, medium, heavy and very heavy. The definitions of the classes were given in terms of the loads that are lifted by the crane.

The first hoistload distribution developed was the 'one cycle' distribution which is the probability distribution of the size of the hoistload for one load lifted, i.e. one crane cycle. The 'one cycle' distribution can be considered to be the frequency distribution of all the loads lifted by a crane over its lifetime.

Information was obtained from crane manufacturers and operators on the loads that are lifted by cranes as well as the level of the overload limit switch. The information was either in the form of production data which could be used to obtain histograms of loads lifted, or descriptions of the loads that are lifted by specific cranes.

The development of the 'one cycle' distributions for the four crane classes was based on the information given by crane manufacturers and operators and the descriptions of the crane classes. Beta distributions were used for the 'one cycle' hoistload distributions.

The extreme value type distributions are the probability distributions of the largest load lifted in a given number of crane cycles (N_{extr}). The extreme hoistload distributions were developed from the 'one cycle' distributions using a simulation technique. Trends of the mean values and standard deviations of the extreme hoistload distributions with respect to N_{extr} were observed. These trends allow the parameters of the extreme hoistload distributions to be determined given a value of N_{extr}. A truncated Normal distribution was shown to be appropriate for the extreme hoistload distributions. The appropriate extreme hoistload distribution can be obtained by using a suitable value of N_{extr} for various limit states and load combinations.

Pectora roborant cultus recti

Chapter 8

Code calibration method

The method of carrying out the code calibration was to perform a reliability analysis, with assumed crane partial load factors, and then to vary the load factors until the reliability met the specified target reliability.

Individual structural elements of the representative structures were considered for the code calibration. Different failure modes for the elements were considered separately, resulting in a value of reliability for each element for each failure mode considered. The probability of failure of the structure was assumed to be equal to the maximum probability of failure of the individual elements.

8.1 Reliability analysis method

The reliability analysis was carried out in two steps: firstly an economic design of the structural element under consideration and secondly the reliability assessment of the economically design member. These two steps will be discussed in detail below.

8.1.1 Economic design

This step entailed designing the member under consideration to exactly comply with the code requirements. Because this is a code calibration exercise, the reliability of the code provisions are of interest and no conservatism in the design of the member can be included.

Conservatism in the design of the member would lead to unconservative code calibration results because the member would be larger (and thus

stronger) than that specified by the code and its reliability would be greater than the code reliability. The reliability of the member is assumed to represent the reliability of the code and the partial load factors are calibrated so that the reliability of the member is equal to the target reliability. If the calibration was carried out on a member which included some conservatism, the calibrated partial load factors would be lower than if the calibration was carried out on a member which didn't include any conservatism, thereby causing the reliability of the code itself to be lower than the target reliability.

The loads imposed on the element for the economic design were the factored design loads and load combinations as specified by the code. Crane loads were taken from prEN 1991-3 [2] and the permanent, wind and roof imposed loads were taken from the South African loading code SABS 0160:1989 [1]. Partial load factors for the crane loads and combination factors for the crane loads and their accompanying loads were assumed. During the calibration process, these factors were varied until the target reliability was achieved.

The resistances of the members were determined by the methods given in the South African steel and concrete design codes, SANS 10162-1:2005 [11] and SABS 0100-1:1992 [10].

The method of carrying out the economic design was to take the member section as it was built in the actual structure and to scale it down, keeping the proportions the same, until its design resistance was exactly equal to the applied design loads. This resulted in impractical member sizes but as this was a theoretical exercise this was not of significance. Practical rounding of the member sizes would have incorporated some conservatism in the member design which is not acceptable as discussed above.

The size of the member obtained from the economic design was used as the nominal size for the reliability assessment. The statistical properties of the member dimensions in relation to the nominal sizes are discussed in Chapter 6.

8.1.2 Reliability assessment

The reliability analysis method was a first order reliability method (FORM) using the Rackwitz-Fiessler procedure of equivalent normal distributions. The FORM analysis was implemented in MATLAB using the matrix method given by Nowak & Collins [15].

Use of FORM is recommended by the Eurocode basis of design prEN 1990 [61] for a Level II type calibration where Level I is a semi-probabilistic method and Level III is a full probabilistic calibration. The initial development of the Eurocodes had an historical and empirical basis and the further development has been based on Level II type calibration [61]. This is thus a recognised and accepted reliability method for use in code calibration.

The reliability analysis was carried out on the economically designed member by considering the actual loads that it was subject to and the real resistance behaviour. The loads and resistances considered for the reliability analysis are discussed in Chapter 5.

8.2 Definition of code objective

The code objective chosen for this code calibration process was the achievement of a target reliability. The target reliabilities vary for the different limit states considered.

8.2.1 Ultimate limit state

A table of fifty year target reliabilities for the ultimate limit state from JCSS [36] is given in Table 8.1. These target reliabilities are based on a cost benefit analysis taking into consideration the relative cost of safety measures and the consequences of failure of the structure.

Table 8.1: 50 year target reliabilities

Relative cost of safety measure	Consequences of failure		
	Small	Moderate	Large
Large	1.7	2.0	2.6
Moderate	2.6	3.2	3.5
Small	3.2	3.5	3.8

The fifty year target reliability used for calibration of the Eurocodes is given in the Eurocode basis of design, prEN 1990 [61] as $\beta_T = 3.8$ where it is stated that the achieved reliabilities should be as close as possible to the target reliability.

The approach taken in the calibration of the South African codes differs from the Eurocodes in that the target reliability is seen as the minimum level of

reliability. The target reliability used in the calibration of the South African codes is given by Kemp *et al.* [9] and Milford [62] as $\beta_T = 3.0$ for ductile failure modes. This target reliability was obtained from the implicit reliability of existing acceptable practice at the introduction of limit states design codes of practice in South Africa.

Due to the fact that this code calibration is for the determination of partial load factors for the crane loads in the proposed SANS 10160, the target reliability that has been selected is that used for calibration of the South African codes of $\beta_T = 3.0$.

8.2.2 Accidental limit state

The accidental load case considered was that of the crane running into the end stops on the end of the runway. The end stop, or buffer, forces are classified in prEN 1991-3 as accidental actions.

It is estimated that, in South Africa, the case of the crane running into the end stops could occur 10 times during the lifetime of the crane. This is too high a probability of occurrence for this load case to be treated as an accidental load situation for which the probability of occurrence should be very small. The load situation of the crane running into the end stops, though classified as an accidental action in prEN 1991-3, will be treated, for the calibration, as an ultimate limit state due to its relatively high probability of occurrence.

When selecting a target reliability for the accidental load situation, the cost of the structural elements which resist the loads and the consequences of failure were considered. The elements that resist the longitudinal buffer forces are the end stops and the longitudinal crane bracing. The cost of these structural elements is only a small proportion of the total cost of the crane and the support structure. Failure of the end stops or longitudinal bracing due to the crane running into the end stops could have large safety or financial consequences due to damage to the support structure or crane and interruption of the industrial process.

The table of target reliabilities from JCSS [36], which relates the relative cost of safety measures to consequences of failure for a 25 year design life, is given in Table 8.2. From Table 8.2, the recommended target reliability for a situation where the relative cost of safety measures is small and the consequences of failure are large is $\beta_T = 4.0$. This is the value that will be

used for the calibration of the partial load factors for the buffer forces due to the crane running into the end stops.

Table 8.2: 25 year target reliabilities

Relative cost of safety measure	Consequences of failure		
	Small	Moderate	Large
Large	2.0	2.3	2.8
Moderate	2.8	3.4	3.6
Small	3.4	3.6	4.0

8.2.3 Fatigue

Guidelines are given in the Eurocode basis of design prEN 1990 [61] on the target reliability for fatigue. The 50 year target reliability for office and industrial type structures is given as ranging from $\beta_T = 1.5$ to 3.8 depending on the degree of inspectability, reparability and damage tolerance. These lower and upper limits of fatigue reliability correspond to the 50 year target reliabilities for serviceability limit state and ultimate limit state respectively. This implies that if the structural element under consideration is easily inspectable, reparable and has a high damage tolerance then fatigue is considered a serviceability limit state, however in the opposite case fatigue is considered an ultimate limit state.

Gulvanessian *et al.* [63] divide structures into damage-tolerant and damage-intolerant with respect to fatigue and state that if a structure is damage-tolerant (i.e. inspectable and reparable) then fatigue may be considered as a serviceability limit state.

Suggestions are given in SANS 2394:2004 [64] on target reliability levels for fatigue. The suggested values range from $\beta_T = 2.3$ to 3.1 depending on the possibility of inspection. The lower value is higher than the lower target reliability value given by prEN 1990. A target reliability of $\beta_T = 1.5$ is given for irreversible serviceability limit states by SANS 2394:2004. The case of elements subject to fatigue being inspectable and reparable cannot be considered an irreversible limit state because with correct maintenance the fatigue damage is reversible, however, it does have maintenance consequences similar to an irreversible serviceability situation.

The elements subject to fatigue in crane support structures are primarily the crane girders and columns, including corbel connections. These elements are generally accessible for inspection and repair therefore in this investigation fatigue will be considered as a serviceability limit state with a target reliability of $\beta_T = 1.5$.

8.3 Definition of code format

The code format is defined by Faber & Sørensen [8] as the number and type of partial load factors, characteristic values of loads, load combination rules and number and type of load combination factors.

Characteristic values of loads are defined in the prEN 1990 [61] as the most representative value of the load and may be taken as a mean value, an upper or lower value or a nominal value which is not statistically based. The characteristic values of the weights of the crane and hoistload in the new proposed code will be kept the same as those specified in SABS 0160:1989. The characteristic values of the crane self weight (bridge and crab) are taken as the nominal values obtained from the crane manufacturer. The most representative value of the hoistload is the nominal capacity of the crane, i.e. the safe working load. Cranes in practice are always referred to by their capacity and so to use any other value as the characteristic value would be confusing for the designer.

The partial load factors, load combination rules and load combination factors will be discussed separately for the different limit states.

8.3.1 Ultimate limit state

The load combination rules and number and type of load combination factors are specified by SABS 0160:1989.

The definition of the code format here will concentrate on the number and type of crane partial load factors. Four code formats were considered and are discussed below in increasing order of complexity.

1. One partial load factor applied to the calculated characteristic wheel loads

   This is the most basic format and constitutes current practice for crane loads, being used in both SABS 0160:1989 and prEN 1991-3. The advantage of this format is its simplicity and familiarity for designers.

2. Two partial load factors, one applied to the crane self weight and one applied to the hoistload

   The next level of complexity in the code formats was to factor the self weight and hoistload separately before the calculation of the design wheel loads. This format takes into account the difference in variabilities of the self weight and hoistload and the higher bias of the hoistload.

3. As for format 1 but with an additional factor applied to the calculated design horizontal loads

   The wheel loads are calculated as for format 1 and the characteristic vertical wheel load is factored by the crane partial load factor while the characteristic horizontal wheel load is factored by the product of the crane partial load factor and the additional partial factor for the horizontal load.

4. As for format 2 but with an additional factor applied to the calculated design horizontal loads

   The crane self weight and hoistload are factored separately as for format 2 and then the design wheel loads are calculated. The horizontal wheel load is then factored further by the additional partial factor.

   Formats 3 and 4 take into account the greater uncertainty in the calculation of the horizontal loads than the vertical loads.

With increasing complexity in the code format, greater consistency is expected in the level of reliability. For practical purposes, this greater consistency should be weighed up against the increased complexity for the designer. One measure that could be implemented to decrease the perceived complexity for formats 3 and 4, would be to include the additional partial factor for the horizontal loads as part of the wheel load calculation procedure instead of treating it separately and explicitly as a partial load factor. The disadvantage in this approach is that it decreases the rationality and transparency of the code.

The partial load factors for each code format are defined in Table 8.3.

8.3.2 Accidental limit state

The two code formats that were considered for the accidental limit state are the same as code formats 1 and 2 for the ultimate limit state.

Table 8.3: Definitions of crane partial load factors

Symbol	Definition
γ_C	Crane partial load factor applied to wheel loads for formats 1 & 3
γ_{Csw}	Crane partial load factor applied to crane self weight for formats 2 & 4
γ_{Ch}	Crane partial load factor applied to hoistload for formats 2 & 4
γ_H	Additional partial load factor applied to horizontal wheel loads for formats 3 & 4

8.3.3 Fatigue

Two fatigue assessment methods have been considered in this investigation, the method recommended in prEN 1991-3 of calculating a fatigue damage equivalent load and the method implied by SABS 0160:1989 where the responsibility rests on the support structure designer to simulate the crane behaviour for the calculation of the fatigue damage.

In the case where both alternatives were given in the code, it would be preferable for the code format to be the same for both methods.

One way of achieving this would be to apply a fatigue partial load factor to the characteristic crane wheel loads. This design wheel load would then be used either for the calculation of the fatigue damage equivalent load, which is directly proportional to the crane wheel load, or for the calculation of the fatigue damage directly in the case when the crane behaviour is simulated. In this way only one partial load format for fatigue need be specified in the code.

The disadvantage in this approach is that currently the fatigue assessment is carried out with unfactored loads, implying a partial load factor for fatigue of $\gamma_F = 1.0$. Changing this could meet with resistance from designers.

An alternative approach, in the case when the fatigue design is carried out using the method given in prEN 1991-3, would be to include the partial load factor in the λ factors given for the calculation of the fatigue damage equivalent load. This would result in a less transparent code but would retain the familiar code format.

8.4 Calibration method

8.4.1 Ultimate limit state

The procedure that was followed for the code calibration was that given by Ter Haar & Retief [53]. The procedure is carried out in two steps:

1. Calibration of the crane partial load factors

   A single load case is considered for the calculation of partial load factors to achieve the target reliability. For this calibration the crane only load case was considered first for the determination of the crane partial load factors.

2. Calibration of the combination factors

   The partial load factors calculated for the single load case are used in combinations of time dependent loads for the calculation of combination factors to achieve the target reliability. The time dependent load combinations considered here were crane with wind loads and crane with roof imposed loads.

8.4.1.1 Calibration of crane partial load factors

The calibration of the crane partial load factors was carried out considering the crane only load case. The elements that were considered were those elements that are subject to predominantly crane loads, i.e. the crane girders and crane columns.

Parametric studies were carried out to determine the effect of important parameters on the reliability. The practical range of each parameter was defined and the value that resulted in the lowest reliability was identified for use in the calibration of the partial load factors and combination factors. The parametric studies for the crane only calibration are outlined below.

1. Class of the crane

   The four classes of crane as allowed for in prEN 1991-3 and as modelled in Chapter 7 were considered.

2. The number of crane cycles considered for the extreme hoistload distribution (N_{extr}).

N_{extr} was considered in the range of 100 to 10^6 cycles. One million cycles was considered a reasonable maximum of the number of cycles a crane is likely to perform over its lifetime. This relates to the crane performing 8 cycles an hour, 16 hours a day, 6 days a week, 52 weeks a year for 25 years.

3. The ratio between the weight of the hoistload and the total weight of the crane (hoistload and self weight).

   In the selection of the representative cranes, the capacities covered the full range of capacities, however, the spans of the representative cranes covered only the most likely values of crane bridge spans with the shortest span being that of the 5t crane at 19.2 m and the longest span being that of the 260t crane at 28.5 m.

   One of the crane properties that is affected by the span of the crane is the ratio of hoistload to total crane weight. The longer the span, the stronger, and hence heavier, the crane bridge needs to be to support the hoistload.

   A database of cranes that includes small standard cranes and large process cranes obtained from various crane manufacturers and operators showed the ratio of hoistload to total crane weight to range from 0.3 to 0.85. The list of cranes together with the ratios of hoistload to total crane weight are given in Appendix D.

   An inspection of the ratios and the crane data shows that as expected, the cranes with higher ratios of hoistload to total crane weight have relatively short spans compared with cranes having a lower ratio of hoistload to total crane weight. The cranes with higher ratios of hoistload to total crane weight are all standard cranes which would probably be class one or two cranes.

4. The load effects caused by the horizontal and vertical crane wheel loads.

   For the investigation of the relative effects of the horizontal and vertical crane wheel loads, different elements were considered that were normally subject to various ratios of horizontal and vertical wheel loads. An element subject only to vertical crane loads was the column for the 5t crane for the load case of crane load combination 1 with maximum vertical loads. An element subject only to horizontal loads was the auxiliary

girder for the 260t crane. This parametric study was of interest for the calibration of code formats 3 and 4 only.

All the elements mentioned above for all the crane only load cases were considered for the parametric studies. Due to the fact that the constraint for the calibration process was that the reliability should always be greater than the target reliability, the scenarios that resulted in the lowest reliability were identified as the critical cases. Crane partial load factors were determined that resulted in the reliability of the critical cases being equal to the target reliability.

8.4.1.2 Calibration of combination factors

The load combination method that was used was Turkstra's rule [65]. The probability distribution of the maximum value of the leading load was considered together with the probability distribution of the maximum value of the accompanying load for the time period when the leading load is active. For example in the case of wind as the leading load and crane loads as the accompanying load, the number of cycles taken for N_{extr} for the hoistload distribution is the number of cycles that the crane is likely to perform during an extreme wind event, e.g. a storm.

The two load combinations that were considered were crane with wind loads and crane with roof imposed loads. The elements that were considered for these load combinations were the frame elements (columns and roof trusses) which were subject to crane, wind and roof imposed loads. Permanent loads were included in the load combinations.

The effect of different resistance modes, and hence different bias and uncertainty values, was investigated by carrying out reliability analyses on the various elements with the same loading conditions. The element with the resistance mode which resulted in the lowest reliability was identified as the critical element and together with the load case which resulted in the lowest reliability, was considered the critical case for the code calibration process.

The values of the parameters for the crane only load case that resulted in the lowest reliability were used for the calibration of combination factors. The additional parametric studies that were carried out for each of the combinations are discussed below.

1. The ratio between the load effect caused by permanent load and the total load effect (e.g. permanent, crane and wind).

   This parametric study was carried out to assess the affect of the permanent load on the reliability. Initially a study was carried out considering only crane and permanent load. From the results of this study, the ratio of permanent load to total load for the combinations was selected.

2. The ratio between the load effect caused by crane load and the load effect caused by crane and wind loads.

3. The ratio between the load effect caused by crane load and the load effect caused by crane and roof imposed loads.

8.4.1.3 Verification of partial load factors

The code calibration was carried out on specific selected critical elements and load cases. This resulted in partial load factors and combination factors for which the reliability of the critical element was equal to the target reliability. In order to verify these partial load factors, reliability analyses were carried out on all the selected elements from the representative structures for all the load cases.

The verification of the partial load factors had two main aims. Firstly to ensure that the correct elements and load cases had been identified as critical, i.e. that the reliability of all the elements was above the target reliability. Secondly to investigate the degree of conservatism induced by calibration to the critical cases and to select the optimal code format.

The degree of conservatism was assessed by carrying out a cost analysis. This was carried out for the crane only load case for the crane girders and columns. Both the columns and the girders for the 5t and 260t cranes were steel so the costs of the elements were expressed in terms of their volume. For the 40t crane where the columns are concrete and the girders are steel, the actual monetary costs of the elements were calculated based on the current rates for steel, concrete and reinforcing given below.

The method followed in calculating the cost for each element was to firstly design the element for each load case and to determine which load case resulted in the largest element (i.e. to find the critical load condition). The reliability of the element subject to the critical load case was assessed. The cost was

expressed in relative reliability terms and the resulting cost has been termed the 'excess cost'. The excess cost was calculated by multiplying the volume (or monetary cost) by the difference between the reliability and the target reliability i.e. Volume $\times$ $(\beta - \beta_T)$ or Cost (R) $\times$ $(\beta - \beta_T)$.

The costs were calculated for three ratios of hoistload to total crane weight, r = 0.3, r = 0.5 and r = 0.85. The three cost values were summed to get the total cost for the element.

Rates for steel, concrete and reinforcing

Concrete R750/ m^3 based on 30 MPa concrete with 19 mm stone

Reinforcing R7/kg

Structural steel R18 500/ton = R145 000/ m^3

8.4.2 Accidental limit state

The accidental load situation that was considered was the crane running into the end stops on the end of the runway. The loads resulting from this load case are horizontal longitudinal forces which are resisted by the longitudinal runway bracing.

8.4.2.1 Parametric studies

The parametric studies that were carried out for the accidental limit state were:

1. The number of cycles considered for the extreme hoistload distribution (N_{extr})

   The extreme hoistload distribution models the probability distribution of the largest load that will be lifted in a given number of cycles. The number of cycles selected for N_{extr} was the number of times that the crane is estimated to run into the end stops during its lifetime. The extreme hoistload distribution then models the largest load that the crane is likely to be lifting when it runs into the end stops.

2. Class of the crane

   A parametric study was carried out on the class of the crane, to determine which class results in the lowest reliability for the number of cycles selected for N_{extr} for the accidental load situation.

3. The ratio of the weight of the hoistload to the total crane weight

   The motivation for this parametric study is the same as for the ultimate limit state.

The longitudinal bracing elements resist the end stop forces and are thus the elements considered for the accidental limit state.

8.4.3 Fatigue

8.4.3.1 Parametric studies

Two parametric studies were carried out for the fatigue reliability analysis.

1. The assessment of the effect of using a single slope versus a double slope S-N curve.

   Reliability analyses were carried out considering both a single slope and a double slope S-N curve and the differences between the results were assessed.

2. The load spectrum class.

   Load spectrum classes Q_2 to Q_5 were considered. A comparison between the different classes was made to determine which class resulted in the lowest reliability.

8.4.3.2 Calibration of fatigue partial load factors

The fatigue provisions in prEN 1991-3 were assessed by calculating the bounds of reliability for a given load spectrum class Q. With reference to Table 2.18 on page 51, the combination of the upper bound for both the load spectrum and the number of cycles gives the lower reliability bound whereas the combination of the lower bound for both the load spectrum and the number of cycles gives the upper reliability bound. The combination of the upper bound for the load

spectrum and lower bound for the number of cycles, or vice versa, results in the intermediate values of reliability.

In this investigation fatigue is considered as a serviceability limit state. Calibration of serviceability limit states is carried out with the average values of reliability rather than the minimum values as for ultimate limit states. This is because serviceability is less of a safety issue and more an economic consideration resulting in a softer performance target for serviceability, where the requirements are satisfied with sufficient performance on average.

The intermediate values of reliability can be considered as the average values as will be explained with reference to Figure 8.1 which depicts one block from the table of fatigue classes, Table 2.18 on page 51.

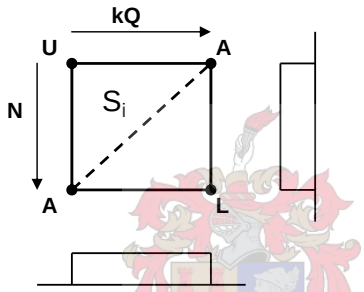

Figure 8.1: Combinations of load spectrum, kQ, and number of cycles, N

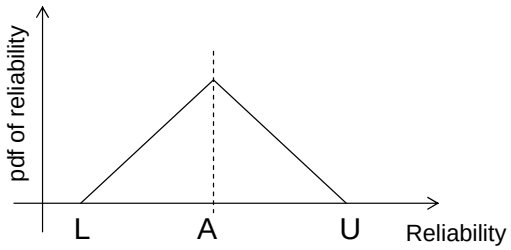

Figure 8.2: Distribution of reliability

If the load spectrum, kQ, and the number of cycles, N, are increasing in the directions shown then the point marked 'U' in the top left hand corner represents the upper bound of reliability with kQ and N at a minimum. Similarly the point marked 'L' in the lower right hand corner represents the lower

bound of reliability. The two points marked 'A' in the upper right hand corner and the lower left hand corner represent the combinations of the minimum of kQ and maximum of N and vice versa. These two points give the intermediate levels of reliability which are the same, or very close, for both points. The broken line joining these two points consists of combinations of kQ and N that also result in this intermediate level of reliability. If the distributions of kQ and N are considered to be uniform then the most likely combinations fall along the dotted line joining the two 'A' points as shown in Figure 8.2. These are therefore the most likely (or average) combinations and will be used for the calibration process. All combinations of kQ and N which are between the diagonal line and the point marked 'U' will have reliabilities between the intermediate line and the upper bound and all combinations between the diagonal line and the point marked 'L' will have reliabilities between the intermediate line and the lower bound.

The method of calibration was to apply a partial load factor to the maximum wheel load before calculating the fatigue damage equivalent load and to assess the reliability of the resulting element. The partial load factor was varied until the average value of reliability was equal to the target reliability.

The calibration of the fatigue partial load factor was also carried out for the second method of fatigue design of simulating the behaviour of the crane. As discussed in Chapter 5, the economic design of the element was carried out according to the prEN 1991-3 fatigue design method and the damage resulting from the simulated crane behaviour was calculated. Using this damage and the calibration results from the prEN 1991-3 fatigue method, the fatigue partial load factor was determined for the fatigue analysis method of simulating the crane behaviour.

8.5 Summary

The two step method of carrying out the reliability analysis was discussed. The first step is the economic design of the member under consideration to ensure that the member is designed to exactly complies with the code requirements with no conservatism included. The second step is the reliability analysis of this economically designed member.

The code objective was defined as meeting a given target reliability. The recommended target reliabilities were considered.

For the ultimate limit state the target reliability was chosen as $\beta_T = 3.0$ as is the norm for the calibration of the South African codes. The accidental limit state was treated as an ultimate limit state because of the relatively high probability of occurrence of the accidental load case, given in prEN 1991-3, of the crane running into the end stops. The target reliability was based on the fact that the cost of the elements which resist the accidental loads is small in comparison to the consequences of failure. A target reliability of $\beta_T = 4.0$ was selected. For these two limit states the constraint was that the reliability must be greater than or equal to the target reliability.

Fatigue was considered as a serviceability limit state with a target reliability of $\beta_T = 1.5$, because crane girders and columns are generally inspectable and reparable. As for serviceability limit states, which are more of an economic consideration than a safety issue, the constraint was that the average reliability for the fatigue should be equal to the target reliability.

The code format was discussed, the characteristic values of the loads and load combination rules have been taken as in SABS 0160:1989. The number and type of partial load factors and combination factors to be considered for the calibration have been defined.

Four code formats were considered for the ultimate limit state considering applying one partial load factor to the calculated characteristic wheel load or two separate factors to the hoistload and self weight before the design wheel loads are calculated. An additional factor applied to the horizontal wheel loads was also included.

The code formats for the accidental limit state consisted of either applying one partial load factor to the calculated characteristic longitudinal load or applying separate partial load factors to the crane self weight and hoistload before calculating the design longitudinal load.

The code format for fatigue consisted of applying a partial load factor to the characteristic crane wheel loads before the calculation of the fatigue damage equivalent load or the simulation of the crane behaviour.

The parametric studies that were carried out for each limit state and load combination were discussed. The parametric studies were carried out to determine the critical values of various parameters to be used in the code calibration.

The parameters that will be assessed for the ultimate limit state for the calibration of the crane partial load factors, are the class of the crane, the number of cycles considered for N_{extr} for the determination of the extreme

hoistload distribution, the ratio of hoistload to total crane weight to take into account shorter or long crane bridge spans and varying ratios of vertical and horizontal wheel loads.

The calibration of the combination factors for the ultimate limit state combinations of permanent and crane with wind or roof imposed loads considered the following parameters for investigation: the ratio of permanent load to total load and the ratio of crane load to crane and wind or crane and roof imposed loads, in order to cover the range of possible loading situations.

The parametric studies that were carried out for the accidental limit state of the crane running into the end stops were the class of crane, the number of cycles considered for N_{extr} and the ratio of hoistload to total crane weight.

The parameters that were investigated for the reliability assessment of fatigue were the use of either a single or double slope S-N curve and the effect of different load spectrum classes as given by prEN 1991-3.

The two step procedure for the calibration of the partial load factors and combination factors for the ultimate limit state was discussed. The first step consists of determining the crane partial load factors by considering the crane only load case. In the second step the combination factors are determined using the calibrated crane partial load factors.

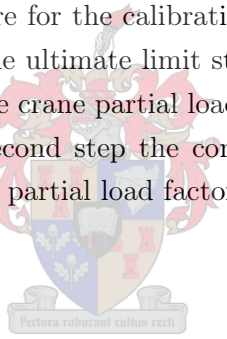

Chapter 9

Code calibration results

Results are presented here of the parametric studies and code calibration of the ultimate limit state, accidental limit state and fatigue.

9.1 Ultimate limit state

The calibration of partial load factors and combination factors for the ultimate limit state was carried out in two stages as discussed in Chapter 8. The first stage was the calibration of the crane partial load factors considering the crane only load case. The second stage was the calibration of the combination factors for crane loads with wind or roof imposed loads using the crane partial load factors determined in stage one.

9.1.1 Crane load only

The elements that were considered for the crane only load case were the crane girders and crane columns. The results of the parametric studies that were outlined in Chapter 8 are given, followed by the calibration results.

9.1.1.1 Results of parametric studies

The first set of parametric studies that was carried out investigated the effect of the class of the crane and the number of cycles taken for the extreme hoistload distribution (N_{extr}). The variation of reliability with N_{extr} was plotted for the four different classes of crane. Values of the partial load factor were assumed for this parametric study. Investigations were carried out for all the crane

girders and columns and the results were found to be consistent for all the cases. Figure 9.1 shows a typical graph with results from this investigation for the 5t crane column considering crane load combination 5 which includes both vertical and horizontal crane wheel loads. The results of this investigation are not influenced by the code format, the value of the crane partial load factor or the ratio of the hoistload to total crane weight. Code format 1 was chosen for simplicity, the value of the crane partial load factor was taken as the value in SABS 0160:1989 of $\gamma_C = 1.6$ and the ratio of hoistload to total crane weight was taken as r = 0.85.

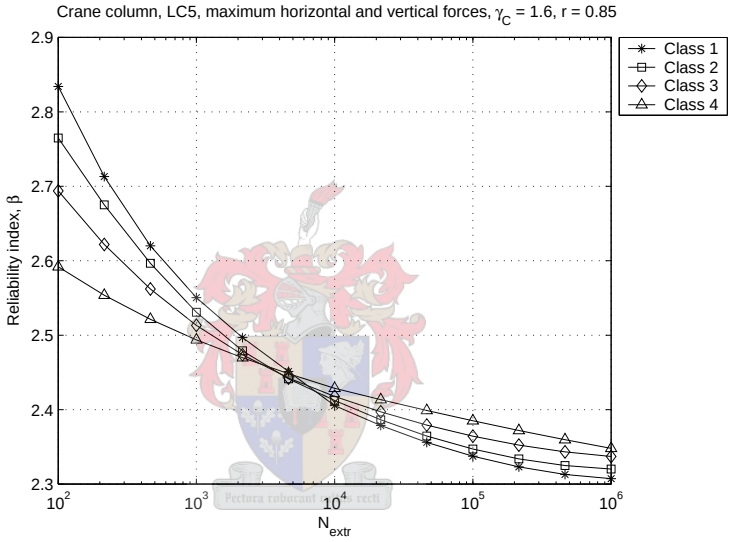

Figure 9.1: Parametric study into class of crane and N_{extr}

It can be seen from Figure 9.1 that the reliability decreases as N_{extr} increases as expected from the trends of the extreme hoistload distributions. The lowest reliability is achieved with a class one crane and N_{extr} equal to one million cycles. These are the values of the parameters that will be used for the code calibration process.

The second parametric study carried out was to investigate the effect of the ratio of hoistload to total crane weight, i.e. the crane self weight and the hoistload. The code format does have an effect in this investigation with a difference in results observed between the code formats that factor the calculated characteristic wheel loads (1 & 3) and the code formats that factor the

hoistload and self weight separately (2 & 4). The inclusion of an additional partial load factor for the horizontal loads, as in code formats 3 & 4 does not have a significant effect on the results of this parametric study. For the sake of simplicity, the results are presented here for code formats 1 and 2 only.

The reliability curves for the horizontal loads from crane load combination 1 (LC1) differed from the curves for the vertical loads from the same load combination and the horizontal and vertical loads from crane load combination 5 (LC5). This is shown in Figures 9.2 & 9.3. Figure 9.2 shows the results for the 260t crane auxiliary girder subject to only horizontal wheel loads from LC1. Figure 9.3 shows the results for the 260t crane main girder for LC5. Figure 9.3 is typical for elements subject to vertical loads from either crane load combination or horizontal loads from LC5. Values of the crane partial factors were assumed for these investigations and are shown in the figures.

The difference between the shapes of the graphs for the auxiliary girder and the main girder is due to the different relative sensitivities of the reliability analysis to the self weight components of the crane and the hoistload. Figure 9.4 shows the variation of the sensitivity factors with the ratio of hoistload to total crane weight for the 260t auxiliary girder and main girder with the same values of the parameters as in the previous figures.

The shape of Figure 9.3 is typical of most of the elements and load combinations. The elements that did not display this behaviour are those dominated by horizontal loads from LC1 and are listed below:

1. 5t crane column with LC1 maximum horizontal loads
2. 40t crane girder with LC1 maximum horizontal loads, stress in the top flange
3. 40t crane girder with LC1 maximum vertical loads, stress in the top flange
4. 40t crane concrete column with LC1
5. 260t crane auxiliary girder with LC1

None of these elements were the critical elements for the calibration so the parametric study focussed mainly on the more typical cases as shown in Figure 9.3.

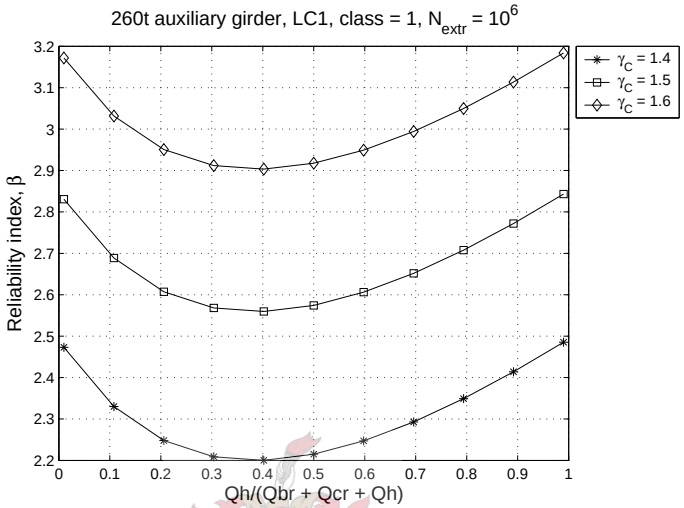

(a) Code format 1

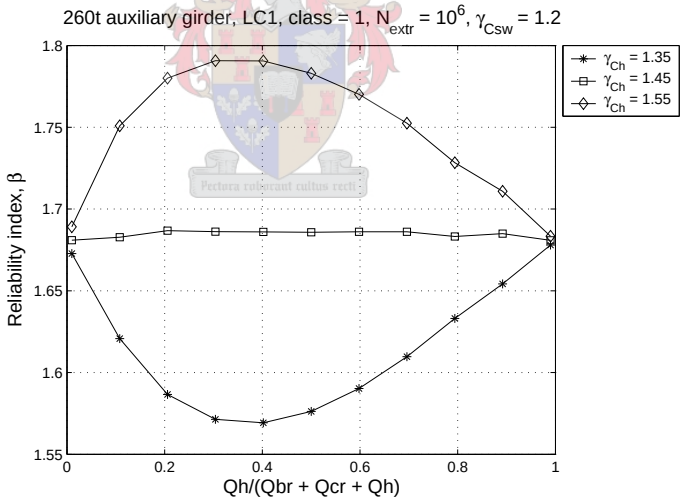

(b) Code format 2

Figure 9.2: 260t crane auxiliary girder, LC1

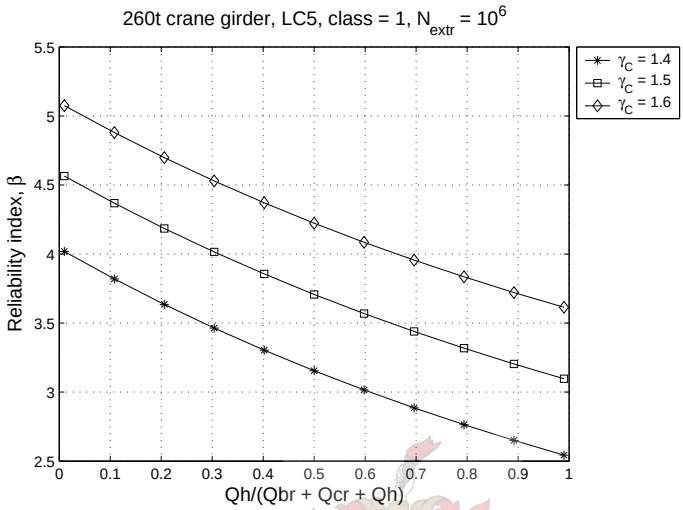

(a) Code format 1

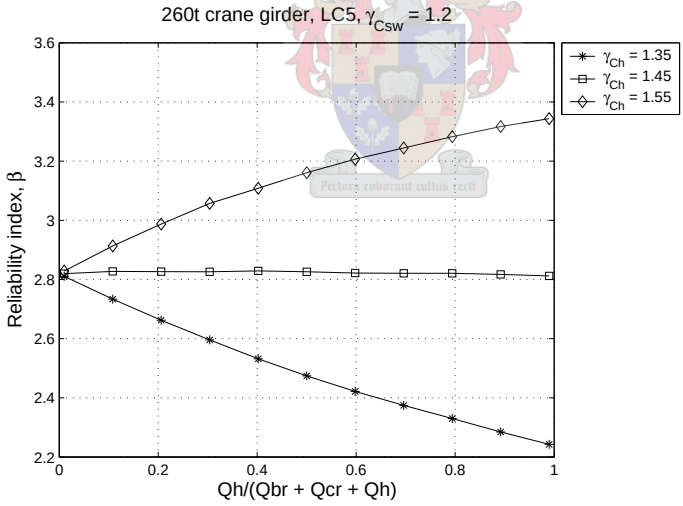

(b) Code format 2

Figure 9.3: 260t crane main girder, LC5

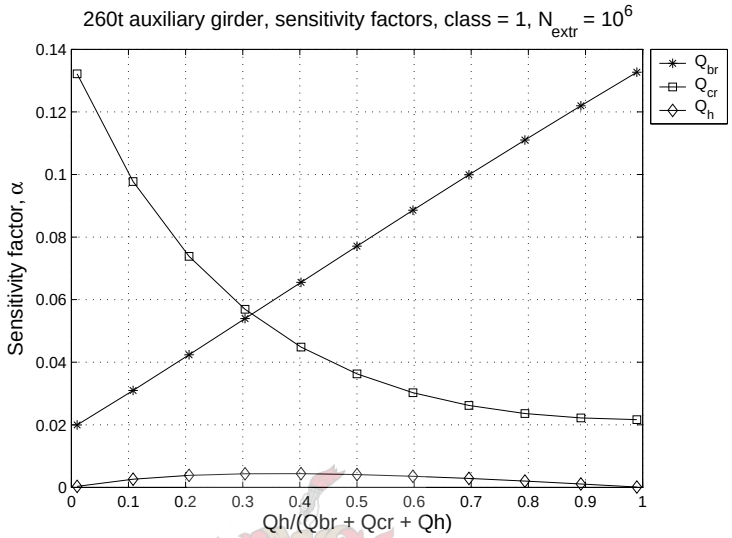

(a) 260t crane auxiliary girder, LC1

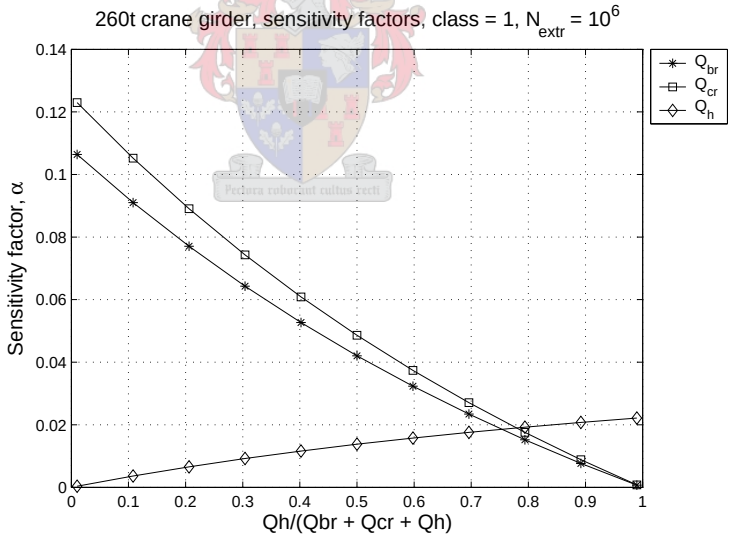

(b) 260t crane main girder, LC5

Figure 9.4: Sensitivity factors for LC1 & LC5

Considering code format 1 and referring to Figure 9.3(a) it was observed that the reliability index decreases as the ratio of hoistload to total crane weight increases. The practical range of ratios is r = 0.3 to 0.85. The lowest level of reliability is obtained at a ratio of r = 0.85 for a class one crane.

The table of crane descriptions with the ratios of hoistload to total crane weight (given in Appendix D) was assessed to determine whether there are class one cranes in the region of higher ratios of hoistload to total crane weight in order to ensure that the combination of class one crane and r = 0.85 is not unnecessarily conservative. It was observed that the cranes in the region of higher ratios of hoistload to total crane weight were all small standard cranes which are likely to be class one or two cranes therefore the combination of a class one crane with r = 0.85 is likely in practice and is thus not over conservative. The value of r = 0.85 is therefore the critical value of this parameter which will be considered for the calibration.

Considering code format 2 and referring to Figure 9.3(b) it was observed that depending on the values of the partial load factors applied to the self weight and hoistload, the reliability either increases or decreases as the ratio of hoistload to total crane weight increases. It can also be seen that it is possible to choose values of the partial load factors so that the reliability remains constant over the range of ratios. This is an advantage of code format 2 in that it is possible to fulfil the code calibration objective of attaining a consistent reliability over a range of parameters.

The next parametric study carried out was to investigate the relative effects of vertical and horizontal crane wheel loads. The element chosen for this investigation was the 5t crane column because of the load situations it is subject to. Two loading situations were considered, LC1 maximum vertical loads (no horizontal loads) and LC5 vertical and horizontal loads. Results of this investigation are shown in Figures 9.5 & 9.6 for code formats 1 and 2 respectively. The value of the reliability index at r = 0.85 is shown on the graphs in Figure 9.5.

It can be seen clearly from Figures 9.5 & 9.6 that the inclusion of horizontal loads leads to a decrease in reliability. For code format 1 from Figure 9.5 the critical level of reliability, with $\gamma_C = 1.5$, for the vertical only load case is $\beta = 2.68$ compared to the vertical and horizontal load case where $\beta = 2.03$. The same is seen for code format 2 in Figure 9.6 where the vertical load only case results in $\beta = 2.35$ compared to the horizontal load case where $\beta = 1.78$.

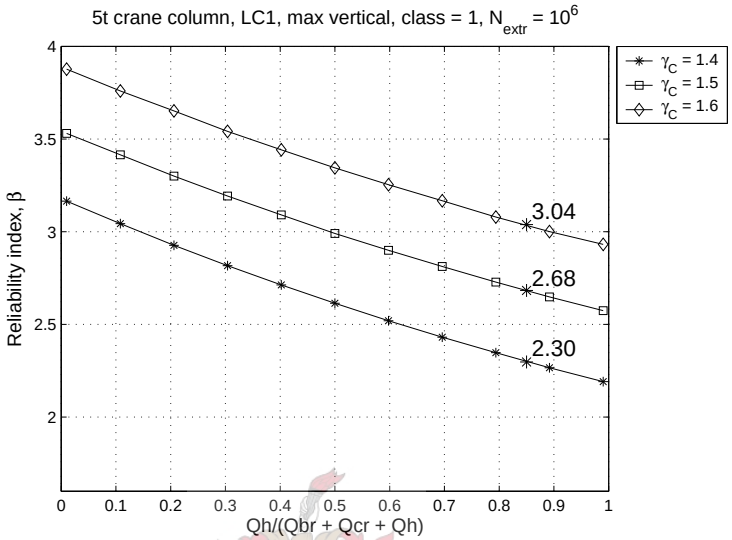

(a) Vertical loads only

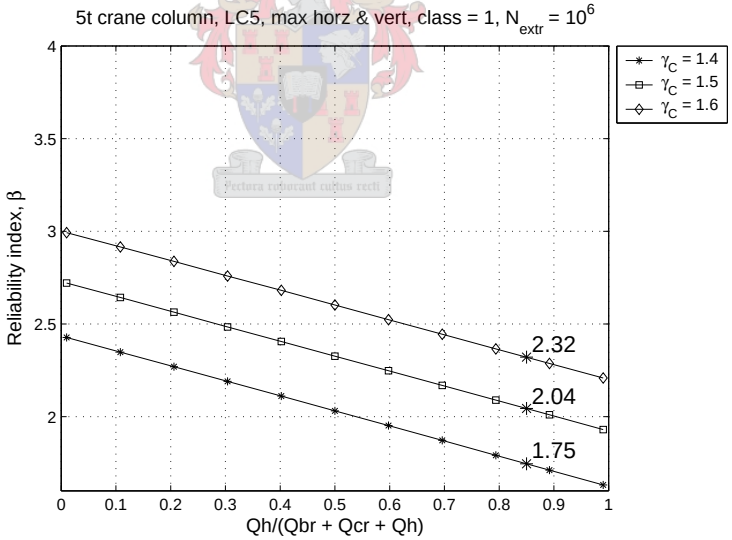

(b) Vertical and horizontal loads

Figure 9.5: Influence of vertical and horizontal loads, code format 1

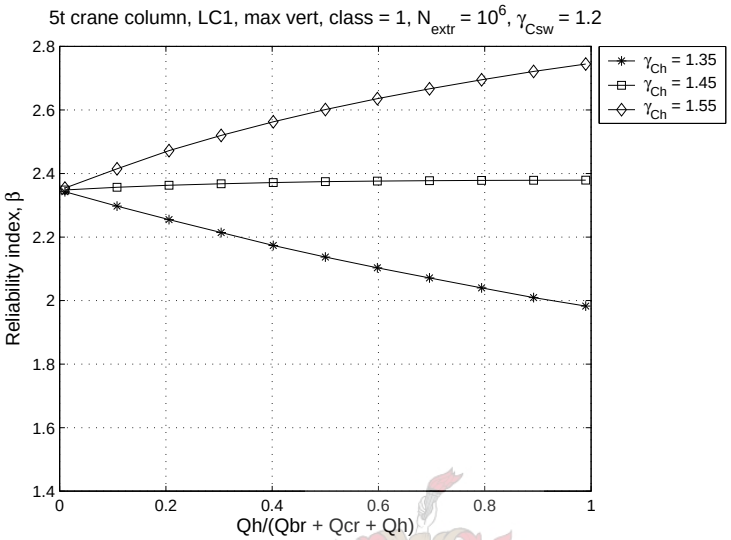

(a) Vertical loads only

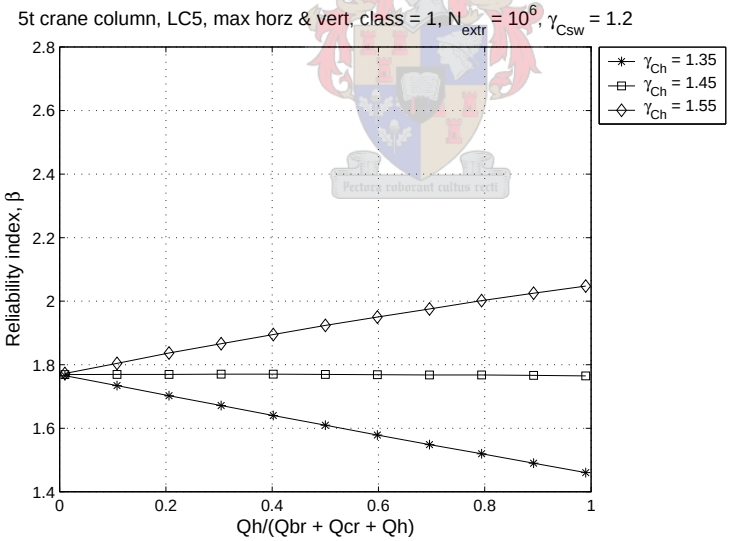

(b) Vertical and horizontal loads

Figure 9.6: Influence of vertical and horizontal loads, code format 2

This reduction in reliability with the inclusion of horizontal wheel loads is expected because of the higher modelling uncertainty for the calculation of the horizontal loads than the vertical loads. Code formats 3 and 4 (as discussed in Chapter 8) have been included in this investigation because of this decrease in reliability with increasing horizontal loads.

9.1.1.2 Reliability of current practice

An assessment of the reliability of current practice was carried out on the crane loading provisions in SABS 0160:1989 [1] and the Eurocode crane loading provisions in prEN 1991-3 [2].

The assessment of the reliability of current practice was carried out with the 40t crane which can be considered to be the 'most representative' crane in South Africa as discussed in Chapter 3. The element that was considered was the crane girder subject to its own weight and crane loads.

The economic design of the girder was carried out for each code considering the critical crane load combinations from that code, the critical load combinations are given in Chapter 4. The partial load and resistance factors were taken as given in each code and are shown in Table 9.1.

Table 9.1: Current partial safety factors in SABS 0160:1989 and prEN 1991-3

Partial load or resistance factor	SABS 0160:1989	prEN 1991-3
Partial load factor for permanent loads	1.2	1.35
Partial load factor for crane loads	1.6	1.35
Partial resistance factor for steel	0.9	1/1.1

For the reliability analysis, the actual crane loads imposed on the girder were assumed to be represented by the prEN 1991-3 crane load models with the inclusion of the modelling uncertainties discussed in Chapter 6, as is the case for all the reliability analyses.

The assessment was carried out for SABS 0160:1989 crane classes 2 - 4 and prEN 1991-3 hoist classes 1 - 4. SABS 0160:1989 class 1 cranes have been omitted as they are hand operated cranes and this investigation deals only with electric overhead travelling cranes.

The results from the assessment of current practice are shown in Figure 9.7. The variation of the reliability with respect to the number of cycles taken

for the extreme hoistload distribution (N_{extr}) is shown in Figure 9.7(a) with a ratio of hoistload to total crane weight of r = 0.5. This is the actual ratio of the 40t crane. The variation of reliability with the ratio of hoistload to total crane weight is shown in Figure 9.7(b).

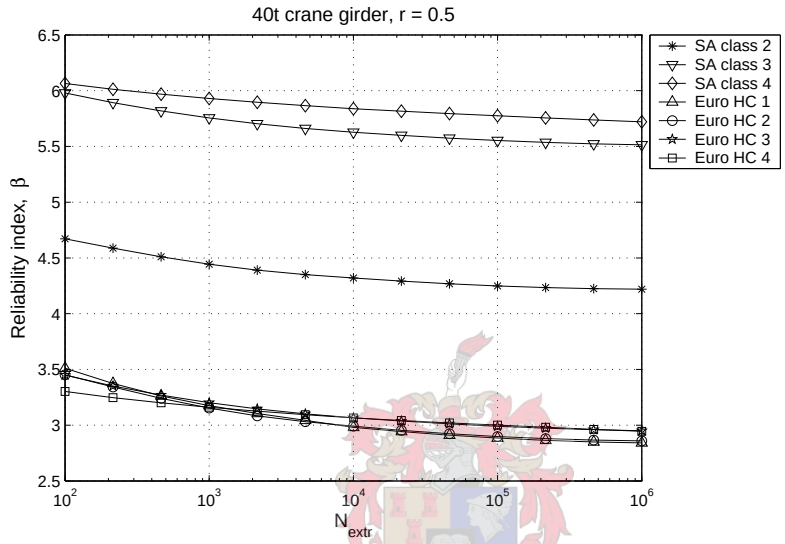

(a) Variation with N_{extr}

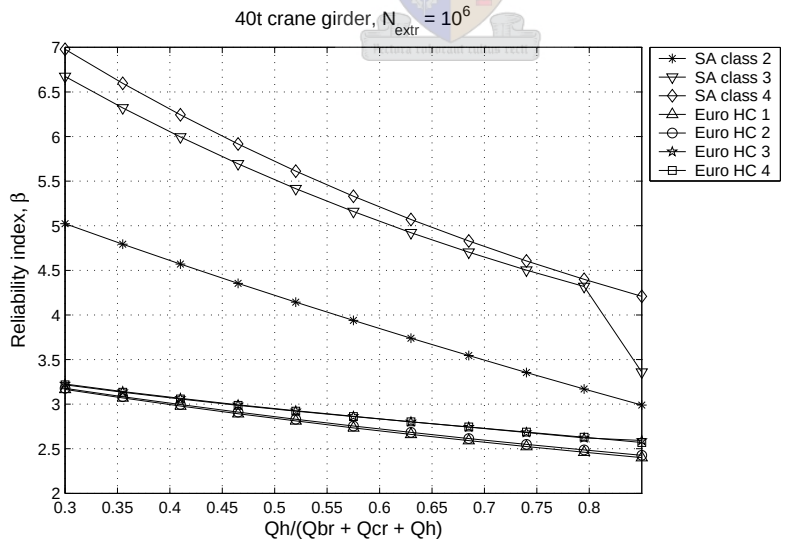

(b) Variation with ratio of hoistload to total crane weight

Figure 9.7: Assessment of reliability of current practice

Considering Figure 9.7(a), the trend of the reliability is the same as is observed in Figure 9.1 in that the reliability decreases as N_{extr} increases.

It can be seen that SABS 0160:1989 has a higher reliability than prEN 1991-3 for this case of the 40t crane girder.. The level of reliability of SABS 0160:1989 at $N_{extr} = 10^6$ cycles, ranges from $\beta = 4.2$ for the class 2 crane to $\beta = 5.75$ for the class 4 crane whereas prEN 1991-3 has a reliability of $\beta \approx 2.8$ to 3.0.

The level of reliability of prEN 1991-3 is lower than is expected and could be partly due to two conservative assumptions that have been made regarding the loading. The first assumption is the upper limit of 1.25 SWL for the 'one cycle' distribution which results in the mean of the extreme hoistload distribution at $N_{extr} = 10^6$ cycles being close to 1.25 SWL. The second conservative assumption is that the position of the crab is assumed to be deterministic at the extreme of its travel closest to the wheel being considered resulting in the maximum possible wheel load always being obtained.

The large difference between the classes for SABS 0160:1989 in Figure 9.7 is partly due to the method of calculating the wheel loads for the economic design. The vertical and horizontal wheel load are dependent on the class of the crane as is explained in Chapter 4 and shown in the calculations in Appendix A. In contrast, the prEN 1991-3 hoist class affects only the dynamic factor for the vertical loads for LC1.

The second reason for the large difference in reliability between the classes for SABS 0160:1989 is the failure mode for the reliability analysis is sometimes dominated by horizontal loads and sometimes by vertical loads. The class 2 crane and the class 3 crane at a ratio of hoistload to total crane weight of r = 0.85 in Figure 9.7(b) have failure modes dominated by horizontal loads and therefore have a lower reliability. This can be seen from the sensitivity factors for the class 2 and 3 cranes at $N_{extr} = 10^6$ cycles and r = 0.5 as shown in Figures 9.8 & 9.9.

Where:

mf V – represents the modelling uncertainty in the calculation of the vertical wheel loads

mf H – represents the modelling uncertainty in the calculation of the horizontal wheel loads

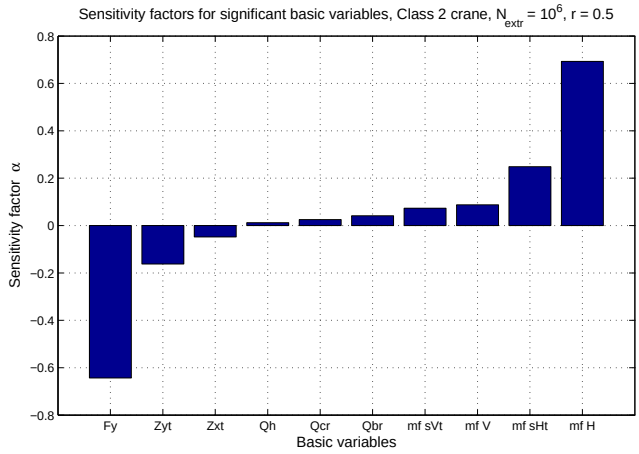

Figure 9.8: Sensitivity factors for class 2 crane, SABS 0160:1989

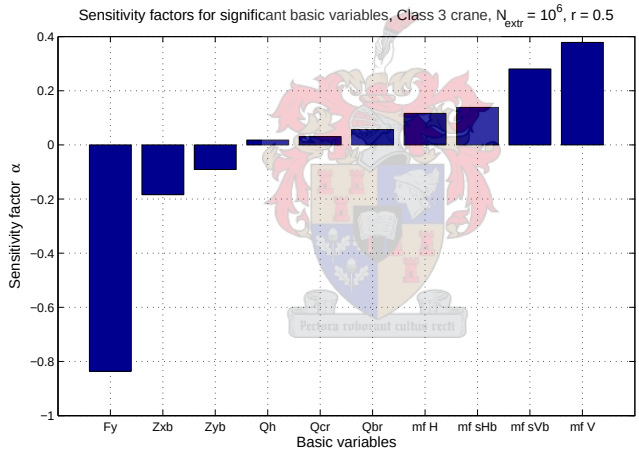

Figure 9.9: Sensitivity factors for class 3 crane, SABS 0160:1989

It can be seen in Figures 9.8 & 9.9 that the class 2 crane is much more sensitive to the modelling uncertainty for the calculation of the horizontal wheel loads than the class 3 crane.

9.1.1.3 Calibration of partial load factors

The critical elements that resulted in the lowest reliability were identified for use in the code calibration procedure. Of the crane girders and columns for the three representative cranes, the element with the lowest reliability was the

5t crane column. The complete set of results of the calibration process are given in Appendix E where it can be seen that the 5t crane column has the lowest reliability. Two load cases were identified for the code calibration:

1. 5t crane column subject to LC1 maximum vertical loads. This load case consists of only vertical loads.
2. 5t crane column subject to LC5. This load case consists of both vertical and horizontal loads.

The calibration of the partial load factors for the different code formats was carried out as outlined below.

1. Calibration of the partial load factors for code formats 1 and 2

   These load factors were calibrated considering LC5 consisting of vertical and horizontal loads.

2. Calibration of the partial load factors for code formats 3 and 4

   a) The crane partial load factors (γ_C, γ_{Csw}, γ_{Ch}) for code formats 3 and 4 were calibrated considering LC1 consisting of only vertical loads

   b) The load factors for the horizontal loads for code formats 3 and 4 were calibrated using the partial load factors from step (a) and considering LC5 consisting of vertical and horizontal loads.

The calibration was carried out considering the critical values of the parameters determined above, i.e. class 1 crane, $N_{extr} = 10^6$ cycles, r = 0.85. The partial load factors were varied until the reliability was equal to the target reliability of $\beta_T = 3.0$.

The results of the code calibration are given in Table 9.2. Figures 9.10 - 9.12 show the reliability graphs for the critical elements with the calibrated partial load factors.

Table 9.2: Calibrated partial load factors

Code format	γ_C	γ_{Csw}	γ_{Ch}	γ_H
1	1.907			
2		1.617	1.963	
3	1.590			1.261
4		1.354	1.623	1.271

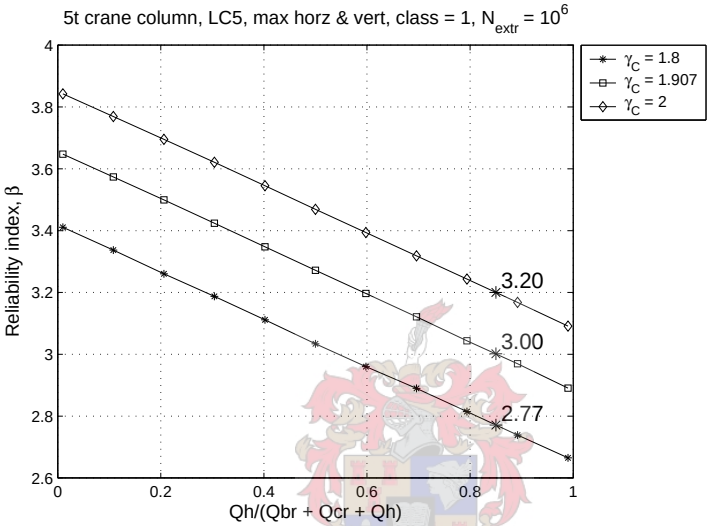

(a) Code format 1

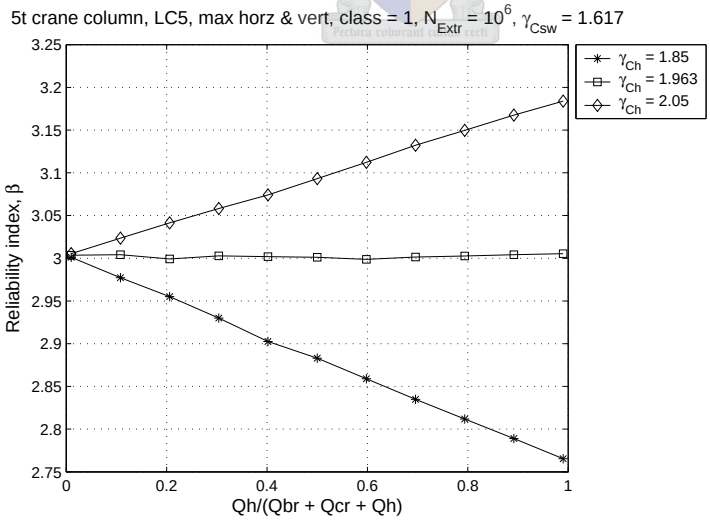

(b) Code format 2

Figure 9.10: Crane only calibration, code formats 1 and 2

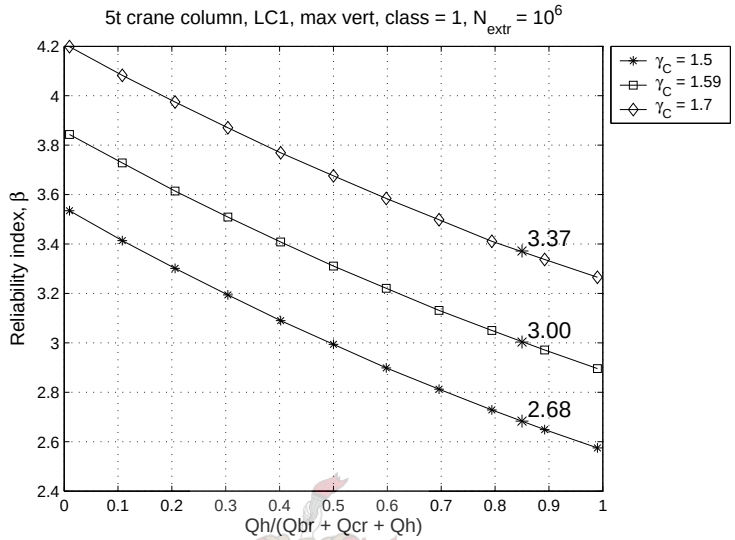

(a) Code format 3

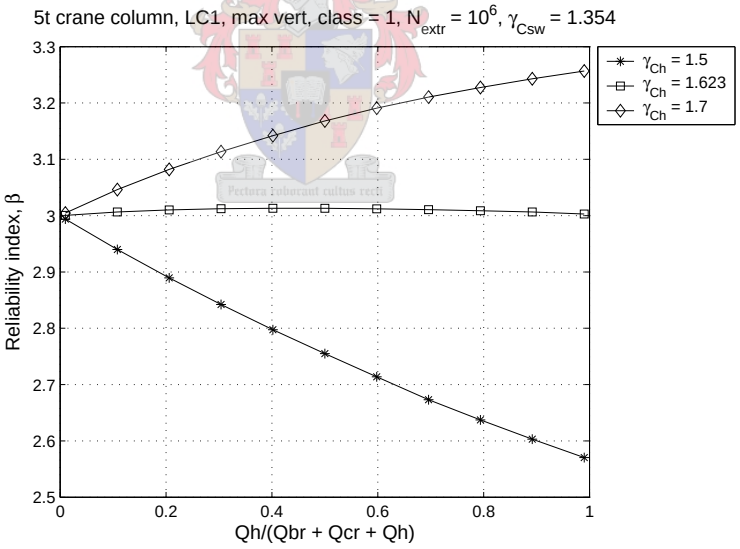

(b) Code format 4

Figure 9.11: Crane only calibration, code formats 3 and 4 step (a)

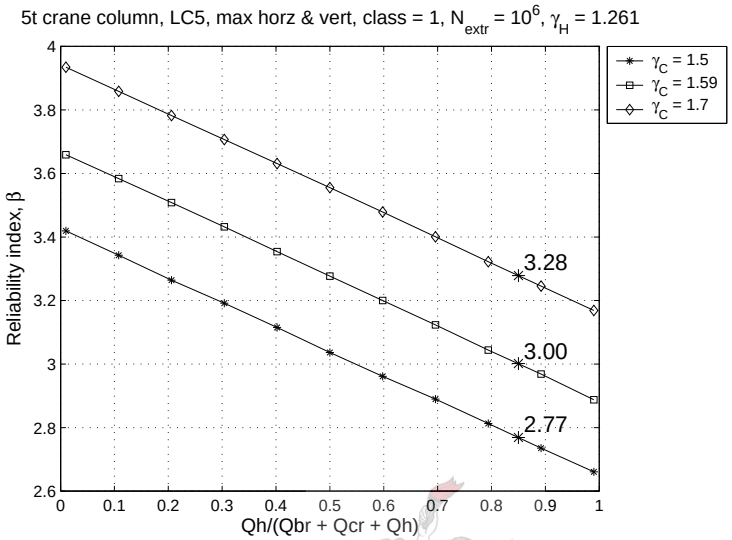

(a) Code format 3

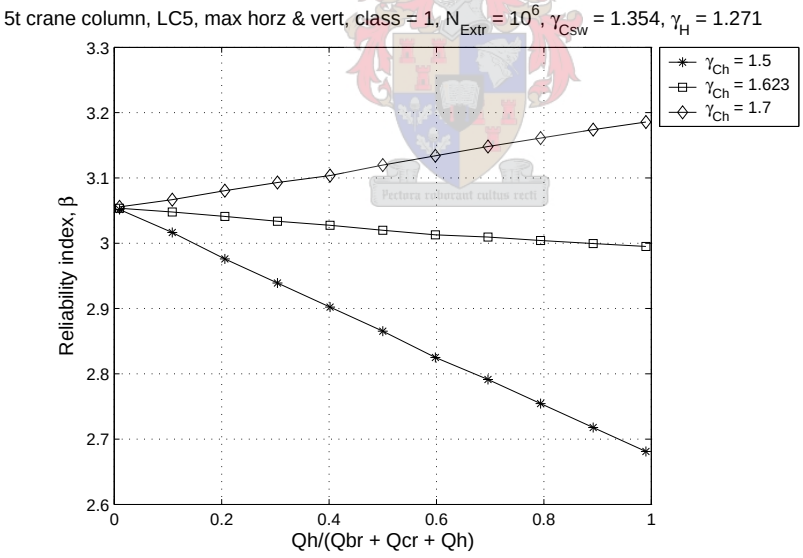

(b) Code format 4

Figure 9.12: Crane only calibration, code formats 3 and 4 step (b)

9.1.1.4 Verification of partial load factors

The final step in the crane only calibration was to verify the results. This consisted of ensuring that the reliability of all the elements was not below the target reliability and assessing the degree of conservatism.

The reliability graphs for all the crane girders and columns from the three representative cranes were plotted using the calibrated partial load factors and it was observed that in all cases the reliability was above the target reliability. The minimum reliabilities for the various elements and load cases ranged from $\beta = 3.00$ - 5.55. The reliability graphs for all the girders and columns with the calibrated partial load factors are given in Appendix E.

The second step in the verification of the partial load factors was to assess the degree of conservatism for the support structures as a whole. The excess costs of the elements for the three representative cranes were calculated as described in Chapter 8. Figures 9.13 - 9.15 give the results of the cost analyses.

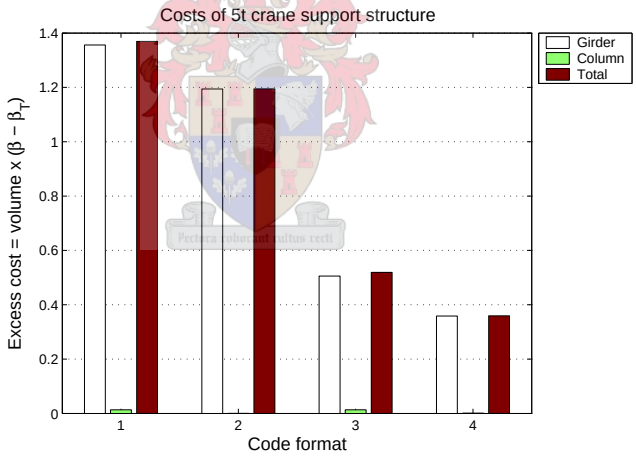

Figure 9.13: Excess cost of the 5t crane support structure

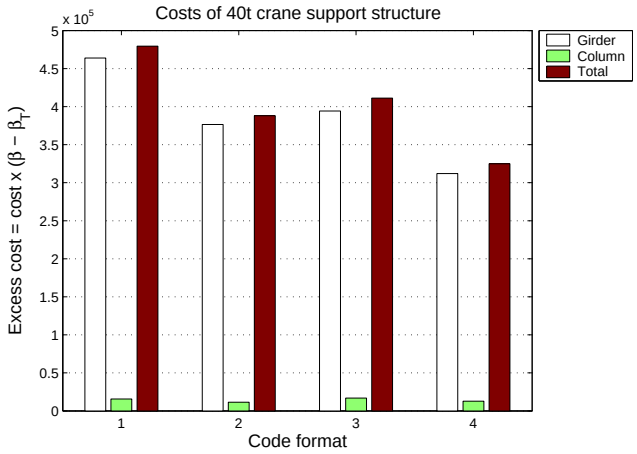

Figure 9.14: Excess cost of the 40t crane support structure

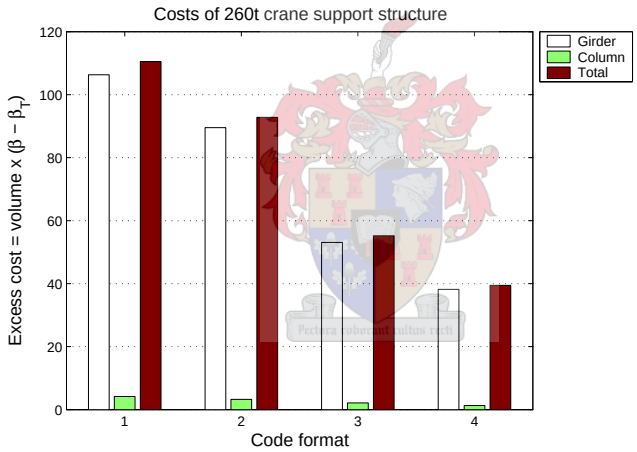

Figure 9.15: Excess cost of the 260t crane support structure

It can be clearly seen from Figures 9.13 - 9.15 that the degree of conservatism of the support structures reduces with increasing complexity of the code format. Two progressions of the increase in complexity of the code format were identified:

1. Code formats $1 \rightarrow 2 \rightarrow 4$

   The lowest level of complexity is code format 1 with one partial load factor applied to the calculated characteristic wheel load. The next level of complexity is code format 2 where two separate partial load factors

are applied to the crane self weight and hoistload before the calculation of the design wheel loads. The third level of complexity is code format 4 where an additional partial load factor, to code format 2, is applied to the horizontal wheel loads.

2. Code formats 1 → 3 → 4

   This progression starts and ends the same as the previous one but the intermediate step is seen as applying one partial load factor to the calculated characteristic wheel loads and an additional factor to the horizontal wheel loads.

For both of these progressions, there is a decrease in the degree of conservatism as indicated by the excess cost of the support structure. Code format 4 has the least conservatism and can thus be considered the code format which best meets the code calibration objective.

9.1.2 Combinations of time varying loads

The element that was selected for the investigation into crane loads combined with other time varying loads was the column for the 5t crane with LC5 maximum horizontal load. This was the element with the lowest reliability.

The code format did not have an effect on the results of these investigations so code format 4 has been chosen. The results are shown with the calibrated values of the crane partial load factors. The critical values of the parameters discussed previously have been used here, i.e. ratio of hoistload to total crane weight r = 0.85; $N_{extr} = 10^6$ cycles and class 1 crane in the case of the crane load being the leading load.

9.1.2.1 Results of parametric studies

The first parametric study that was carried out for the combination of crane loads with wind or roof imposed loads was an investigation into the influence of permanent loads. In order to carry out this investigation a combination of crane and permanent loads only was considered.

SABS 0160:1989 gives two load combinations for the crane and permanent loads:

1. 1.2(Permanent) + γ_C(Crane)

2. 1.5(Permanent)

Both of these load combinations were considered in this investigation. Figure 9.16 shows the variation of the reliability index with varying ratios of crane load to crane and permanent load.

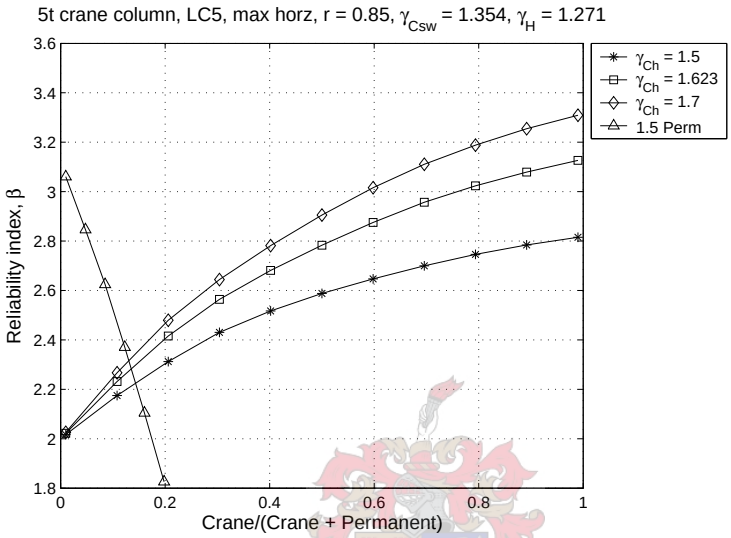

Figure 9.16: Crane and Permanent loads

As can be seen from Figure 9.16, the reliability decreases as the ratio of permanent load increases. The assessment of the code provisions for permanent loads is not within the scope of this project, therefore the ratio of permanent loads to total loads will be kept very small (p = 0.01), i.e. ratio of crane load to crane and permanent load close to one, in the following investigations.

The second parametric study that was carried out was an investigation into the class of crane and the number of cycles considered for N_{extr} for the crane load as the accompanying load.

From Figure 9.1 it was observed that the class 1 crane has the lowest reliability for $N_{extr} > 5\,000$ cycles. In the case where crane loads are the accompanying loads for wind or roof imposed loads, N_{extr} would be chosen to be the number of cycles the crane is likely to perform during an extreme wind event or roof loading which is unlikely to be more than 5 000. From Figure 9.1 it was observed that for $N_{extr} < 5\,000$ cycles, a class 4 crane gives the lowest reliability. Therefore for the assessment of the reliability of crane loads as the

accompanying load combined with other time varying loads, a class 4 crane will be considered.

The number of cycles that a crane is likely to perform during an extreme wind event (e.g. a storm) or roof loading event (e.g. roof maintenance) would be in the range of 10 - 100. An assessment of the effect of this range in values of N_{extr} has been carried out by considering a combination of wind and crane loads for the wind load dominant case. A nominal value of the crane combination factor has been chosen as $\psi_{CW} = 0.6$. Figure 9.17 shows the results of this parametric study in the form of a graph of reliability versus the ratio of crane load to crane and wind load. It can be seen that the difference in N_{extr} has a very small effect on the reliability. A variation in N_{extr} has a larger effect on the class 1 - 3 cranes but some conservatism will be included for these classes due to the class 4 crane being considered as the calibration case. A similar, validating, parametric study will be carried out for the class 1 crane after the calibration has been carried out to ensure that the reliability is above the target reliability.

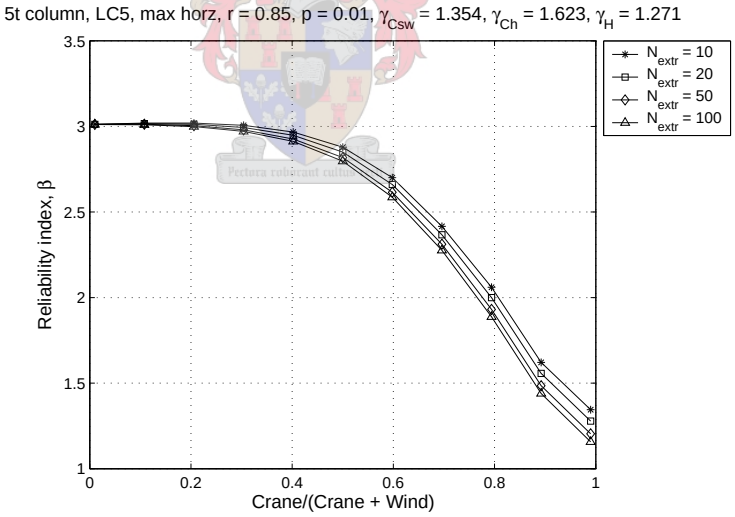

Figure 9.17: Effect of N_{extr} for crane load as accompanying load

A value of $N_{extr} = 20$ cycles was considered reasonable for the number of cycles a crane will perform during an extreme wind or roof loading event and has been used for the calibration.

9.1.2.2 Combination of crane and wind loads

The two load combinations that were considered for the combination of crane and wind loads and the partial load factors for permanent and wind loads are given below.

1. Crane dominant: γ_P(Permanent) + γ_C(Crane) + $\psi_{WC}1.3$(Wind)
2. Wind dominant: γ_P(Permanent) + $\psi_{CW}\gamma_C$(Crane) + 1.3(Wind)

Where:

γ_P – partial load factor for permanent loads

γ_P = 1.2 when the permanent loads are in unfavourable combination with crane and wind loads

γ_P = 0.9 when the permanent loads are in favourable combination with the crane and wind loads

γ_C – represents conceptually the factoring of the crane loads by whichever code format is being considered

In the case where the crane load was the accompanying load, the crane partial load factors (γ_C, γ_{Csw}, γ_{Ch}) were multiplied by the crane combination factor.

The reliability was determined as a function of the ratio of crane load to crane and wind load. The ratios are expressed in terms of the unfactored, characteristic values.

Figure 9.18 shows the reliability of the column with varying ratios of crane load to crane and wind load. Figure 9.18(a) shows the case where wind is the leading load and Figure 9.18(b) shows the case where the crane load is the leading load. It can be seen from these graphs that the values of the combination factors which keep the reliability constant, in the pertinent range of ratios, for each case are:

1. Combination factor applied to wind loads: $\psi_{WC} = 0$
2. Combination factor applied to crane loads: $\psi_{CW} = 0.65$

Figure 9.19 shows the combined graph for the crane dominant and the wind dominant cases with these combination factors.

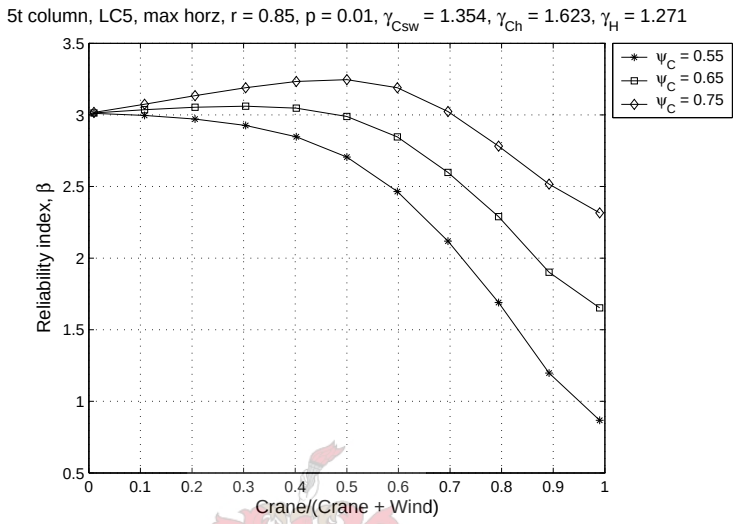

(a) Wind dominant

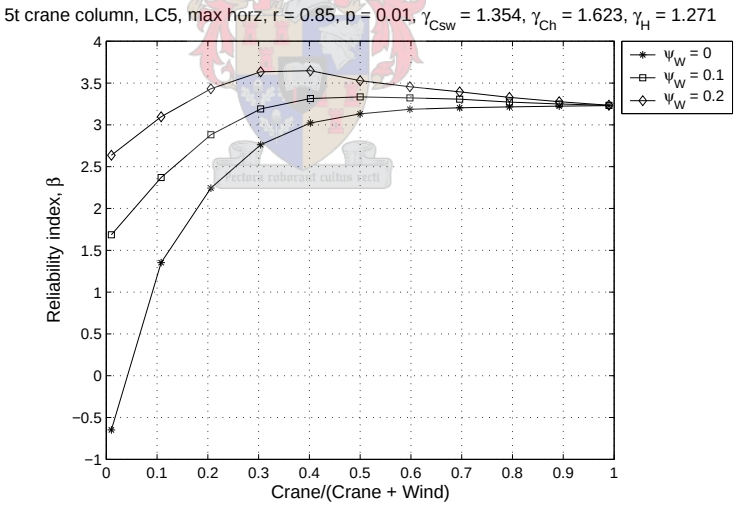

(b) Crane dominant

Figure 9.18: Calibration of combination factors for crane and wind loads

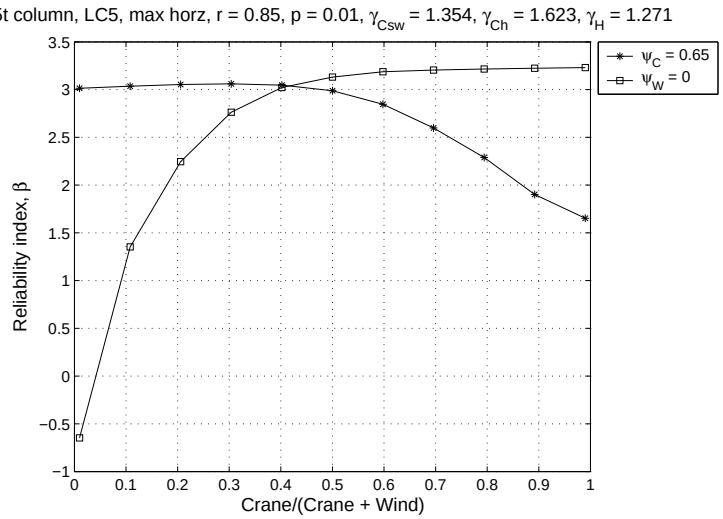

Figure 9.19: Calibrated combination factors for crane and wind

The investigation into the sensitivity of a class one crane to the number of cycles considered for N_{extr} is shown in Figure 9.20 with $\psi_{CW} = 0.65$. Comparing this graph with Figure 9.17 it was observed that the class 1 crane is more sensitive to N_{extr} but that sufficient conservatism is incorporated in the combination factor so that the reliability does not fall below the target reliability. Therefore no further investigation is required into the exact number of cycles to be considered for N_{extr}.

9.1.2.3 Combination of crane and roof imposed loads

The two load combinations that were considered for the combination of crane and roof imposed loads and the partial load factors for permanent and roof imposed loads are given below:

1. Crane dominant: 1.2(Permanent) + γ_C(Crane) + ψ_{RC}1.6(Roof imposed)

2. Roof dominant: 1.2(Permanent) + $\psi_{CR}\gamma_C$(Crane) + 1.6(Roof imposed)

In the same way as for the combination of crane and wind loads, γ_C represents conceptually the crane partial load factors from whichever code format is being considered.

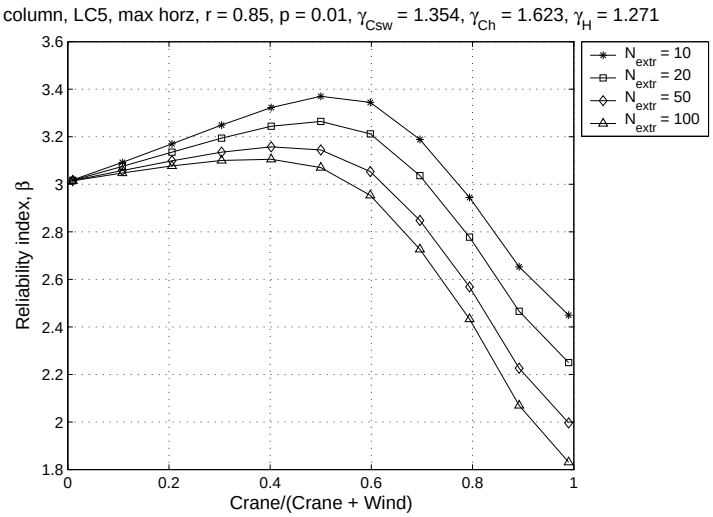

Figure 9.20: Sensitivity of class 1 crane to N_{extr}

The crane combination factor ψ_{CR} was applied to the crane loads by multiplying the crane partial load factors (γ_C, γ_{Csw}, γ_{Ch}) by the combination factor.

The reliability of the column was determined as a function of the ratio of crane load to crane and roof imposed load. The ratio is expressed in terms of the unfactored, characteristic loads.

Results are shown in Figure 9.21 for the calibration of the combination factors for crane and roof imposed loads. Figure 9.21(a) shows the full reliability graph and Figure 9.21(b) shows the more relevant range of reliabilities between zero and five.

The reliability curves which relate to the crane dominant case are the mostly horizontal curves and are labelled on the figures, the reliability curves which relate to the roof dominant case are the curves with the steeper gradients and are also labelled on the figures.

The roof dominant curve could not be presented for ratios of crane load to crane and roof loads of less than 0.35 because the reliability was too large and the numerical FORM analysis method broke down. The trend of the curves is clearly increasing though, into the region of reliability greater than 5 which is not in the critical range.

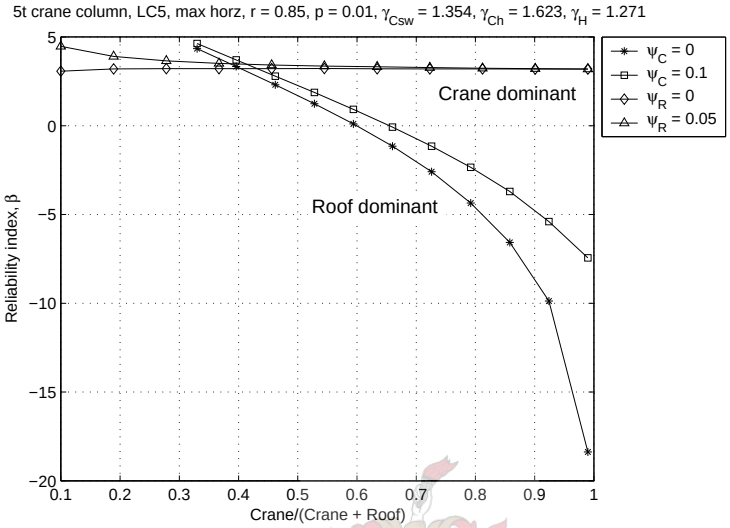

(a) Full range of reliability

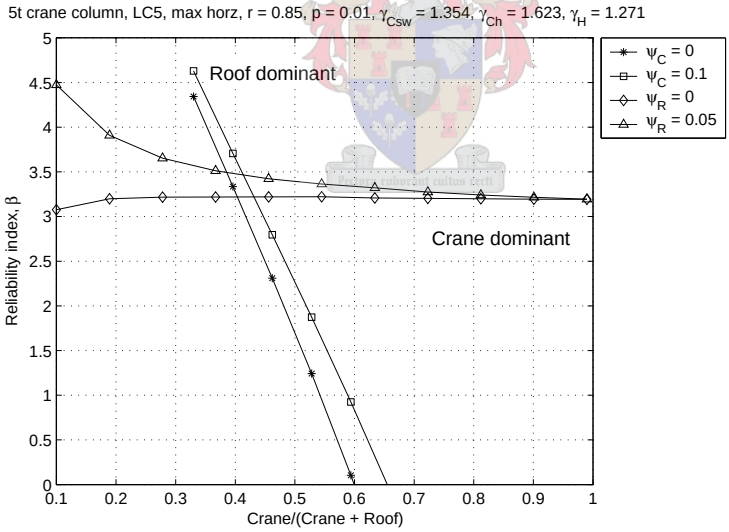

(b) Relevant range of reliability

Figure 9.21: Calibration of combination factors for crane and roof imposed loads

From Figure 9.21, for ratios of crane load to crane and roof imposed load less than 0.4, the roof dominant case has a higher reliability than the crane dominant case, even with a crane combination factor of $\psi_{CR} = 0$. This can be explained from the parameters of the statistical model for the lifetime maximum roof imposed loads. The mean value of the lifetime maximum roof loads is:

$$\mu_R = \frac{R_{nom}}{3.75}$$

With such a large bias in the roof imposed loads, design of members according to these loads is over conservative, hence the large reliability for small ratios of crane to crane and roof loads.

Considering Figure 9.21, for ratios of crane load to crane and roof load greater than 0.4, the crane dominant case has the higher reliability, even in the case where the combination factor for roof loads $\psi_{RC} = 0$. Again, the statistical model for the roof imposed loads explains this phenomenon. The point-in-time roof imposed load for combination with other time varying loads is taken to be zero. This means that any combination factor for roof loads greater than zero is conservative and essentially results in loads taken into account in the design which are not present for the reliability analysis.

These results indicate that the combination of crane load with roof imposed load is not a rational load combination and the two load cases should rather be treated separately as:

1. Crane dominant: 1.2(Permanent) + γ_C(Crane)
2. Roof dominant: 1.2(Permanent) + 1.6(Roof imposed)

In other words, the appropriate values of the combination factors are:

1. Combination factor applied to roof loads: $\psi_{RC} = 0$
2. Combination factor applied to crane loads: $\psi_{CR} = 0$

9.2 Accidental limit state

The accidental limit state considered the crane load case which are classified as accidental loads in prEN 1991-3. This accidental load case consists of the crane running into the end stops on the end of the runway causing longitudinal forces which are resisted by the longitudinal runway bracing. The 40t crane was taken to be representative for this load case.

9.2.1 Results of parametric studies

The first two parametric studies that were carried out were investigations into the class of crane that resulted in the lowest reliability and the number of cycles that was considered for N_{extr}.

The code format did not have an effect on the results of these parametric studies so for the sake of simplicity, code format one has been selected.

The number of cycles considered for N_{extr} is the number of times that this action is likely to occur over the lifetime of the crane. The extreme hoistload distribution then models the probability distribution of the largest load that will be lifted when the crane runs into the end stops. This load case is not classified under crane loads arising from normal operation, being classified as an accidental load situation in prEN 1991-3, and therefore should not occur very often. Low values of the number of cycles have been considered, in the range $5 \leq N_{extr} \leq 35$.

Figure 9.22 shows the reliability analysis curves for the four classes of crane for the range of N_{extr} given above, for code format one, with the accidental partial load factor, $\gamma_C = 1.0$.

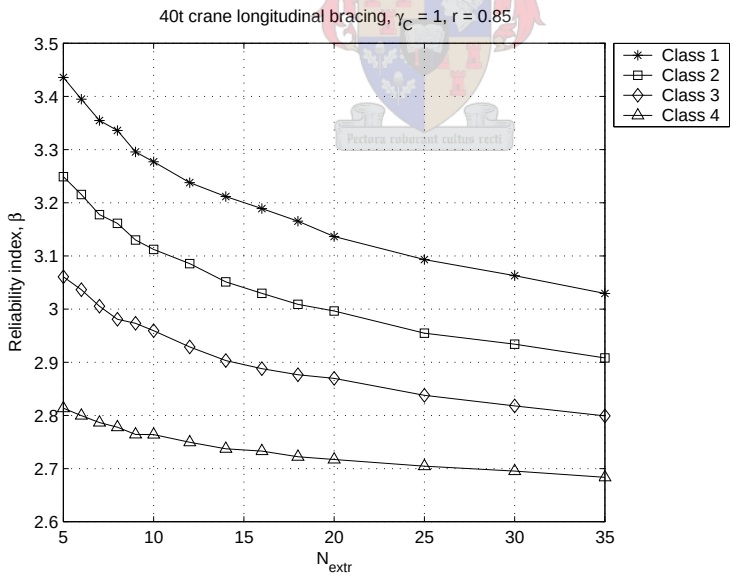

Figure 9.22: Effect of class and cycles for accidental limit state

From Figure 9.22, it was observed that the class four crane gives the lowest reliability and that, as expected, the reliability decreases with increasing N_{extr}. The decrease in reliability from $N_{extr} = 5$ cycles to $N_{extr} = 35$ cycles is not large, ranging from $\beta = 2.81$ for $N_{extr} = 5$ to $\beta = 2.68$ for $N_{extr} = 35$.

The number of cycles that was selected for N_{extr} for the calibration of the accidental limit state was $N_{extr} = 10$. The reliability implications of calibration with $N_{extr} = 10$ in the event of the actual number of cycles being larger will be investigated after the calibration has been carried out.

9.2.2 Calibration of partial load factors

Figure 9.23 shows the reliability curves with the calibrated partial load factors for code formats one and two.

It was found that the partial load factors that resulted in reliabilities equal to the target reliability of $\beta_T = 4.0$ were:

- Code format 1:
  - $\gamma_C = 1.196$
- Code format 2:
  - $\gamma_{Csw} = 1.344$
  - $\gamma_{Ch} = 1.448$

The partial load factors applied separately to the crane self weight and hoistload before the calculation of the design forces, for code format 2 are significantly larger than the partial load factor for code format 1 because the buffer forces are proportional to the square root of the weights of the crane and hoistload.

9.2.3 Verification of partial load factors

As mentioned above, the number of cycles selected for N_{extr} for the calibration was 10. The number of cycles was selected to be small due to the fact that the crane running into the end stops should only occur infrequently, however, 10 cycles was an arbitrary selection.

Figure 9.24 shows the effect on the reliability of selecting different numbers of cycles for N_{extr}. Code format one is shown, applying the calibrated partial load factor.

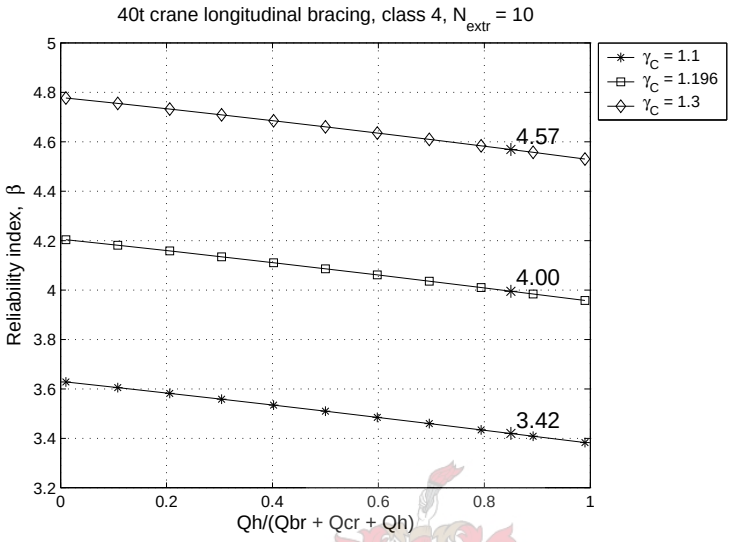

(a) Code format 1

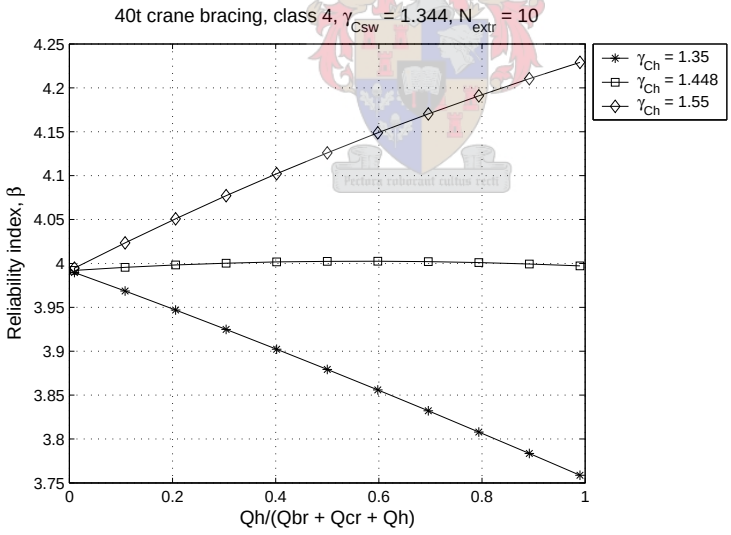

(b) Code format 2

Figure 9.23: Calibration of partial load factors for accidental limit state

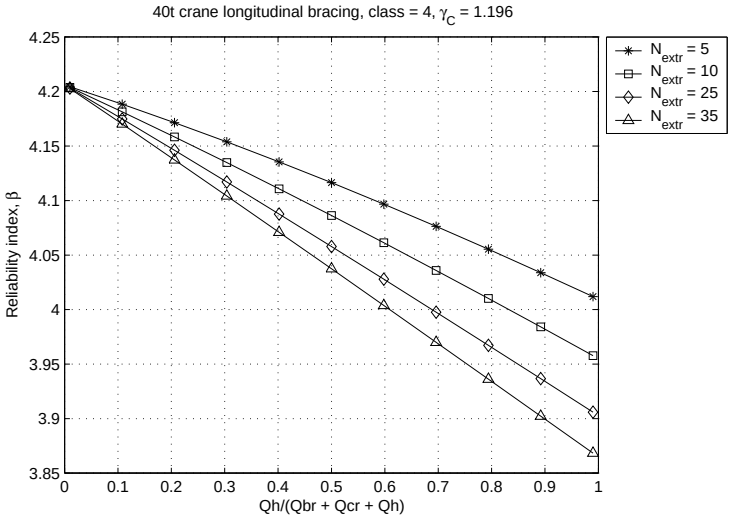

Figure 9.24: Effect of different values of N_{extr} on accidental limit state reliability, class 4

It can be seen from Figure 9.24 that the reliability falls below the target reliability of $\beta_T = 4.0$ for the larger values of N_{extr} for ratios of hoistload to total crane weight greater than 0.6. It has been noted before that the cranes with higher ratios of hoistload to total crane weight tend to be class one cranes. Figure 9.25 shows the effect on the reliability of selecting different numbers of cycles for N_{extr} for a class one crane using the partial load factors calibrated for the class 4 crane.

From Figure 9.25, for the class one crane, the reliability remains above the target reliability of $\beta_T = 4.0$ for all ratios of hoistload to total crane weight for all values of N_{extr}.

It is thus concluded that calibrating the partial load factors for a class four crane with $N_{extr} = 10$ cycles ensures that the reliability remains above the target reliability of $\beta_T = 4.0$ for all relevant ranges of parameters.

9.3 Fatigue

The results of the reliability assessment of fatigue are discussed first for the fatigue loading method given in prEN 1991-3 and these results are then applied to the alternative method of assessing fatigue where the detailed crane behaviour is considered.

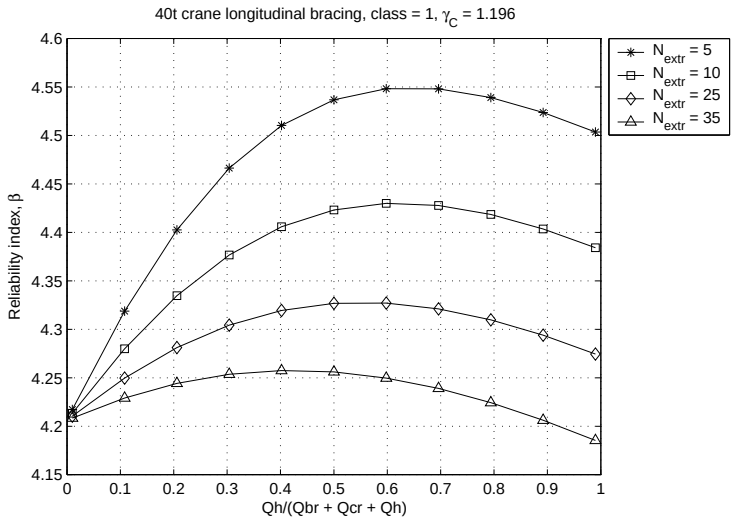

Figure 9.25: Effect of different values of N_{extr} on accidental limit state reliability, class 1

The fatigue provisions in prEN 1991-3 were assessed by calculating the bounds of reliability for a given load spectrum class Q, as discussed in Chapter 8. An upper bound, lower bound and average value of reliability were obtained for each load spectrum class. The reliability was determined as a function of the number of cycles the crane will perform over its lifetime.

9.3.1 Results of parametric studies

The first parametric study carried out for fatigue was the assessment of the effect of using a single or a double slope S-N curve. A typical graph is shown in Figure 9.26 which gives the reliability of the 40t crane girder fatigue at the bottom of the intermediate stiffener, for load spectrum class Q_5.

Comparing the graph obtained considering a single slope S-N curve with that considering a double slope S-N curve, it is seen that there is a tendency for the reliability to increase in the region of higher cycles for the double slope S-N curve, most markedly so for the lower bound. This is due to the fact that the designs carried out with higher cycles would have a higher λ factor resulting in a larger beam. When the actual crane movement is simulated, a larger proportion of the stresses would fall into the lower region than those for a smaller beam. With a double slope S-N curve these lower stresses result in less damage than for a single slope S-N curve resulting in a higher reliability.

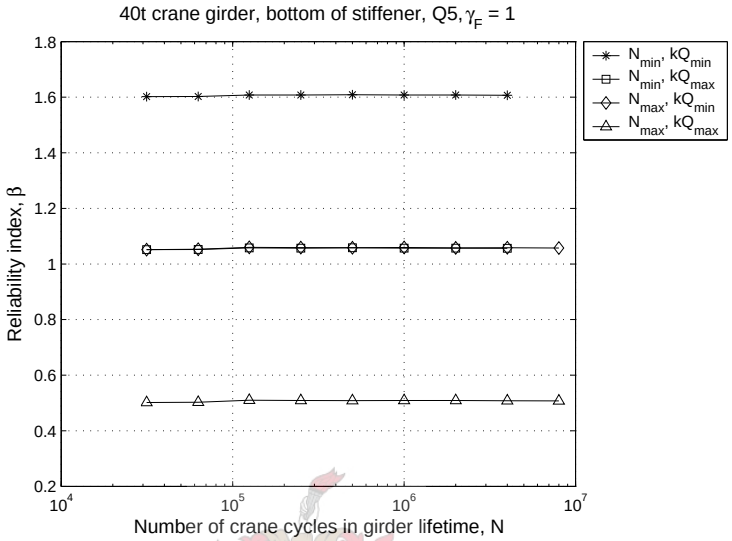

(a) Single slope S-N curve

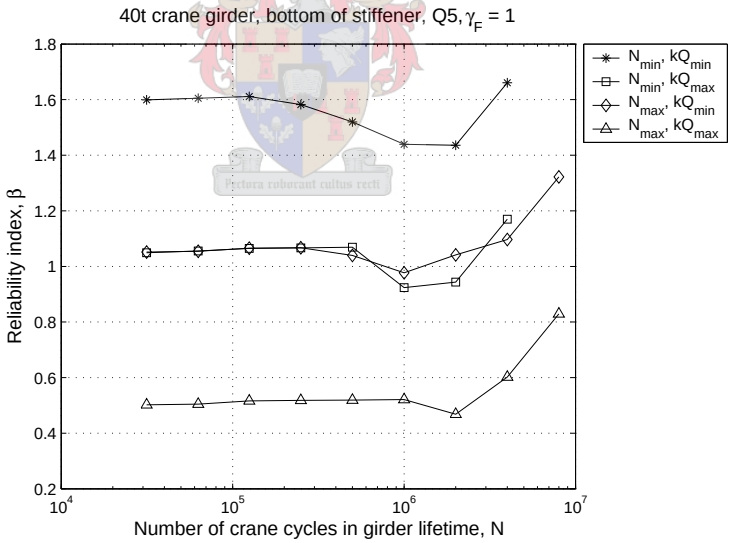

(b) Double slope S-N curve

Figure 9.26: Effect of single or double slope S-N curve

The second phenomenon that is observed is that when a double slope S-N curve is considered, there is a dip in reliability in the region of 2×10^5 cycles, more pronounced in the upper bound. This is due to the fact that there are more uncertainties involved in using a double slope S-N curve. This can be observed from Figures 9.27 - 9.29 which give the sensitivity factors for reliability analyses carried out on the 40t crane girder bottom of intermediate stiffener for load spectrum class Q_5. Figure 9.27 shows the sensitivity factors for a reliability analysis considering a single slope S-N curve at 2×10^6 cycles. Figures 9.28 & 9.29 show the sensitivity factors for reliability analyses considering a double slope S-N curve, Figure 9.28 is at 1.25×10^5 cycles and Figure 9.29 is at 2×10^6 cycles. Figures 9.27 & 9.28 are almost identical because with 1.25×10^5 cycles the stresses are in the upper region of the S-N curve and only the first slope is considered with m = 3 as for the single slope S-N curve. Figure 9.29 shows the additional uncertainty which is included for a double slope S-N curve in the variable S_o which is the level of stress at which the gradient of the S-N curve changes.

For simplification purposes, a single slope S-N curve has been considered for the further investigations as the double slope S-N curve does not significantly change the trend of the reliability.

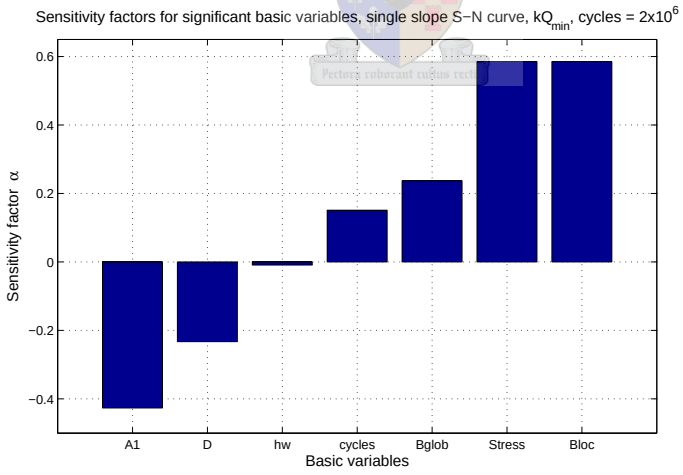

Figure 9.27: Sensitivity factors for a single slope S-N curve at 2×10^6 cycles

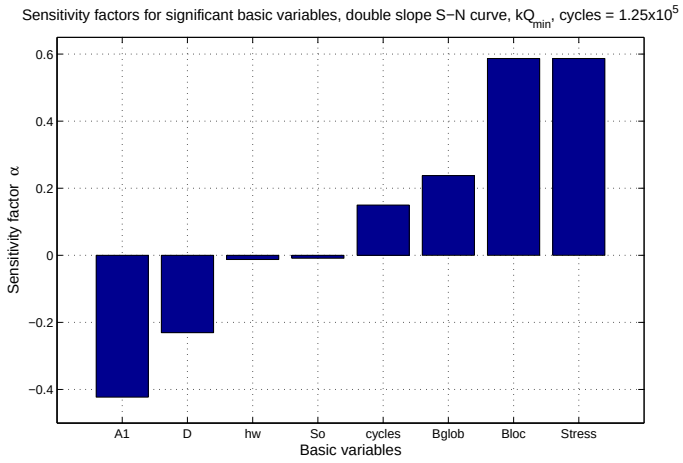

Figure 9.28: Sensitivity factors for a double slope S-N curve at 1.25×10^5 cycles

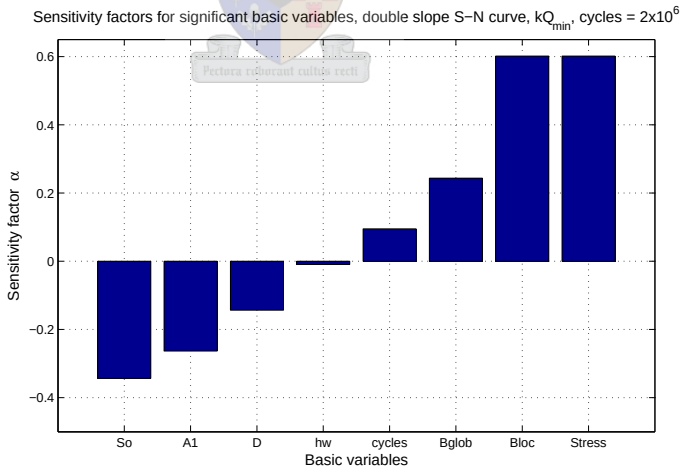

Figure 9.29: Sensitivity factors for a double slope S-N curve at 2×10^6 cycles

The second parametric study carried out was to assess the difference in reliability between the load spectrum classes. Figure 9.30 gives the reliability bounds for the 40t crane girder bottom of the intermediate stiffener. Figure 9.30(a) shows results for load spectrum class Q_2 and Figure 9.30(b) shows results for load spectrum class Q_5.

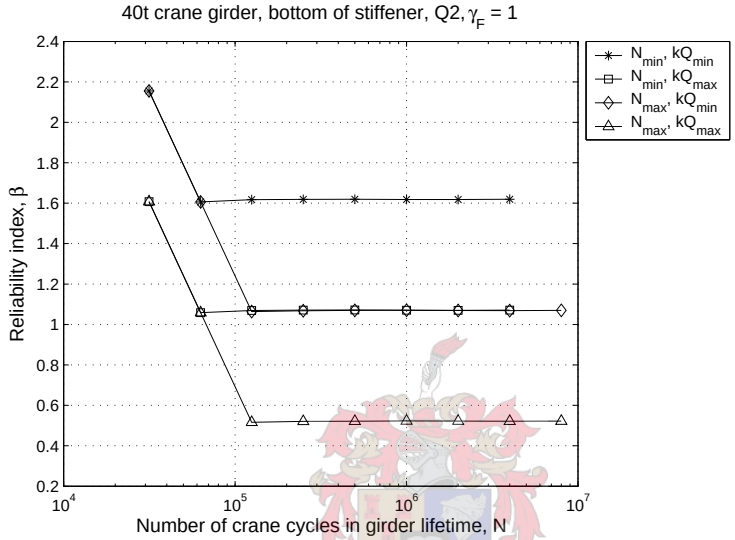

(a) Load spectrum class Q_2

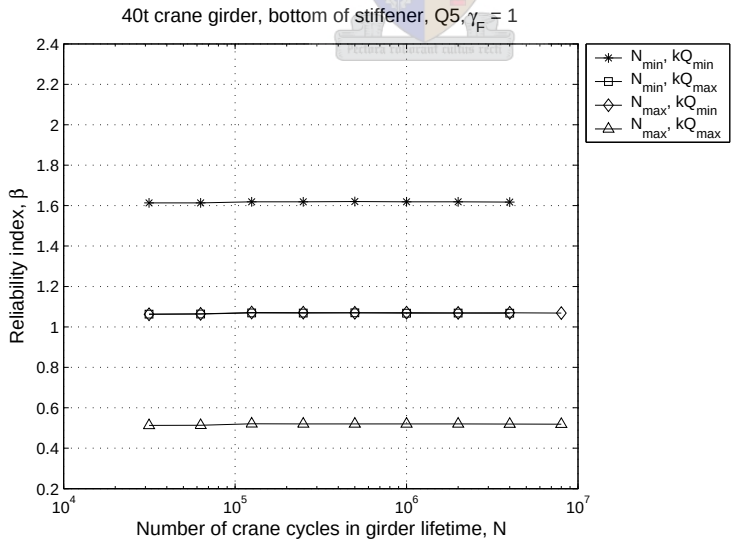

(b) Load spectrum class Q_5

Figure 9.30: Effect of different load spectrum classes

An initial steep downwards slope is observed in the graph for load spectrum class Q_2. This can be explained by referring to Table 2.18 on page 51 and considering load spectrum class Q_2. The first four fatigue classes are all S_0 and therefore for a number of cycles up to 1.25×10^5 the same λ factor is used for the design. This results in over design of elements subject to a lower number of cycles and hence a greater reliability. After the initial downwards slope, horizontal lines are obtained where the level of reliability is the same for class Q_2 and class Q_5.

The same trend of the results was observed for the 5t crane corbel to column welded connection, however, a different trend was observed for the 40t crane girder top flange to web weld. Figure 9.31 shows results for the 40t crane girder top flange to web weld, again comparing load spectrum classes Q_2 and Q_5.

The difference between the graphs obtained for the fatigue at the bottom of the stiffener and the fatigue at the top flange to web weld can be explained by considering the calculation of the λ factors. The λ factors for the normal stresses have been derived considering a single slope S-N curve with m = 3 [2]. This results in the constant reliability observed for the graphs generated for a single slope S-N curve for the 40t crane girder at the bottom of the stiffener which displays the same behaviour as the 5t crane corbel connection. The graphs for the 40t crane girder considering the fatigue of the top flange to web weld are not horizontal as with the other elements. This is because the stresses involved are a combination of shear and normal stresses. The stress considered for the fatigue analysis was the resulting principal stress and the S-N curve for the normal stress was used with the slope given previously of m = 3. The lambda factor for the calculation of the shear stresses in the design was derived considering a single slope S-N curve with a slope of m = 5 [2]. This would result in lower reliability for the higher cycles if the reliability was assessed with an S-N curve with a slope of m = 3. The trend of the reliability values for the upper and lower bounds and the average value is not significantly affected with the values centered on those for the other elements.

The 40t crane girder, fatigue at the bottom of the intermediate stiffener was considered for the calibration process. The load spectrum class considered was Q_5 with a single slope S-N curve.

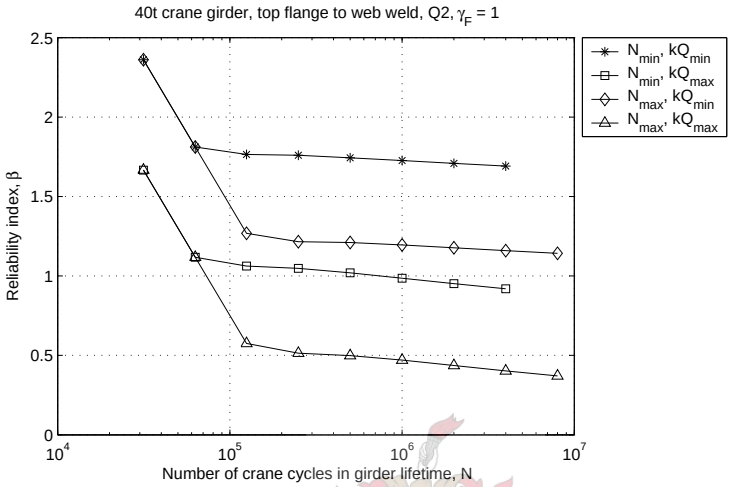

(a) Load spectrum class Q_2

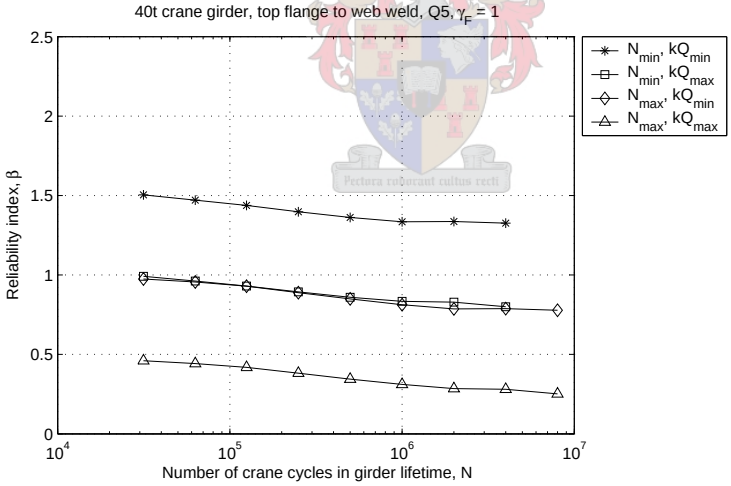

(b) Load spectrum class Q_5

Figure 9.31: 40t crane girder, top flange to web weld

9.3.2 Calibration of partial load factors

Considering the 40t crane girder bottom of the intermediate stiffener, in Figure 9.30(b), the upper bound of the reliability is $\beta_U \approx 1.6$, the lower bound is $\beta_L \approx 0.5$ and the average value is $\beta_A \approx 1.0$. It was found that applying a partial load factor of $\gamma_F = 1.25$, the average value of the reliability reached the target reliability of $\beta_T = 1.5$. The resulting reliability for the three elements for load spectrum class Q_5 are shown in Figures 9.32 - 9.34.

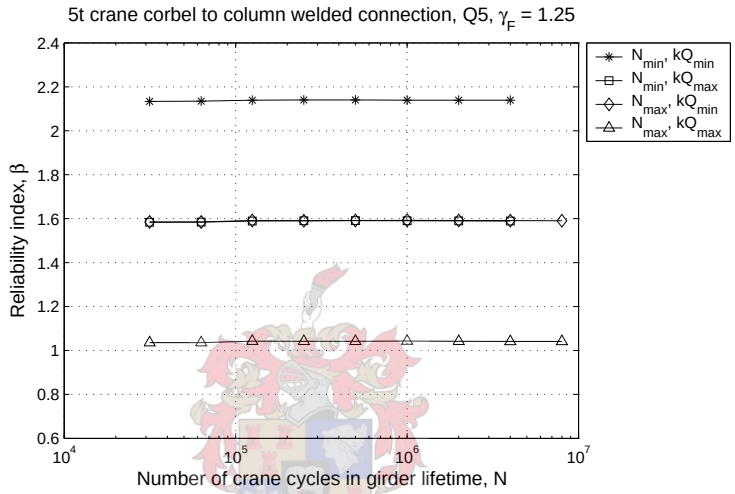

Figure 9.32: Calibration results for 5t crane corbel to column connection

9.3.3 Simulation of crane behaviour

The second method of assessing fatigue that could be included in the code is recommending crane load combinations to be considered for fatigue and the responsibility is then on the support structure designer to simulate the crane behaviour to determine the fatigue damage in the element.

This method of considering fatigue was assessed by carrying out the economic design of each element using the prEN 1991-3 method and then simulating the crane behaviour and assessing the resulting fatigue damage in the element.

This was carried out for each element for the average level of reliability combination of maximum number of cycles and minimum load spectrum for load spectrum class Q_5. The average damage for all the elements for each

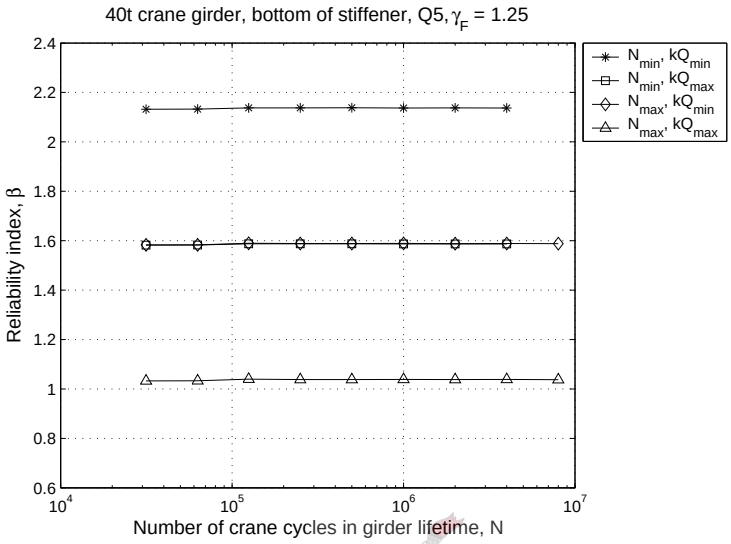

Figure 9.33: Calibration results for 40t crane girder bottom of stiffener

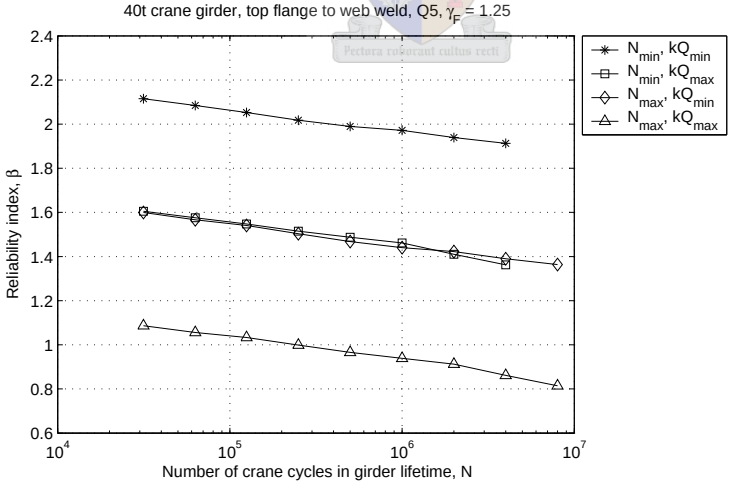

Figure 9.34: Calibration results for 40t crane girder top flange to web weld

point on the reliability curve was calculated and taken to represent the fatigue damage resulting from the true crane behaviour on the economically designed elements.

Considering the case when the fatigue partial load factor was $\gamma_F = 1.0$, the average fatigue damage resulting from the simulated crane behaviour on the elements which had been economically design according to the prEN 1991-3 method was 0.851. This indicates that there is some conservatism built into the prEN 1991-3 method.

Considering the case when the fatigue partial load factor was $\gamma_F = 1.25$, which results in a reliability equal to the target reliability, the average fatigue damage resulting from the simulated crane behaviour was 0.419.

A fatigue design equation in terms of fatigue damage can be considered in the form of:

$$D \geq d \tag{9.3.1}$$

Where:

D – fatigue resistance

d – fatigue damage resulting from simulated crane behaviour

In this case, the fatigue damage at failure is treated as the resistance and the fatigue damage resulting from the simulated crane behaviour is treated as the loading.

To achieve a target reliability of $\beta_T = 1.5$, the actual, nominal, fatigue damage in the elements was 0.419. When designing according to prEN 1991-3, the design value of the fatigue damage resulting from simulated crane behaviour was 0.851.

The partial factor which should be applied to the fatigue damage to obtain the target reliability is therefore:

$$\gamma_d = \frac{d_{\text{des}}}{d_{\text{nom}}} = \frac{0.851}{0.419} = 2.03 \tag{9.3.2}$$

Partial factors are traditionally applied to loads rather than to load effects, such as fatigue damage, so the partial factor obtained above will be reformulated so as to relate it to the crane wheel load rather than the fatigue damage resulting from the wheel load.

For an S-N curve with a constant slope of m = 3, the fatigue damage is calculated using the equation given below:

$$d = \sum_i \frac{(S_i)^3}{A} \frac{n_i}{N} \tag{9.3.3}$$

The damage is therefore proportional to the cube of the stress. Assuming that the stress is linear with respect to the load, the partial load factor which should be applied to the crane wheel load to achieve a target reliability of $\beta_T = 1.5$ is:

$$\begin{aligned} \gamma_F &= \sqrt[3]{\gamma_d} = \sqrt[3]{\frac{d_{\text{des}}}{d_{\text{nom}}}} \\ &= \sqrt[3]{\frac{0.851}{0.419}} \\ &= 1.26 \end{aligned} \tag{9.3.4}$$

This value of the fatigue partial load factor of $\gamma_F = 1.26$ corresponds well with the value of $\gamma_F = 1.25$ obtained considering the reliability graphs.

The above discussion was based on a structural element that had been economically designed according to the fatigue design method given in prEN 1991-3. The damage in the economically designed element due to the simulation of the crane behaviour was calculated and was found to be 0.851 for a fatigue partial load factor of $\gamma_F = 1.0$.

The second method of fatigue assessment entails carrying out the design of the girder by simulating the crane behaviour to determine the fatigue damage and taking the fatigue resistance as the fatigue damage at failure equal to 1.0. In this case the design method is the same as the method that was used to assess the fatigue damage in the girder designed according to the prEN 1991-3 method. Whereas for design according to prEN 1991-3, with a fatigue partial load factor of $\gamma_F = 1.0$ the damage from simulating the crane behaviour is 0.851, carrying out the design by simulating the crane behaviour would result in a corresponding fatigue damage of 1.0.

The required fatigue partial load factor applied to the crane loads in the case where the design is carried out by simulating the crane behaviour is given by:

$$\begin{aligned}\gamma_F &= \sqrt[3]{\frac{d_{\text{des}}}{d_{\text{nom}}}} \\ &= \sqrt[3]{\frac{1}{0.419}} \\ &= 1.34\end{aligned} \tag{9.3.5}$$

The partial load factor is larger than that required for design according to the prEN 1991-3 method because of the in built conservatism in the prEN 1991-3 method which is not present when considering the crane behaviour for the design.

9.4 Summary

The partial load factors and combination factors that resulted from the code calibration exercise are given in Tables 9.3 & 9.4.

Table 9.3: Calibrated partial load factors

Partial load factor	Symbol	Calibrated value
Crane partial load factor, code format 1	γ_C	1.907
Self weight partial load factor, code format 2	γ_{Csw}	1.617
Hoistload partial load factor, code format 2	γ_{Ch}	1.963
Crane partial load factor, code format 3	γ_C	1.590
Horizontal partial load factor, code format 3	γ_H	1.261
Self weight partial load factor, code format 4	γ_{Csw}	1.354
Hoistload partial load factor, code format 4	γ_{Ch}	1.623
Horizontal partial load factor, code format 4	γ_H	1.271
Partial load factor for accidental load, code format 1	γ_C	1.196
Partial load factor for accidental load applied to crane self weight, code format 2	γ_{Csw}	1.344
Partial load factor for accidental load applied to hoistload, code format 2	γ_{Ch}	1.448
Partial load factor for fatigue loads for prEN 1991-3 design method	γ_F	1.25
Partial load factor for fatigue loads for design by considering the crane behaviour	γ_F	1.34

Table 9.4: Calibrated combination factors

Combination factor	Symbol	Calibrated value
Combination factor for crane loads when combined with wind loads	ψ_{CW}	0.65
Combination factor for wind loads when combined with crane loads	ψ_{WC}	0
Combination factor for crane loads when combined with roof imposed loads	ψ_{CR}	0
Combination factor for roof imposed loads when combined with crane loads	ψ_{RC}	0

Pectora roborant cultus recti

Chapter 10

Discussion of results

The sensitivity factors for the reliability analyses showed that the modelling uncertainties in the calculation of the vertical and horizontal crane wheel loads were the dominant parameters. These were also the basic variables for which there was the least information available for the stochastic modelling. Sensitivity studies on the parameters of the modelling uncertainties are discussed in this chapter. The further work which could be carried out on the investigation of code calibration for crane support structures is discussed.

10.1 Sensitivity factors

The selection of the 5t crane column for the code calibration procedure was due to it having the lowest reliability of all the structural elements considered. The sensitivity factors from the reliability analysis were assessed to investigate the reason for this.

The sensitivity factors for a reliability analysis on the 5t crane column with LC5 for a class 1 crane with the ratio of hoistload to total crane weight r = 0.85 and $N_{extr} = 10^6$ cycles for code format 4, are given in Figure 10.1.

It was observed from the sensitivity factors that the modelling uncertainties have the most significant effect on the reliability. The reason why the 5t crane column has a lower reliability than the other elements is that the dominant loading is bending due to the horizontal crane wheel loads. The modelling factors for the uncertainty in the calculation of the horizontal loads and the bending moments obtained from the structural analysis program have large variations in comparison with the other variables, resulting in a low reliability.

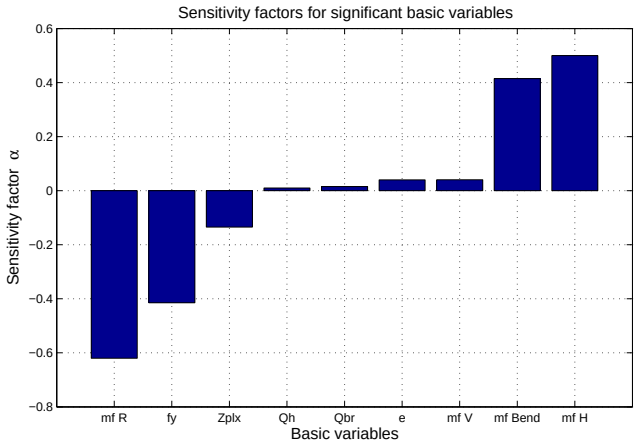

Figure 10.1: Sensitivity factors for the 5t crane column

Where:

mf R – modelling factor for the uncertainty in the resistance of the column

fy – yield stress of steel

Zplx – plastic section modulus of the column

Qh – weight of the hoistload

Qbr – weight of the crane bridge

e – eccentricity of the vertical wheel load

mf V – modelling uncertainty in the vertical wheel load calculations

mf Bend – modelling uncertainty in the bending moments obtained from the structural analysis program

mf H – modelling uncertainty in the calculation of the horizontal wheel loads

It was the general trend for all of the elements for the modelling factors to be the dominant variables, especially the modelling factors allowing for uncertainties in the calculation of the wheel loads. The parameters of these modelling factors were estimated because there was no literature available, as discussed in Chapter 6. The parameters of these modelling factors are therefore uncertain. In order to investigate the effect of different coefficients

of variation for these modelling factors, a sensitivity study was carried out on the reliabilities of the crane girders and columns.

10.1.1 Sensitivity of reliability to modelling uncertainty parameters

Four sets of coefficients of variation were considered for the modelling uncertainties for the calculation of the wheel loads:

cov1 $\delta_V = 5\%$ $\delta_H = 10\%$

cov2 $\delta_V = 5\%$ $\delta_H = 15\%$

cov3 $\delta_V = 10\%$ $\delta_H = 15\%$

cov4 $\delta_V = 10\%$ $\delta_H = 20\%$

The code calibration as presented in Chapter 9 was based on cov2.

In order to assess the sensitivity of the code calibration results to variations in the modelling uncertainties, the reliability of the girders and elements were calculated in a similar manner to the cost analysis for the verification of the results presented in Chapter 9. Following the same method of finding the critical load case for each element and assessing its reliability with respect to that load case, the minimum level of reliability of each element was assessed. The calibrated crane partial load factors were used for this assessment and it was observed that the code format did not have an effect on the trend of the results so code format 4 has been considered here. The minimum reliability for each of the crane girders and columns for each of the sets of modelling uncertainty parameters are shown in Figure 10.2.

As expected, the reliability decreases as the coefficients of variation of the modelling uncertainties increase. The difference in decrease between the different sets of coefficients of variation is due to the different influences of the vertical and horizontal wheel loads on each element. For example, the 5t crane column is loaded primarily by horizontal wheel loads, and there is therefore only a very small change in the reliability between cov2 and cov3 where there is only an increase in the coefficient of variation of the modelling uncertainty in the calculation of the vertical wheel loads. Similarly for the 5t crane girder which is loaded primarily by vertical wheel loads there is only a small change in reliability between cov1 & cov2 and cov3 & cov4.

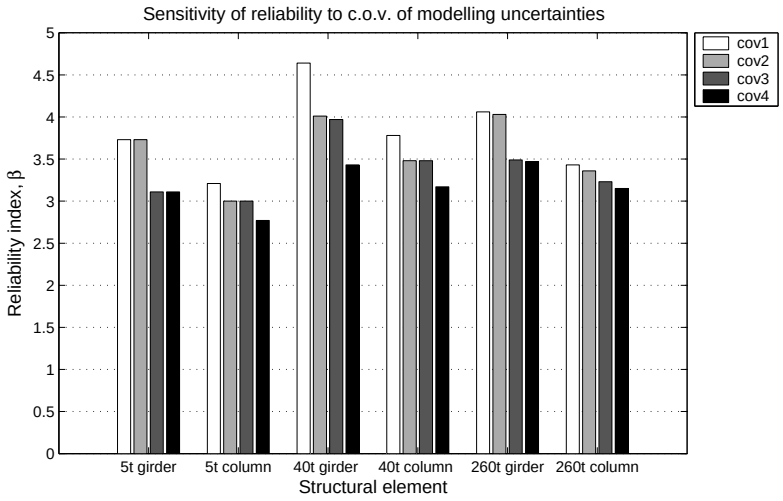

Figure 10.2: Sensitivity of reliability to c.o.v. of modelling uncertainties

The element chosen for the code calibration was the element which had the lowest reliability, i.e. the 5t crane column. The resulting conservatism for the other crane girders and columns ensures that as the coefficients of variation of the modelling uncertainties increase, though the reliabilities of these elements decrease they do not fall below the target reliability of $\beta_T = 3.0$. The reliability for the critical element, however, does fall below the target reliability with a reliability of $\beta = 2.77$ for cov4.

This sensitivity analysis shows that, though the majority of the elements have sufficient conservatism to meet the code calibration requirements for a range of coefficients of variation of the modelling uncertainties, more investigation is needed into the modelling uncertainties in the calculation of the crane wheel loads. The information that would assist in the improvement of the modelling uncertainty parameters would be a comparison between measured wheel loads to calculated wheel loads, both vertical and horizontal. The information would be most valuable if the comparison was carried out over a range of parameters similar to the parameters considered in this study but also including the stiffness of the crane and support structure.

10.1.2 Sensitivity of partial load factors to modelling uncertainty parameters

The modelling uncertainty for the calculation of the horizontal wheel loads was the modelling factor that had the greatest influence on the crane partial load factors and was the modelling factor for which there was the least information available to determine statistical parameters.

The crane partial load factors which are influenced by the modelling uncertainty for the calculation of the horizontal loads are:

γ_C – partial load factor applied to characteristic crane wheel loads in code format 1

γ_{Csw} – partial load factor applied to crane self weight in code format 2

γ_{Ch} – partial load factor applied to hoistload in code format 3

γ_H – additional partial load factor applied to horizontal wheel loads for code formats 3 & 4

A sensitivity study was carried out on the partial load factors mentioned above. The bias and coefficient of variation of the modelling uncertainty of the calculation of the horizontal wheel loads were varied and the partial load factor required to obtain a reliability equal to the target reliability of $\beta_T = 3.0$, was calculated.

Only partial load factors γ_C, applied to the characteristic wheel load, and γ_H, the additional factor applied to the horizontal wheel load are considered for the sensitivity study. The results from the sensitivity studies for these two partial load factors are similar and were judged to be representative of the sensitivity of the load factors to the modelling uncertainty parameters.

The results of the sensitivity study are shown in Figures 10.3 & 10.4. The sensitivity of the crane partial load factor, γ_C, for code format 1, to the modelling uncertainty parameters is shown in Figure 10.3. The sensitivity of the additional partial load factor applied to the horizontal wheel loads, γ_H, is shown in Figure 10.4, the values of γ_H do not vary significantly from code format 3 to 4, therefore Figure 10.4 shows the results for code format 3.

The bias of the modelling uncertainty, λ_{mfH}, is defined as the ratio of mean horizontal wheel load to calculated characteristic horizontal wheel load:

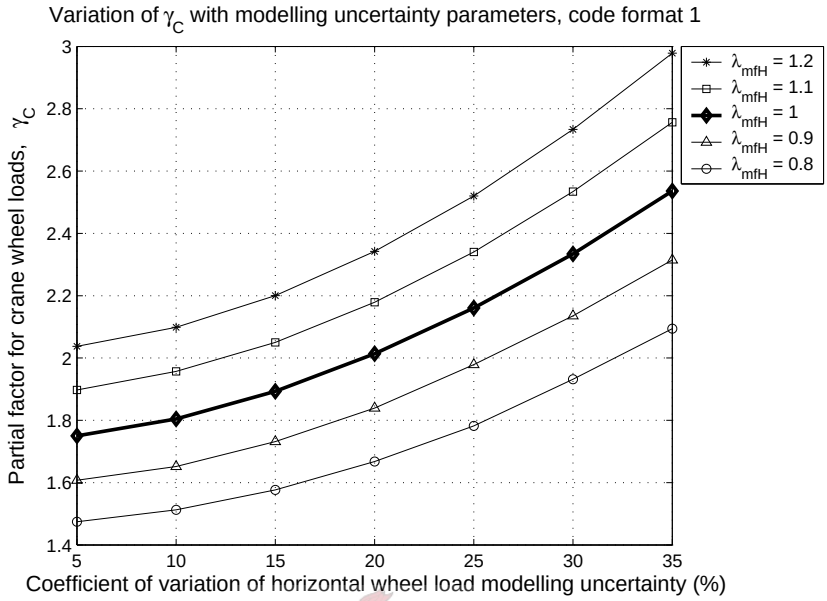

Figure 10.3: Sensitivity of γ_C to horizontal wheel load modelling uncertainty parameters

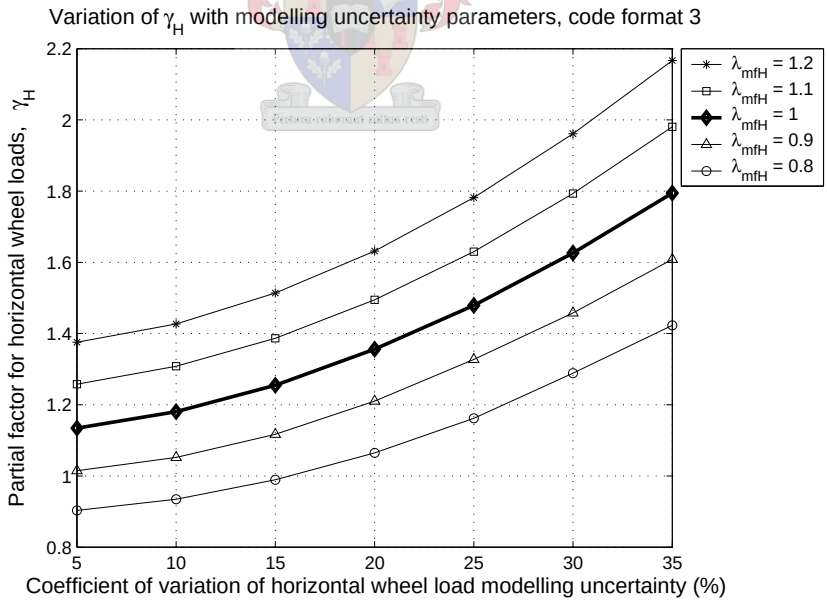

Figure 10.4: Sensitivity of γ_H to horizontal wheel load modelling uncertainty parameters

$$\lambda_{mfH} = \frac{\bar{H}}{H_c} \tag{10.1.1}$$

In other words, a bias greater than one indicates an unconservative model which consistently underestimates the value of the wheel loads and conversely a bias less than one indicates a conservative model which consistently overestimates the value of the wheel loads.

The trends of the partial load factors are:

1. As the bias increases, the required partial load factor to achieve a target reliability of $\beta_T = 3.0$ also increases.

2. As the coefficient of variation increases, the partial load factor also increases, with the curve becoming steeper in the region of larger coefficients of variation.

The parameters of the modelling uncertainty for the horizontal loads that were used for the code calibration were:

$$\lambda_{mfV} = 1.0 \qquad \delta_{mfV} = 15\%$$

These values resulted in partial load factors of:

$\gamma_C = 1.907$

$\gamma_H = 1.261$

Load models which have been rationally developed, such as the crane load models in prEN 1991-3, are unlikely to have a high bias (i.e. be unconservative) combined with a large coefficient of variation. Therefore, considering Figures 10.3 & 10.4, the curve for a bias of 1.2 is unlikely to realistically go beyond a coefficient of variation of modelling uncertainty of 5% and for a bias of 1.1, the coefficient of variation is unlikely to be larger than 15%. This trend suggests a reasonable upper limit of $\gamma_C = 2.3$ and $\gamma_H = 1.5$.

This sensitivity study confirms the fact that the results of the code calibration are indeed sensitive to the parameters of the modelling uncertainty for the calculation of the horizontal wheel loads and that more investigation is required into these parameters.

10.2 Code format

10.2.1 Ultimate limit state

Four code formats were considered for the ultimate limit state and have been discussed in section 8.3. They are briefly outlined below:

1. One partial load factor applied to the calculated wheel load

2. Two partial load factors, one applied to the crane self weight and one applied to the hoistload

3. As for format 1 but with an additional factor applied to the calculated horizontal loads

4. As for format 2 but with an additional factor applied to the calculated horizontal loads

It can be clearly seen from the cost analyses for the girders and columns presented in Figure 9.13 - 9.15 that the code format which results in the lowest cost support structure is code format 4. This code format allows for the different bias and variability between the crane self weight and hoistload by applying different partial load factors to each. It also allows for the higher level of uncertainty in the calculation of the horizontal wheel loads than the vertical wheel loads by applying an additional partial load factor to the calculated horizontal wheel loads.

Code format 4 best fulfils the requirements of the code calibration exercise in that it achieves the most consistent level of reliability over a range of loading conditions and crane parameters resulting in the most economic support structures.

The disadvantage of code format 4 is that it entails more partial load factors than the current code format and is therefore a more complicated code format for designers. One method of ameliorating this problem would be to include the additional partial load factor for the horizontal loads in the calculation model for the wheel loads. This would result in a code format more consistent with current practice at the expense, however, of transparency.

10.2.2 Accidental limit state

Characteristic loads are used in SABS 0160:1989 for the assessment of accidental load situations, this implies a partial load factor of 1.0. In order to achieve the target reliability of $\beta_T = 4.0$ for the accidental limit state the following partial load factors were required:

- Code format 1:
  - $\gamma_C = 1.196$
- Code format 2:
  - $\gamma_{Csw} = 1.344$
  - $\gamma_{Ch} = 1.448$

In order to keep the familiar code format, one manner in which these factors may be included in the code is to incorporate them into the dynamic factor ϕ_7.

These partial load factors have been calibrated on the assumption that the crane will collide with the end stops 10 times during the life of the structure, resulting in this load situation being treated as an ultimate limit state. If sufficiently reliable measures were in place (e.g. limit switches) to prevent the crane colliding with the end stops, the choice may be made available to the designer to reduce the partial load factor or to follow current practice of using characteristic loads. If this assumption was made and the crane did occasionally collide with the end stops, this would lead to a reduction in reliability of the support structure. In order to assess the level of reliability for this situation an investigation was carried out into the effect of retaining the current practice of using characteristic values for the assessment of the accidental limit state. Figures 10.5 to 10.8 show the reliability curves for all four classes of crane with various values of N_{extr} and ratios of hoistload to total crane weight, using characteristic loads for the design.

For the practical range of ratios of hoistload to total crane weight, the reliabilities range from $\beta = 2.68$ for the class four crane to $\beta = 3.43$ for a class one crane. These values of reliability are all much lower than the target reliability of $\beta_T = 4.0$.

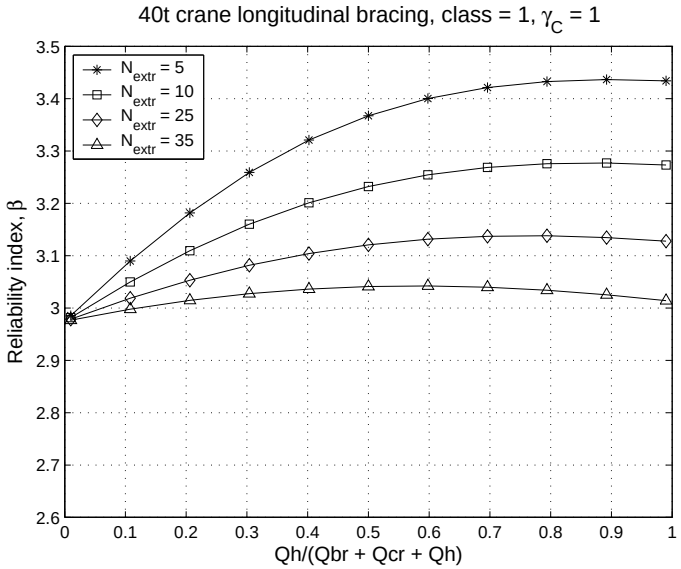

(a) Class 1

Figure 10.5: Reliability of bracing elements for accidental limit state, Class 1

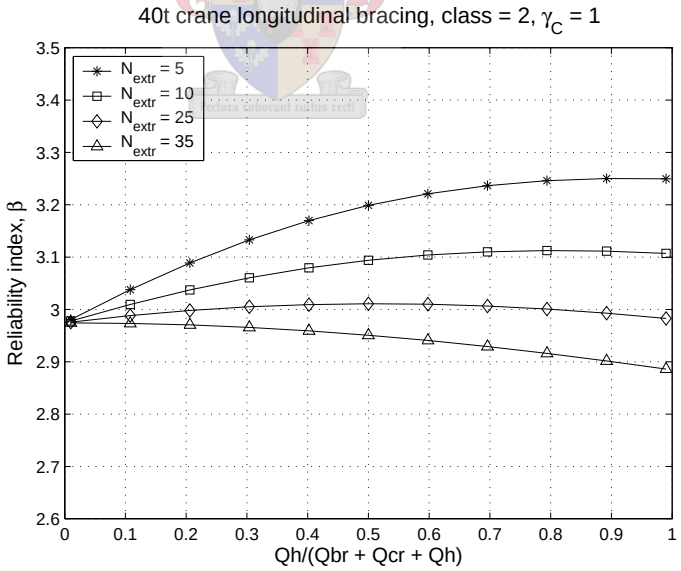

(a) Class 2

Figure 10.6: Reliability of bracing elements for accidental limit state, Class 2

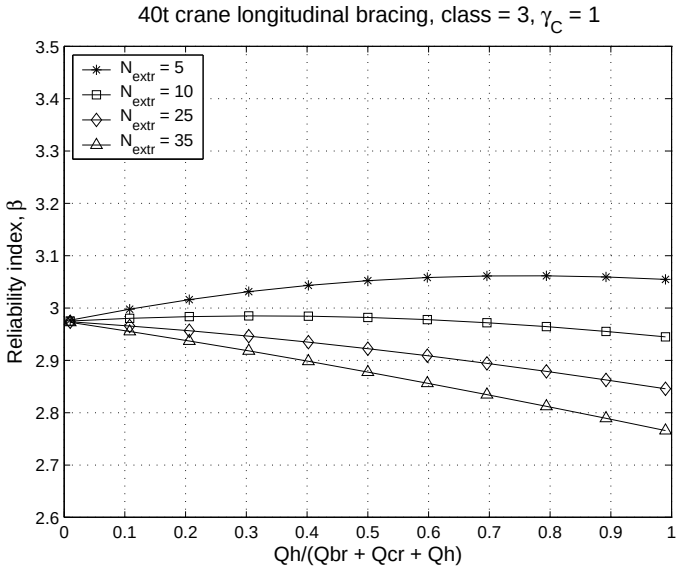

(a) Class 3

Figure 10.7: Reliability of bracing elements for accidental limit state, Class 3

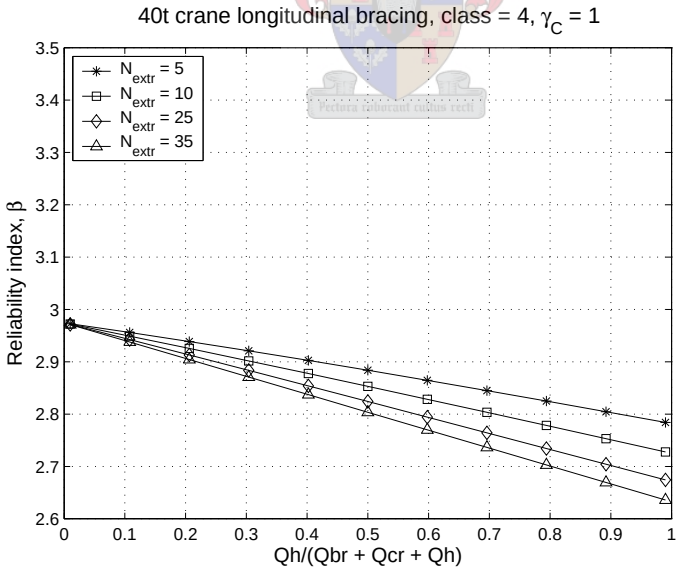

(a) Class 4

Figure 10.8: Reliability of bracing elements for accidental limit state, Class 4

10.2.3 Fatigue

The current partial load factor for fatigue in SABS 0160:1989 [1] is 1.0, i.e. characteristic loads are used for the fatigue analysis. The code calibration results showed that when using the fatigue loading method in prEN 1991-3, a partial load factor of 1.25 applied to the crane wheel loads is required to obtain the target reliability of $\beta_T = 1.5$. This would be a deviation from current practice and could lead to opposition from designers. This could be dealt with in a similar manner to the horizontal load partial factor in the ultimate limit state, in that the fatigue partial load factor could be included in the λ factors which are used to calculate the fatigue damage equivalent load. The code would then keep the current format with the disadvantage of a loss of transparency.

Very little information is given in the prEN 1991-3 as to the development of the λ factors so it could be argued that this fatigue design method is not transparent and the inclusion of a partial load factor into the λ factors could therefore not decrease the transparency.

10.3 Further work

10.3.1 Multiple cranes

This code calibration exercise dealt only with loads imposed by a single crane. Many industrial buildings consist of more than one bay with a crane in each bay or more than one crane in one bay, therefore the combined actions of more than one crane are of interest.

Due to the spatial and temporal variability of crane loading, a time dependent approach is recommended for the assessment of the combination of more than one crane.

A study of the combination of two cranes for column loading has been carried out by Pasternak *et al.* [14] where the crane vertical loads on the column were modelled as intermittent trapezoidal wave renewal processes. An upcrossing approach was used to determine the mean upcrossing rate function and the cumulative distribution function of the maximum value of the combined loading for a given time period.

When considering combinations of intermittent wave renewal processes the following items need to be determined (Wen [66]):

1. Load occurrence rate
2. Intensity variation
3. Duration of each pulse
4. Simultaneous occurrence of different loads

The intensity variation of the pulses was modelled by Pasternak *et al.* [14] considering two random variables, namely the hoistload and the position of the crab. The hoistload models given by Köppe [13] were used which have been shown in Chapter 7 to be unsuitable for hook cranes in South Africa. In future work on the combination of more than one crane in South Africa the hoistload models developed in Chapter 7 could be used. Two distributions were considered by Pasternak *et al.* [14] for the distribution of the crab position, viz. a uniform distribution (modelling the crab working evenly across the crane bridge) and a left triangular distribution (modelling the crab working predominantly to the left side of the crane bridge). Further crab position distributions which could be considered are a centre triangular distribution (modelling the crab working predominantly in the centre of the crane bridge) and a 'concentrated distribution' where the crab is always at the extreme of its travel as is the case with many ladle cranes.

The load occurrence rate and duration of each pulse would depend on the speed of the crane, the length of the runway and the characteristics of the crane operation.

Combination factors for two cranes are given by Pasternak *et al.* [14], expressed as a given percentile of the maximum combined load divided by the sum of the given percentiles for the individual loads.

Further work is required, however, on the combination of more than one crane for codification due to the fact that the results given by Pasternak *et al.* [14] use the hoistload distributions developed by Köppe [13] and that the results are given for time periods of only up to one year whereas the lifetime of a crane support structure is usually 25 years.

A further limitation of the work carried out by Pasternak *et al.* [14] is that only vertical loads on columns have been considered. The combination of horizontal loads should also be considered for the full assessment of combinations of cranes.

10.3.2 Probabilistic optimisation

The target reliabilities selected for the code calibration for the three limit states considered, were based on current practice and recommendations given by JCSS [36], prEN 1990 [61] and SANS 2394:2004 [64]. The target reliabilities were treated as the minimum allowable value of reliability for all practical ranges of parameters. This stringent condition could be moderated by carrying out a probabilistic cost optimisation exercise to determine the optimal reliability level taking into account the risks associated with crane support structures.

In order to carry out the probabilistic optimisation, a risk assessment of crane support structures would be required to identify possible unfavourable situations and to determine their consequences. Ultimate limit state type failures could be considered as well as serviceability limit states and fatigue. One aspect that could be considered is the frequency of inspection and maintenance required for fatigue considerations.

The four classes of crane should be considered separately for the probabilistic optimisation because the characteristics of the risks for the four different classes are likely to differ.

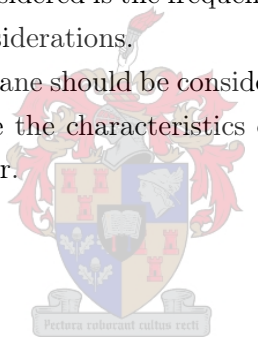

Chapter 11

Conclusions

Electric overhead travelling cranes are used in industrial applications for moving loads around the industrial area. Cranes often form an integral part of the industrial process and any down time can have severe financial implications for the owner. Cranes move over the industrial area lifting heavy loads, therefore any failure of the crane or the support structure which causes the load or crane to fall could become a serious safety hazard.

Due to the importance of the smooth running and safety of cranes, the correct design of the crane support structure is a very important issue when designing an industrial building which will contain cranes. Many problems have been encountered with crane support structures, particularly fatigue problems.

Codes of practice on loadings on buildings provide load models to calculate the wheel loads that cranes impose on their support structures. Two aspects of the crane loading provisions in the South African code of practice on loadings on buildings, SABS 0160:1989 [1], were identified for investigation. These two aspects were:

1. Crane load models

   A comparison between the crane load models in SABS 0160:1989 [1] and those in prEN 1991-3 [2], ISO 8686-1:1989 [5], DIN 15018 Part 1 1984 [4] and AS1418.1-1994 [6] indicated that the SABS 0160:1989 crane load models are over-simplistic.

   Updating of the South African crane load models by adoption of the prEN 1991-3 load models is currently under consideration by the South African loading code committee, and for this, an assessment of the prEN

1991-3 crane load models is required to determine their suitability for inclusion into the updated South African loading code, proposed SANS 10160.

2. Reliability of crane support structures

   Reliability based code calibration has not previously be applied to crane support structures are there is therefore no reliability basis for the crane partial load factor in SABS 0160:1989. The load factor which is applied to the crane loads is the imposed load factor, which has been calibrated for floor loads in office buildings, of $\gamma_L = 1.6$. In contrast the crane partial load factor in prEN 1991-3 is the same as the load factor applied to permanent loads, of 1.35.

   The difference between the partial load factors in the two codes and the lack of a reliability basis for the crane partial load factor in SABS 0160:1989, indicated a need for a reliability assessment of the crane load models.

   The aims of the reliability assessment of the crane load models were to assess the level of reliability of current practice and, if necessary, to determine suitable partial load factors to achieve the required level of reliability.

Both of these issues were dealt with as a code calibration problem, where the code that was being considered, was the crane loading code. The code calibration consisted of two parts, firstly calibration to current practice and secondly the reliability calibration.

Both of these calibration procedures were carried out on specific example structures. An investigation was carried out into the crane parameters which affect the loads as calculated by prEN 1991-3 and the range and distribution of these parameters for cranes in South Africa. The critical parameters were found to be the crane bridge span and the capacity of the crane.

Three representative cranes were selected to cover the range of the parameters. The full range of capacities was covered but the spans covered only the most likely range. The effect of shorter or longer spans was taken into account in the parametric study on the ratio of hoistload to total crane weight, that was carried out for the reliability calibration. The representative cranes were:

- 5t crane, 19.2 m span

- 40t crane, 23.8 m span
- 260t crane, 28.5 m span

The support structures were also shown to be representative of those found in practice.

The selection of the representative cranes and the calibration to current practice has been discussed in Warren *et al.* [67].

11.1 Calibration to current practice

The aims of the calibration to current practice were:

1. To assess the crane load models from prEN 1991-3 for their suitability for adoption into proposed SANS 10160.
2. To assess the implications of adopting the crane load models from prEN 1991-3 on the cost of the support structure and the design effort required for the crane support structure.

11.1.1 Crane load models from prEN 1991-3

The crane load situations that are allowed for in SABS 0160:1989 and prEN 1991-3 were compared and are summarised in Table 11.1.

The crane load models in prEN 1991-3 model in more detail the different vertical loads, taking into account specific situations for the dynamic effects of lifting loads, running on rails etc.

A comparison between the horizontal load cases shows that both codes consider acceleration of the crane, skewing and crane buffer forces but that the load case for misalignment of the crane wheels or rails is not covered by prEN 1991-3.

The misalignment load case in SABS 0160:1989 takes into account the situation where either the rails or wheels are misaligned in a 'toe-out' or 'toe-in' manner causing horizontal transverse wheel loads, which tend to pull the rails together or push them apart. The misalignment forces are due to transverse friction on the rails and can occur when the alignment of the wheels and rails are both within specified alignment tolerances.

The misalignment load case is one of the critical load cases in SABS 0160:1989 and its inclusion in the SABS 0160:1989 crane loading provisions

Table 11.1: Summary of crane loads considered by the codes

Crane load	SABS 0160:1989	prEN 1991-3
Vertical		
Generic dynamic amplification	X	
Hoisting a load off the ground		X
Running on rails		X
Release of payload		X
Test loads		X
Horizontal transverse		
Acceleration of crane		X
Acceleration of crab	X	
Skewing	X	X
Misalignment	X	
Crab buffer forces		X
Horizontal longitudinal		
Acceleration of crane	X	X
Crane buffer forces	X	X

implies that it was deemed to be necessary to consider this load situation. Therefore, when the crane load models are updated, a misalignment load model should be included.

An assessment of the prEN 1991-3 crane load models showed that they were more sophisticated than the SABS 0160:1989 models in that more crane parameters were taken into account. The comparison between the load effects resulting from horizontal loads from prEN 1991-3 and SABS 0160:1989 demonstrated the greater sophistication of the prEN 1991-3 load models by the fact that the load effect ratios due to horizontal loads depended on the span and wheel spacing of the crane.

prEN 1991-3 load models also take into account in more detail the dynamic factors for different load situations (e.g. hoisting a load, acceleration of the crane), thereby more accurately modelling the mechanism behind the load.

Considering all the above points, it is likely that the prEN 1991-3 crane load models more accurately model the crane behaviour than the crane load models from SABS 0160:1989.

11.1.2 Fatigue loading in prEN 1991-3

SABS 0160:1989 does not specify crane loads to be considered for fatigue load assessment of the crane support structure. The onus is therefore on the designer to model the crane behaviour, i.e. the load cases to be considered for fatigue, the range of hoistloads, the crab positions and the movement of the crane along the runway.

The approach of prEN 1991-3 is to normalise the maximum crane wheel load resulting in a constant amplitude load for two million cycles which is then used to calculate the fatigue stresses. The normalisation is carried out by applying a factor to the maximum crane wheel load depending on the number of cycles that the crane will perform over its lifetime and the load spectrum of the crane.

The method of normalising the wheel load was derived from the fatigue design procedure of the crane itself and the applicability of this method to the support structure is questionable.

An issue of concern that was identified was the definition of the load spectrum. The definition of the load spectrum in prEN 1991-3, considers the change in wheel load that the crane will experience, from the minimum load to the wheel load being considered for a particular load being lifted. For fatigue design of the support structure it would be more reasonable to consider the change in load that the support structure would experience, from zero, before the crane moves onto the particular girder or column, to the value of the wheel load, when the crane is on the particular girder or column.

A modified load spectrum definition was presented that considered the change in load that the support structure would experience rather than the change in load that the crane would experience. This load spectrum definition, however, does not cover the case of a continuous girder which could experience a negative load effect when the crane is on the adjacent span and a positive load effect when the crane is on the span being considered. This highlights the fact that it is more difficult to apply this fatigue design method to the support structure than to the crane because of the variety of support structure configurations.

The advantage of the fatigue assessment method given in prEN 1991-3 is that it is simpler to use than a full simulation of the crane behaviour. It should be conservative though, as with all simplified methods. The degree of conservatism included in this method will be discussed in Section 11.2 on

reliability of the support structures.

An alternative method of including crane fatigue loading recommendations in proposed SANS 10160 is to identify the crane load combinations which are to be considered for the fatigue assessment. The support structure designer is then responsible for modelling the crane behaviour for the fatigue design.

The crane load combinations given in prEN 1991-3 include combinations which will not be critical for ultimate limit state but which could be used for a fatigue assessment. The load combinations to be considered for fatigue would be those that consist of frequently occurring actions such as hoisting, acceleration of the crane bridge, acceleration of the crab. Skewing of the crane in plan is viewed as an infrequently occurring load situation (ENV 1993-6 [35]) and therefore should not be included in the fatigue assessment.

The advantage of this method is that it allows the designer to assess the effect of each crane load on the fatigue damage and to be able to tailor the crane behaviour modelling to fit each crane installation.

11.1.3 Implications of adopting crane load models from prEN 1991-3

Two issues were investigated in assessing the implications of adopting the crane load models from prEN 1991-3 into proposed SANS 10160: the cost of the support structure and the design effort required for the design of the support structure.

11.1.3.1 Cost of the support structure

The costs of the support structure designed considering crane wheel loads from the models in SABS 0160:1989 and prEN 1991-3 were compared by considering the load effects in the crane girders, columns and longitudinal bracing of the three representative cranes. In order to assess the effect of the crane class on the load effects, the comparison was carried out assuming that the cranes were either class or hoist class 2, 3 or 4. The class 2 cranes were compared with the hoist class 2 cranes etc.

The load effects due to vertical crane wheel loads showed that, on average, the vertical loads due to the prEN 1991-3 load models were 10% smaller than those due to the SABS 0160:1989 load models. The ratios of the load effects due to the vertical loads did not vary across the crane classes.

The load effects influenced by horizontal transverse loads ranged from the prEN 1991-3 load models resulting in loads 56% to 217% of the SABS 0160:1989 loads. The difference depended on the geometry of the crane, specifically the span and the wheel spacing. The loads from prEN 1991-3 were the smallest when considering the 260t, crane which has a span to wheel spacing ratio of 2.4, and the largest when considering the 40t crane, which has a span to wheel base ratio of 5.4. The ratios of horizontal transverse loads (SABS 0160:1989/prEN 1991-3) were different for the various classes of crane, increasing with increasing class. The horizontal loads from prEN 1991-3 do not change with the class of crane as in SABS 0160:1989, so the variation in ratios was due to the change in magnitude of the SABS 0160:1989 loads.

The buffer forces calculated from prEN 1991-3 resulted in forces with magnitudes in between those obtained from the simple method and the more detailed method in SABS 0160:1989. The simple method gives the largest forces as would be expected from a simplified method. Both prEN 1991-3 and the more detailed method in SABS 0160:1989 consider the resilience of the buffers but prEN 1991-3 results in larger loads because it includes the weight of the hoistload whereas SABS 0160:1989 does not.

The effect on the cost of the support structure of adopting the prEN 1991-3 crane load models into proposed SANS 10160 would depend on the class and geometry of the crane. The horizontal forces in SABS 0160:1989 depend on the class of the crane and those in prEN 1991-3 do not. The horizontal forces in prEN 1991-3 take into account the geometry of the crane, the span and wheel spacing, unlike those in SABS 0160:1989 which take into account only the crane self weight, hoistload and number of wheels. For lower class cranes with a large span to wheel spacing ratio, the prEN 1991-3 load models give larger horizontal forces than the SABS 0160:1989 load models. For higher class cranes and cranes with small span to wheel spacing ratio, the prEN 1991-3 load models result in smaller horizontal forces than the SABS 0160:1989 load models. The vertical loads from prEN 1991-3 would on average result in lighter girders.

Considering the longitudinal bracing, design using the prEN 1991-3 load models would result in heavier bracing members if the detailed method in SABS 0160:1989 had previously been used, or lighter bracing if the simplified method had previously been used.

No general trend can be identified for the change in the cost of the support

structure by design according to the prEN 1991-3 crane load models rather than the SABS 0160:1989 crane load models due to the difference in the approach taken to calculate the horizontal transverse loads.

11.1.3.2 Design effort

The design effort required for the design of the support structure was considered by dividing the design process into the calculation of the crane loads and the subsequent design of the support structure.

It was found that slightly more crane information is required for the calculation of the crane loads according to prEN 1991-3 than SABS 0160:1989. Calculating the crane loads according to prEN 1991-3 also required more pages of calculations than according to SABS 0160:1989.

Two critical load combinations were identified for each code, therefore the same design effort would be required for the subsequent design of the support structure, which in itself entails vastly more design effort than the calculation of the loads.

Slightly more design effort is required for the prEN 1991-3 crane load models than the SABS 0160:1989 models, however, with the use of computer spreadsheets this would probably be a once-off effort and is therefore insignificant.

11.2 Reliability calibration

The reliability code calibration was carried out on individual elements of the support structures of the representative cranes. The elements that were considered were those that were influenced by crane loads, i.e. the crane girders, crane columns, roof columns, roof truss members and longitudinal runway bracing.

The limit states considered for the reliability assessment of the crane support structures were ultimate limit state, accidental limit state and fatigue.

The calibration did not follow the convention for general code calibration of separating loads and resistances but, because specific structures were being considered, the limit states equations were developed including both loads and resistances.

11.2.1 Stochastic modelling

The stochastic models for most of the basic variables were obtained from literature. There was no literature available on the basic variables relating to crane loading so these were developed for this investigation.

The crane wheel loads were modelled by considering the crane self weight and hoistload as basic variables and including a modelling uncertainty factor to take into account the uncertainty in the calculation of the wheel loads.

11.2.1.1 Modelling uncertainties

There was no literature available on modelling uncertainties in the calculation of the crane loads; therefore the statistical parameters for these modelling uncertainties were developed for this investigation

Three crane load modelling uncertainties were included to take into account the various crane load models.

1. Uncertainty in the calculation of the vertical wheel loads
2. Uncertainty in the calculation of the horizontal transverse wheel loads
3. Uncertainty in the calculation of the horizontal longitudinal loads due to the crane colliding with the end stops.

The modelling uncertainty for the vertical wheel loads was investigated by carrying out a numerical assessment of various crane configurations to determine the increase in vertical loads due to one wheel losing contact with the rail. The modelling uncertainty for the horizontal longitudinal loads was assessed from experimental data available on end stop forces. However, there was no information available on which to base the parameters of the modelling uncertainty for the horizontal transverse loads, so the parameters were estimated using judgement.

The sensitivity factors from the reliability analysis and the sensitivity study carried out on the partial load factors showed that the modelling uncertainty for the horizontal transverse loads was a critical variable. In the light of this, more information should be gathered to improve the parameters for this modelling uncertainty. Difficulties arise in that there is no available experimental or numerical modelling data. One option would be to conduct an expert survey but here too, difficulties are encountered. The experts in crane support

structure design in South Africa are currently unfamiliar with the prEN 1991-3 crane load models and horizontal crane wheel loads are inherently difficult to assess because of the lack of observational data, unlike roof or floor imposed loads where the loads are due to the weight of visible objects.

A solution to the problem of determining the parameters of the modelling uncertainty in the horizontal transverse loads is to obtain data on actual horizontal loads that cranes impose on their support structures. This data could be obtained from laboratory experiments or numerical modelling of crane structures. In order to be comprehensive, a range of crane parameters should be considered.

11.2.1.2 Stochastic modelling of the hoistload

There were no crane load models, suitable for the code calibration, presented in the literature. Although Pasternak *et al.* [14] and Köppe [13] have developed crane load models they are not suitable for the code calibration of crane loads for use in South Africa. Therefore stochastic models for crane loads were developed for this investigation in the form of statistical models for the hoistloads lifted by cranes.

The stochastic models for the hoistload that were developed for the code calibration were both arbitrary point-in-time and extreme value type distributions. The stochastic modelling of the hoistload has been discussed in Warren *et al.* [68].

For the purpose of this study, cranes were divided into four classes according to a description of the loads that are lifted and hoistload distributions developed for each class.

'One cycle' distributions were developed which model the probability distribution of the load lifted by a crane for one crane cycle, i.e. one load lifted. This distribution can be considered as the frequency distribution of the loads that a crane lifts over its lifetime. The 'one cycle' distributions were developed from data and descriptions of loads lifted obtained from crane operators as well as the descriptions of the class of crane.

Beta distributions were used for the 'one cycle' hoistload distributions because they have lower and upper bounds and because of the ease of fitting the required shape.

The upper bound of the hoistload distributions was set higher than the

overload limit switch level of 110% overload because, according to the crane operators, the overload limit switches do get turned off to lift larger loads. The level chosen for the upper limit was 125% overload which is the value of the test load that the crane lifts after installation. This value can be considered to be an extreme upper bound for the upper limit of the distribution.

The extreme distributions were developed on the principle that reliability is always expressed in terms of a time period and the extreme load distributions model the largest load that is likely to occur during that time period. When considering cranes, a given time period can be related to a number of crane cycles and the extreme hoistload distribution can be considered to be the probability distribution of the largest load that the crane will lift in a given number of cycles, termed N_{extr}.

The extreme hoistload distributions were developed from the 'one cycle' distributions using a simulation technique. Curves were fitted to the observed trends in the mean values and standard deviations which allow interpolation and extrapolation to obtain the parameters of the extreme hoistload distribution for $N_{extr} \leq 2 \times 10^6$ cycles.

Extreme hoistload distributions can be obtained for various limit states and load combinations by selecting the appropriate number of cycles.

The hoistload distributions that were developed are not dependent on the specific representative cranes but are general distributions which could be used for future reliability assessment of crane support structures, including time variant assessments of one crane or combinations of more than one crane.

11.2.2 Code calibration

The reliability assessment for the code calibration was carried out in two steps. The first step was the economic design of the member being considered where the design was carried out so that the member exactly complied with the code requirements. The second step was to carry out the reliability analysis of the economically designed member. This procedure ensured that the reliability of the code itself was being assessed.

11.2.2.1 Ultimate limit state

The objective for the code calibration was the achievement of a target reliability. The target reliability selected for the ultimate limit state was the value

used for the calibration of the South African codes of $\beta_T = 3.0$, with the constraint that the reliability obtained must be greater than or equal to this target reliability.

Four partial load factor formats were considered for the ultimate limit state. The first and simplest code format considered was the current practice for both SABS 0160:1989 and prEN 1991-3. The remaining three code formats were more complex formats which were included for this investigation to take into account the different characteristics of the crane self weight and hoistload, and the vertical and horizontal forces. The effect of the different code formats on the consistency of the reliability over a range of parameters was investigated.

The four code formats are discussed in detail in Section 8.3 on page 180 and are outlined briefly below:

1. One partial load factor, γ_C, applied to the calculated characteristic wheel loads.

2. Two partial load factors, one applied to the crane self weight, γ_{Csw}, and one applied to the hoistload, γ_{Ch}.

3. As for format 1 but with an additional factor applied to the calculated design horizontal loads, γ_H.

4. As for format 2 but with an additional factor applied to the calculated design horizontal loads, γ_H.

As with all design codes, increased sophistication of the code format leads to greater consistency in the reliability which must be weighed up against the increased complexity of the code.

The calibration of the ultimate limit state was carried out in two steps: firstly, calibration of the crane partial load factors considering a crane load only case and secondly, calibration of the combination factors considering combinations of crane loads with other time varying loads.

The calibration was carried out on the critical structural element which had the lowest reliability which was found to be the 5t crane column.

Parametric studies were carried out to determine the values of critical parameters which resulted in the lowest reliability, these critical values were used for the calibration. The parametric studies that were carried out, and the critical values of these parameters, were:

1. Class of crane: the lowest reliability was obtained with a class one crane

2. Number of cycles considered for the extreme value distribution: $N_{extr} = 10^6$ cycles. This can be considered to be a reasonable upper limit of the number of cycles that a crane is likely to perform over its lifetime.

3. Ratio between hoistload and total crane weight: r = 0.85. This ratio takes into account shorter or longer crane bridge spans than the spans of the representative cranes.

It was also found that the higher the ratio of horizontal load effect to vertical load effect, the lower the reliability.

The calibrated partial load factors that were obtained for the crane only load case are given in Table 11.2. The partial load factors were calibrated using the extreme hoistload distributions that were developed for the code calibration, with the assumption that the crane could be overloaded to 125% SWL, the modelling uncertainties discussed above and considering the crab always at the extreme of its travel.

Table 11.2: Calibrated partial load factors

Code format	γ_C	γ_{Csw}	γ_{Ch}	γ_H
1	1.91			
2		1.62	1.96	
3	1.59			1.26
4		1.35	1.62	1.27

Verification of the calibrated partial load factors was carried out to ensure that the reliability of all the elements was above the target reliability and to assess the conservatism over a range of parameters for the four code formats.

It was found that code format 4 resulted in the most consistent level of reliability and hence the minimum conservatism. This would thus be the code format that best meets the code calibration objective of achieving a consistent target reliability. As mentioned above, consistent reliability and code simplicity are two mutually opposing goals and one has to be traded off against the other when it comes to deciding on the code format for the design code.

Two combinations of crane loads with other time varying loads were considered. The load combination equations are given below:

1. Crane and wind loads

    a) Crane dominant: γ_P(Permanent) + γ_C(Crane) + ψ_{WC}1.3(Wind)

    b) Wind dominant: γ_P(Permanent) + $\psi_{CW}\gamma_C$(Crane) + 1.3(Wind)

2. Crane and roof imposed loads

    a) Crane dominant: γ_P(Permanent) + γ_C(Crane) + ψ_{RC}1.6(Roof imposed)

    b) Roof dominant: γ_P(Permanent) + $\psi_{CR}\gamma_C$(Crane) + 1.6(Roof imposed)

Where:

γ_C – represents conceptually the factoring of the crane loads by whichever code format is being considered

The crane partial load factors that were calibrated for the crane only case were used in the calibration of the combination factors.

The combination factors for the combination of crane and wind loads were selected so as to result in constant reliability over the pertinent range of ratios of crane load to crane and wind load. The appropriate value of the combination factor applied to the crane loads was found to be $\psi_{CW} = 0.65$ and the appropriate value of the combination factor applied to the wind loads was found to be $\psi_{WC} = 0$.

The combination of crane and roof imposed loads resulted in very high reliability levels for the roof dominant case when designing the element for roof loads only. Constant levels of reliability equal to the reliability of the crane only load case, were obtained for the crane dominant case when designing for crane loads only. The combination of crane loads and roof imposed loads is therefore not a rational one.

The load combinations that resulted from this investigation are thus:

1. γ_P(Permanent) + γ_C(Crane)

2. γ_P(Permanent) + 0.65γ_C(Crane) + 1.3(Wind)

3. γ_P(Permanent) + 1.6(Roof imposed)

11.2.2.2 Accidental limit state

The accidental limit state that was considered was the crane running into the end stops causing horizontal longitudinal forces which are resisted by the longitudinal bracing. This load situation is classified as an accidental load in prEN 1991-3, though it was estimated to occur 10 times during the lifetime of the crane. This load situation was therefore considered as an ultimate limit state because of its relatively high probability of occurrence.

The target reliability selected was $\beta_T = 4.0$ because of the low cost of the longitudinal bracing elements and end stops in proportion to the consequences of failure.

The code formats considered for the accidental limit state were code formats one and two as given for the ultimate limit state.

The parametric studies that were carried out for the accidental limit state and the critical values of the parameters were:

1. Class of crane: the lowest reliability was obtained with a class 4 crane
2. Number of cycles considered for the extreme hoistload distribution: N_{extr} = 10 cycles

The calibrated partial load factors were:

- Code format 1:
  - $\gamma_C = 1.196$
- Code format 2:
  - $\gamma_{Csw} = 1.344$
  - $\gamma_{Ch} = 1.448$

These partial load factors are all greater than 1.0 indicating that the current practice of using the characteristic loads for the accidental limit state is unconservative.

The variation of the reliability with the ratio of hoistload to total crane weight was small, therefore code format 1 does not include significant conservatism in the lower ratios of hoistload to total crane weight. Code format 1

is a simpler format than code format 2 and, since it does not include significant over conservatism, would be the most suitable code format the accidental loads.

The calibration of the accidental load situation of the crane running into the end stops was carried out on the assumption that it would occur 10 times during the lifetime of the crane and was therefore considered as an ultimate limit state. In the event of the crane having sufficiently reliable systems to stop the crane before collision with the end stops, the choice could be left to the designer to reduce the partial load factor, or follow the current practice of using characteristic loads.

11.2.2.3 Fatigue

Fatigue was considered as a serviceability limit state with the objective that the average value of reliability should meet a target reliability of $\beta_T = 1.5$ because of the general inspectability of fatigue effects.

The code format that was considered for fatigue was code format one, as given for the ultimate limit state, consisting of applying one partial load factor, γ_F, to the characteristic crane wheel loads.

The fatigue reliability was assessed by determining the bounds of reliability for a given load spectrum class. The parametric studies that were carried out for fatigue were:

1. Considering a single slope or double slope S-N curve: the trend of the results did not differ significantly between the two curves so for simplicity, a single slope S-N curve was considered.

2. The load spectrum class considered: the load spectrum class was taken as Q_5 which was representative of the reliability for all the classes without the initial conservative area included in the other load spectrum classes.

The fatigue reliability was assessed for the prEN 1991-3 method of normalising the maximum wheel load and the results used to determine a partial load factor for the method of simulating the crane behaviour. The partial load factors are given in Table 11.3.

The partial load factor for fatigue assessment using the method given in prEN 1991-3 is less than that for the simulation of the crane behaviour. This

Table 11.3: Partial load factors for fatigue

Fatigue assessment method	Partial load factor, γ_F
prEN 1991-3	1.25
Simulating crane behaviour	1.34

indicates that the method given in prEN 1991-3 is slightly conservative, but not sufficiently so to be able to use the characteristic loads for the design.

Current practice is to use the characteristic loads for the fatigue assessment and the inclusion of a fatigue partial load factor in the code could meet with some resistance from designers. If the option to include only the fatigue assessment method given by prEN 1991-3 was taken, the fatigue partial load factor could be included in the factors used for the normalisation of the maximum wheel loads. This could be seen to be reducing the rationality and transparency of the code, though the fatigue method given by prEN 1991-3 is not completely transparent.

If it was decided to include both the fatigue assessment method from prEN 1991-3 and the method of simulating the crane behaviour; including two fatigue partial load factors, one for each method, would be undesirable from the perspective of code complexity. A method of simplifying the code format would be to specify only the fatigue partial load factor calibrated for simulation of the crane behaviour of $\gamma_F = 1.34$. This would result in designs using the method from prEN 1991-3 being conservative but this is appropriate for a simplified method.

11.3 Recommendations

The prEN 1991-3 crane load models have been shown to be more sophisticated and thus more likely to accurately model the crane wheel loads, than the crane load models in SABS 0160:1989. The crane load models from prEN 1991-3 should thus be included in proposed SANS 10160, with the addition of a load model for misalignment of the crane wheels or rails.

Of the four code formats considered for the crane partial load factors for the ultimate limit state, code format 4 resulted in the most consistent level of reliability and should be adopted in the code. The different partial load factors for the crane self weight, hoistload and horizontal loads, model the different

sources of uncertainty in the crane wheel loads and this is therefore the most transparent code format.

Code format 4 would result in an increase in code complexity from the current practice of applying one partial load factor to the characteristic wheel loads. The advantages of a more consistent reliability with less conservatism, resulting in more economic structures, outweigh the increased complexity of the code. With the use of computers and spreadsheets for load calculations, the increased complexity of the code format could be easily incorporated into the design process.

The issue of code complexity versus consistent reliability requires consideration though, and a less complex code format may be deemed to be more suitable for a code of practice. One method of simplifying code formats 3 or 4 for inclusion into the design code would be to include the additional partial load factor for the horizontal loads into the horizontal load models.

The calibrated crane partial load factors are reproduced in Table 11.4.

Table 11.4: Calibrated partial load factors

Code format	γ_C	γ_{Csw}	γ_{Ch}	γ_H
1	1.91			
2		1.62	1.96	
3	1.59			1.26
4		1.35	1.62	1.27

These partial load factors are all larger than the factors in SABS 0160:1989 and prEN 1991-3 indicating that the current level of reliability for crane support structures is inadequate.

The calibration of the combination factors for combinations of crane loads with wind loads or roof imposed loads resulted in only three rational load combinations that should be included in the design code:

1. γ_P(Permanent) + γ_C(Crane)
2. γ_P(Permanent) + 0.65γ_C(Crane) + 1.3(Wind)
3. γ_P(Permanent) + 1.6(Roof imposed)

A partial load factor should be included in the code for the accidental load situation of the crane colliding with the end stops. Because the structural

elements which resist the accidental loads have a low cost in proportion to the total cost of the structure and because of the serious safety and financial implications of failure, partial load factors greater than 1.0 should be included in proposed SANS 10160 for accidental loads. In the event that a crane has reliable measures to prevent collision with the end stops, an option should be available for the designer to reduce the partial load factor or follow current practice of using the characteristic loads for the design of these elements.

In order to keep the current code format of using characteristic loads for the assessment of the accidental situations, the partial load factors could be included in the dynamic factor ϕ_7.

Both the fatigue methods considered, the method in prEN 1991-3 of normalising the wheel load and the method of recommending load cases and for the support structure designer to model the crane behaviour, should be included into proposed SANS 10160.

The current method of using characteristic loads for the fatigue assessment was shown to be unconservative. The fatigue partial load factors that were obtained are reproduced in Table 11.5.

Table 11.5: Partial load factors for fatigue

Fatigue assessment method	Partial load factor, γ_F
prEN 1991-3	1.25
Simulating crane behaviour	1.34

If both methods are to be included in the code, the recommendation would be to include only one fatigue partial load factor of $\gamma_F = 1.34$. This would result in the fatigue assessment method from prEN 1991-3 being conservative, which is appropriate for a simplified method.

11.4 Further work

No literature was available on the modelling uncertainties for the calculation of the crane wheel loads therefore these models were developed for use in the code calibration. The modelling uncertainty for the calculation of the horizontal transverse loads was the variable for which the least information was available and the statistical parameters were therefore estimated. This modelling uncertainty was identified by the sensitivity factors and sensitivity

studies to be a critical variable requiring further investigation. Experimental or numerical investigations into the horizontal wheel loads that cranes impose on the support structures would provide the necessary information to be able to derive more accurate modelling uncertainties. The reliability procedures developed here can then be used to update and improve the partial factors derived in this study. Since the results presented here necessarily have to be on the conservative side to reflect the uncertainty in the true modelling uncertainty, the validated modelling factor variables are expected to result in more economical partial load factors.

In the code calibration, only single cranes were considered. Many industrial buildings consist of multiple bays with one or more cranes in each bay. An extension of the code calibration could be the calibration of combinations of more than one crane, using the stochastic models of hoistloads presented here.

A risk assessment and probabilistic cost optimisation could be carried out to determine the optimal levels of reliability for ultimate limit state, accidental limit state and fatigue.

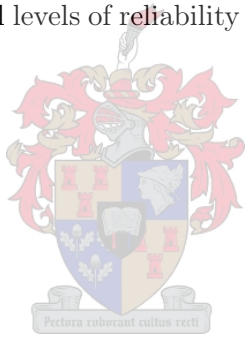

References

[1] SABS 0160:1989: Code of Practice, The general procedures and loadings to be adopted in the design of buildings. The Council of the South African Bureau of Standards, 1990.

[2] prEN 1991-3: Eurocode 1991: Actions on structures, Part 3: Actions induced by cranes and other machinery. prEN 1991-3. European Committee for Standardisation, CEN TC250/SC1, 2002.

[3] SANS 10160: Working document on SANS 10160: Basis of structural design and actions for buildings and industrial structures, Section 10: Actions induced by cranes and machinery. Personal communication with Working Group 61M of STANSA.

[4] DIN 15018 Part 1 1984: Deutsche Norm: Cranes, steel structures, verification and analysis. Beuth Verlag GmbH, Berlin, nov 1984.

[5] ISO 8686-1:1989: International Standard: Cranes - Design principles for loads and load combinations, Part 1: General. International Organisation for Standardization, Geneva, Switzerland, nov 1989.

[6] AS1418.1-1994: Cranes (including hoists and winches) Part 1: General requirements. Standards Australia, 1994.

[7] ASCE 7-98: Minimum design loads for buildings and other structures. American Society of Civil Engineers, jan 1998.

[8] Faber, M.H. and Sørensen, J.D.: Reliability based code calibration. Joint Committee on Structural Safety, Workshop on Code Calibration, Zurich, mar 2002.

[9] Kemp, A.R., Milford, R.V. and Laurie, J.A.P.: Proposals for a comprehensive limit states formulation for South African structural codes. *The Civil Engineer in South Africa*, vol. 29, no. 9, pp. 351–360, sep 1987.

[10] SABS 0100-1:1992: Code of Practice, The structural use of concrete, Part 1: Design. The Council of the South African Bureau of Standards, 1992.

[11] SANS 10162-1:2005: Code of Practice, The structural use of steel, Part 1: Limit-states design of hot-rolled steelwork. The Council of the South African Bureau of Standards, 2005.

[12] Hansen, P.F. and Sørensen, J.D.: Reliability-based code calibration of partial safety factors. Joint Committee on Structural Safety, Workshop on Code Calibration, Zurich, mar 2002.

[13] Köppe, U.: Nutzlastkollektive von kranen. *Hebezeuge und Fördermittel*, vol. 21, no. 2, pp. 36–39, 1981.

[14] Pasternak, H., Rozmarynowski, B. and Wen, Y.-K.: Crane load modelling. *Structural Safety*, vol. 17, pp. 205–224, 1996.

[15] Nowak, A.S. and Collins, K.R.: *Reliability of Structures.* McGraw-Hill, 2000.

[16] Crane Aid Morris Cranes: Personal communication. jul 2005.

[17] Verlinde Cranes: Personal communication. jul 2005.

[18] Demag Cranes and Components: Personal communication. mar 2003.

[19] Condra Cranes: Personal communication. jul 2005.

[20] Ricker, D.T.: Tips for avoiding crane runway problems. *American Institute of Steel Construction Engineering Journal*, pp. 181–205, Fourth quarter 1982.

[21] Lobov, N.A.: Calculation of dynamic loads on an overhead travelling crane. *Russian Engineering Journal*, vol. 56, no. 1, pp. 44–48, 1976.

[22] Lobov, N.A.: Loads of an overhead travelling crane caused by transverse and rotatory motions of the bridge girder. *Soviet Engineering Research*, vol. 62, no. 6, pp. 31–35, 1982.

[23] Lobov, N.A.: Overhead travelling crane loads when track-wheel flanges contact the rails. *Soviet Engineering Research*, vol. 64, no. 7, pp. 22–26, 1984.

[24] Lobov, N.A.: Loads on an overhead travelling crane when it moves with a constant skew setting of the girder. *Soviet Engineering Research*, vol. 66, no. 12, pp. 13–17, 1986.

[25] Spitsyna, D.N. and Anoskin, I.V.: Investigation into the dynamics of the metal structures of foundry cranes when accelerating. *Soviet Engineering Research*, vol. 66, no. 5, pp. 25–30, 1986.

[26] Dunaiski, P.E., Barnard, H., Krige, G. and Mackenzie, R.: Review of provision of loads to structures supporting overhead travelling cranes. In: Zingoni, A. (ed.), *Proceedings of the International Conference on Structural Engineering Mechanics and Computation*, pp. 1321–1328. Elsevier, apr 2001.

[27] EN 13001-2: Crane safety - General design - Part 2: Load effects. European Committee for Standardisation, dec 2004.

[28] Lynch, L.: Keeping out of trouble. *Hoist*, feb 2001.

[29] SAISC: *South African Structural Steelwork Specification for Construction.* 1st edn. The Southern African Institute of Steel Construction, Johannesburg, 2000.

[30] Rowswell, J.C.: *Crane Runway Systems.* Master's thesis, Department of Civil Engineering, University of Toronto, aug 1987.

[31] Prokon: Structural analysis computer program, version W2.1.09. Prokon Software Consultant Ltd, dec 2004.

[32] Ellingwood, B., Galambos, T.V., MacGregor, J.G. and Cornell, C.A.: Development of a probability based load criterion for American National Standard A58. NBS Special Publication 577, National Bureau of Standards, US Department of Commerce, Washington DC, jun 1980.

[33] Kwan, K.H. and Liauw, T.C.: Computer aided design of reinforced concrete members subjected to axial compression and biaxial bending. *The Structural Engineer*, vol. 63B, no. 2, pp. 34–40, jun 1985.

[34] Nawy, E.G.: *Reinforced Concrete, a Fundamental Approach.* 3rd edn. Prentice Hall, New Jersey, 1995.

[35] ENV 1993-6: Eurocode 1993: Design of steel structures, Part 6: Crane supporting structures. Draft ENV 1993-6. European Committee for Standardisation, CEN TC250/SC3, 1999.

[36] JCSS: Joint committee on structural safety - Probabilistic model code. JCSS internet publication: http://www.jcss.ethz.ch/, 2001.

[37] Galambos, T.V. and Ravindra, M.K.: Properties of steel for use in LRFD. *ASCE Journal of the Structural Division*, vol. 104, no. ST9, pp. 1459–1468, sep 1978.

[38] Bjorhovde, R., Galambos, T.V. and Ravindra, M.K.: LRFD criteria for steel beam-columns. *ASCE Journal of the Structural Division*, vol. 104, no. ST9, pp. 1371–1387, sep 1978.

[39] Ellingwood, B. and Reinhold, T.A.: Reliability analysis of steel beam columns. *ASCE Journal of the Structural Division*, vol. 106, no. ST12, pp. 2560–2564, dec 1980.

[40] Cooper, P.B., Galambos, T.V. and Ravindra, M.K.: LRFD criteria for plate girders. *ASCE Journal of the Structural Division*, vol. 104, no. ST9, pp. 1389–1407, sep 1978.

[41] Ravindra, M.K. and Galambos, T.V.: Load and resistance factor design for steel. *ASCE Journal of the Structural Division*, vol. 104, no. ST9, pp. 1337–1353, sep 1978.

[42] MacGregor, J.G., Mirza, S.A. and Ellingwood, B.: Statistical analysis of resistance of reinforced and prestressed concrete members. *ACI Journal Proceedings*, vol. 80, pp. 167–176, may-jun 1983.

[43] Mirza, S.A., Hatzinikolas, M. and MacGregor, J.G.: Statistical descriptions of strength of concrete. *ASCE Journal of the Structural Division*, vol. 105, no. ST6, pp. 1021–1037, jun 1979.

[44] Grant, L.H., Mirza, S.A. and MacGregor, J.G.: Monte carlo study of strength of concrete columns. *American Concrete Institute Journal*, vol. 75, no. 8, pp. 348–358, aug 1978.

[45] Ellingwood, B.: Statistical analysis of RC beam-column interaction. *ASCE Journal of the Structural Division*, vol. 103, no. ST7, pp. 1377–1388, jul 1977.

[46] Mirza, S.A. and MacGregor, J.G.: Variability of mechanical properties of reinforcing bars. *ASCE Journal of the Structural Division*, vol. 105, no. ST5, pp. 921–937, may 1979.

[47] Mirza, S.A. and MacGregor, J.G.: Variations in dimensions of reinforced concrete members. *ASCE Journal of the Structural Division*, vol. 105, no. ST4, pp. 751–766, apr 1979.

[48] Fisher, J.W., Galambos, T.V., Kulak, G.L. and Ravindra, M.K.: Load and resistance factor design criteria for connectors. *ASCE Journal of Structural Engineering*, vol. 104, no. ST9, pp. 1427–1441, sep 1978.

[49] Ruiz, S.E. and Aguilar, J.C.: Reliability of short and slender reinforced-concrete columns. *ASCE Journal of Structural Engineering*, vol. 120, no. 6, pp. 1850–1865, jun 1994.

[50] SABS 0100-2:1992: Code of Practice, The structural use of concrete, Part 2: Materials and execution of work. The Council of the South African Bureau of Standards, 1992.

[51] Lu, R., Luo, Y. and Conte, J.P.: Reliability evaluation of reinforced concrete beams. *Structural Safety*, vol. 14, no. 4, pp. 277–298, jul 1994.

[52] de Villiers, P.J.: *Imposed Loads for Inaccessible Roofs of Light Industrial Steel Buildings.* Master's thesis, Civil Engineering, University of Stellenbosch, apr 2003.

[53] Ter Haar, T.R. and Retief, J.V.: Development of a methodology for structural code calibration. ISI Report R00/1, University of Stellenbosch, dec 2000.

[54] Kohlhaas, S.: Impact forces on end stops for overhead travelling crane support structures. Tech. Rep., University of Stellenbosch, dec 2004.

[55] Holický, M.: Conventional probabilistic models of basic variables. Tech. Rep., Klokner Institute, Czech Technical University in Prague, jun 2002.

[56] Kotoguchi, H., Leonard, J.W. and Shiomi, H.: Statistical evaluation of steel beam-column resistance. *Engineering Structures*, vol. 7, no. 2, pp. 143–147, apr 1985.

[57] Rojiani, K.B. and Woeste, F.E.: A probabilistic analysis of steel beam-columns. *Engineering Structures*, vol. 4, no. 4, pp. 233–241, oct 1982.

[58] Personal communication with The Southern African Institute of Steel Construction: Commentary on SANS 10162: Part 1: Limit-States Design of hot-rolled steelwork. 2005.

[59] Maddox, S.J.: *Fatigue strength of welded structures.* 2nd edn. Abington Publishing, 1991.

[60] Van der Walt, S.J.: Reliability based determination of load models for EOTC support structures. Current Masters study, Civil Engineering, University of Stellenbosch.

[61] prEN 1990: Eurocode - Basis of structural design: Draft prEN 1990. European Committee for Standardisation, jul 2001.

[62] Milford, R.V.: Target safety and SABS 0160 load factors. *The Civil Engineer in South Africa*, vol. 30, no. 10, pp. 475–481, oct 1988.

[63] Gulvanessian, H., Calgaro, J.-A. and Holický, M.: *Designer's guide to EN 1990, Eurocode: Basis of structural design.* Thomas Telford Publishing, London, 2002.

[64] SANS 2394:2004: General principles on reliability for structures. The Council of the South African Bureau of Standards, 2004.

[65] Melchers, R.E.: *Structural Reliability Analysis and Prediction.* 2nd edn. John Wiley and Sons, New York, 1999.

[66] Wen, Y.-K.: Statistical combination of extreme loads. *ASCE Journal of the Structural Division*, vol. 103, no. ST5, pp. 1079–1093, may 1977.

[67] Warren, J.S., Dunaiski, P.E. and Retief, J.V.: A comparison between crane induced load effects from SABS and Eurocode. In: *Proceedings of the Second International Conference on Structural Engineering, Mechanics and Computation.* Balkema, jul 2004.

[68] Warren, J.S., Retief, J.V. and Dunaiski, P.E.: Reliability models of overhead traveling crane loading for code calibration. In: *Proceedings of the Ninth International Conference on Structural Safety and Reliability.* Millpress, jun 2005.

List of Figures

List of Tables

Pectora roborant cultus recti

Appendix A

Load calculations

Example load calculations for the 40t representative crane described in Chapter 3 are given below.

A.1 Crane loads according to SABS 0160:1989

Diagrams showing the load combinations are in Figures 4.1 - 4.5 on page 86.

The information about the crane which is required for the calculation of the load according to SABS 0160:1989 [1] is given in Table A.1.

Table A.1: Crane information required for SABS 0160:1989

Crane parameter	
Weight of crane bridge	298 kN
Weight of crab	98 kN
Nominal weight of hoistload	400 kN
Total number of wheels	4
Maximum vertical wheel load	335 kN
Minimum vertical wheel load	75 kN
Buffer type	Hydraulic PUDZ II ϕ 63

The crane is a process crane in a car stamping plant which is under continuous use and is classified according to SABS 0160:1989 [1] as a class 3 crane.

A.1.1 Vertical loads

A.1.1.1 Static vertical loads

The static vertical loads are as given by the crane manufacturer:

$$V_{s,max} = 335\,\text{kN}$$

$$V_{s,min} = 75\,\text{kN}$$

A.1.1.2 Dynamic vertical loads

The impact factor for the dynamic loads is 1.25 for a class 3 crane.

$$V_{d,max} = 335 \times 1.25 = 419\,\text{kN}$$

$$V_{d,min} = 75 \times 1.25 = 94\,\text{kN}$$

A.1.2 Horizontal transverse loads

A.1.2.1 Acceleration or braking of the crab

The factor for the calculation of the horizontal transverse loads due to acceleration or braking of the crab is 0.15 for a class 3 crane.

$$\begin{aligned} H_a &= 0.15 \times (Q_{cr} + Q_h) \\ &= 0.15\,(98 + 400) \\ &= 18.7\,\text{kN} \end{aligned}$$

A.1.2.2 Misalignment of rails or wheels

The factor for the calculation of the horizontal transverse loads due to the misalignment of the rails or wheels is 0.15 for a class 3 crane.

$$\begin{aligned} H_b &= 0.15 \times \frac{Q_{br} + Q_{cr} + Q_h}{\text{Total number of crane wheels}} \\ &= 0.15 \times \frac{298 + 98 + 400}{4} \\ &= 29.9\,\text{kN} \end{aligned}$$

A.1.2.3 Skewing of the crane in plan

$$H_c = 1.5 \times H_b = 44.8\,\text{kN}$$

A.1.3 Horizontal longitudinal load

The horizontal longitudinal load is caused by the acceleration and braking of the crane bridge.

$$\begin{aligned} H_L &= 0.1 \times (\text{sum of maximum static wheel loads on rail}) \\ &= 0.1 \times 2 \times 335 \\ &= 67.0\,\text{kN} \end{aligned}$$

A.1.4 End stop forces

Method (a): The force on each end stop caused by the crane bridge running into the end stops on the end of the runway is given by:

$$H_e = Q_{br} + Q_{cr} = 396\,\text{kN}$$

Method (b): Taking the resilience of the buffers into account, assuming the ends stops are rigid, and the crane travelling at full rated speed, taking only the weight of the crane bridge and crab.

$$\begin{aligned} E_{kin} &= 0.5mv^2 \\ &= 0.5\,(29800 + 9800)\,(0.833)^2 \\ &= 13739J \end{aligned}$$

$$\begin{aligned} H_e &= k\frac{E_{kin}}{s} \\ &= 1.1\frac{13739}{0.1} \times 10^{-3} \\ &= 151\,\text{kN} \end{aligned}$$

Where:

k – buffer characteristic factor, degree of plasticity

s – buffer stroke length

A.2 Crane loads according to prEN 1991-3

The crane loads have been calculated using the models in prEN 1991-3. Diagrams showing the factored load combinations are shown in Figures 4.6 - 4.13 on page 88.

The information about the crane that is required to calculate the loads is given in Table 3.3 on page 75.

A.2.1 Dynamic factors

ϕ_1 – vibrational excitation of the crane structure due to lifting of the hoistload off the ground.

$$\phi_{1,\min} = 0.9$$

$$\phi_{1,\max} = 1.1$$

ϕ_2 – dynamic effects of transferring the hoistload from the ground to the crane.

$$\phi_2 = \phi_{2\,\min} + \beta_2 v_h$$

The crane is HC 3 therefore $\phi_{2\,\min} = 1.15$ and $\beta_2 = 0.51$.

$$\phi_2 = 1.15 + (0.51)(10/60) = 1.235$$

ϕ_4 – dynamic effect induced when travelling on rail tracks or runways.
The rails are welded and ground smooth therefore:

$$\phi_4 = 1.0$$

ϕ_5 – effects caused by drive forces
Forces change smoothly therefore $1 \leq \phi_5 \leq 1.5$

$$\phi_5 = 1.25$$

ϕ_6 – dynamic effects of test load.

$\phi_{6,dyn}$ – when test load moved by the drives in the way the crane is used.

$$\phi_{6,dyn} = 0.5(1 + \phi_2) = 0.5(1 + 1.235) = 1.118$$

$\phi_{6,stat}$ – when a test load is not moved by the drives

$$\phi_{6,stat} = 1.0$$

ϕ_7 – elastic effects of impact on buffers

$$\phi_7 = 1.25 + 0.7(\xi - 0.5) = 1.25 + 0.7(0.9 - 0.5) = 1.53$$

A.2.2 Load combinations

The crane load combinations as specified by prEN 1991-3 are given in Table A.2.

Table A.2: Crane load combinations

		Groups of loads								
		ULS							Test load	Accidental
		1	2	3	4	5	6	7	8	9
1	Self weight of crane	ϕ_1	ϕ_1	1	ϕ_4	ϕ_4	ϕ_4	1	ϕ_1	1
2	Hoist load	ϕ_2	ϕ_3	-	ϕ_4	ϕ_4	ϕ_4	η[1]	-	1
3	Acceleration of crane bridge	ϕ_5	ϕ_5	ϕ_5	ϕ_5	-	-	-	ϕ_5	-
4	Skewing of crane bridge	-	-	-	-	1	-	-	-	-
5	Acceleration or braking of crab or hoist block	-	-	-	-	-	1	-	-	-
6	Test load	-	-	-	-	-	-	-	1	-
7	Buffer force	-	-	-	-	-	-	-	-	ϕ_7

[1] η is the part of the hoist load that remains when the payload is removed, but is not included in the self weight of the crane

A.2.3 Vertical loads

A.2.3.1 Load combination 1

ϕ_1(Self weight) + ϕ_2(Hoistload)

Maximum wheel load:

$$\begin{aligned} Q_{r,\max} &= \frac{1}{2}\left[\phi_1 \frac{Q_{br}}{2} + \frac{l - e_{\min}}{l}\left(\phi_1 Q_{cr} + \phi_2 Q_h\right)\right] \\ &= \frac{1}{2}\left[1.1\frac{298}{2} + \frac{23800 - 1650}{23800}\left(1.1 \times 98 + 1.235 \times 400\right)\right] \\ &= 362\,\text{kN} \end{aligned}$$

Minimum wheel load:

$$\begin{aligned} Q_{r,\min} &= \frac{1}{2}\left[\phi_1 \frac{Q_{br}}{2} + \frac{e_{\min}}{l}\left(\phi_1 Q_{cr} + \phi_2 Q_h\right)\right] \\ &= \frac{1}{2}\left[1.1\frac{298}{2} + \frac{1650}{23800}\left(1.1 \times 98 + 1.235 \times 400\right)\right] \\ &= 103\,\text{kN} \end{aligned}$$

A.2.3.2 Load combination 3 and 7

(Self weight) + η(Hoistload)

Maximum wheel load:

$$\begin{aligned} Q_{r,\max} &= \frac{1}{2}\left[\frac{Q_{br}}{2} + \frac{l - e_{\min}}{l}\left(Q_{cr}\right)\right] \\ &= \frac{1}{2}\left[\frac{298}{2} + \frac{23800 - 1650}{23800}\left(98\right)\right] \\ &= 120\,\text{kN} \end{aligned}$$

Minimum wheel load:

$$\begin{aligned} Q_{r,\min} &= \frac{1}{2}\left[\frac{Q_{br}}{2} + \frac{e_{\min}}{l}\left(Q_{cr}\right)\right] \\ &= \frac{1}{2}\left[\frac{298}{2} + \frac{1650}{23800}\left(98\right)\right] \\ &= 78\,\text{kN} \end{aligned}$$

A.2.3.3 Load combination 4, 5 and 6

ϕ_4(Self weight) + ϕ_4(Hoistload)

Maximum wheel load:

$$\begin{aligned} Q_{r,\max} &= \frac{\phi_4}{2}\left[\frac{Q_{br}}{2} + \frac{l - e_{\min}}{l}\left(Q_{cr} + Q_h\right)\right] \\ &= \frac{1}{2}\left[\frac{298}{2} + \frac{23800 - 1650}{23800}\left(98 + 400\right)\right] \\ &= 306\,\text{kN} \end{aligned}$$

Minimum wheel load:

$$\begin{aligned} Q_{r,\min} &= \frac{\phi_4}{2}\left[\frac{Q_{br}}{2} + \frac{e_{\min}}{l}\left(Q_{cr} + Q_h\right)\right] \\ &= \frac{1}{2}\left[\frac{298}{2} + \frac{1650}{23800}\left(98 + 400\right)\right] \\ &= 92\,\text{kN} \end{aligned}$$

A.2.3.4 Load combination 4, 5 and 6

(Self weight) + (Hoistload)

Maximum wheel load:

$$\begin{aligned} Q_{r,\max} &= \frac{1}{2}\left[\frac{Q_{br}}{2} + \frac{l - e_{\min}}{l}\left(Q_{cr} + Q_h\right)\right] \\ &= \frac{1}{2}\left[\frac{298}{2} + \frac{23800 - 1650}{23800}\left(98 + 400\right)\right] \\ &= 306\,\text{kN} \end{aligned}$$

Minimum wheel load:

$$\begin{aligned} Q_{r,\min} &= \frac{1}{2}\left[\frac{Q_{br}}{2} + \frac{e_{\min}}{l}\left(Q_{cr} + Q_h\right)\right] \\ &= \frac{1}{2}\left[\frac{298}{2} + \frac{1650}{23800}\left(98 + 400\right)\right] \\ &= 92\,\text{kN} \end{aligned}$$

A.2.4 Horizontal loads

A.2.4.1 Longitudinal and transverse loads caused by acceleration and braking of crane

Horizontal longitudinal force:

$$H_L = \phi_5 K \frac{1}{n_r}$$

Where:

n_r – is the number of rails

Drive force K:

$$\begin{aligned} K &= \alpha \sum Q_{r,\min} \\ &= \alpha m_w Q_{r,\min} \qquad (m_w = \text{number of single wheel drives}) \\ &= (0.2)(2)(78) \\ &= 31.2\,\text{kN} \end{aligned}$$

Therefore:

$$H_L = (1.25)(31.2)\frac{1}{2} = 19.5\,\text{kN}$$

Horizontal transverse forces:

$$H_{T,1} = \phi_5 \xi_2 \frac{M}{a}$$

$$H_{T,2} = \phi_5 \xi_1 \frac{M}{a}$$

Position of center of mass of crane:

$$\begin{aligned} \xi_1 &= \frac{\sum Q_{r,\max}}{\sum Q_r} \\ &= \frac{(2)(306)}{298 + 98 + 400} \\ &= 0.769 \end{aligned}$$

$$\xi_2 = 1 - \xi_1 = 0.231$$

Moment caused by drive forces not acting at the center of mass:

$$\begin{aligned} M = Kl_s &= K\left(\xi_1 - 0.5\right) l \\ &= (31.2)(0.769 - 0.5)(23.8) \\ &= 199.75\,\text{kNm} \end{aligned}$$

Therefore:

$$H_{T,1} = (1.25)(0.231)\left(\frac{199.75}{4.4}\right) = 13.1\,\text{kN}$$

$$H_{T,2} = (1.25)(0.769)\left(\frac{199.75}{4.4}\right) = 43.6\,\text{kN}$$

A.2.4.2 Horizontal loads and the guide force caused by skewing

Guide force:

$$S = f\lambda_{s,j}\sum Q_r$$

Horizontal longitudinal forces:

$$H_{s,i,j,L} = f\lambda_{s,i,j,L}\sum Q_r$$

Horizontal transverse forces:

$$H_{s,i,j,T} = f\lambda_{s,i,j,T}\sum Q_r$$

Where:

i – is the rail number

j – is the wheel pair number

L – stands for longitudinal forces

T – stands for transverse forces

Non positive factor:

$$f = 0.3\left(1 - \exp\left(-250\alpha\right)\right) \leq 0.3$$

Skewing angle:

$$\begin{aligned}
\alpha &= \alpha_F + \alpha_v + \alpha_o \leq 0.015 \\
\alpha_F &= \frac{0.75x}{a} \qquad (x = \text{ clearance between rail and wheel flange}) \\
&= \frac{0.75(25)}{4400} = 4.26 \times 10^{-3} \\
\alpha_v &= \frac{y}{a} \qquad (y = \text{ wear of rail and guide means} \geq 0.10b) \\
&= \frac{0.10(100)}{4400} = 2.27 \times 10^{-3} \\
\alpha_o &= 0.001 \\
\therefore \alpha &= 7.53 \times 10^{-3}
\end{aligned}$$

$$f = 0.3\left(1 - \exp\left(-250 \times 7.53 \times 10^{-3}\right)\right) = 0.254$$

Combination of wheel pairs - Independent, fixed/fixed.

Distance to instantaneous slide pole:

$$h = \frac{\sum e_j^2}{\sum e_j} = \frac{4400^2}{4400} = 4400\,\text{mm}$$

force factors:

$$\lambda_{s,j} = 1 - \frac{\sum e_j}{nh} = 1 - \frac{4400}{2 \times 4400} = 0.5$$

$$\lambda_{s,i,j,L} = 0$$

$$\lambda_{s,1,1,T} = \frac{\xi_2}{n}\left(1 - \frac{e_j}{h}\right) = \frac{0.231}{2} = 0.115$$

$$\lambda_{s,2,1,T} = \frac{\xi_1}{n}\left(1 - \frac{e_j}{h}\right) = \frac{0.769}{2} = 0.385$$

$$\lambda_{s,i,2,L} = 0$$

Where:

n – is the number of wheel pairs

e_j – is the distance of wheel pair j from the guide means

Guide force:

$$\begin{aligned} S &= f\lambda_{s,j}\sum Q_r \\ &= (0.254)(0.5)(298+98+400) = 101.1\,\text{kN} \end{aligned}$$

Transverse forces:

$$H_{s,1,1,T} = f\lambda s,1,1,T\sum Q_r = (0.254)(0.115)(796) = 23.25\,\text{kN}$$

$$H_{s,2,1,T} = f\lambda s,2,1,T\sum Q_r = (0.254)(0.385)(796) = 77.80\,\text{kN}$$

A.2.4.3 Horizontal forces caused by acceleration or braking of the crab

The forces are assumed by the code to be less than the buffer forces related to movement of the crab and are not calculated.

A.2.4.4 Buffer forces related to movements of the crab

The payload is free to swing, therefore:

$$\begin{aligned} H_{B2} &= 0.10\,(Q_{cr}+Q_h) \\ &= 0.10(98+400) = 49.8\,\text{kN} \end{aligned}$$

Force on one wheel = 24.9 kN.

A.2.4.5 Test loads

Dynamic test load – 10% overload:

$$Q_{T,dyn} = \phi_{6,dyn}110\%Q_h = 1.118(1.10)(400) = 492\,\text{kN}$$

Static test load – 25% overload

$$Q_{T,stat} = \phi_{6,stat}125\%Q_h = 1.0(1.25)(400) = 500\,\text{kN}$$

Maximum test load is static load.

Vertical wheel loads - Load Combination 8: ϕ_1(Self weight) + ϕ_6(Test load)

Maximum wheel load:

$$\begin{aligned} Q_{r,\max} &= \frac{1}{2}\left[\phi_1 \frac{Q_{br}}{2} + \frac{l - e_{\min}}{l}\left(\phi_1 Q_{cr} + \phi_6 Q_T\right)\right] \\ &= \frac{1}{2}\left[1.1\frac{298}{2} + \frac{23800 - 1650}{23800}\left(1.1 \times 98 + 500\right)\right] \\ &= 365\,\text{kN} \end{aligned}$$

Minimum wheel load:

$$\begin{aligned} Q_{r,\min} &= \frac{1}{2}\left[\phi_1 \frac{Q_{br}}{2} + \frac{e_{\min}}{l}\left(\phi_1 Q_{cr} + \phi_6 Q_T\right)\right] \\ &= \frac{1}{2}\left[1.1\frac{298}{2} + \frac{1650}{23800}\left(1.1 \times 98 + 500\right)\right] \\ &= 103\,\text{kN} \end{aligned}$$

A.2.4.6 Buffer forces related to crane movement

The equation given for the calculation of the end stop forces in prEN 1991-3 is:

$$H_{B,1} = \phi_7 u \sqrt{m_c S_B}$$

Where:

ϕ_7 – dynamic factor taking into account plasticity of buffer

u – long travel speed of crane taken as 70% of maximum speed

m_c – mass of crane and hoistload

S_B – spring constant of buffer

Buffer maximum forces $F_{max} = 200\,\text{kN}$ and maximum deflection $s_{max} = 100\,\text{mm}$.

$$\begin{aligned} S_B &= \frac{F_{max}}{s_{max}} \\ &= 2 \times 10^6\, N/m \end{aligned}$$

$$\begin{aligned} H_{B,1} &= \phi_7 u \sqrt{m_c S_B} \\ &= (0.53)(0.583)\sqrt{(29800 + 9800 + 40000)\, 2 \times 10^6} \\ &= 356\,\text{kN} \end{aligned}$$

A.3 Roof Imposed loads

The roof imposed loads were calculated using the method given in Clause 5.4.4 SABS 0160:1989 [1].

(5.4.4.3) Inaccessible roof – a uniformly distributed load applied to the roof with a value of:

$$\omega = \left(0.3 + \frac{15 - A}{6}\right)\,\text{kN/m}^2 \geq 0.3\,\text{kN/m}^2$$

Where:

A – is the tributary area of the member being considered in m^2

For one frame:

$$A = 45 \times 8 = 360\,\text{m}^2$$

$$\therefore \omega = 0.3\,\text{kN/m}^2$$

Force per unit length of roof:

$$q = \omega \times 8 = 2.4\,\text{kN/m}$$

This force is multiplied by the tributary length of the purlin to get the force per purlin/frame connection.

A.4 Wind loads

The wind loads were calculated using the method given in Clause 5.5 in SABS 0160:1989 [1]. An outline of the building as considered for the calculation of wind loads is given in Figure A.1.

Regional wind speed = 40 m/s

Mean return period = 50 years

Terrain category 3 - built up industrial

Height of structure = 18400mm on tall side, (14190mm on short side)

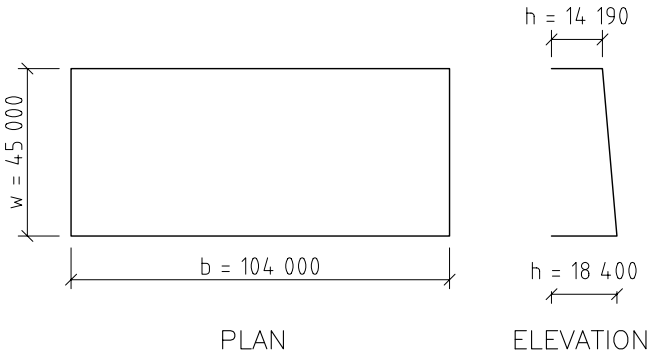

Figure A.1: Building outline for wind calculations

(Table 5 SABS 0160:1989 [1]) Wind speed multiplier:

$$k_{z,tall} = 0.814$$

$$k_{z,short} = 0.769$$

Characteristic wind speed:

$$V_{z,tall} = k_{z,tall} V = 32,56\,\mathrm{m/s}$$

$$V_{z,short} = k_{z,short} V = 30.76\,\mathrm{m/s}$$

Velocity pressures:

$$q_z = k_p {V_z}^2$$

$$k_p = 0.6 \qquad \text{(0m above sea level)}$$

$$q_{z,tall} = 0.6(32.56)^2 = 636\,\mathrm{N/m^2}$$

$$q_{z,short} = 0.6(30.76)^2 = 568\,\mathrm{N/m^2}$$

Building plan ratio:

$$\frac{b}{w} = \frac{104}{45} = 2.31$$

Building height ratio:

$$\frac{h}{w} = \frac{184}{450} = 0.41$$

The surface pressure coefficients were taken from Tables 6 and 8 in SABS 0160:1989 [1]. Figures A.2 & A.3 show the surface pressure coefficients.

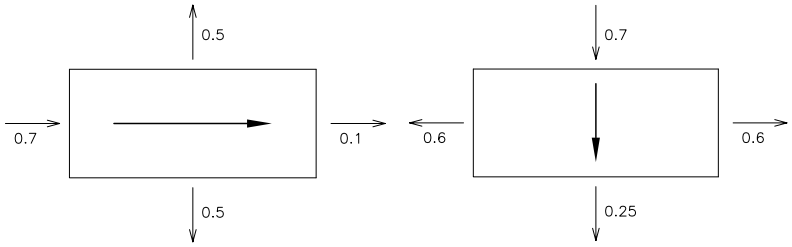

(a) Wind along (b) Wind across

Figure A.2: Surface pressure coefficients on walls

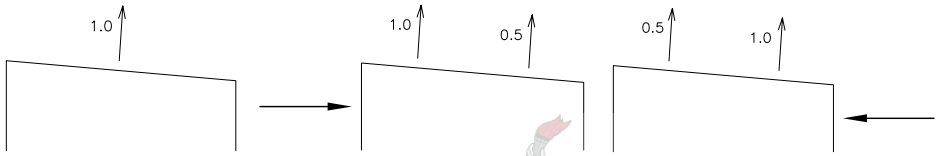

(a) Wind along (b) Wind across from tall side (c) Wind across from short side

Figure A.3: Surface pressure coefficients on roof

The wind load per purlin/frame or girt/frame connection:

$$W_n = (\text{frame spacing}) \times (\text{pressure coefficient}) \times (\text{velocity pressure}) \times (\text{purlin/girt spacing})$$

A.4.0.7 Load Case 1 - Wind along

Walls:

$$\text{Tall} : W_n = (8)(0.5)(0.636)s_g = 2.544s_g \,\text{kN}$$

$$\text{Short} : W_n = (8)(0.5)(0.568)s_g = 2.272s_g \,\text{kN}$$

Roof:

$$W_n = (8)(1.0)(0.636)s_p = 5.088s_p \,\text{kN}$$

$$\text{Horizontal component} : W_{n,h} = W_n \sin 4^\circ = 0.355s_p \,\text{kN}$$

$$\text{Vertical component} : W_{n,v} = W_n \cos 4^\circ = 5.076s_p \,\text{kN}$$

A.4.0.8 Load Case 2a - Wind across from the tall side

Walls:

$$\text{Tall} : W_n = (8)(0.7)(0.636)s_g = 3.562s_g \,\text{kN}$$

$$\text{Short} : W_n = (8)(0.25)(0.568)s_g = 1.136s_g \,\text{kN}$$

Roof (windward):

$$W_n = (8)(1.0)(0.636)s_p = 5.088s_p \,\text{kN}$$

$$\text{Horizontal component} : W_{n,h} = W_n \sin 4^\circ = 0.355s_p \,\text{kN}$$

$$\text{Vertical component} : W_{n,v} = W_n \cos 4^\circ = 5.076s_p \,\text{kN}$$

Roof (leeward):

$$W_n = (8)(0.5)(0.636)s_p = 2.544s_p \,\text{kN}$$

$$\text{Horizontal component} : W_{n,h} = W_n \sin 4^\circ = 0.178s_p \,\text{kN}$$

$$\text{Vertical component} : W_{n,v} = W_n \cos 4^\circ = 2.538s_p \,\text{kN}$$

A.4.0.9 Load Case 2b - Wind across from the short side

Walls:

$$\text{Tall} : W_n = (8)(0.25)(0.636)s_g = 1.272s_g \,\text{kN}$$

$$\text{Short} : W_n = (8)(0.7)(0.568)s_g = 3.181s_g \,\text{kN}$$

Roof (windward):

$$W_n = (8)(1.0)(0.636)s_p = 5.088s_p \,\text{kN}$$

$$\text{Horizontal component} : W_{n,h} = W_n \sin 4^\circ = 0.355s_p \,\text{kN}$$

$$\text{Vertical component} : W_{n,v} = W_n \cos 4^\circ = 5.076s_p \,\text{kN}$$

Roof (leeward):

$$W_n = (8)(0.5)(0.636)s_p = 2.544s_p \,\text{kN}$$

$$\text{Horizontal component} : W_{n,h} = W_n \sin 4^\circ = 0.178s_p \,\text{kN}$$

$$\text{Vertical component} : W_{n,v} = W_n \cos 4^\circ = 2.538s_p \,\text{kN}$$

A.5 Permanent loads

The permanent loads on the frame consisted of:

1. Sheeting and utilities

   Weight of sheeting, assume $6\,\text{kg/m}^2$
   Weight of utilities, assume $1\,\text{kg/m}^2$
   Force per purlin/frame connection:

$$F_{su} = (6+1)(8)(9.81) \times 10^{-3} s_p = 0.55 s_p\,\text{kN}$$

2. Purlins

   Purlin section: $225 \times 75 \times 20 \times 2.5$ CFC, weight = 7.78kg/m.
   Force per purlin/frame connection:

$$F_p = (7.78)(8)(9.81) \times 10^{-3} = 0.61\,\text{kN}$$

3. Monitors

   Frame section: $150 \times 65 \times 20 \times 2.5$ CFC, weight = $5.92\,\text{kg/m}$.
   Length of frame = $1500 \times 2 + 4490 = 7490\,\text{mm}$
   One frame per purlin, force per purlin = $(7.49)(5.92)(9.81) \times 10^{-3} = 0.43\,\text{kN}$
   Two false rafters $45 \times 45 \times 5\text{L}$, weight = $3.38\,\text{kg/m}$
   Two girts $45 \times 45 \times 5\text{L}$, weight = $3.38\,\text{kg/m}$
   Force per unit length of roof = $4(3.38)(9.81) \times 10^{-3} = 0.133\,\text{kN/m}$
   Force per purlin/frame connection from frames, rafters and girts:

$$F_m = 0.43 + (0.133)(2.15) = 0.716\,\text{kN}$$

4. Self weight

   The self weight of the structural elements is calculated by Prokon and included in the 'Permanent' load case for analysis.

Pectora roborant cultus recti

Appendix B

Load Effects

B.1 5t crane girder

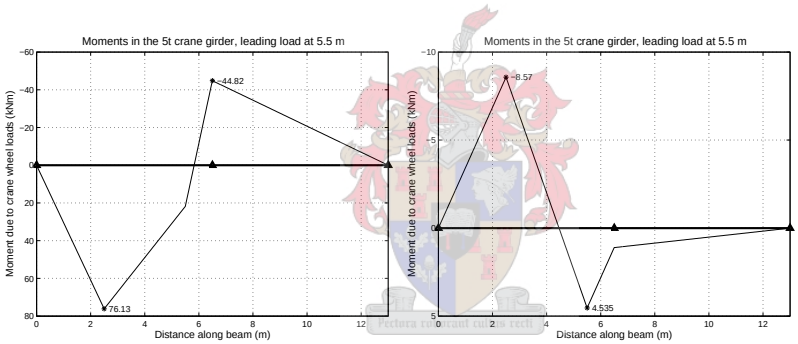

(a) Vertical moments (b) Horizontal moments

Figure B.1: 5t crane girder, maximum positive vertical moment, LC1

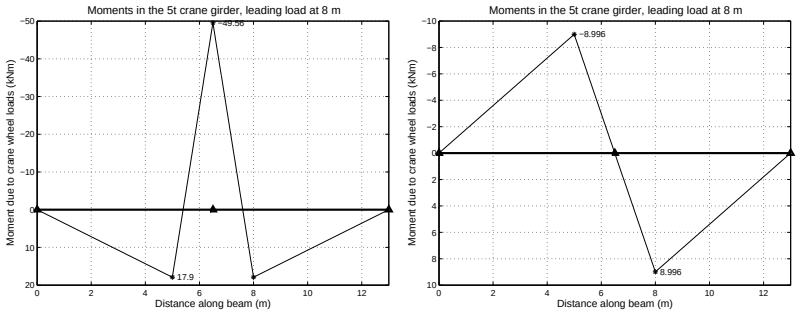

(a) Vertical moments (b) Horizontal moments

Figure B.2: 5t crane girder, maximum negative vertical moment, LC1

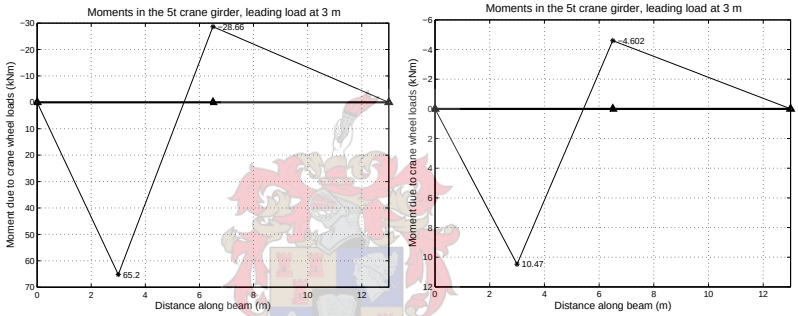

(a) Vertical moments (b) Horizontal moments

Figure B.3: 5t crane girder, maximum horizontal moment, LC1

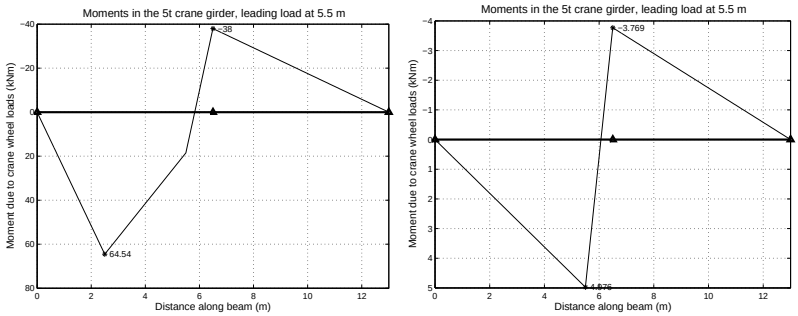

(a) Vertical moments (b) Horizontal moments

Figure B.4: 5t crane girder, maximum positive vertical moment, LC5

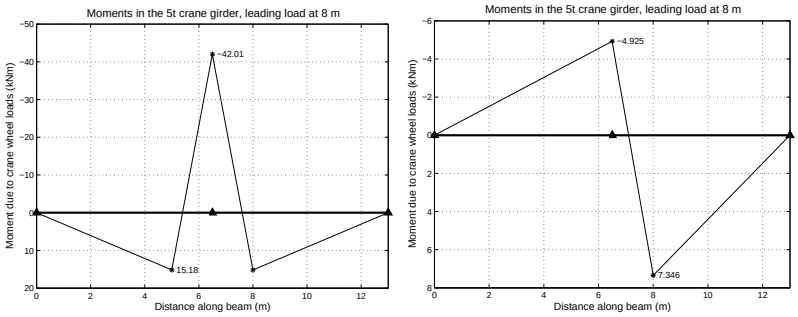

(a) Vertical moments (b) Horizontal moments

Figure B.5: 5t crane girder, maximum negative vertical moment, LC5

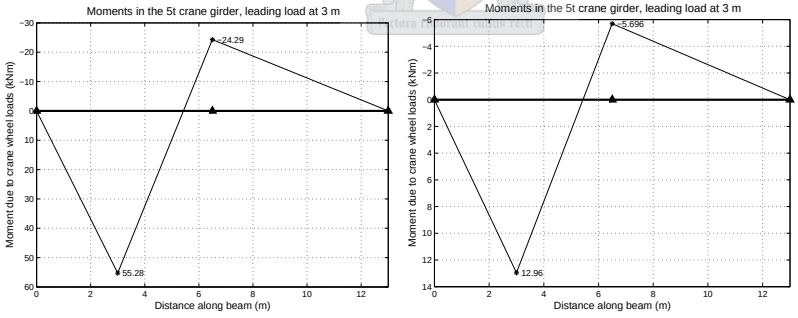

(a) Vertical moments (b) Horizontal moments

Figure B.6: 5t crane girder, maximum horizontal moment, LC5

Pectora roborant cultus recti

Appendix C

Graphs for stochastic modelling of hoistload

C.1 Class 1 cranes

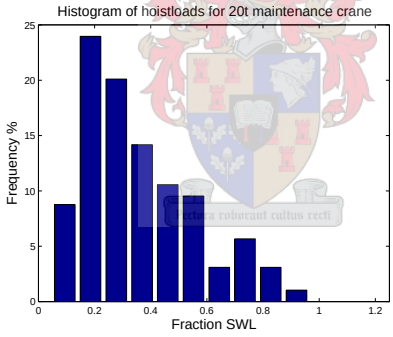

Figure C.1: 20t class 1 crane (produced from data)

C.1.0.10 Maintenance crane

For 80% of the cycles the crane lifts less than half the SWL. Crane does sometimes lift the SWL.

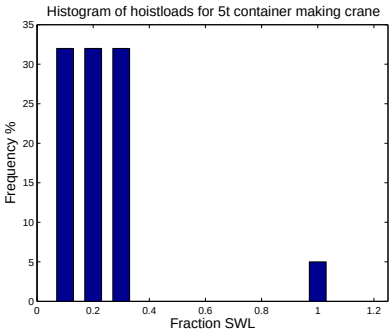

Figure C.2: 3.2t class 1 crane (produced from descriptions)

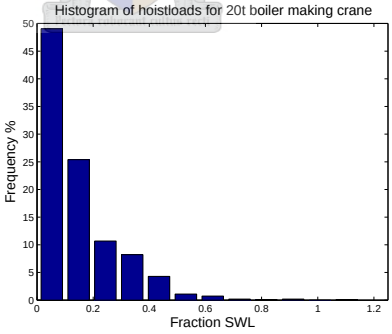

Figure C.3: 20t class 1 crane (produced from data)

C.2 Class 2 cranes

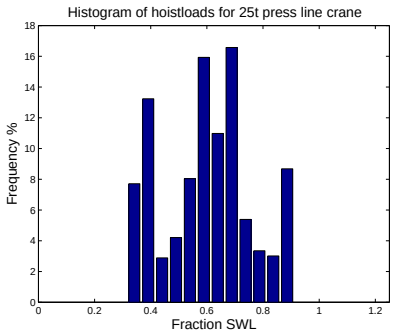

Figure C.4: 25t class 2 crane (produced from data)

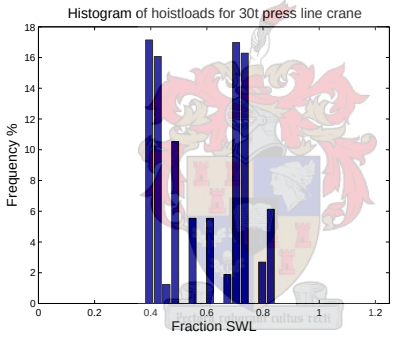

Figure C.5: 30t class 2 crane (produced from data)

C.2.0.11 Coil handling crane

Coils range from 5% SWL to 70% SWL. Most coils are in the range 40% SWL to 50% SWL.

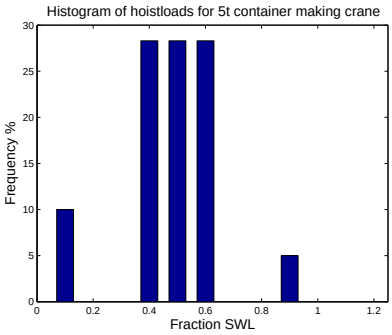

Figure C.6: 5t class 2 crane (produced from descriptions)

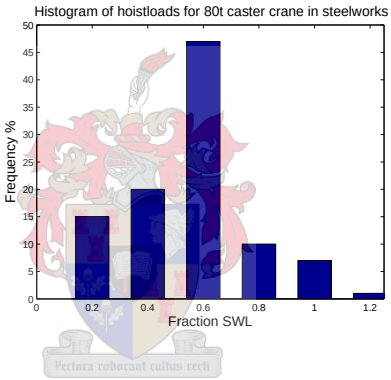

Figure C.7: 80t class 2 crane (produced from descriptions)

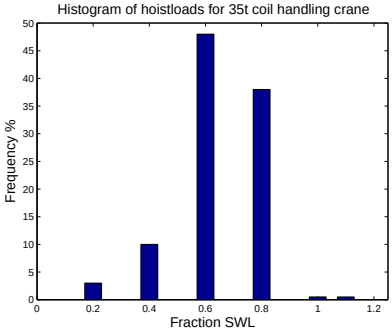

Figure C.8: 35t class 2 crane (produced from descriptions)

C.3 Class 3 cranes

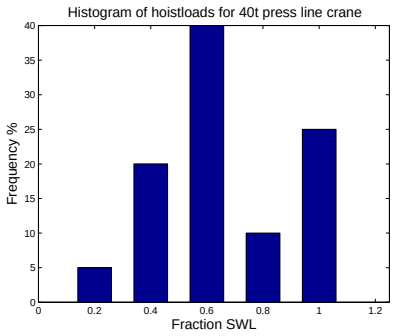

Figure C.9: 40t class 3 crane (produced from descriptions)

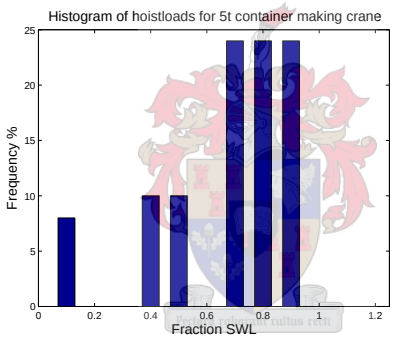

Figure C.10: 5t class 3 crane (produced from descriptions)

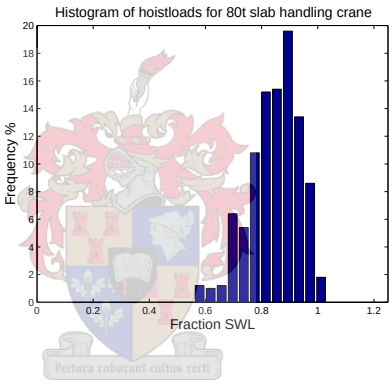

Figure C.11: 80t class 3 crane (produced from data)

C.4 Class 4 cranes

C.4.0.12 Ladle crane at a steelworks

Full ladles range from 98% SWL to 110% SWL. The empty ladle is 32% SWL.

C.4.0.13 Ladle crane at a steelworks

Always lifts SWL, the empty ladle is 27% SWL.

C.5 Extreme hoistload distributions

Equations are given below for the means and standard deviations of the extreme hoistload distributions.

C.5.0.14 Class 1

$$\mu_1 = \begin{cases} 0.0143{N_{extr}}^3 - 0.1575{N_{extr}}^2 + 0.6225N_{extr} + 0.3188 & \left(N_{extr} \leq 10^4\right) \\ -0.0861 \cdot 10^{-3}{N_{extr}}^3 - 0.0052{N_{extr}}^2 + 0.0749N_{extr} + 0.9953 & \left(N_{extr} \geq 10^4\right) \end{cases} \tag{C.5.1}$$

$$\log_{10}(\sigma_1) = -0.3334 \log_{10}(N_{extr}) - 0.4614 \tag{C.5.2}$$

C.5.0.15 Class 2

$$\mu_2 = \begin{cases} -0.0220{N_{extr}}^2 + 0.1923N_{extr} + 0.7850 & \left(N_{extr} \leq 10^4\right) \\ -0.0065{N_{extr}}^2 + 0.0805N_{extr} + 0.9864 & \left(N_{extr} \geq 10^4\right) \end{cases} \tag{C.5.3}$$

$$\log_{10}(\sigma_2) = -0.2922 \log_{10}(N_{extr}) - 0.6874 \tag{C.5.4}$$

C.5.0.16 Class 3

$$\mu_3 = \begin{cases} 0.0021{N_{extr}}^3 - 0.0329{N_{extr}}^2 + 0.1852N_{extr} + 0.8552 & \left(N_{extr} \leq 10^4\right) \\ -0.0044{N_{extr}}^2 + 0.0571N_{extr} + 1.0443 & \left(N_{extr} \geq 10^4\right) \end{cases} \tag{C.5.5}$$

$$\log_{10}(\sigma_3) = -0.2346 \log_{10}(N_{extr}) - 0.9835 \tag{C.5.6}$$

C.5.0.17 Class 4

$$\mu_4 = \begin{cases} 0.0016{N_{extr}}^3 - 0.0194{N_{extr}}^2 + 0.0992N_{extr} + 1.0128 & \left(N_{extr} \leq 10^4\right) \\ -0.0011{N_{extr}}^2 + 0.0241N_{extr} + 1.1204 & \left(N_{extr} \geq 10^4\right) \end{cases} \tag{C.5.7}$$

$$\log_{10}\left(\sigma_4\right) = -0.1675 \log_{10}\left(N_{extr}\right) - 1.3613 \tag{C.5.8}$$

Appendix D

Ratios of hoistload to total crane weight

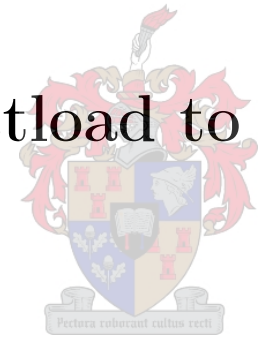

r	Crane description	Weight of bridge kN	Weight of crab kN	Crane Capacity kN
0.30	Standard 1t 15m	22.37	0.83	10
0.35	Charging crane 160t 28.5m	2000	1000	1600
0.37	Warehouse crane 35t 30m	468	120	350
0.38	Standard 1t 12,5m	15.47	0.83	10
0.40	Coil handling crane 45t 30m	545	139	450
0.43	Standard 1t 10m	12.67	0.83	10
0.44	Ladle crane 260t 28.5m	1970	1298	2600
0.45	Container making crane 5t 19.2m	55	6.4	50
0.45	Standard 2t 15m	23.28	1.12	20
0.45	Roll shop crane 40t 24.5m	353	133	400
0.48	Standard 10t 20m span	100	10	100
0.48	Caster crane 80t 31.75m	670.1	204.5	800
0.48	Standard 3,2t 16,5m	31.5	2.8	32
0.50	Standard3,2t 15m	29	3.5	32

r	Crane description	Weight of bridge kN	Weight of crab kN	Crane Capacity kN
0.51	Standard2,5t 15m	23.29	1.21	25
0.52	Standard 3,2t 15,5m	26.7	2.8	32
0.52	Standard2,5t 12,5m	21.59	1.21	25
0.53	Standard15t 20m span	118	15	150
0.54	Standard 1t 7,5m	7.67	0.83	10
0.55	Rolling mill crane 16t 20m	114	17	160
0.57	Press line crane 25t 22.86m	157	33	250
0.57	Standard 20t 20m	128.5	20	200
0.57	Standard 2,5t 11m	17.29	1.21	25
0.58	Standard 3,2t 11,2m	20	2.8	32
0.59	Standard 10t 15m span	31	3.5	50
0.60	Standard 2t 9m	12.08	1.12	20
0.61	Standard 3,2t 10m	17.7	2.8	32
0.61	Mould shop crane 65t 21m	300	116	650
0.62	Press line crane 20t 19m	99	25	200
0.62	Tool Repair crane 20t 18,76m	99	25	200
0.62	Roll shop crane 80t 14.5m	353	133	800
0.62	Standard 5t 14,5m	27.4	2.8	50
0.63	Standard 2t 7,5m	10.38	1.12	20
0.65	Standard 6,3t 14m	29	4.6	63
0.66	Standard 10t 15m span	43.4	7	100
0.67	Standard 3,2t 8m	13.1	2.8	32
0.67	Standard 5t 12.5m	22	2.8	50
0.67	Standard 2.5t 8m	11.09	1.21	25
0.67	Standard 6.3t 13m	25.8	4.6	63
0.68	Maintenance crane 10t 14.1m	37	9	100
0.71	Standard 5t 9.7m	17.8	2.8	50
0.71	Standard 6.3t 11m	20.8	4.6	63
0.73	Standard 3.2t 6m	9.2	2.8	32
0.74	Standard 8t 11.5m	23.7	4.6	80

r	Crane description	Weight of bridge kN	Weight of crab kN	Crane Capacity kN
0.75	Standard 5t 8.3m	14.1	2.8	50
0.75	Standard 6.3t 8.5m	16.1	4.6	63
0.75	Standard 2.5t 5.5m	6.99	1.21	25
0.77	Standard 8t 9.5m	19	4.6	80
0.78	Standard 10t 10m	22.9	4.9	100
0.79	Standard 5t 6m	10.5	2.8	50
0.79	Standard 6.3t 6.5m	11.9	4.6	63
0.80	Standard 8t 8m	15.5	4.6	80
0.81	Standard 10t 8.5m	19.3	4.9	100
0.85	Standard 10t 6m	13.2	4.9	100

Pectora roborant cultus recti

Appendix E

Code calibration results

E.1 Ultimate limit state - crane only

E.1.1 5t crane girder

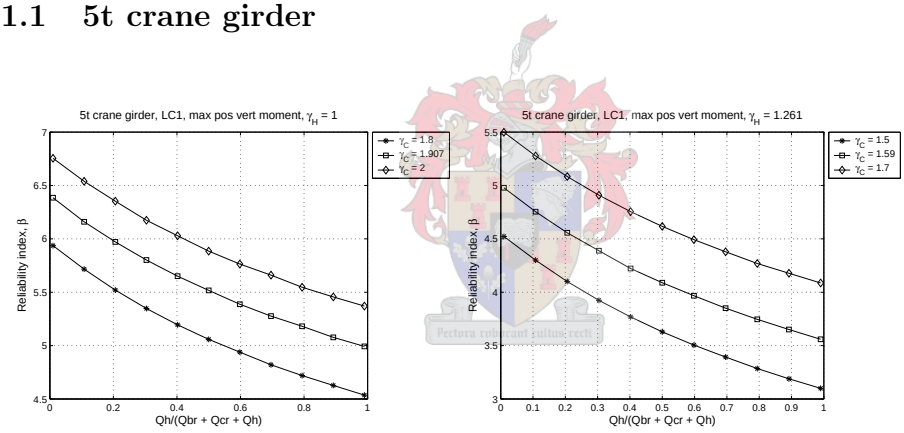

(a) Code format 1 (b) Code format 3

Figure E.1: LC1 maximum positive vertical moment, code formats 1 & 3

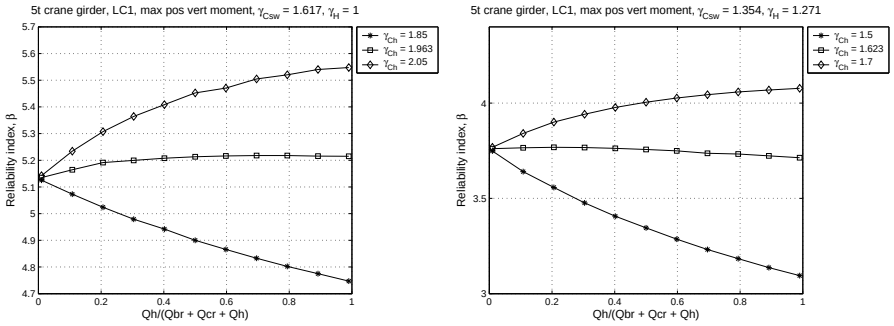

(a) Code format 2 (b) Code format 3

Figure E.2: LC1 maximum positive vertical moment, code formats 2 & 4

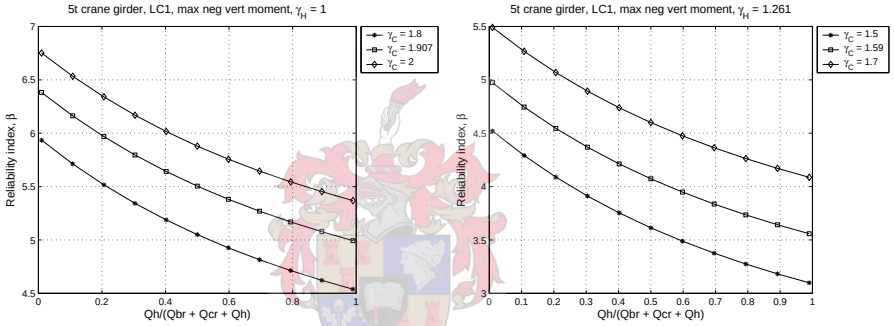

(a) Code format 1 (b) Code format 3

Figure E.3: LC1 maximum negative vertical moment, code formats 1 & 3

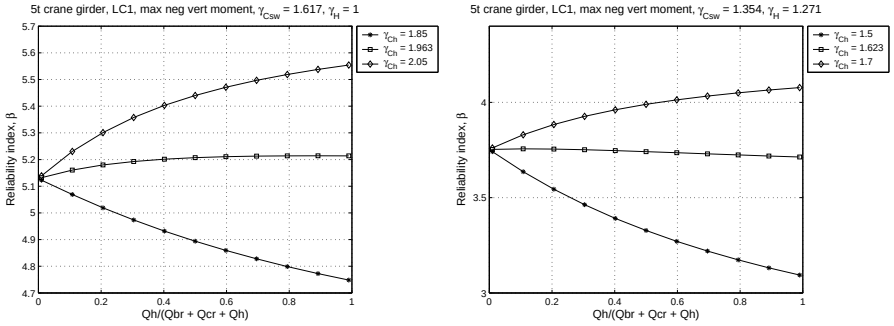

(a) Code format 2 (b) Code format 3

Figure E.4: LC1 maximum negative vertical moment, code formats 2 & 4

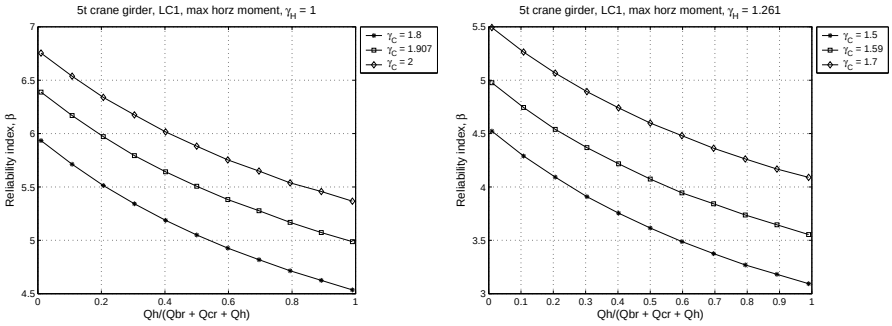

(a) Code format 1 (b) Code format 3

Figure E.5: LC1 maximum horizontal moment, code formats 1 & 3

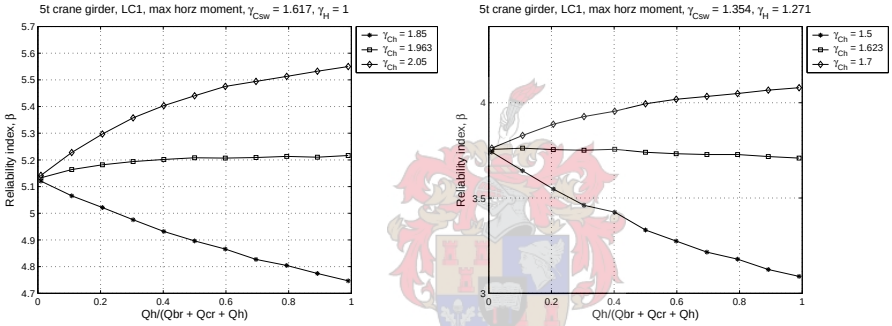

(a) Code format 2 (b) Code format 3

Figure E.6: LC1 maximum horizontal moment, code formats 2 & 4

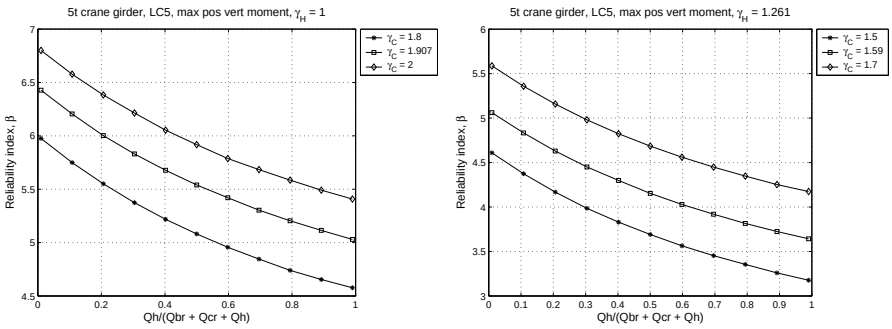

(a) Code format 1 (b) Code format 3

Figure E.7: LC5 maximum positive vertical moment, code formats 1 & 3

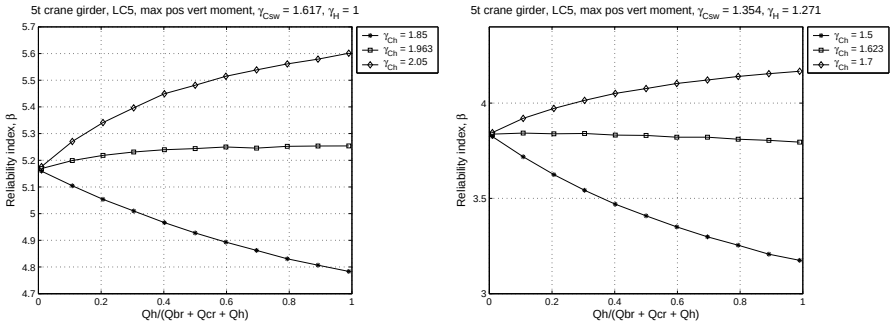

(a) Code format 2 (b) Code format 3

Figure E.8: LC5 maximum positive vertical moment, code formats 2 & 4

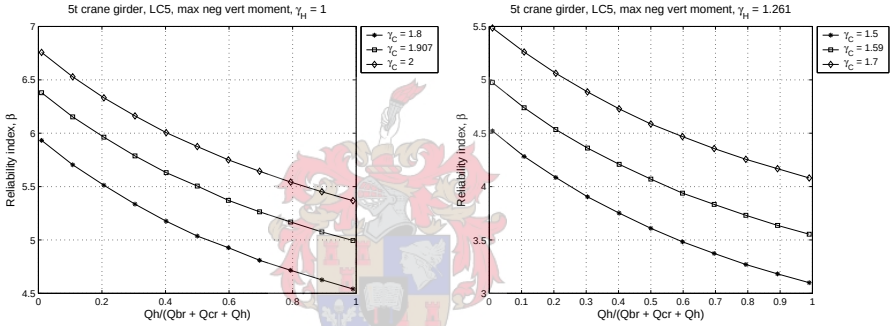

(a) Code format 1 (b) Code format 3

Figure E.9: LC5 maximum negative vertical moment, code formats 1 & 3

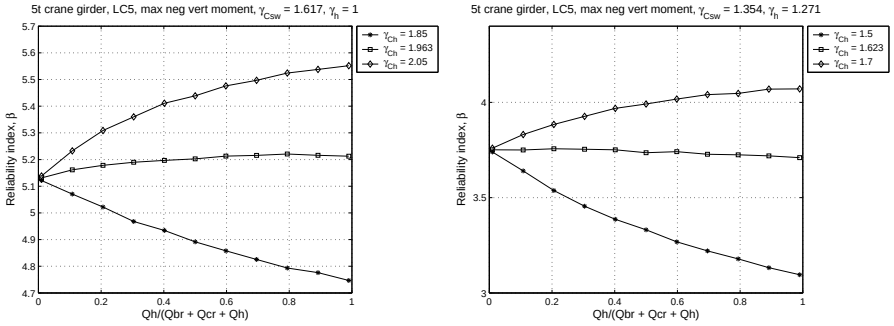

(a) Code format 2 (b) Code format 3

Figure E.10: LC5 maximum negative vertical moment, code formats 2 & 4

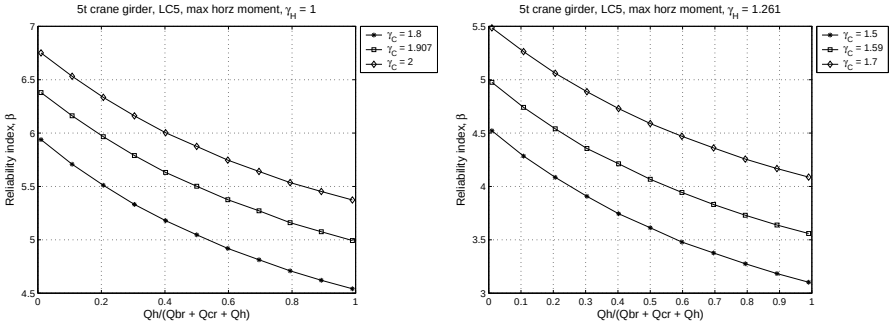

(a) Code format 1 (b) Code format 3

Figure E.11: LC5 maximum horizontal moment, code formats 1 & 3

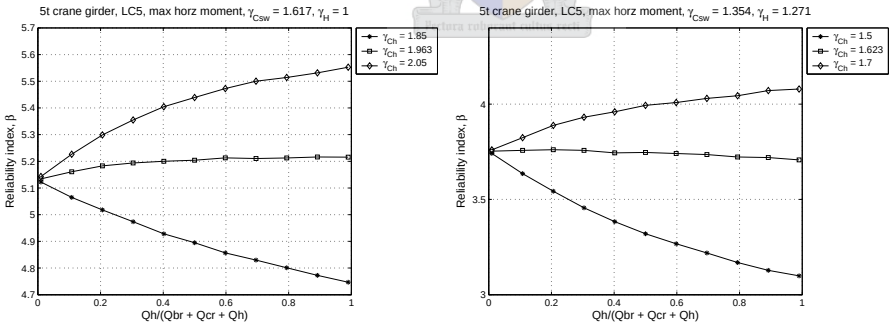

(a) Code format 2 (b) Code format 3

Figure E.12: LC5 maximum horizontal moment, code formats 2 & 4

E.1.2 5t crane column

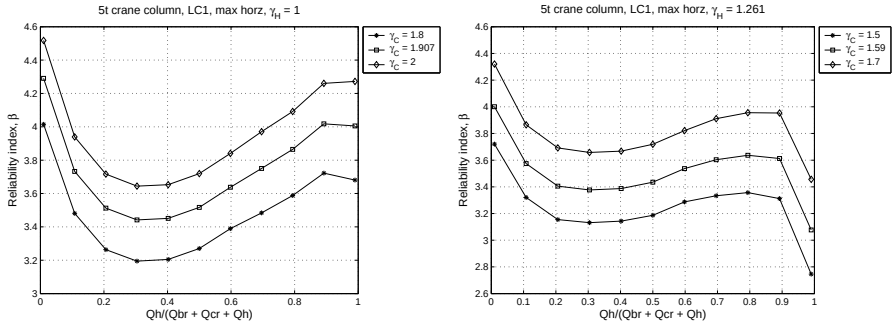

(a) Code format 1 (b) Code format 3

Figure E.13: LC1 maximum horizontal, code formats 1 & 3

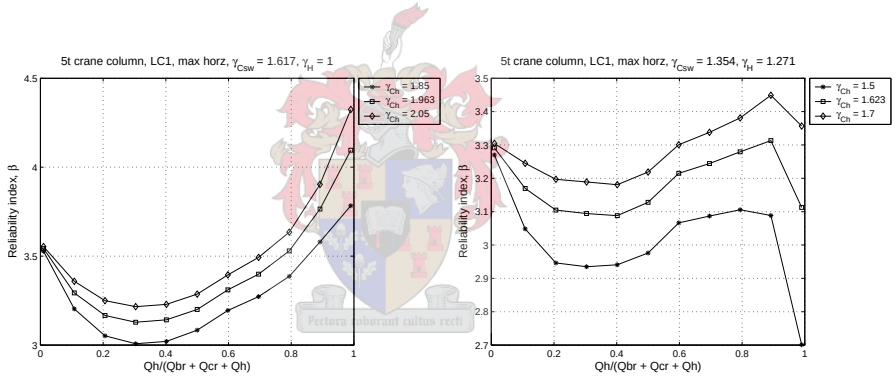

(a) Code format 2 (b) Code format 3

Figure E.14: LC1 maximum horizontal, code formats 2 & 4

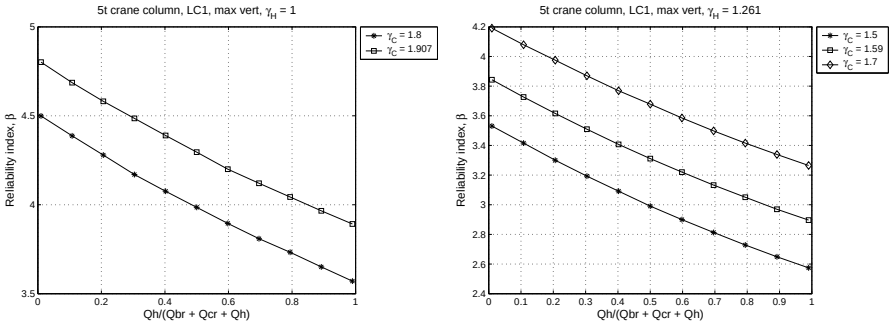

(a) Code format 1 (b) Code format 3

Figure E.15: LC1 maximum vertical, code formats 1 & 3

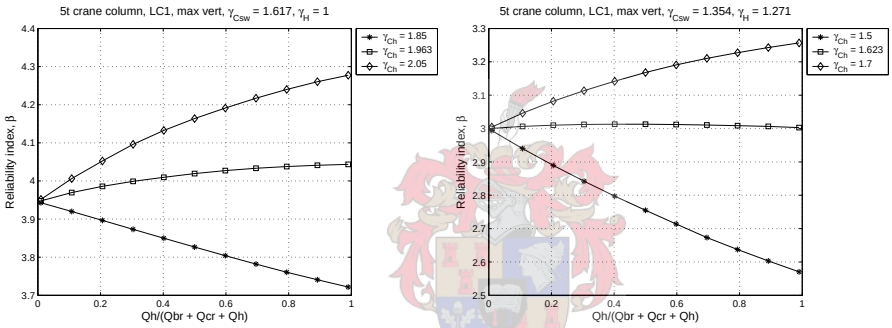

(a) Code format 2 (b) Code format 3

Figure E.16: LC1 maximum vertical, code formats 2 & 4

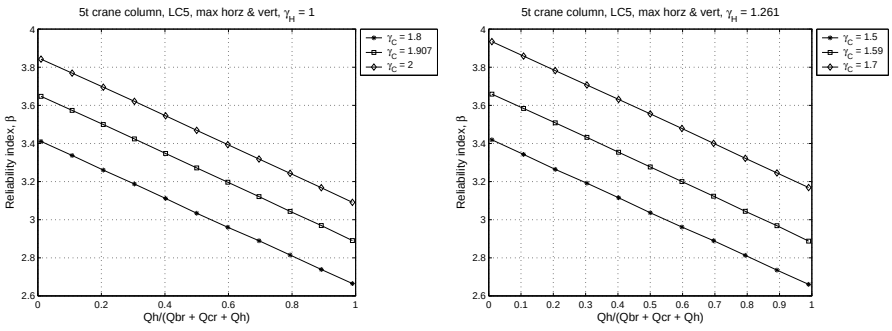

(a) Code format 1 (b) Code format 3

Figure E.17: LC5, code formats 1 & 3

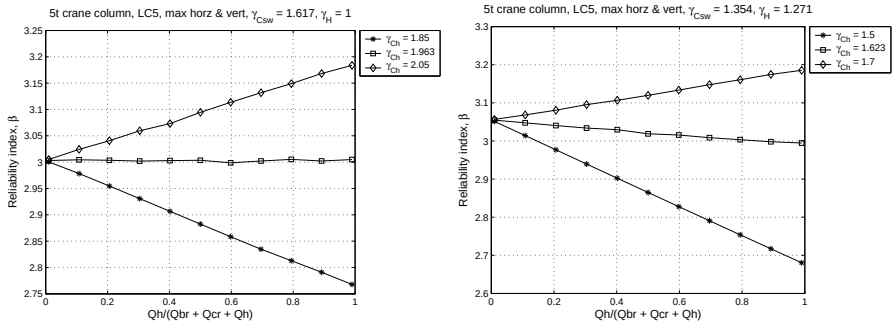

(a) Code format 2 (b) Code format 3

Figure E.18: LC5, code formats 2 & 4

E.1.3 40t crane girder

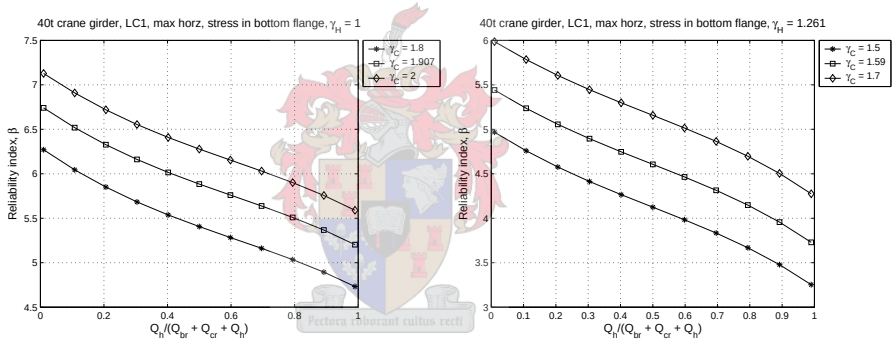

(a) Code format 1 (b) Code format 3

Figure E.19: LC1 maximum horizontal moment, bottom flange, code formats 1 & 3

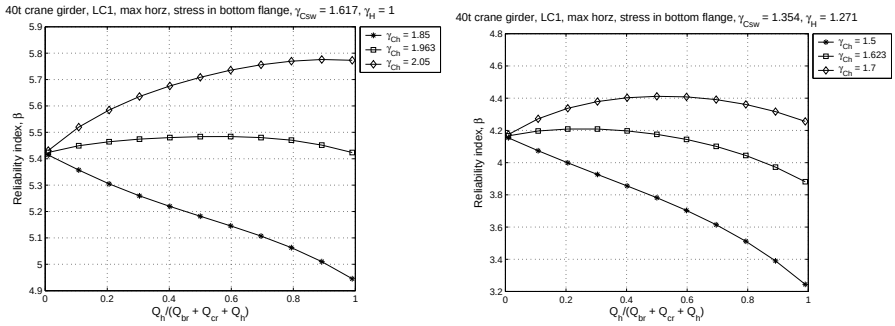

(a) Code format 2 (b) Code format 3

Figure E.20: LC1 maximum horizontal moment, bottom flange, code formats 2 & 4

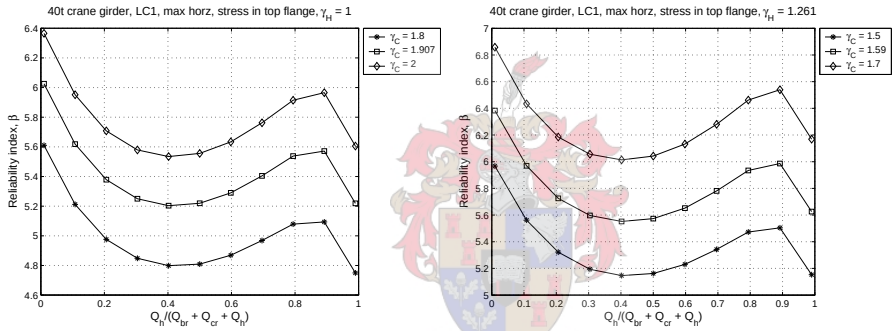

(a) Code format 1 (b) Code format 3

Figure E.21: LC1 maximum horizontal moment, top flange, code formats 1 & 3

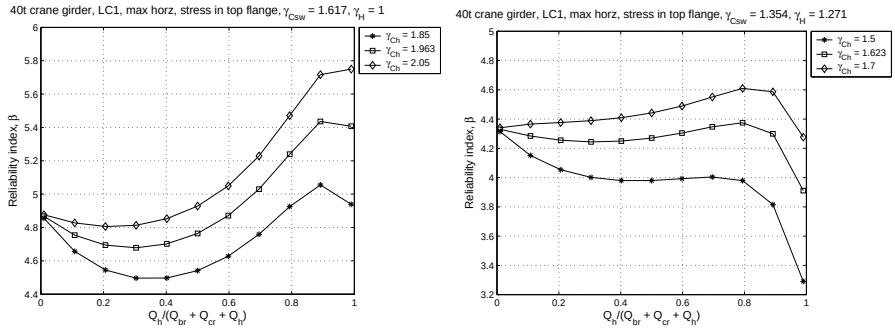

(a) Code format 2 (b) Code format 3

Figure E.22: LC1 maximum horizontal moment, top flange, code formats 2 & 4

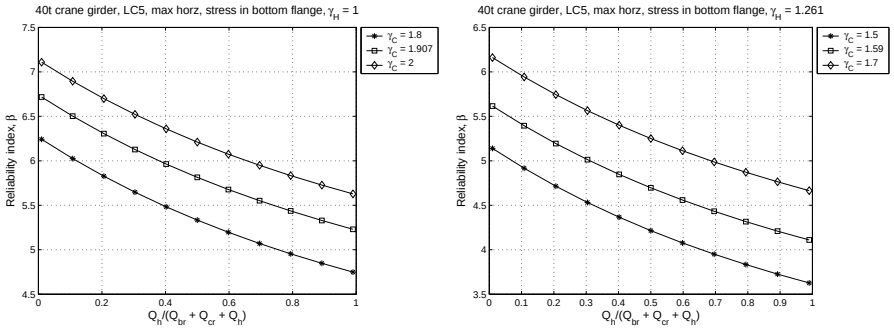

(a) Code format 1 (b) Code format 3

Figure E.23: LC5 maximum horizontal moment, bottom flange, code formats 1 & 3

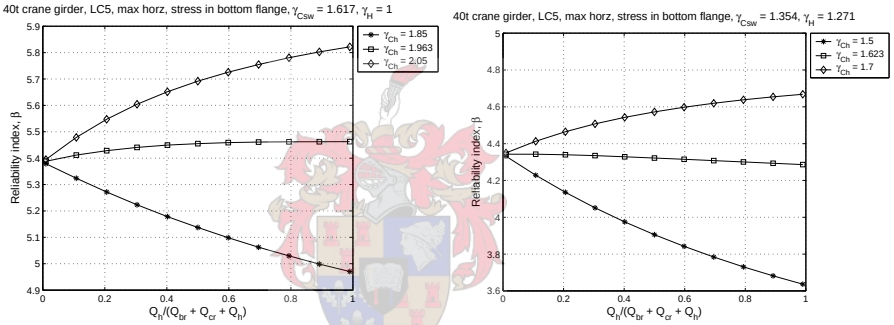

(a) Code format 2 (b) Code format 3

Figure E.24: LC5 maximum horizontal moment, bottom flange, code formats 2 & 4

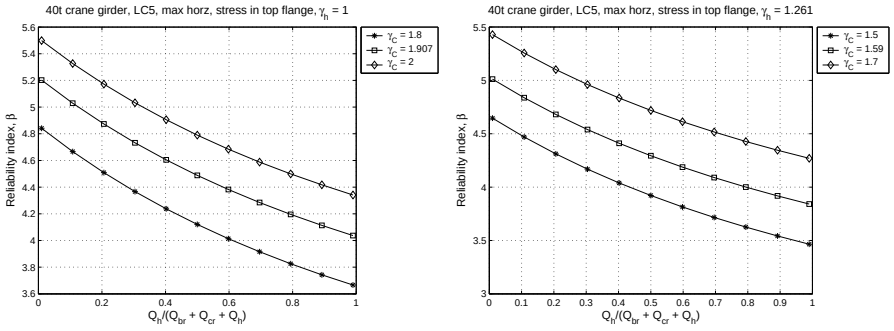

(a) Code format 1 (b) Code format 3

Figure E.25: LC5 maximum horizontal moment, top flange, code formats 1 & 3

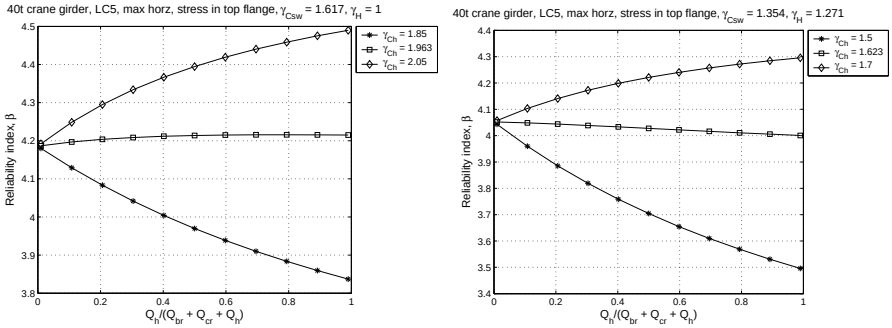

(a) Code format 2 (b) Code format 3

Figure E.26: LC5 maximum horizontal moment, top flange, code formats 2 & 4

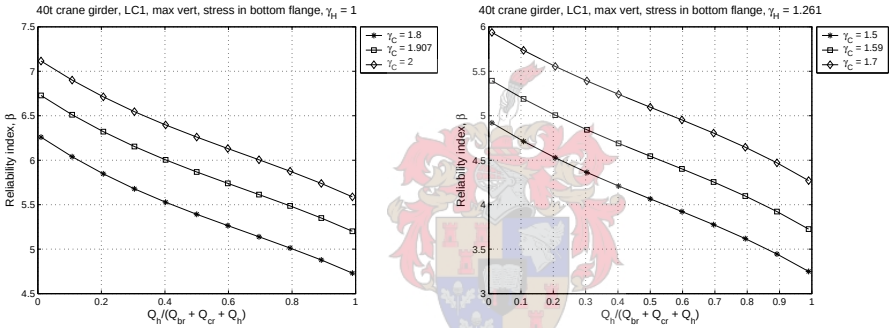

(a) Code format 1 (b) Code format 3

Figure E.27: LC1 maximum vertical moment, bottom flange, code formats 1 & 3

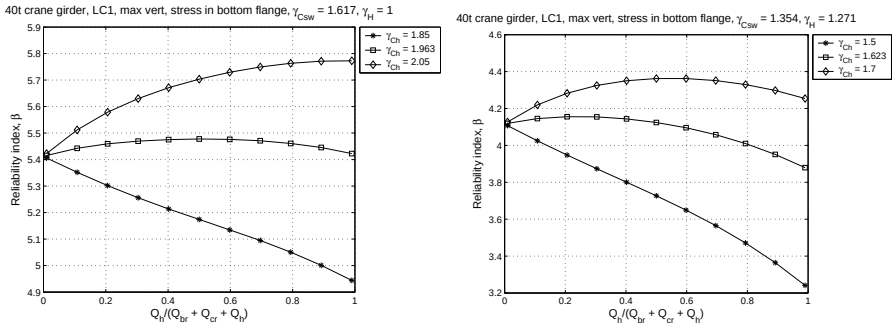

(a) Code format 2 (b) Code format 3

Figure E.28: LC1 maximum vertical moment, bottom flange, code formats 2 & 4

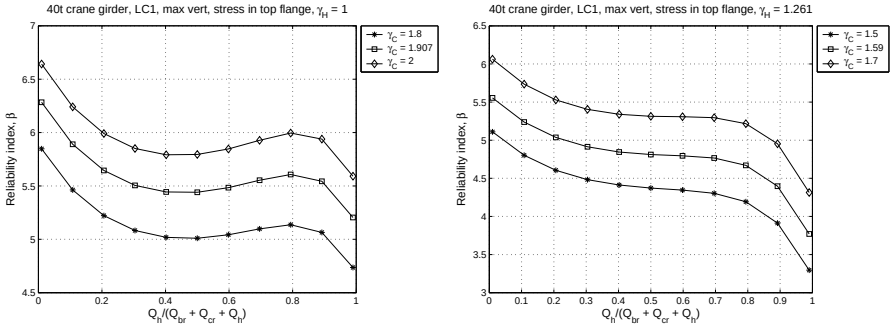

(a) Code format 1 (b) Code format 3

Figure E.29: LC1 maximum vertical moment, top flange, code formats 1 & 3

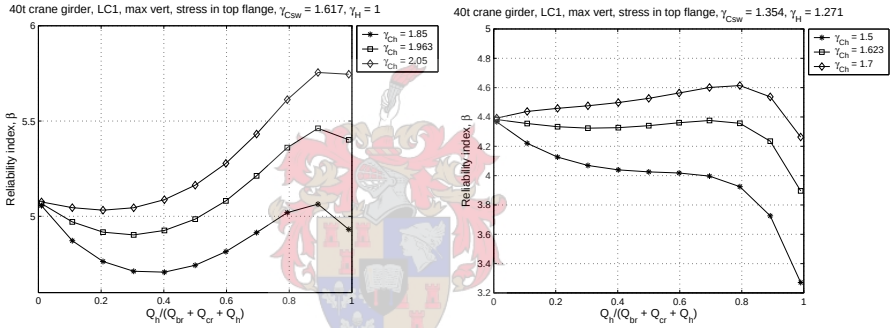

(a) Code format 2 (b) Code format 3

Figure E.30: LC1 maximum vertical moment, top flange, code formats 2 & 4

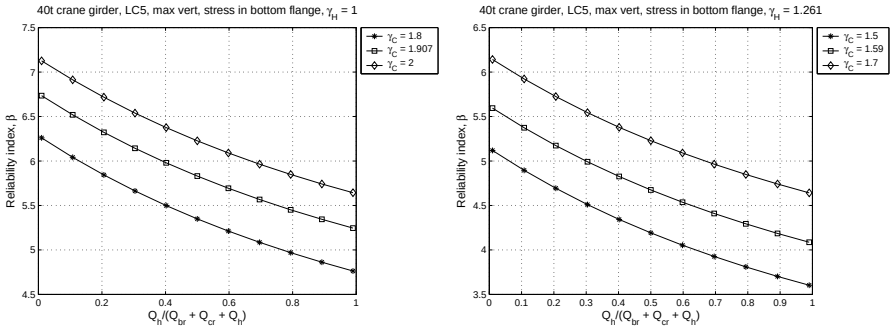

(a) Code format 1 (b) Code format 3

Figure E.31: LC5 maximum vertical moment, bottom flange, code formats 1 & 3

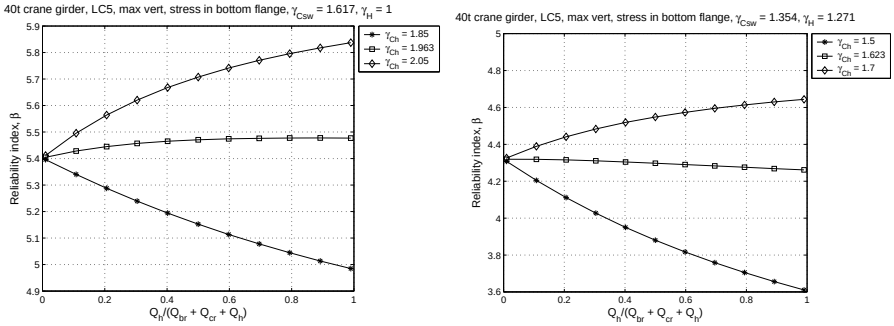

(a) Code format 2 (b) Code format 3

Figure E.32: LC5 maximum vertical moment, bottom flange, code formats 2 & 4

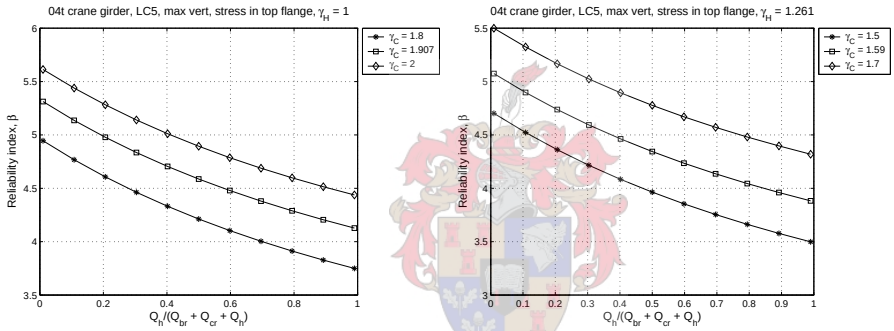

(a) Code format 1 (b) Code format 3

Figure E.33: LC5 maximum vertical moment, top flange, code formats 1 & 3

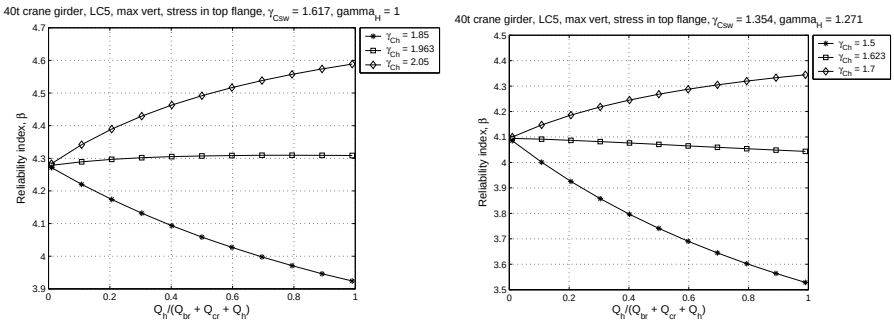

(a) Code format 2 (b) Code format 3

Figure E.34: LC5 maximum vertical moment, top flange, code formats 2 & 4

E.1.4 40t crane column

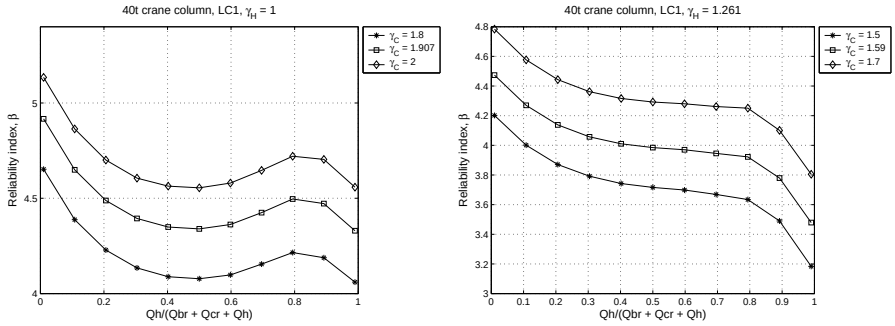

(a) Code format 1 (b) Code format 3

Figure E.35: LC1, code formats 1 & 3

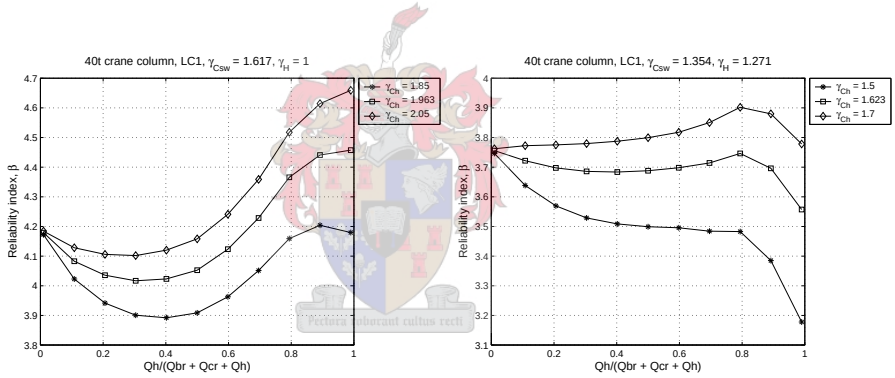

(a) Code format 2 (b) Code format 3

Figure E.36: LC1, code formats 2 & 4

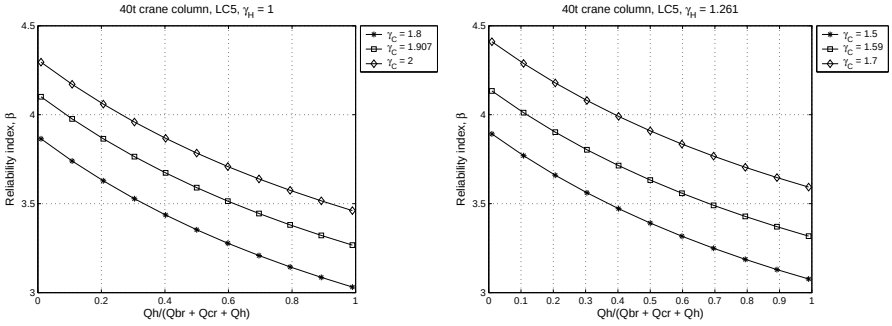

(a) Code format 1 (b) Code format 3

Figure E.37: LC5, code formats 1 & 3

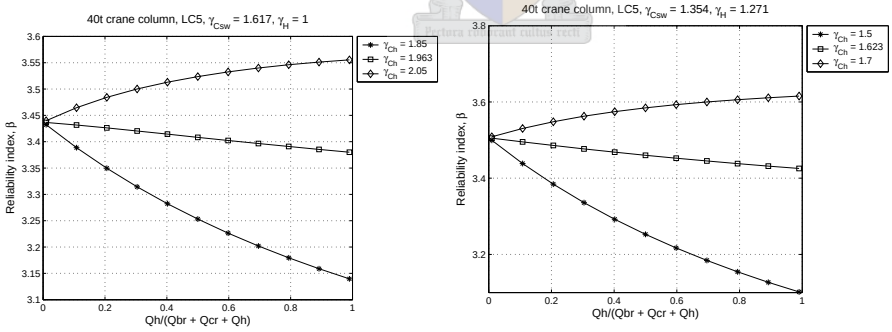

(a) Code format 2 (b) Code format 3

Figure E.38: LC5, code formats 2 & 4

E.1.5 260t crane girder

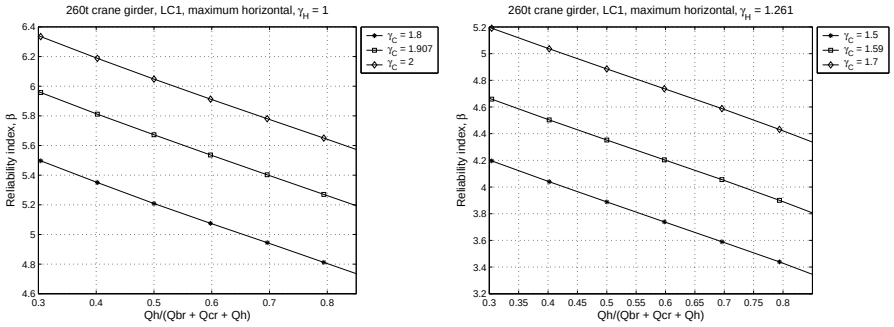

(a) Code format 1 (b) Code format 3

Figure E.39: LC1 maximum horizontal force, code formats 1 & 3

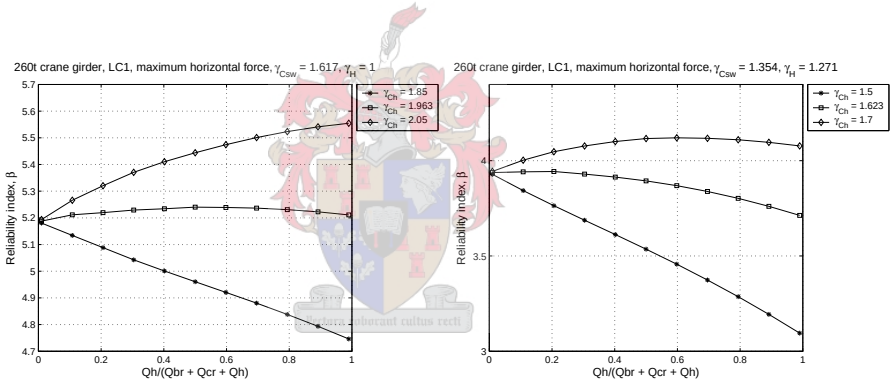

(a) Code format 2 (b) Code format 3

Figure E.40: LC1 maximum horizontal force, code formats 2 & 4

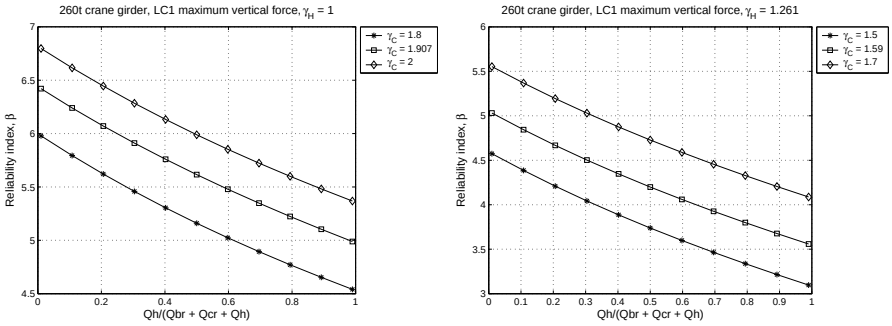

(a) Code format 1 (b) Code format 3

Figure E.41: LC1 maximum vertical force, code formats 1 & 3

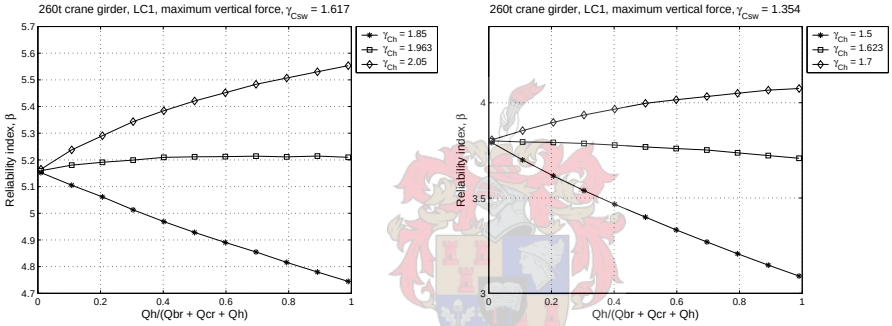

(a) Code format 2 (b) Code format 3

Figure E.42: LC1 maximum vertical force, code formats 2 & 4

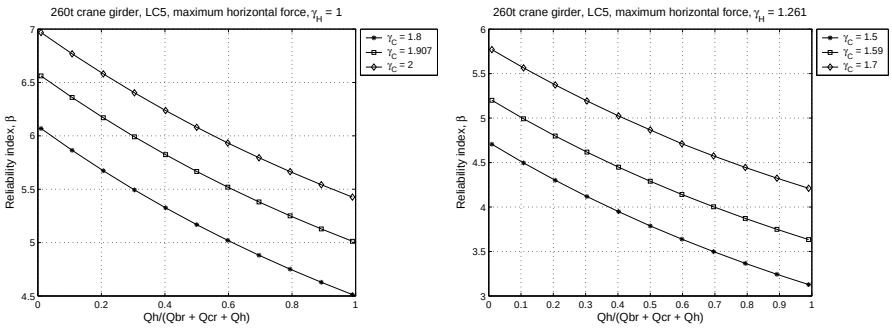

(a) Code format 1 (b) Code format 3

Figure E.43: LC5 maximum horizontal force, code formats 1 & 3

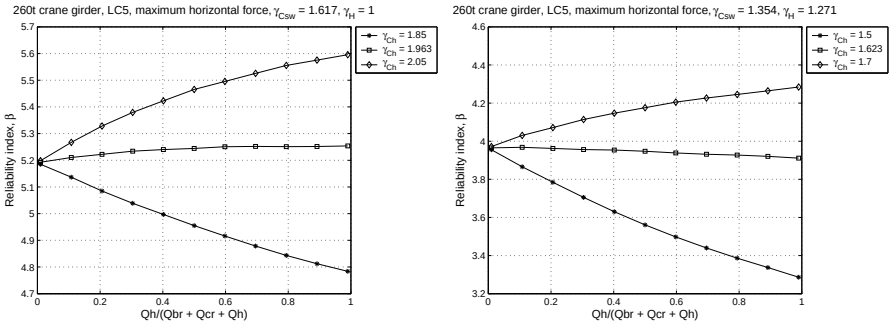

(a) Code format 2 (b) Code format 3

Figure E.44: LC5 maximum horizontal force, code formats 2 & 4

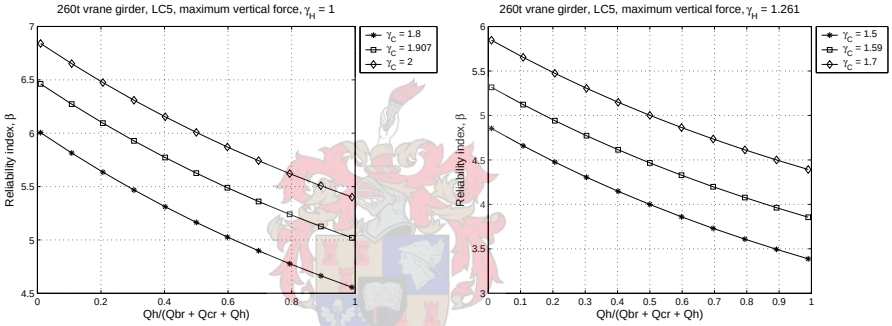

(a) Code format 1 (b) Code format 3

Figure E.45: LC5 maximum vertical force, code formats 1 & 3

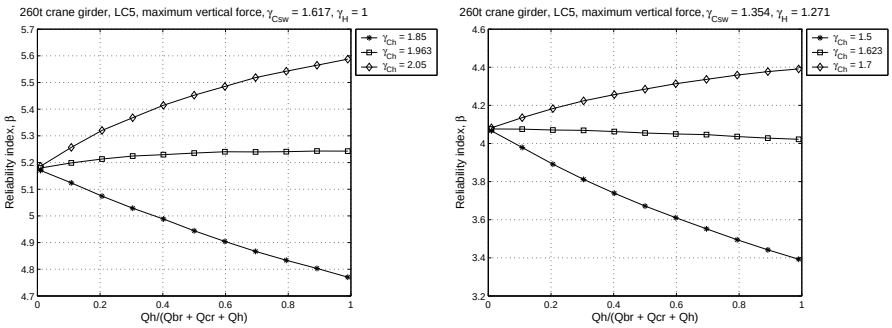

(a) Code format 2 (b) Code format 3

Figure E.46: LC5 maximum vertical force, code formats 2 & 4

E.1.6 260t crane auxiliary girder

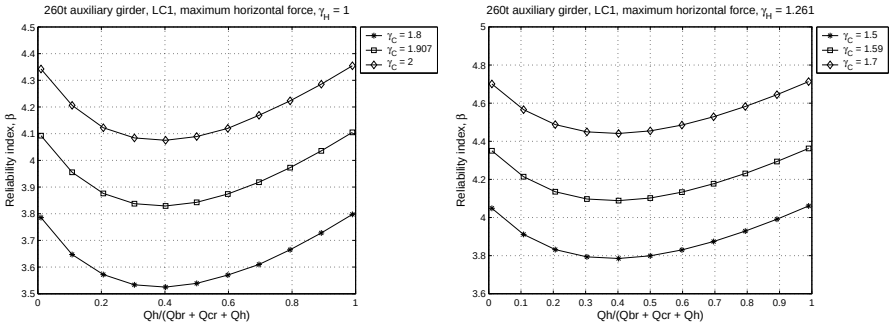

(a) Code format 1 (b) Code format 3

Figure E.47: LC1 maximum horizontal force, code formats 1 & 3

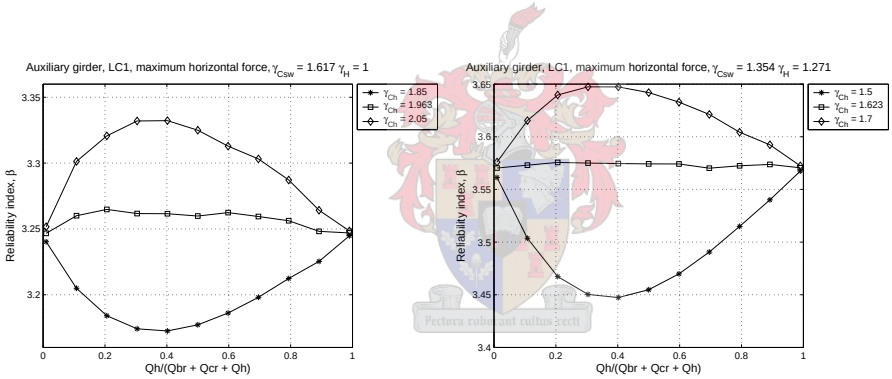

(a) Code format 2 (b) Code format 3

Figure E.48: LC1 maximum horizontal force, code formats 2 & 4

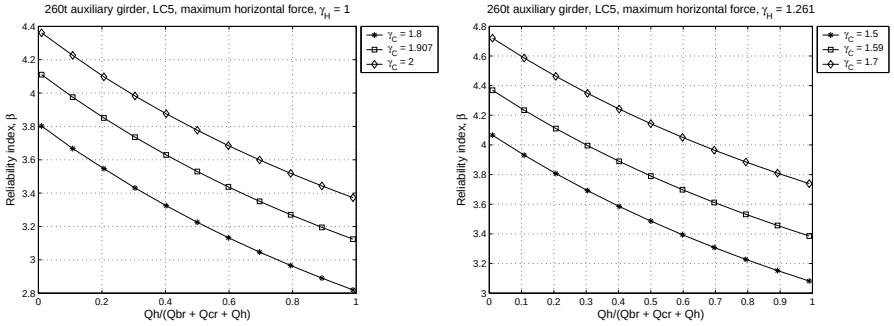

(a) Code format 1 (b) Code format 3

Figure E.49: LC5 maximum horizontal force, code formats 1 & 3

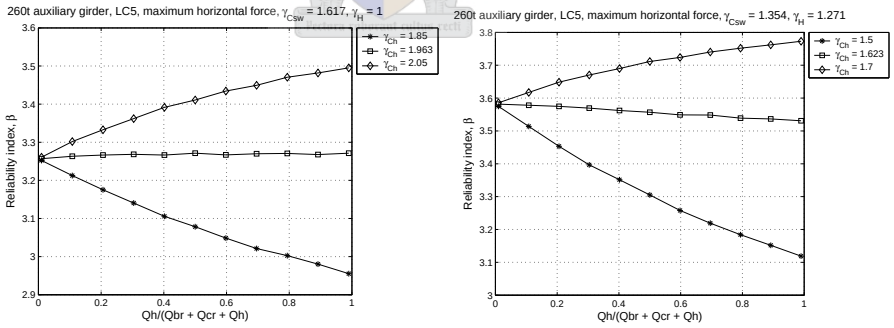

(a) Code format 2 (b) Code format 3

Figure E.50: LC5 maximum horizontal force, code formats 2 & 4

E.1.7 260t crane column

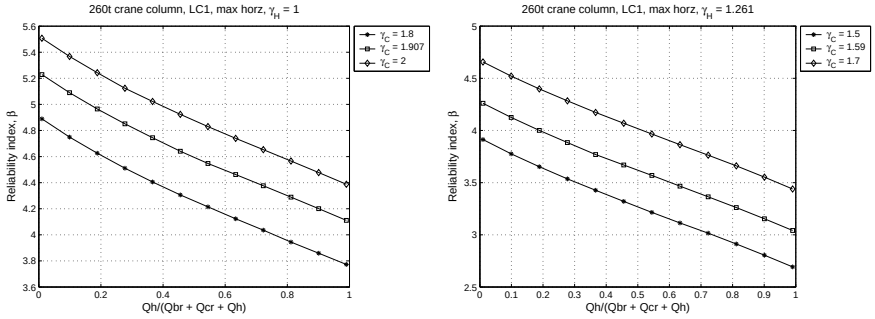

(a) Code format 1 (b) Code format 3

Figure E.51: LC1 maximum horizontal force, code formats 1 & 3

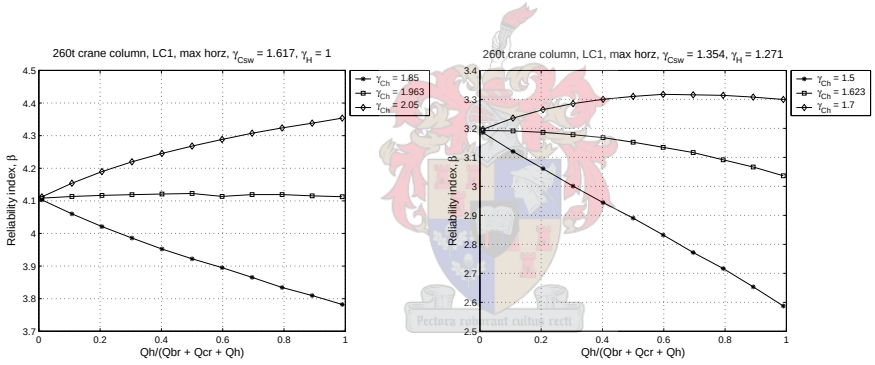

(a) Code format 2 (b) Code format 3

Figure E.52: LC1 maximum horizontal force, code formats 2 & 4

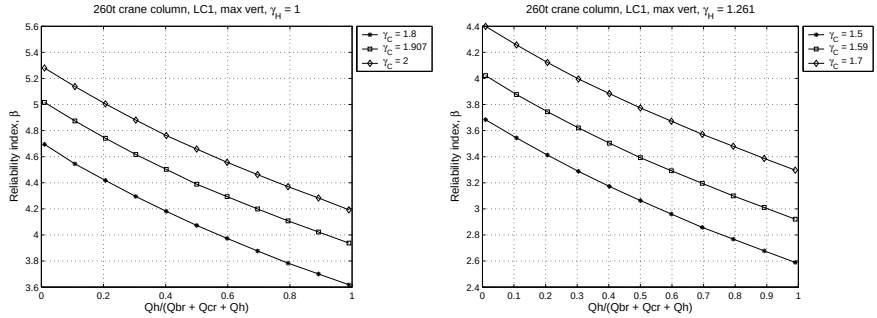

(a) Code format 1 (b) Code format 3

Figure E.53: LC1 maximum vertical force, code formats 1 & 3

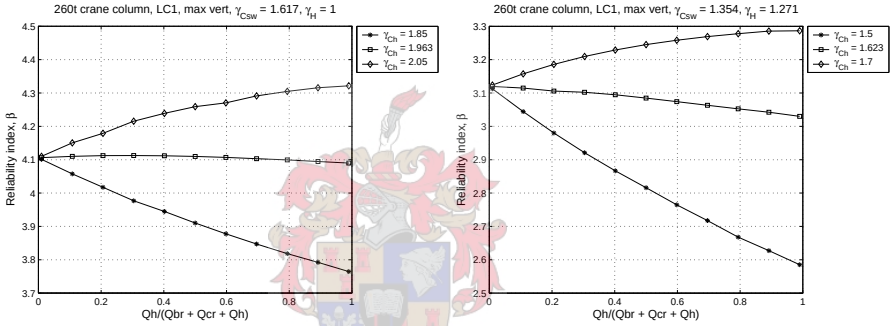

(a) Code format 2 (b) Code format 3

Figure E.54: LC1 maximum vertical force, code formats 2 & 4

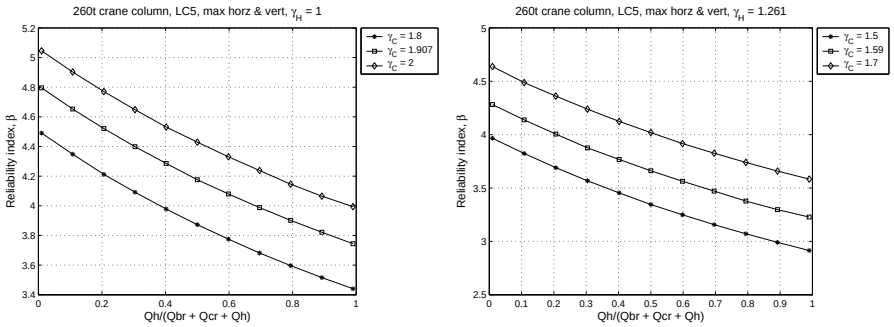

(a) Code format 1 (b) Code format 3

Figure E.55: LC5, code formats 1 & 3

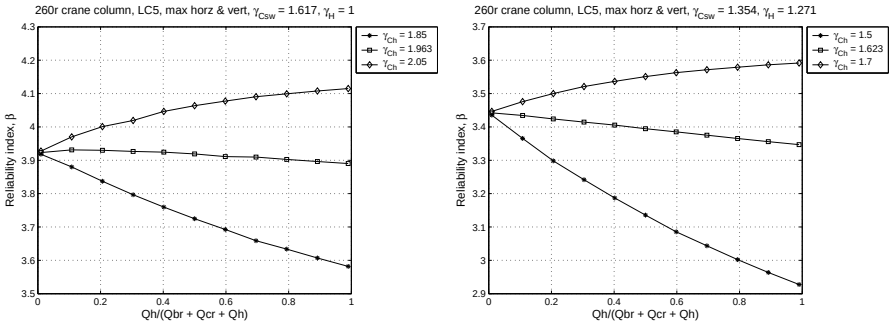

(a) Code format 2 (b) Code format 3

Figure E.56: LC5, code formats 2 & 4

E.2 Fatigue

E.2.1 5t crane corbel to column welded connection

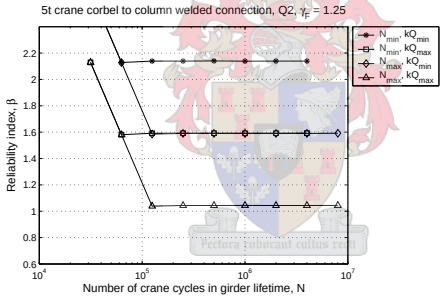

Figure E.57: 5t crane corbel to column connection, load spectrum class Q_2

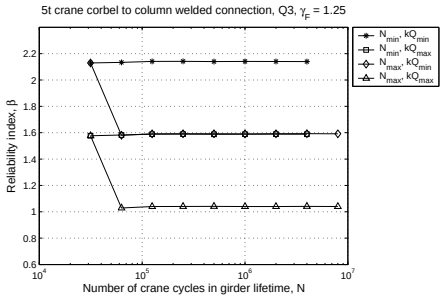

Figure E.58: 5t crane corbel to column connection, load spectrum class Q_3

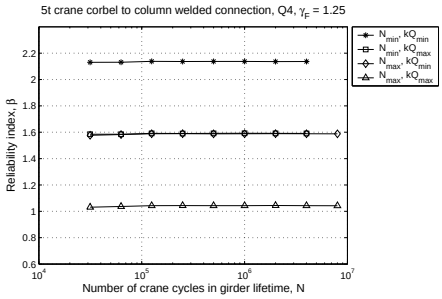

Figure E.59: 5t crane corbel to column connection, load spectrum class Q_4

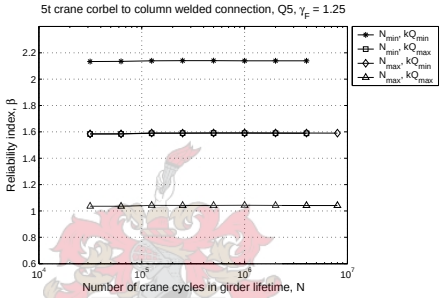

Figure E.60: 5t crane corbel to column connection, load spectrum class Q_5

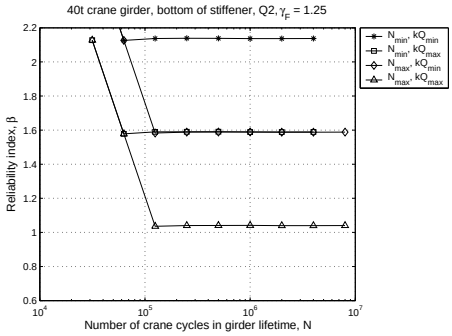

Figure E.61: 40t crane girder intermediate stiffener, load spectrum class Q_2

E.2.2 40t crane girder bottom of intermediate stiffener

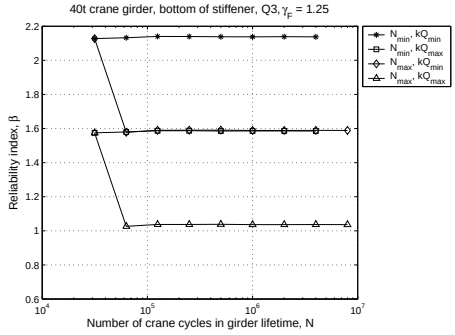

Figure E.62: 40t crane girder intermediate stiffener, load spectrum class Q_3

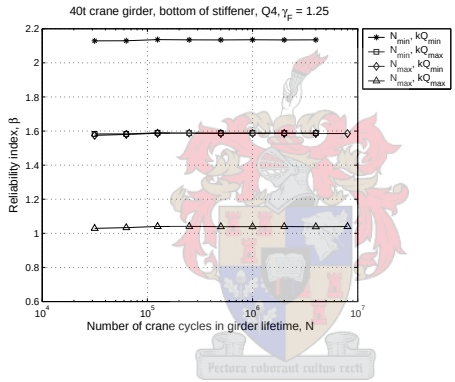

Figure E.63: 40t crane girder intermediate stiffener, load spectrum class Q_4

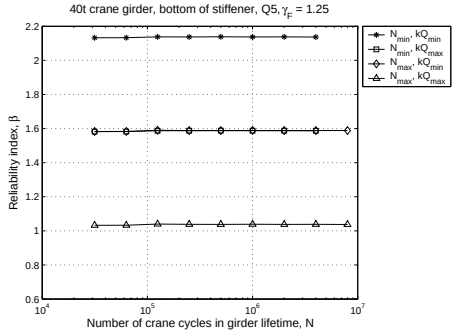

Figure E.64: 40t crane girder intermediate stiffener, load spectrum class Q_5

E.2.3 40t crane girder top flange to web weld

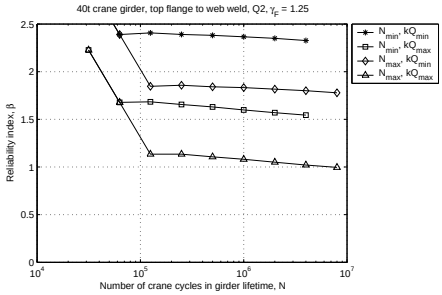

Figure E.65: 40t crane girder top flange to web weld, load spectrum class Q_2

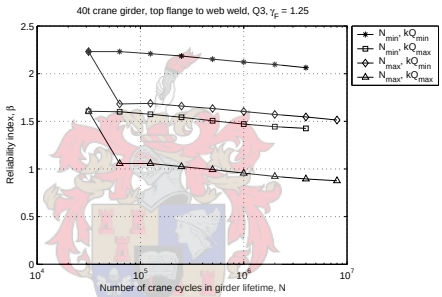

Figure E.66: 40t crane girder top flange to web weld, load spectrum class Q_3

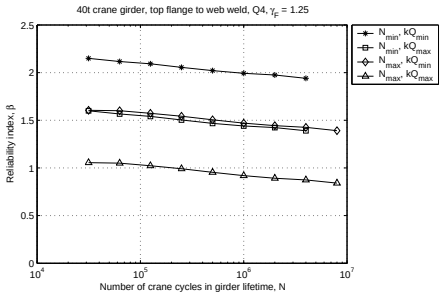

Figure E.67: 40t crane girder top flange to web weld, load spectrum class Q_4

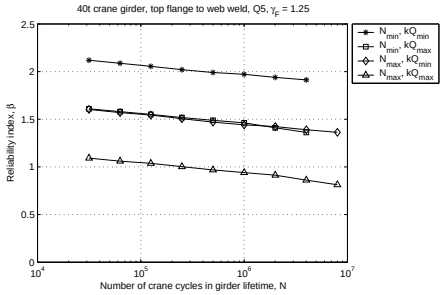

Figure E.68: 40t crane girder top flange to web weld, load spectrum class Q_5

Pectora roborant cultus recti